ICLIAD 66 (4), 347-482, 2025

p-ISSN 0535-5133
e-ISSN 2477-9393

Volumen 66
No. 4
Diciembre
2025

Investigación Clínica

65 Aniversario

Universidad del Zulia
Facultad de Medicina
Instituto de Investigaciones Clínicas
"Dr. Américo Negrette"
Maracaibo, Venezuela

Investigación Clínica

https://sites.google.com/site/revistainvestigacionesclinicas

Revista arbitrada dedicada a estudios humanos, animales y de laboratorio relacionados con la investigación clínica y asuntos conexos.

La Revista es de Acceso Abierto, publicada trimestralmente por el Instituto de Investigaciones Clínicas "Dr. Américo Negrette", de la Facultad de Medicina, de la Universidad del Zulia, Maracaibo, Venezuela.

Investigación Clínica está indizada en Science Citation Index Expanded (USA), Excerpta Medica/EMBASE y Scopus (Holanda), Tropical Diseases Bulletin y Global Health (UK), Biblioteca Regional de Medicina/BIREME (Brasil), Ulrich's Periodicals, Journal Citation Reports (USA), Index Copernicus (Polonia), SIIEC Data Bases, Sección Iberoamérica (Argentina) e Infobase Index (India), Redalyc y las bases de datos: SciELO (www.Scielo.org.ve), Revencyt, LILACS, LIVECS, PERIODICA y web de LUZ: http://www.produccioncientificaluz.org/revistas

Para cualquier otra información dirigir su correspondencia a:

Dra. Elena Ryder, Editora
Instituto de Investigaciones Clínicas
"Dr. Américo Negrette"
Facultad de Medicina, Universidad del Zulia
Maracaibo, Venezuela.

Teléfono:
+58-0414-6305451

Correos electrónicos:
elenaryder@gmail.com
riclinicas@gmail.com

Páginas web:
https://sites.google.com/site/revistainvestigacionesclinicas

http://www.produccioncientificaluz.org/revistas

For any information please address correspondence to:

Dr. Elena Ryder, Editor
Instituto de Investigaciones Clínicas
"Dr. Américo Negrette"
Facultad de Medicina, Universidad del Zulia
Maracaibo, Venezuela.

Phone:
+58-0414-6305451

E-mails:
elenaryder@gmail.com
riclinicas@gmail.com

Web pages:
https://sites.google.com/site/revistainvestigacionesclinicas

http://www.produccioncientificaluz.org/revistas

Universidad del Zulia
Publicación auspiciada por el
Vicerrectorado Académico
Serbiluz-CONDES

CODEN: ICLIAD
Versión impresa ISSN: 0535-5133
Depósito legal pp 196002ZU37
Versión electrónica ISSN: 2477-9393
Depósito legal ppi 201502ZU4667

Artes finales:
Lisbeny Valencia
lisbenyvalencia@gmail.com

ASESORES CIENTÍFICOS (2025-2027)

Invest Clin 66(4): 347 - 348, 2025 https://doi.org/10.54817/IC.v66n4a00

EDITORIAL
Honestidad en investigación: Papel de las revistas científicas como mecanismo de control.

En el mundo de la ciencia, la honestidad, es una cualidad indispensable, por lo cual debe estar presente en toda investigación. Sin embargo, en la práctica, esto no siempre se cumple y es por ello que las editoriales de algunas revistas científicas, han establecido criterios, que ayuden a detectar fraude, o lo que es lo mismo, deshonestidad, en un trabajo de investigación [1].

Un comportamiento honesto en un investigador científico, es actuar (de acuerdo con la RAE) [2], de forma honrada, razonable y justa, en todo el proceso de investigación, desde que concibe la hipótesis del trabajo, hasta su publicación y desde luego, siempre sujeto a la verdad, aunque ella contradiga el propósito o los resultados del trabajo.

Desafortunadamente, la falta de honestidad es frecuente en muchos aspectos del comportamiento del individuo, y el investigador científico también puede estar sujeto a la tentación de "modificar" la verdad, en aras de producir un trabajo [3,4].

La competitividad en el mundo de la ciencia, es muy alta y el investigador, específicamente en el medio académico, debe demostrar su actividad, mediante un mínimo anual de publicaciones en revistas acreditadas de su especialidad, de lo contrario, pone en peligro su ascenso en el escalafón, o lo que es peor, su estabilidad en la institución. Por esta razón, se han conocido casos, de trabajos publicados en revistas de alto rango científico, donde se han hecho evidentes el plagio, la manipulación de los resultados, así como la fabricación.

En otros casos, el investigador recurre a la "amistad", para que lo incluyan en la lista de autores, o lo que es peor, se apropia de las ideas de otro cuando escribe un artículo, o modifica los resultados para obtener una diferencia estadística que apoye la hipótesis de trabajo. En otras ocasiones, los evaluadores conciben fuertes sospechas de que los autores, no fueron los que realizaron la investigación.

Otra forma de deshonestidad es colocar referencias que no se han consultado, o lo que es peor, omitir las de otro autor, cuyas ideas han sido clave para la concepción y desarrollo de la investigación. Se da también el caso de publicar gráficos y tablas de otros autores, sin las debidas referencias y permisos. En estas situaciones, cabe el beneficio de la duda, si el investigador actuó con o sin malicia o si pudiera tratarse de investigadores noveles, que desconocen las normas de publicación.

Actualmente, es frecuente que el investigador recurra a los llamados "Promotores", para ayudarle a encontrar una revista que publique su trabajo. Este procedimiento sin considerarlo incorrecto, pudiera dar paso a situaciones controversiales.

Otro aspecto que hay que considerar es el avance de la tecnología, que mientras ofrece excelente ayuda para obtener información sobre el tema a investigar, también ofrece mayor oportunidad de cometer fraude, como puede suceder con el mal uso de la "Inteligencia Artificial", que es una gran herramienta para la búsqueda de información, pero que a la vez crea la posibilidad de escribir un trabajo para publicación, que en realidad no se ha realizado. Esto no es solo deshonesto, sino que es criminal, ya que di-

chos resultados falsificados, son llevados a la práctica clínica, afectando la salud de poblaciones de pacientes.

Desafortunadamente, las situaciones mencionadas, se han visto frecuentemente durante años recientes. Por lo tanto, las revistas de investigación, tienen el reto cada vez mayor, de detectar fraude en un trabajo de investigación y es tarea de sus árbitros y del Comité Editorial, el revisar acuciosamente los artículos que se reciben, para evitar que ello suceda.

María Diez Ewald
ORCID 0000-0002-7161-5307

Honesty in research: the role of scientific journals as a control mechanism.

The publication of false results and the appropriation of ideas, are examples of dishonesty in research. Artificial intelligence and the use of "Promoters", while useful when correctly used, could be a source for committing fraud. Although these issues are observed sporadically, the responsibility to identify fraud in a manuscript lies with its reviewers and the editorial staff.

REFERENCIAS

1. **Elsevier.** Policies & guidelines for authors [internet]. Amsterdam: Elsevier. Disponible en: https//www: Elsevier.com/researcher/autor/policies-and-guidelines.
2. **Real Academia Española**. Diccionario de la lengua española [Internet]. 23ª ed. Madrid: RAE; 2025. Disponible en: https://dle.rae.es.
3. **Robert JS**. Misconduct in research. What is it? How widespread is it? And What should we do about it? Account Res. 2023; 30 (7): 439-458. *https://doi.org/10.1080/08989621.2021.2020110.*
4. **Rodrigues F, Gupta P, Khan AP, Chatterjee T, Sandhu NK, Gupta L**. The cultural contest of plagiarism and research misconduct in the Asian region. J Korean Med Sci. 2023; 38(12): e88. *https://doi.org/10.3346/jkms.2023.38.e88.*

Invest Clin 66(4): 349 - 364, 2025 https://doi.org/10.54817/IC.v66n4a01

The role of amyloid and tau biomarkers in assessing the effectiveness of drug treatment for Alzheimer's disease.

Jiao Sun[1], Yingchun Ling[2], Jie Chen[2] and Mingyong Zhao[3]

[1]Department of Pharmacy, Shaoxing Seventh People's Hospital, Shaoxing, Zhejiang Province, China.
[2]Department of Clinical Laboratory, Shaoxing Seventh People's Hospital, Shaoxing, Zhejiang Province, China.
[3]Department of Geriatrics Shaoxing Seventh People's Hospital, Shaoxing, Zhejiang Province.

Keywords: Amyloid Beta-Peptides; Tau Proteins; Phosphorylated Tau; P-Tau-181, Alzheimer Disease; Drug Therapy.

Abstract. This study aimed to explore the role of amyloid and tau biomarkers in evaluating the effectiveness of drug therapy for Alzheimer's disease (AD). A retrospective analysis was performed in 150 AD patients admitted to our hospital from October 2022 to January 2024, and 50 healthy people were selected as the control group. The basic information of patients, including cognitive function and daily living ability, as well as amyloid and tau biomarkers, was compared between the two groups. AD patients were treated with donepezil hydrochloride and memantine tablets, and were divided into valid and invalid groups based on efficacy. Binary logistic regression analysis was used to identify factors affecting the effectiveness of AD drug treatment, with the predictive accuracy being assessed using ROC curves. This study revealed that compared with the control group, the MMSE (Mini-Mental State Examination), MoCA (Montreal Cognitive Assessment), and Aβ1-42 in the AD group decreased, while T-tau and P-Tau-181 increased ($p<0.05$). Drug treatment was considered effective in 107 out of 150 AD patients. Education years, daily exercise, Aβ1-42, T-tau, and P-Tau-181 are all factors that affect the effectiveness of AD drug treatment. The changes in serum levels of Aβ1-42, T-tau, and P-Tau-181 can all be used to evaluate the effectiveness of AD drug treatment, with AUC values of 0.869, 0.815, and 0.800, respectively. The combined evaluation of the three factors has an AUC of 0.977. Drug therapy can improve the clinical efficacy of most AD patients. The years of education, exercise, Aβ1-42, T-tau and P-Tau-181 are the influencing factors of the efficacy of AD drug treatment. The efficacy of AD drug treatment can be evaluated by detecting the changes of serum Aβ1-42, T-tau and P-Tau-181 levels in clinical practice, and the combined evaluation value of the three is higher than the individual values.

Correspondence author: Yingchun Ling. Department of Clinical Laboratory, Shaoxing Seventh People's Hospital, Shaoxing, Zhejiang Province. China. Email: sxdqrm2025@hotmail.com

El papel de los biomarcadores de amiloide y tau en la evaluación de la eficacia del tratamiento farmacológico para la enfermedad de Alzheimer.

Invest Clin 2025; 66 (4): 349 – 364

Palabras clave: Péptidos Beta-Amiloide; Proteínas Tau; Proteína Tau Fosforilada; P-Tau- 181; Enfermedad de Alzheimer; Terapia Farmacológica.

Resumen. El objetivo de este estudio es explorar el papel de los biomarcadores de amiloide y tau en la evaluación de la eficacia de la farmacoterapia para la enfermedad de Alzheimer (EA). Se realizó un análisis retrospectivo de 150 pacientes con EA ingresados en nuestro hospital entre octubre de 2022 y enero de 2024, y se seleccionaron 50 personas sanas como grupo control. Se compararon la información básica, la función cognitiva, la capacidad para realizar las actividades de la vida diaria, así como los biomarcadores de amiloide y tau entre ambos grupos. Los pacientes con EA fueron tratados con tabletas de hidrocloruro de donepezilo y memantina, y se dividieron en un grupo de pacientes que respondieron al tratamiento y otro grupo de pacientes que no respondieron, en función de la eficacia del mismo. Se utilizó un análisis de regresión logística binaria para identificar los factores que afectan la eficacia del tratamiento farmacológico de la EA, y se evaluó la precisión predictiva mediante curvas ROC. Los resultados de este estudio revelan que, en comparación con el grupo control, en el grupo de EA, las puntuaciones en las escalas MMSE, MoCA y los niveles de Aβ1-42 disminuyeron, mientras que los niveles de T-tau y P-Tau-181 aumentaron ($p<0,05$). Después del tratamiento farmacológico, 107 de los 150 pacientes con EA mostraron una respuesta favorable. Los años de educación, el ejercicio diario, los niveles de Aβ1-42, T-tau y P-Tau-181 son todos factores que afectan la eficacia del tratamiento farmacológico de la EA. Los cambios en los niveles séricos de Aβ1-42, T-tau y P-Tau-181 pueden servir para evaluar la eficacia del tratamiento farmacológico de la EA, con valores de área bajo la curva (AUC) de 0,869, 0,815 y 0,800, respectivamente. La evaluación combinada de estos tres factores tiene un AUC de 0,977. La farmacoterapia puede mejorar la eficacia clínica en la mayoría de los pacientes con EA. Los años de educación, el ejercicio, los niveles de Aβ1-42, T-tau y P-Tau-181 son los factores que influyen en la eficacia del tratamiento farmacológico de la EA. La eficacia del tratamiento farmacológico de la EA puede evaluarse detectando los cambios en los niveles séricos de Aβ1-42, T-tau y P-Tau-181 en la práctica clínica. Además, el valor de la evaluación combinada de estos tres biomarcadores es mayor que la evaluación de estos factores individualmente.

Received: 02-07-2025 Accepted: 12-07-2025

INTRODUCTION

Alzheimer's disease (AD) is a degenerative neurological disorder, clinically manifested as memory impairment and irreversible progressive memory loss, among others. In addition, patients may also experience language and visual-spatial disorders, which mainly affect the elderly [1, 2]. With the increase of aging, the incidence rate of AD is increasing year by year, and its impact on the social economy is also increasingly significant [3]. At present, AD is mainly relying on drug treatment supplemented by comprehensive measures such as psychological and cognitive interventions [4]. In terms of drug therapy, cholinesterase inhibitors, glutamate receptor antagonists, and other cognitive enhancement drugs are mainly used [5]. However, due to the complexity and multifactorial nature of AD disease, as well as the challenges faced in evaluating the effectiveness and safety of drugs [6, 7], and that drug therapy can alleviate patients' clinical symptoms, the clinical efficacy is not satisfactory, and additional methods are needed to improve patients' quality of life and cognitive abilities [8, 9]. Therefore, it is necessary to explore biomarkers to evaluate the effectiveness of drugs in order to develop personalized treatment plans tailored to the specific conditions of patients and enhance their clinical efficacy.

Research has shown that the excessive deposition of amyloid-β (Aβ) in cerebral blood vessels and the aggregation of tau protein to form neurofibrillary tangles are the primary pathological mechanisms of AD [10,11]. Aβ is a peptide generated by the amyloid precursor protein (APP) [12, 13], and its primary forms are Aβ1-42 and Aβ1-40, which are important biomarkers in AD [14]. Studies have shown that excessive deposition of Aβ1-42 promotes neuroinflammation, neuronal death and cognitive dysfunction [15]. For mild AD patients, Aβ begins to accumulate abnormally in the early stages of the disease, and soluble Aβ1-42 levels decrease; however, the damage to nerve cells and neural networks is relatively mild at this time. Timely anti-amyloid treatment can effectively prevent the progression of the disease [16]. Tau protein plays a crucial role in maintaining the stability of the microtubule structure, facilitating axonal transport, and regulating neuronal function [17]. However, in AD patients, the abnormal phosphorylation and aggregation of the Tau protein lead to the formation of neurofibrillary tangles, which destroy the cellular structure and trigger neuronal death [18]. Among them, phosphorylated tau protein 181 (P-Tau-181) is a phosphorylated form of T-tau [19]. Under normal circumstances, the content of P-Tau-181 in blood or spinal fluid is minimal. Therefore, detection of P-Tau-181 levels can reflect neural or cognitive function [20].

However, there is currently no report on whether amyloid protein and tau biomarkers can be used to evaluate the effectiveness of drug therapy. Therefore, this study examines the role of serum Aβ1-42, P-Tau-181, and T-tau biomarkers in evaluating the effectiveness of AD drug therapy, aiming to provide personalized treatment plans for patients and thereby improve treatment outcomes, to provide further laboratory evidence for drug treatment and clinical reference for saving patients' lives and improving prognosis.

MATERIALS AND METHODS

Subjects

Regression analysis was conducted on 150 AD patients admitted to our hospital between February 2023 and January 2024. Fifty healthy individuals were included as the control group. Through multidisciplinary consultations in neurology, psychiatry, rehabilitation, and other fields, comprehensive evaluations and confirmations of AD patients were conducted using EEG and head MRI examinations (Fig. 1).

Inclusion criteria: ①Meet the diagnostic criteria for AD [21], age≥55 years; ②Com-

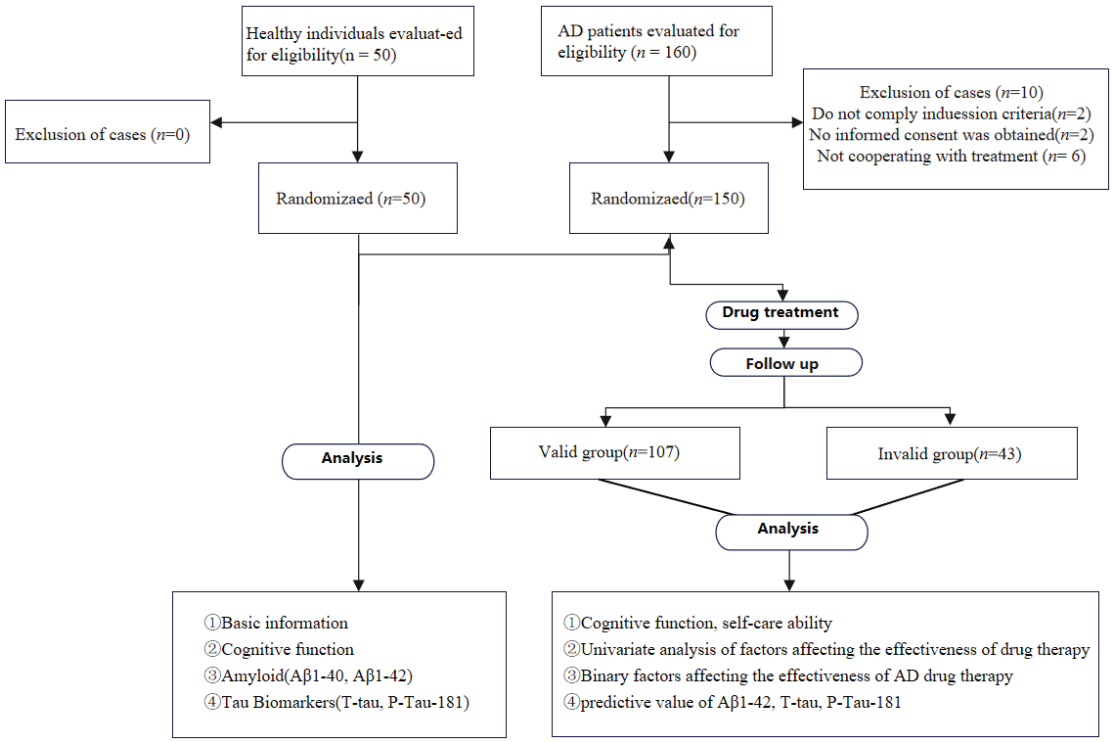

Fig. 1. Study design drawing.

plete clinical data; ③Could communicate fluently in Mandarin, understand the questionnaire content, and complete various survey evaluations; ④Good compliance; ⑤Expected survival period≥6 months; ⑥Tolerate the treatment plan related to this study; ⑦A score of≥27 on the Mini Mental State Examination (MMSE) and/or≥26 on the Montreal Cognitive Assessment Scale (M0CA) for healthy individuals during the same period.

Exclusion criteria: ①Patients with comorbidities of other mental illnesses; ②Long-term use of sedatives and sleeping pills; ③Individuals who are allergic to the medication used in this study; ④Serious infectious diseases of body organs; ⑤Not willing to comply with the follow-up and evaluation plan of this study.

Ethical considerations

This study strictly adheres to the principles of the Declaration of Helsinki, and all research procedures comply with international ethical standards. Has obtained approval from the ethics committee of Shaoxing Seventh People's Hospital. All participants have signed an informed consent form. In emergencies, the consent form may be signed by a representative or guardian of the individual. All data involved in the research process has been anonymized to ensure the privacy and confidentiality of participants' identities.

Therapeutic approaches

All AD patients received drug treatment: oral donepezil hydrochloride (Shaanxi Fangzhou Pharmaceutical Co., Ltd., GYZZ H20030583, specification: 5 mg), one tablet per day. The dose was adjusted four weeks later, the maximum dose was two tablets/per day. if severe insomnia occurred, they were administered in the morning. Oral administration of Meijingang tablets (Hangzhou Baishan Technology Co., Ltd., national drug approval number H20213931, specifi-

cation: 5mg), one tablet/per day, increasing by one tablet/per day per week, the maximum dose was four tablets/per day. Regular monitoring of the patient's blood pressure and provision of medication guidance and education was carried out during nursing. Appropriate sleep schedules were arranged to ensure adequate sleep. The diet was guided to be light, to avoid overeating, stimulating foods, and smoking and alcohol consumption. Moreover, specific psychological counselling was provided, tailored to the patient's situation and treatment for three months.

Detection of indicators

Clinical data: Relevant indicators and clinical data of patients were collected within 24 hours after admission, including gender, age, BMI, clinical symptoms, imaging data, and relevant laboratory examination indicators, as well as basic diseases. Using an electronic blood pressure measuring device (model: HEM-7124, Manufacturer: Omron Company), systolic and diastolic blood pressure values were recorded. Five mL of venous blood was extracted from the patient, the serum separated and an automated chemical analyzer used to detect blood calcium, fasting blood glucose, homocysteine (Hcy), and creatinine (Cr), Urea (BUN), total cholesterol (TC), triglycerides (TG), low-density and high-density lipoprotein cholesterol (LDL, HDL). Jinan Xinrun Medical Equipment Co., Ltd, provided the instruments and supporting reagent kits. The ELISA method was used to detect serum neuregulin1 (NRGl) and Klotho protein. The kit was purchased from Tinglai Biological Company with item number J19117 and validated by at least two intermediate-level pathologists. If there was any objection, the result was reviewed and confirmed by a physician with a senior professional title or above to ensure the reliability of the results.

Cognitive function: Evaluated with the MMSE test (Mini-Mental State Examination)[22], with 1 point for correct answers and 0 point for incorrect answers. The score is proportional to cognitive function. Scores higher than 26 indicate normal cognition. At least one day later, the MoCA test [23] was performed, which covers eight cognitive domains related to visual spatial execution ability, naming, memory, abstract thinking, etc. Scores above 25 indicate normal cognitive. The total score for both tables is 30 points.

Daily living ability: The AD Patient Activities of Daily Living Cooperative Study Scale (ADCS-ADL) was used to evaluate it[24]. The scale encompasses Basic Activities of Daily Living (BADL) and Instrumental Activities of Daily Living (IADL). The BADL section evaluates more basic activities such as dressing, eating, and toileting. The IADL section encompasses complex daily or social activities, such as visiting, working, and performing household chores, that require more cognitive function. The total score is 22 and 56 points. The lower the score, the lower the activity ability.

Amyloid and Tau biomarkers: venous blood was collected from all participants on an empty stomach and measured in real-time using an ELISA method according to diagnosis and treatment needs. The kit was purchased from Fujirebio Corporation in Japan and operated strictly according to the kit instructions.

Follow-up

After three months of drug treatment, a clinical efficacy evaluation was conducted on 150 patients [25], who were divided into three groups: significantly effective (with basic recovery of mental symptoms, complete orientation, MMSE and MoCA scores increased by≥4 points, and self-care ability); effective (with improvement of main mental symptoms, basic orientation, MMSE and MoCA scores increased by 1-3 points, slightly delayed response, and basic self-care ability); and ineffective (not meeting the above criteria). The significant and effective were included in the valid group, and the ineffective in the invalid group.

Outcome measures

Clinical data, cognitive function, and biomarker levels (amyloid and tau) were compared between AD patients and healthy individuals. The effectiveness of drug therapy compared the indicators of cognitive and self-care abilities between the effective and ineffective treatment groups. Factors influencing the effectiveness of drug therapy were evaluated by determining the values of serum Aβ1-42, T-tau, and P-Tau-181 levels in predicting the effectiveness of drug therapy in AD patients.

Statistical analysis

SPSS25.0 software package was used to analyze the data; the count data were expressed as an example (%), and the chi-square test was applied. Measurement data were presented as mean ± SD ($\bar{x}\pm s$), and a t-test was conducted. An ROC curve was constructed, and the corresponding AUC was computed to assess the effectiveness of drug therapy in AD patients. $p<0.05$ was considered statistically significant.

RESULTS

Baseline data

No statistical difference was observed in the baseline characteristics between the two groups ($p>0.05$, Table 1).

Cognitive function and biological indicators

The AD group exhibited decreased MMSE, MoCA, and Aβ1-42 levels, as well as increased T-tau and p-tau-181 levels, compared to the control group ($p<0.05$, Table 2).

Clinical efficacy

After three months of drug treatment, among the 150 AD patients, significant effective, effective and ineffective cases were 62, 45 and 43 cases, respectively, so 107 cas-

Table 1. Baseline comparison between Alzheimer's Disease patients and controls.

Group	*n*	Age (years)	Gender		BMI (kg/m²)	Years of Education (years)
			Male	Female		
Control group	50	66.30±6.08**	24 *(48.00)	*26 (52.00)	23.24±1.10**	9.04±2.99**
AD group	150	65.45±5.81**	*91 (60.67)	*59 (39.33)	23.53±1.76**	9.22±4.08**
t/χ2-value		-0.890	2.462		1.362	0.334
p-value		0.375	0.117		0.175	0.739

AD: Alzheimer's Disease; BMI: Body Mass Index. The data is presented as * n (%), or** mean ± SD

Table 2. Comparison of indicators between Alzheimer's Disease and control groups.

Group	*n*	MMSE	MoCA	Aβ1-40	Aβ1-42	T-tau	P-Tau-181
Control group	50	28.50±0.99	27.74±0.83	317.79±17.38	188.66±17.77	461.68±26.01	49.77±6.48
AD group	150	12.50±1.65	11.51±1.71	322.89±31.29	163.76±26.03	497.59±46.13	62.11±12.67
t-value		-82.144	-89.167	1.439	-7.567	6.746	8.929
p		<0.001	<0.001	0.152	<0.001	<0.001	<0.001

Abbreviations: AD: Alzheimer's Disease; MMSE: Mini-Mental State Examination; MoCA: Montreal Cognitive Assessment; Aβ1-40: Amyloid-beta 1-40; Aβ1-42: Amyloid-beta 1-42; T-tau: Total tau protein; P-Tau-181: Phosphorylated tau protein at threonine 181. Data Expression: The data is presented as mean ± standard deviation (SD).

Table 3. Comparison of MMSE, MoCA, BADL, IADL between valid and invalid groups.

Group	*n*	MMSE		MoCA	
		Before treatment	After treatment	Before treatment	After treatment
Valid group	107	12.44±1.67	20.33±5.20*	11.59±1.79	19.26±4.81*
Invalid group	43	12.65±1.60	12.21±2.65	11.33±1.49	11.05±2.47
t-value		-0.710	12.580	0.854	13.735
p		0.471	<0.001	0.395	<0.001

Group	*n*	BADL		IADL	
		Before treatment	After treatment	Before treatment	After treatment
Valid group	107	8.32±1.47	16.43±3.06*	18.71±1.41	29.56±5.56*
Invalid group	43	8.16±1.79	9.28±1.32*	19.02±1.54	21.35±2.40*
t-value		0.505	19.996	-1.200	12.625
p value		0.616	<0.001	0.232	<0.001

Compared with before the treatment, *p<0.05.

Abbreviations: AD: Alzheimer's Disease; MMSE: Mini-Mental State Examination; MoCA: Montreal Cognitive Assessment; BADL: Basic Activities of Daily Living; IADL: Instrumental Activities of Daily Living. Data Expression: The data is presented as mean ± standard deviation (SD).

es were included in the valid group, accounting for 71.33%. There were 43 cases in the invalid group, accounting for 28.67%.

Cognitive function and self-care ability

The MMSE, MoCA, BADL, and IADL scores of the valid group were higher than those of the invalid group ($p<0.05$, Table 3).

Univariate analysis of factors affecting the effectiveness of drug therapy in AD

Compared with the invalid group, the valid group had longer years of education, engaged in daily exercise, had higher levels of Aβ1-42, and lower levels of T-tau and P-Tau-181 ($p<0.05$, Table 4).

Logistic regression analysis of factors influencing the effectiveness of AD drug therapy

Analyzing the statistically significant factors in univariate analysis, with the effectiveness of AD drug treatment as the dependent variable (effectiveness=0, ineffectiveness=1), education years (actual value), daily exercise (yes=1, no=0), Aβ1-42 (actual value), T-tau (actual value), P-Tau-181 (actual value) as independent variables, binary logistic regression analysis was conducted. The results showed that education years, daily exercise, Aβ1-42, T-tau, and P-Tau-181 were all factors affecting the effectiveness of AD drug treatment ($p<0.05$, Table 5).

The predictive value of Aβ1-42, T-tau, P-Tau-181 in AD drug therapy

The AUC values for predicting the efficacy of AD drug treatment using serum Aβ1-42, T-tau, and P-Tau-181 levels were 0.869, 0.815, and 0.800, respectively, with cut-off values of 154.67 (ng/L), 517.95 (ng/L), and 63.66 (ng/L). The sensitivities were 76.74%, 69.77%, and 72.09%, respectively, and the specificities were 83.18%, 81.31%, and 71.03%. The AUC of the joint prediction of the three factors is 0.954, with a cut-off value of 0.292, a sensitivity of 90.70%, and a specificity of 93.46%, See Fig. 2 and Table 6.

Table 4. Univariate analysis of factors affecting the effectiveness of drug therapy in Alzheimer's disease patients.

Factors	n	Valid group (n=107)	Invalid group (n=43)	t/χ^2-value	*p*
Age (years)		65.30±5.97	65.81±5.43	-0.490	0.625
Gender					
Male	91	68 (63.55)	23 (53.49)		
Female	59	39 (66.45)	20 (46.51)		
Duration of disease (years)		3.14±0.44	3.23±0.57	-0.952	0.345
BMI (kg/m^2)		23.51±1.76	23.59±1.78	-0.247	0.805
Systolic pressure (mmHg)		130.04±16.01	128.81±12.28	0.450	0.653
Diastolic pressure (mmHg)		79.21±8.08	79.51±10.48	-0.167	0.868
Years of Education (years)		10.93±3.82	4.95±2.42	12.298	<0.001
Drinking					
Yes	109	80 (74.77)	29 (67.44)	2.511	0.113
No	41	27 (25.23)	14 (32.56)		
Family history					
Yes	15	10 (9.35)	5 (11.63)	0.177	0.674
No	135	97 (90.65)	38 (88.37)		
Diabetes					
Yes	34	21 (19.63)	13 (30.23)	1.969	0.161
No	116	86 (80.37)	30 (69.77)		
Hyperlipidemia					
Yes	50	32 (29.91)	18 (41.86)	1.972	0.160
No	100	75 (70.09)	25 (58.14)		
Marital status					
Married	117	87 (81.31)	30 (69.77)	2.381	0.123
Other	33	20 (18.69)	13 (30.23)		
Daily exercise					
Yes	100	85 (79.44)	15 (34.88)	27.402	<0.001
No	50	22 (20.56)	28 (65.12)		
Blood calcium (mmol/L)		2.28±0.17	2.32±0.14	-1.499	0.136
Fasting blood glucose (mmol/L)		4.95±1.01	4.98±0.79	-0.144	0.886
Hcy (μmol/L)		17.72±3.11	17.96±2.90	-0.436	0.664
Cr (μmol/L)		57.66±6.31	57.73±4.60	-0.073	0.942
BUN (mmol/L)		5.38±1.28	5.28±0.89	0.551	0.582
TC (mmol/L)		4.92±1.04	4.97±0.69	-0.382	0.703
TG (mmol/L)		1.28±0.18	1.30±0.20	-0.557	0.579

Table 4. CONTINUATION

Factors	n	Valid group (n=107)	Invalid group (n=43)	t/χ^2-value	*p*
LDL (mmol/L)		2.75±0.32	2.76±0.39	-0.289	0.773
HDL (mmol/L)		1.26±0.14	1.27±0.10	-0.352	0.726
NRGl (ng/L)		340.62±27.22	332.20±30.48	1.665	0.100
Aβ1-40 (ng/L)		321.83±29.51	325.53±35.56	-0.653	0.515
Aβ1-42 (ng/L)		173.90±24.76	138.50±24.76	8.464	<0.001
T-tau (ng/L)		483.43±41.57	532.83±37.49	12.298	<0.001
P-Tau-181 (ng/L)		57.97±9.96	72.41±12.91	-6.590	<0.001

Abbreviations: BMI: Body Mass Index; Hcy: Homocysteine; Cr: Creatinine; BUN: Blood Urea Nitrogen; TC: Total Cholesterol; TG: Triglycerides; LDL: Low-Density Lipoprotein; HDL: High-Density Lipoprotein; NRGl: Neurogranin; Aβ1-40: Amyloid-beta 1-40; Aβ1-42: Amyloid-beta 1-42; T-tau: Total tau protein; P-Tau-181: Phosphorylated tau protein at threonine 181. Data Expression: The data is presented as mean ± standard deviation (SD) or n(%).

Table 5. Logistic regression analysis of factors influencing the efficacy of drug treatment in Alzheimer's disease patients.

Factors	B	SE	Wald/χ2	p	OR	95%CI
Years of Education	-0.487	0.146	11.125	0.001	0.614	0.461-0.818
Daily exercise	-2.148	0.939	5.235	0.022	0.117	0.019-0.735
Aβ1-42	-0.065	0.022	8.400	0.004	0.937	0.897-0.979
T-tau	0.032	0.012	7.841	0.005	1.033	1.010-1.056
P-Tau-181	0.107	0.039	7.691	0.006	1.113	1.032-1.200

Abbreviations: AD: Alzheimer's Disease; B: Regression Coefficient; SE: Standard Error; OR: Odds Ratio; 95% CI: 95% Confidence Interval; Aβ1-42: Amyloid-beta 1-42; T-tau: Total Tau Protein; P-Tau-181: Phosphorylated Tau Protein at Threonine 181.

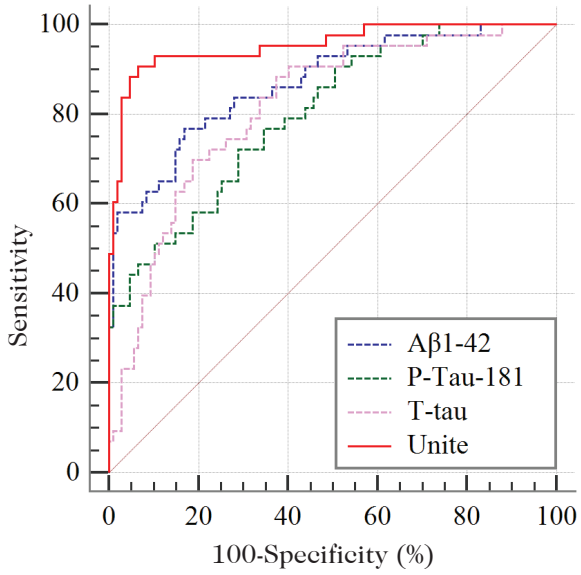

Fig. 2. ROC curves for predicting the therapeutic effect of AD drugs using Aβ1-42, T-tau, P-Tau-181.

Table 6. Diagnostic Value of A β1-42, T-tau, P-Tau-181 in the Efficacy of Alzheimer's disease drug therapy.

Indicators	AUC	p	Best Cut-off Value	Sensitivity (%)	Specificity (%)	95% CI
Aβ1-42	0.869	<0.001	154.67	76.74	83.18	0.805-0.919
T-tau	0.815	<0.001	517.95	69.77	81.31	0.743-0.874
P-tau-181	0.800	<0.001	63.66	72.09	71.03	0.727-0.861
Unite	0.954	<0.001	0.292	90.70	93.46	0.908-0.982

Abbreviations: AUC: Area Under the Curve; 95% CI: 95% Confidence Interval; Aβ1-42: Amyloid-beta 1-42; T-tau: Total Tau Protein; P-Tau-181: Phosphorylated Tau Protein at Threonine 181.

DISCUSSION

AD is a global public health and social care issue, with 10 million AD patients in China [26], and the patient population is becoming younger. Early prevention and treatment, as well as improving the effectiveness and safety of drug therapy, are important means to delay disease progression and enhance quality of life. Aβ1-42 is a protein fragment produced by enzymatic hydrolysis of APP, which can be used as an effective indicator of cognitive function [27]. Tau protein can stabilize microtubules in nerve cells and is closely associated with cognitive impairment[28]. Relevant studies have shown [29, 30], that the Aβ1-42, T-tau and P-tau-181 proteins can be used to evaluate the occurrence of cognitive impairment in AD patients. Compared with healthy individuals, serum Aβ1-42 levels are decreased, and T-tau and P-Tau-181 levels are increased in AD patients, which is consistent with the results of this study. This suggests that the changes in the above proteins can serve as potential biomarkers for predicting AD patients. However, there is currently no report on whether they can evaluate the effectiveness of drug therapy in AD patients.

This study demonstrated effective clinical efficacy in 107 of 150 AD patients (71.33%) after three months of drug treatment, while in 43 cases, it was ineffective, accounting for 28.67%. The MMSE, MoCA, BADL, and IADL scores of the valid group were higher than those of the invalid group. This suggests that donepezil hydrochloride and memantine tablets can enhance the efficacy, cognitive function, and self-care abilities of most patients. It is speculated that donepezil hydrochloride is an acetylcholinesterase inhibitor, which increases the concentration of acetylcholine by inhibiting its activity and reducing its breakdown, thereby improving patients' cognitive function and neurotransmission function [31]. Moreover, this process is reversible and can help stabilize the level of acetylcholine in the body[32]. Meijingang tablets are a non-competitive NMDA antagonist that can reduce neurotoxicity by blocking excessive glutamate activation of NMDA receptors, thereby protecting neurons and enhancing cognitive function[33]. The combination of the two can exert a synergistic effect, further improving the clinical efficacy, cognitive function, and self-care ability of AD patients. However, there are still a few patients with unsatisfactory treatment outcomes. Therefore, we need to explore further the factors that affect the effectiveness of drug therapy, such as education level, physical activity, and severity of the disease, so that the medical staff can adjust the dosage and type of drugs according to the patient's condition on time, in order to improve the efficacy of drug treatment.

Logistic regression analysis showed that education years, daily exercise, Aβ1-42, T-tau, and P-Tau-181 are influencing factors on the effectiveness of AD drug treatment. It is speculated that this may be because the length of education is closely related to the cognitive reserve of the brain, which is the

brain's ability to maintain cognitive abilities by activating and utilizing previously experienced neural networks, and serves as a resource for processing information and solving problems [34]. Patients with longer educational years are tipically able to accumulate more knowledge and problem-solving skills, have higher cognitive reserves, maintain higher treatment compliance when facing treatment, better understand the importance of medication treatment, and take medication according to medical orders, thereby improving treatment effectiveness[35]. Furthermore, patients with higher education are more likely to seek ways to obtain support from their families and society [36], and to receive more help and encouragement during the treatment process. Patients with lower education may have poorer cognitive function and self-care abilities, lack understanding of the disease, have greater disease uncertainty, and thus lack attention and cooperation in treatment, which affects treatment efficacy [37]. Daily exercise is considered an important non-pharmacological intervention that can improve brain health, enhance neuroplasticity, promote blood circulation, increase oxygen supply to the brain [38], enhance muscle strength, and improve cardiovascular function. It helps dementia patients maintain good physical fitness, reduce functional decline caused by physical reasons, and improve functional outcomes. Exercise also promotes the recovery of the endocrine and immune system function [39], and helps reduce AD-related pathological processes such as inflammation and oxidative stress, improving clinical outcomes. Studies have shown that for AD patients receiving medication treatment, regular physical exercise can not only alleviate potential side effects such as fatigue and depression caused by medication, but also improve patients' compliance with treatment. For example, dance, as a physical and mental exercise method, emphasizes calmness and relaxation during movement, and requires concentration to achieve a harmonious unity of consciousness and movement, thereby achieving the effects of physical and mental balance and spiritual relaxation [40]. In addition, exercise can enhance dopamine binding ability in the brain, delay neurodegenerative changes, delay memory decline symptoms, and regulate the secretion of neurotransmitters such as norepinephrine. This can promote memory recovery and enhance sensory input, reaction speed, and other cognitive functions, thereby achieving cognitive improvement [41]. In addition, exercise can reduce NLRP3 inflammation and improve the redox balance, which together slow the progression of AD[42]. Therefore, higher education levels and daily exercise are factors that affect the effectiveness of AD drug treatment.

Aβ deposition is one of the pathological changes in AD, which can easily cause neurotoxicity, inflammatory reactions, etc., leading to neuronal dysfunction, death, and other phenomena [43]. Moreover, Aβ1-42 is a protein fragment produced by enzymatic hydrolysis of APP, the abnormal processing of APP in AD patients reduces the production of soluble Aβ1-42, leading to neuroinflammation and neuronal damage, including interference with nerve signal transmission, triggering inflammatory reactions, damaging the stability of neurons and synaptic connections, ultimately resulting in pathological changes and degenerative damage to the nervous system, causing cognitive impairment and other symptoms [44]. The reduction of Aβ1-42 may also affect the pathological state of other key molecules, such as the Tau protein, further accelerating disease progression. In addition, the reduction of Aβ1-42 also inhibits the activity of gamma-secretase, thereby reducing the clearance of Aβ deposition and forming a vicious cycle[45]. Under normal circumstances, tau protein maintains the stability and function of neuronal microtubules [46]. However, in AD, the T-tau protein undergoes excessive phosphorylation, transforming it from a microtubule-binding protein to the primary component of neurofibrillary tangles,

which in turn causes neuronal degeneration and cognitive dysfunction. P-Tau-181, a phosphorylated T-tau form, exhibits neurotoxicity, promoting neuronal death and dysfunction, thus impacting AD progression [47]. Therefore, low serum Aβ1-42 levels and high levels of T-tau and P-Tau-181 in patients can affect the effectiveness of drug treatment. Consequently, we speculate that the effectiveness of drug therapy can be evaluated by monitoring changes in the levels of the three factors. This study confirmed through ROC curve analysis that the level changes of the three have a good assessment value, and the value of joint analysis of the three is higher. The reason may be that they each play unique and complementary roles in the pathogenesis of AD patients, and together affect cognitive function and drug efficacy. Combined detection provides a more comprehensive reflection of the effectiveness of drug treatment in patients, thereby improving their predictive value.

Although this study analyzed clinical data from AD patients and explored early predictors of the effectiveness of drug therapy, it has some limitations. This study is a retrospective analysis with a small sample size and a relatively short follow-up period of only three months. While this duration was sufficient to observe initial treatment responses, it is important to note that AD is a chronic and progressive condition. A more extended follow-up period would be essential to fully capture the dynamic changes in β-amyloid and tau protein levels, as well as to better understand the long-term effectiveness and potential side effects of the drug therapy. Future research should focus on prospective studies with larger sample sizes and extended treatment cycles to improve the reliability and applicability of the results.

Additionally, the potential heterogeneity of the patient sample is another limitation. This study did not stratify patients based on the stage of disease progression, which could influence the observed treatment responses and biomarker levels. Patients with AD at different stages may exhibit varying degrees of cognitive impairment, biomarker profiles, and treatment efficacy. Therefore, it is crucial to consider the disease stage when interpreting the results and to conduct stratified analyses in future studies to account for this variability. In the future, a comprehensive evaluation should be conducted based on the influence of multiple biomarkers and pathological mechanisms. Moreover, a detailed assessment considering factors such as clinical manifestations, genetic background, and disease severity of patients should be performed to meet the treatment needs of AD patients and to develop more personalized therapeutic strategies.

In conclusion, donepezil hydrochloride combined with memantine tablets can improve the clinical efficacy, function and self-care ability of most patients with AD. However, the efficacy of treatment is not ideal for some patients. Several factors influence the effectiveness of Alzheimer's disease (AD) drug therapy, including years of education, daily exercise, and biomarkers such as Aβ1-42, T-tau, and P-Tau-181. In clinical practice, the effectiveness of AD drug treatment can be assessed by monitoring changes in the levels of these three factors. Additionally, a combined evaluation of all three factors provides a more comprehensive assessment of treatment outcomes.

Acknowledgment

None.

Funding

To explore the mechanism of the NLRP3caspase-1GSDMD pathway mediated by miR-146a-5p to regulate the progression of Alzheimer's disease based on the inflammatory microenvironment (No. 2023A14029).

Study on the mechanism of regulating microglia mitochondria autophagy of

Ginseng Yangrong Decoction to improve cognitive ability of Alzheimer's disease (No. 2024ZL1138).

Conflicts of interest

The authors declare that they have no financial conflicts of interest.

Consent to publish

The manuscript has neither been previously published nor is it under consideration by any other journal. The authors have all approved the content of the paper.

Consent to participate

We secured a signed informed consent form from every participant.

Ethic approval

This experiment was approved by the Shaoxing Seventh People's Hospital Ethics Committee.

ORCID number of authors

- Jiao Sun (JS): 0009-0006-4570-0221
- Yingchun Ling (YL): 0009-0003-7630-3753
- Jie Chen (JC): 0009-0009-0661-9449
- Mingyong Zhao (MZ): 0009-0008-8142-2235

Author participation

JS: Developed and planned the study, performed experiments, and interpreted results. Edited and refined the manuscript with a focus on critical intellectual contributions. YL, JC: Participated in collecting, assessing, and interpreting the data. Made significant contributions to date interpretation and manuscript preparation. MZ: Provided substantial intellectual input during the drafting and revision of the manuscript.

REFERENCES

1. **Lopez-Lee C, Torres ERS, Carling G, Gan L**. Mechanisms of sex differences in Alzheimer's disease. Neuron. 2024;112(8):1208-1221. *https://doi.org/10.1016/j.neuron.2024.01.024.*
2. **Gustavsson A, Norton N, Fast T, Frölich L, Georges J, Holzapfel D, et al**. Global estimates on the number of persons across the Alzheimer's disease continuum. Alzheimers Dement. 2023;19(2):658-670. *https://doi.org/10.1002/alz.12694.*
3. **2023 Alzheimer's disease facts and figures. Alzheimers Dement.** 2023;19(4):1598-1695. *https://doi.org/10.1002/alz.13016.*
4. **Jucker M, Walker LC**. Alzheimer's disease: From immunotherapy to immunoprevention. Cell. 2023;186(20):4260-4270. *https://doi.org/10.1016/j.cell.2023.08.021.*
5. **Reuben DB, Kremen S, Maust DT**. Dementia Prevention and Treatment: A Narrative Review. JAMA Intern Med. 2024;184(5):563-572. *https://doi.org/10.1001/jamainternmed.2023.8522.*
6. **Rostagno AA**. Pathogenesis of Alzheimer's Disease. Int J Mol Sci. 2022;24(1):107. *https://doi.org/10.3390/ijms24010107.*
7. **Ashrafizadeh M.** Cell Death Mechanisms in Human Cancers: Molecular Pathways, Therapy Resistance and Therapeutic Perspective. JCBT. 2024;1(1):17-40. *http://dx.doi.org/10.62382/jcbt.v1i1.13*
8. **Majidazar R, Rezazadeh-Gavgani E, Sadigh-Eteghad S, Naseri A.** Pharmacotherapy of Alzheimer's disease: an overview of systematic reviews. Eur J Clin Pharmacol. 2022;78(10):1567-1587. *https://doi.org/10.1007/s00228-022-03363-6.*
9. **Jun R**. Advances in Combination Therapy for Gastric Cancer: Integrating Targeted Agents and Immunotherapy. ACPT. 2024;1(1):1-15. *https://doi.org/10.63623/9k14tf70*
10. **Söderberg L, Johannesson M, Nygren P, Laudon H, Eriksson F, Osswald G, et al.** Lecanemab, Aducanumab, and Gantenerumab - Binding Profiles to Different Forms of Amyloid-Beta Might Explain Ef-

ficacy and Side Effects in Clinical Trials for Alzheimer's Disease. Neurotherapeutics. 2023;20(1):195-206. *https://doi.org/10.1007/s13311-022-01308-6.*

11. **Zhang J, Zhang Y, Wang J, Xia Y, Zhang J, Chen L**. Recent advances in Alzheimer's disease: Mechanisms, clinical trials and new drug development strategies. Sig Transduct Target Ther. 2024;9(1):211. *https://doi.org/10.1038/s41392-024-019 11-3.*
12. **Jin J, Xu Z, Zhang L, Zhang C, Zhao X, Mao Y, et al.** Gut-derived β-amyloid: Likely a centerpiece of the gut-brain axis contributing to Alzheimer's pathogenesis. Gut microbes. 2023;15(1):2167172. *https://doi.org/10.1080/19490976.2023.2167172.*
13. **Hur JY**. γ-Secretase in Alzheimer's disease. Exp Mol Med. 2022;54(4):433-446. *https://doi.org/10.1038/s12276-022-007 54-8.*
14. **Chatterjee P, Pedrini S, Doecke JD, Thota R, Villemagne VL, Doré V, et al.** Plasma Aβ42/40 ratio, p-tau181, GFAP, and NfL across the Alzheimer's disease continuum: A cross-sectional and longitudinal study in the AIBL cohort. Alzheimers Dement. 2023;19(4):1117-1134. *https://doi.org/10.1002/alz.12724.*
15. **Zeng XX, Zeng JB**. Systems Medicine as a Strategy to Deal with Alzheimer's Disease. J Alzheimers Dis. 2023;96(4):1411-1426. *https://doi.org/10.3233/JAD-230739.*
16. **Perneczky R, Dom G, Chan A, Falkai P, Bassetti C.** Anti-amyloid antibody treatments for Alzheimer's disease. Eur J Neurol. 2024;31(2):e16049. *https://doi.org/10.1111/ene.16049.*
17. **Young-Pearse TL, Lee H, Hsieh YC, Chou V, Selkoe DJ**. Moving beyond amyloid and tau to capture the biological heterogeneity of Alzheimer's disease. Trends Neurosci. 2023;46(6):426-444. *https://doi.org/10.1016/j.tins.2023.03.005.*
18. **Ossenkoppele R, van der Kant R, Hansson O.** Tau biomarkers in Alzheimer's disease: towards implementation in clinical practice and trials. Lancet Neurol. 2022;21(8):726-734. *https://doi.org/10.1016/S1474-4422(22)00168-5.*
19. **Brickman AM, Manly JJ, Honig LS, Sanchez D, Reyes-Dumeyer D, Lantigua RA, et al.** Plasma p-tau181, p-tau217, and other blood-based Alzheimer's disease biomarkers in a multi-ethnic, community study. Alzheimers Dement. 2021;17(8):1353-1364. *https://doi.org/10.1002/alz.12301.*
20. **Dubois B, von Arnim CAF, Burnie N, Bozeat S, Cummings J.** Biomarkers in Alzheimer's disease: role in early and differential diagnosis and recognition of atypical variants. Alzheimers Res Ther. 2023;15(1):175. *https://doi.org/10.1186/s13195-023-01314-6.*
21. **Brooker D, La Fontaine J, Evans S, Bray J, Saad K**. Public health guidance to facilitate timely diagnosis of dementia: ALzheimer's COoperative Valuation in Europe recommendations. Int J Geriatr Psychiatry. 2014;29(7):682-693. *https://doi.org/10.1002/gps.4066.*
22. **Engedal K, Benth J, Gjøra L, Skjellegrind HK, Nåvik M, Selbæk G.** Normative Scores on the Norwegian Version of the Mini-Mental State Examination. J Alzheimers Dis. 2023;92(3):831-842. *https://doi.org/10.3233/JAD-221068.*
23. **Lima Pereira V, Freitas S, Simões MR, Gerardo B**. Montreal Cognitive Assessment (MoCA): A validation study among prisoners. Crim Behav Ment Health. 2023;33(5):330-341. *https://doi.org/10.1002/cbm.2306.*
24. **Monteiro C, Toth B, Brunstein F, Bobbala A, Datta S, Ceniceros R, et al.** Randomized Phase II Study of the Safety and Efficacy of Semorinemab in Participants with Mild-to-Moderate Alzheimer Disease: Lauriet. Neurology. 2023;101(14):e1391-e1401. *https://doi.org/10.1212/WNL.000000000 0207663.*
25. **Lacorte E, Ancidoni A, Zaccaria V, Remoli G, Tariciotti L, Bellomo G, et al.** Safety and Efficacy of Monoclonal Antibodies for Alzheimer's Disease: A Systematic Review and Meta-Analysis of Published and Unpublished Clinical Trials. J Alzheimers Dis. 2022;87(1):101-129. *https://doi.org/10.3233/JAD-220046.*
26. **Zhang YT, Chen Y, Shang KX, Yu H, Li XF, Yu H.** Effect of Volatile Anesthesia Versus Intravenous Anesthesia on Postoperative Pulmonary Complications in Patients Un-

dergoing Minimally Invasive Esophagectomy: A Randomized Clinical Trial. Anesth Analg. 2024;139(3):571-580. *https://doi.org/10.1213/ANE.0000000000006814.*

27. **Zhu M, Xiao B, Xue T, Qin S, Ding J, Wu Y, et al.** Cdc42GAP deficiency contributes to the Alzheimer's disease phenotype. Brain. 2023;146(10):4350-4365. *https://doi.org/10.1093/brain/awad184.*
28. **Kashif M, Sivaprakasam P, Vijendra P, Waseem M, Pandurangan AK.** A Recent Update on Pathophysiology and Therapeutic Interventions of Alzheimer's Disease. Curr Pharm Des. 2023;29(43):3428-3441. *https://doi.org/10.2174/0113816128264355231121064704.*
29. **Giacomucci G, Mazzeo S, Crucitti C, Ingannato A, Bagnoli S, Padiglioni S, et al.** Plasma p-tau181 as a promising non-invasive biomarker of Alzheimer's Disease pathology in Subjective Cognitive Decline and Mild Cognitive Impairment. J Neurol Sci. 2023;453:120805. *https://doi.org/10.1016/j.jns.2023.120805.*
30. **Yang W, Guan F, Yang L, Shou G, Zhu F, Xu Y, et al.** Highly sensitive blood-based biomarkers detection of beta-amyloid and phosphorylated-tau181 for Alzheimer's disease. Front Neurol. 2024;15:1445479. *https://doi.org/10.3389/fneur.2024.1445479.*
31. **Guo J, Wang Z, Liu R, Huang Y, Zhang N, Zhang R.** Memantine, Donepezil, or Combination Therapy-What is the best therapy for Alzheimer's Disease? A Network Meta-Analysis. Brain Behav. 2020;10(11):e01831. *https://doi.org/10.1002/brb3.1831.*
32. **Buck A, Rezaei K, Quazi A, Goldmeier G, Silverglate B, Grossberg GT.** The donepezil transdermal system for the treatment of patients with mild, moderate, or severe Alzheimer's disease: a critical review. Expert Rev Neurother. 2024;24(6):607-614. *https://doi.org/10.1080/14737175.2024.2355981.*
33. **Zohny SM, Habib MZ, Mohamad MI, Elayat WM, Elhossiny RM, El-Salam MFA, et al.** Memantine/Aripiprazole Combination Alleviates Cognitive Dysfunction in Valproic Acid Rat Model of Autism: Hippocampal CREB/BDNF Signaling and Glutamate Homeostasis. Neurotherapeutics. 2023;20(2):464-483. *https://doi.org/10.1007/s13311-023-01360-w.*
34. **Savarimuthu A, Ponniah RJ.** Cognition and Cognitive Reserve. Integr Psychol Behav Sci. 2024;58(2):483-501. *https://doi.org/10.1007/s12124-024-09821-3.*
35. **Umarova RM, Schumacher LV, Schmidt CSM, Martin M, Egger K, Urbach H, et al.** Interaction between cognitive reserve and age moderates effect of lesion load on stroke outcome. Sci Rep. 2021;11(1):4478. *https://doi.org/10.1038/s41598-021-83927-1.*
36. **Hassan M, Fang S, Malik AA, Lak TA, Rizwan M.** Impact of perceived social support and psychological capital on university students' academic success: testing the role of academic adjustment as a moderator. BMC Psychol. 2023;11(1):340. *https://doi.org/10.1186/s40359-023-01385-y.*
37. **Rosselli M, Uribe IV, Ahne E, Shihadeh L.** Culture, Ethnicity, and Level of Education in Alzheimer's Disease. Neurotherapeutics. 2022;19(1):26-54. *https://doi.org/10.1007/s13311-022-01193-z.*
38. **Iso-Markku P, Kujala UM, Knittle K, Polet J, Vuoksimaa E, Waller K**. Physical activity as a protective factor for dementia and Alzheimer's disease: systematic review, meta-analysis and quality assessment of cohort and case-control studies. Br J Sports Med. 2022;56(12):701-709. *https://doi.org/10.1136/bjsports-2021-104981.*
39. **López-Ortiz S, Lista S, Valenzuela PL, Pinto-Fraga J, Carmona R, Caraci F, et al.** Effects of physical activity and exercise interventions on Alzheimer's disease: an umbrella review of existing meta-analyses. J Neurol. 2023;270(2):711-725. *https://doi.org/10.1007/s00415-022-11454-8.*
40. **Fong Yan A, Nicholson LL, Ward RE, Hiller CE, Dovey K, Parker HM, et al.** The Effectiveness of Dance Interventions on Psychological and Cognitive Health Outcomes Compared with Other Forms of Physical Activity: A Systematic Review with Meta-analysis. Sports Med. 2024;54(5):1179-1205. *https://doi.org/10.1007/s40279-02 3-01990-2.*
41. **The 2023 nonhormone therapy position statement of The North Ameri-**

can Menopause Society. Menopause. 2023;30(6):573-590. *https://doi.org/10.1097/GME.0000000000002200.*

42. **Li X, Jin Y, Ding X, Zhu T, Wei C, Yao L.** Long-term exercise training inhibits inflammation by suppressing hippocampal NLRP3 in APP/PS1 mice. Sports Med Health Sci. 2023;5(4):329-335. *https://doi.org/10.1016/j.smhs.2023.09.009.*
43. **da Rosa MM, de Aguiar Ferreira M, de Oliveira Lima CA, Santos Mendonça AC, Silva YM, Sharjeel M, et al.** Alzheimer's disease: Is there a role for galectins? Eur J Pharmacol. 2021;909:174437. *https://doi.org/10.1016/j.ejphar.2021.174437.*
44. **Wu W, Ji Y, Wang Z, Wu X, Li J, Gu F, et al.** The FDA-approved anti-amyloid-β monoclonal antibodies for the treatment of Alzheimer's disease: a systematic review and meta-analysis of randomized controlled trials. Eur J Med Res. 2023;28(1):544. *https://doi.org/10.1186/s40001-023-01512-w.*
45. **Xiao L, Yang X, Sharma VK, Abebe D, Loh YP.** Hippocampal delivery of neurotrophic factor-α1/carboxypeptidase E gene prevents neurodegeneration, amyloidosis, memory loss in Alzheimer's Disease male mice. Mol Psychiatry. 2023;28(8):3332-3342. *https://doi.org/10.1038/s41380-023-02135-7.*
46. **Scheltens P, De Strooper B, Kivipelto M, Holstege H, Chételat G, Teunissen CE, et al.** Alzheimer's disease. Lancet. 2021;397(10284):1577-1590. *https://doi.org/10.1016/S0140-6736(20)32205-4.*
47. **Cai H, Pang Y, Fu X, Ren Z, Jia L.** Plasma biomarkers predict Alzheimer's disease before clinical onset in Chinese cohorts. Nat Commun. 2023;14(1):6747. *https://doi.org/10.1038/s41467-023-42596-6.*

Invest Clin 66(4): 365 - 377, 2025 https://doi.org/10.54817/IC.v66n4a02

CircRNA_104293 targets miR-497-5p to inhibit the mTOR/STAT3 pathway and mitigate inflammation in Crohn's disease.

Xuerui Yin, Gaigai Huang, Chuan Zheng, Yu Zhou and Rong Chen

Department of Medical Laboratory, The First People's Hospital of Shuangliu District/ West China (Airport) Hospital Sichuan University, Chengdu, China.

Keywords: Crohn Disease; mTOR/STAT3; Inflammation; circRNA_104293; miR-497-5p.

Abstract. Crohn's disease (CD) is a chronic inflammatory bowel disease driven in part by dysregulation of the mTOR/STAT3 signaling pathway, where mTOR activates STAT3 via the PI3K/AKT cascade. Circular RNAs (circRNAs) have recently emerged as essential regulators in inflammatory processes, although their specific roles in CD remain largely unexplored. In this study, circRNA expression profiles from CD patients and healthy controls were analyzed, revealing a significant upregulation of circRNA_104293 in CD tissues. Functional investigations demonstrated that knockdown of circRNA_104293 reduced inflammatory cytokine production and DNA damage markers, and decreased cell apoptosis. Bioinformatic analysis and experimental validation confirmed a direct interaction between circRNA_104293 and miR-497-5p. Furthermore, miR-497-5p inhibition reversed the anti-inflammatory effects of circRNA_104293 silencing. Notably, both rapamycin (an mTOR inhibitor) and miR-497-5p mimics suppressed the mTOR/STAT3 pathway and alleviated inflammatory responses. These findings suggest that the circRNA_104293/miR-497-5p axis contributes to CD progression by modulating the mTOR/STAT3 pathway, highlighting its potential as a novel therapeutic target for the treatment of Crohn's disease.

Corresponding author. Rong Chen. Department of Medical Laboratory, The First People's Hospital of Shuangliu District/West China (Airport) Hospital Sichuan University, No. 120, Chengbei Upper Street, Dongsheng Street, Shuangliu District, Chengdu, 610200,China. Tel: +86 13736798579. Email: chenrong202431@126.com

CircRNA_104293 actúa sobre el miR-497-5p para inhibir la vía mTOR/STAT3 y mitigar la inflamación en la enfermedad de Crohn.

Invest Clin 2025; 66 (4): 365 – 377

Palabras clave: Enfermedad de Crohn; mTOR/STAT3; Inflamación; circRNA_104293; miR-497-5p.

Resumen. La enfermedad de Crohn (CD) es una enfermedad inflamatoria crónica del intestino cuya progresión está parcialmente mediada por la disfunción de la vía de señalización mTOR/STAT3, en la que mTOR activa a STAT3 a través de la cascada PI3K/AKT. Recientemente, los ARN circulares (circRNAs) han surgido como reguladores clave en procesos inflamatorios, aunque sus funciones específicas en la CD aún no están bien definidas. En este estudio se analizaron los perfiles de expresión de circRNAs en pacientes con CD y en controles sanos, y se identificó una sobreexpresión significativa de circRNA_104293 en tejidos de pacientes con CD. Los análisis funcionales mostraron que la reducción de la expresión de circRNA_104293 disminuyó la producción de citocinas inflamatorias y de marcadores de daño al ADN, así como la apoptosis celular. Mediante análisis bioinformático y validación experimental, se confirmó una interacción directa entre circRNA_104293 y miR-497-5p. Además, la inhibición de miR-497-5p revirtió los efectos antiinflamatorios inducidos por el silenciamiento de circRNA_104293. De manera destacada, tanto la rapamicina (un inhibidor de mTOR) como los miméticos de miR-497-5p suprimieron la activación de la vía mTOR/STAT3 y redujeron las respuestas inflamatorias. Estos hallazgos indican que el eje circRNA_104293/miR-497-5p participa en la progresión de la CD mediante la modulación de la vía mTOR/STAT3, lo que resalta su potencial como nuevo objetivo terapéutico para el tratamiento de la enfermedad de Crohn.

Received: 19-06-2025 Accepted: 17-09-2025

INTRODUCTION

Crohn's Disease (CD) is characterized by chronic, repetitive inflammation of the gastrointestinal tract. Its etiology has not been fully clarified, but studies have shown that CD is closely associated with genetic, environmental, and immune factors, as well as changes in the gut microbiota[1]. Patients often present with abdominal pain, diarrhea, weight loss, fever, and other symptoms, which in severe cases can lead to complications such as intestinal obstruction and fistula formation [1, 2]. The mammalian target of rapamycin (mTOR) belongs to the phosphoinositide 3-kinase (PI3K)-related kinase family and is mainly involved in processes such as cell growth, proliferation, metabolism, and autophagy [3]. Signal transducer and activator of transcription 3 (STAT3) is a transcription factor that regulates cell survival, proliferation, and immune responses. In CD, aberrant activation of STAT3 is strongly associated with exacerbated inflammatory responses [4]. The mTOR/STAT3 pathway interacts in CD to co-regulate inflammatory

reactions. For example, mTOR activation has been found to promote STAT3 phosphorylation through the phosphoinositide 3-kinase/protein kinase B (PI3K/AKT) signaling pathway, thereby enhancing its transcriptional activity [5]. This interaction plays a key role in intestinal inflammation in Crohn's disease patients and may lead to its persistence and aggravation. But the specific molecular mechanism is unknown.

Circular RNAs (circRNAs) are molecules with unique circular structures that play an essential role in a variety of diseases [6, 7]. In neurological diseases, circRNA is widely expressed in brain tissue and is closely related to neurodevelopment and signaling, showing abnormal expression in diseases such as cerebral palsy and stroke, and is considered a potential biomarker of neurological diseases due to its stable structure [8,9]. In malignant tumors, some circRNAs can adsorb microRNAs (miRNAs) as "molecular sponges", thereby relieving miRNA inhibition of oncogenes and promoting tumor development [10]. In CD, circRNA 103765 is reported to regulate disease progression [11]. At present, the study of circRNA in CD still needs to be further expanded to fully understand its effects on CD. MicroRNAs (miRNAs) are also closely associated with the progression of various inflammatory diseases [12, 13]. miR-497 has been reported to influence the progression of associated inflammatory diseases by modulating lipopolysaccharide (LPS) -induced inflammation in vivo [14, 15]. Furthermore, miR-497 expression was significantly decreased following LPS treatment of RAW264.7 cells and in a mouse colitis model [16].

Here, we performed sequencing analysis of circRNA expression profiles from CD patients to explore potential therapeutic targets and their molecular mechanisms. Through screening, we found circRNAs that were up- and down-regulated in CD. Further, qPCR was used to detect the expression level of circRNA 104293 in CD patients, and its mechanism of action in CD development was studied in depth. The results of this study are expected to provide a new treatment option for patients with CD.

METHODS

Patients and genome sequencing analysis

Between June 2021 and March 2022, we collected the inflamed colonic tissue samples from CD patients who underwent surgical treatment at our institution. The tissues were obtained from inflamed areas of the colon, confirmed by intraoperative findings and postoperative histopathological examination, and non-inflamed adjacent tissues served as control. Tissue total RNA isolation kit (RC101-01, Vazyme, Nanjing, China) was used for the RNA extraction, and RNA integrity was assessed using an Agilent 2100 Bioanalyzer (Agilent Technologies, USA). High-throughput circRNA microarray analysis was conducted by Aksomics Biotechnology (Shanghai, China). Sample processing was carried out according to the manufacturer's protocol. Briefly, the Seq-Star™ rRNA removal kit (AS-MB-001, Aksomics) was employed for the rRNA removal, and the circRNA purification and fluorescent cRNA transcription were performed using Seq-Star™ RNAClean and smallEnrich Beads (AS-MB-009) and rtStar™ First-Strand cDNA Synthesis Kit (AS-FS-001) from Aksomics. Labeled cRNA concentration and specific activity were determined using a NanoDrop ND-1000 spectrophotometer (Thermo Fisher Scientific, USA). One microgram of labeled cRNA from each sample was fragmented, mixed with hybridization buffer, and loaded onto a Human circular RNA Array V2.0 (8 × 15K format, Aksomics). Hybridization was carried out at 65°C for 17 h in an Agilent Hybridization Oven (model G2545A). After hybridization, the microarrays were washed and fixed with Gene Expression Wash Buffers (Agilent Technologies, USA) and scanned with an Agilent DNA Microarray Scanner (model G2505C).

Differential expression analysis

Differential expression analysis was conducted using the DESeq2 R package. The fold change and statistical significance were calculated based on the log2|(fold change)|>1 and *p-adjust* <0.05.

Cells culture and treatment

In this study, Fetal Human Colon (FHC) cells (normal human colon epithelial cells) were purchased from the Cell Bank of Shanghai Institute of Life Sciences. Cells were cultured in RPMI 1640 medium containing 10% fetal bovine serum (FBS) and 1% penicillin-streptomycin-glutamine (PSG) and adapted for 2-3 days before use in experiments. To induce a general inflammatory response *in vitro*, FHC cells were treated with 500 ng/mL of lipopolysaccharide (LPS) and control cells were treated with serum-free medium. Treated cells were divided into two groups: small interfering RNA (si)-circRNA group and negative control group (siNC). Cells were transfected using Lipofectamine ™ 2000 following kit instructions and cells were collected 48 hours later for subsequent experiments. In addition, inhibitors of miR-497-5p and its negative control (NC) were transfected using Lipofectamine ™ 2000. The mTOR targeting inhibitor rapamycin (Bioengineering Co., A606203) was used for experiments and cells were co-incubated with 100 ng/mL rapamycin to investigate its effect.

Q-PCR assay

To determine the expression levels of miR-497-5p and circRNA 104293, we used qPCR. TRIZOL reagent (R0016, Beyotime, Shanghai, China) was used to extract total RNA and RNA was isolated through centrifugation. The RNA was then dissolved in RNase-free water. Then reverse transcription was performed to synthesize cDNA using BeyoRT™II First Strand cDNA Synthesis Kit (D7168S, Beyotime, Shanghai, China), which was subsequently used as the template for qPCR amplification following the instructions of the SYBR Green kit (D7260, Beyotime). The qPCR cycling conditions included initial denaturation at 95°C for 30s, followed by 39 cycles of 95°C for 5s, 60°C for 30s, and a final extension at 72°C for 5 seconds. The relative expression levels of circRNA_104293 were normalized to GAPDH as an internal control. Gene expression was calculated using the 2-ΔΔCt method.

ELISA assay

After transfection, the cells were washed three times with PBS. Subsequently, 0.5 ml of non-denaturing protein lysis buffer was added to each well and gently mixed to lyse the cells. The lysates were then incubated on ice for 20 minutes. The supernatants were immediately stored at -20°C. The tumor necrosis factor-alpha (TNF-α) ELISA Kit (PT518), interleukin-1 beta (IL-1β) ELISA Kit (PI305), IL-6 ELISA Kit (PI325) and IL-8 ELISA Kit (PI641) were purchased from the Beyotime biotechnology company (Shanghai, China). The levels of inflammatory cytokines in cell lysates were measured using ELISA assays according to the manufacturer's instructions.

Flow cytometry assay

A cell suspension of LPS-treated cells was prepared at a density of 5×10^5/mL and seeded into a 6-well plate. After 24 hours, the cells were transfected with si-circRNA 104293, or si-NC, followed by an additional 24-hour incubation. Post-transfection, the cells were harvested through digestion and centrifugation, then washed three times with ice-cold PBS. Apoptosis was assessed by staining the cells with 5 μL of Annexin V-FITC/PI. The apoptosis rate was subsequently quantified using flow cytometry. This protocol ensured consistent evaluation of cell viability under experimental conditions.

Dual-luciferase reporter gene assay

The TargetScan online tool was employed to predict potential miRNA binding sites on circRNA_104293, specifically identifying complementary sequences for

miR-497-5p. To validate this interaction, wild-type or mutant circRNA_104293 plasmids were constructed by GenePharma (Shanghai, China). The miR-497-5p mimic or negative control was co-transfected with either wild-type or mutant plasmids into FHC cells using Lipofectamine™ 2000 (Invitrogen, USA), with triplicate wells for each condition. After 24 h of post-transfection, the medium was discarded, and the cells were washed three times with PBS. Cell lysis was performed using 100 μL of lysis buffer (RG132S, Beyotime) at room temperature. Firefly and Renilla luciferase activities were measured sequentially using a Dual-Luciferase® Reporter Assay System (E1910, Promega, USA), including LARII reagent and Stop&Glo® reagent, according to the manufacturer's instructions. Luminescence was detected using a Glomax Multi+ Detection System (Promega, USA).

Immunofluorescence assay

Cells were cultured on sterile glass coverslips in 24-well plates and then treated with si-circRNA 104293 as the test and si-NC as the control. After treatment, the coverslips were washed three times with PBS and fixed with 37 g/L formaldehyde for 15 min. Permeabilization was performed using 0.5% Triton X-100 for 10 min, followed by blocking with 100 mL/L bovine serum albumin (BSA) for one h. Primary antibodies specific to dsDNA (ab27156, Abcam) and ssDNA (CBL407, Millipore) were applied at appropriate dilutions, and the samples were incubated overnight at 4°C. The coverslips were then washed three times with PBS and once with distilled water, then incubated with an FITC-conjugated secondary antibody (A-11001, Thermo Fisher Scientific) for one h at room temperature in the dark. Finally, the samples were mounted with glycerol and analyzed using fluorescence microscopy. Fluorescence intensity was quantified in ImageJ by measuring the mean fluorescence per cell and normalizing to control samples.

Western blot assay

Proteins were extracted from treated cells 48 h post-treatment using RIPA lysis buffer supplemented with protease and phosphatase inhibitors. The protein samples were quantified using a BCA protein assay kit (A65453, Thermo Fisher Scientific), and equal amounts of protein (30 μg/lane) were separated on an SDS-PAGE gel and subsequently transferred to a PVDF membrane. And then the membrane was blocked with 5% skim milk in TBST for one hour. After blocking, the membrane was incubated overnight at 4°C with primary antibodies targeting p-mTOR (ab109268, Abcam) and p-STAT3 (ab76315, Abcam). GAPDH (ab8245, Abcam) was used as the loading control. Following three washes with TBST, the sections were incubated with appropriate HRP-conjugated secondary antibodies (ab205719, Abcam). After additional TBST washes, the membrane was treated with a chemiluminiscent substrate (ab5801, Abcam), and protein bands were visualized using a Fusion Fx5 chemiluminescence detector (Vilber).

Statistical analysis

The data were processed using SPSS 21.0 software and R software (version 4.2.0). Differences between the two groups were evaluated using the independent samples t-test. A one-way ANOVA followed by the SNK-q test was used to compare multiple groups. A $p<0.05$ was statistically significant.

RESULTS

CircRNA_104293 was upregulated in CD patients

To identify differentially expressed circRNAs between the control and CD groups, genome-wide sequencing analysis was performed. A total of 415 up-regulated and 234 down-regulated circRNAs were identified (Fig. 1A). Among these, circRNA_103765 exhibited significantly elevated expression, highlighting its potential as a therapeutic

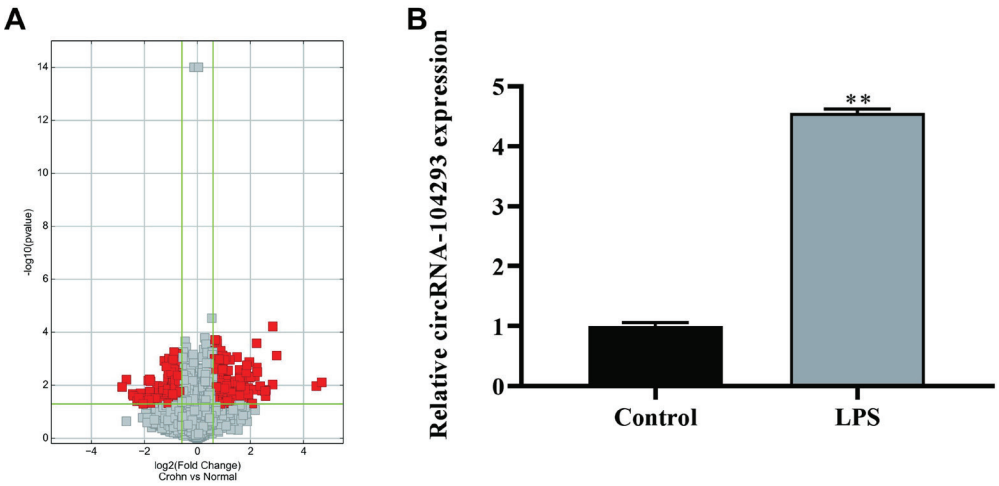

Fig. 1. Elevated circRNA_104293 expressions in Crohn's disease (CD) patients and lipopolysaccharide (LPS)-treated FHC cells. **A.** Volcano plot showing differentially expressed circRNAs in CD patients and controls based on $\log_2|\text{fold change}| > 1$ and an FDR-adjusted p-value < 0.05. **B.** Quantitative (q) PCR was used to compare the levels of circRNA_104293 in fetal human colon (FHC) cells under different treatments, using Student's t-test. (**p < 0.01).

target for CD. Further validation was conducted in LPS-treated FHC cells, where circRNA_104293 showed significantly higher expression than in controls (Fig. 1B). This finding underscores its potential role in inflammatory conditions.

Si-circRNA_104293 suppressed inflammation levels.

The transfection efficiency of si-circRNA_104293 and si-NC was evaluated using q-PCR. Results demonstrated that si-circRNA_104293 effectively reduced circRNA_104293 expression in LPS-treated FHC cells, confirming successful transfection (Fig. 2A). To assess the impact of si-circRNA_104293 on inflammation, ELISA was performed, revealing a significant decrease in pro-inflammatory cytokines TNF-α, IL-1β, IL-6, and IL-8 (Fig. 2B). These findings suggest that si-circRNA_104293 effectively attenuates inflammatory responses. Additionally, flow cytometry indicated that si-circRNA_104293 markedly inhibited apoptosis in LPS-treated FHC cells (Fig. 2C), further supporting its role in mitigating cellular damage under inflammatory conditions.

CircRNA_104293 targeted miR-497-5p

TargetScan was used to identify the interaction between circRNA_104293 and miR-497-5p (Fig. 3A). A dual luciferase reporter assay confirmed this binding relationship, showing that the miR-497-5p mimic reduced luciferase activity in the circRNA_104293-WT group (Fig. 3B). This indicated that circRNA_104293 directly targets and negatively regulates miR-497-5p. Further validation using q-PCR revealed that miR-497-5p expression was lower in the LPS-treated group compared to controls (Fig. 3C). Additionally, silencing circRNA_104293 led to a notable increase in miR-497-5p levels (Fig. 3D), further supporting the regulatory role of circRNA_104293 in suppressing miR-497-5p expression. These findings collectively demonstrate that circRNA_104293 targets and downregulates miR-497-5p.

Si-circRNA_104293 reduced inflammation

LPS-treated cells were divided into three groups: si-NC + NC-inhibitor, si-circRNA_104293 + miR-497-5p-inhibitor, and si-circRNA_104293 + NC-inhibitor, to investigate the roles of circRNA_104293 and

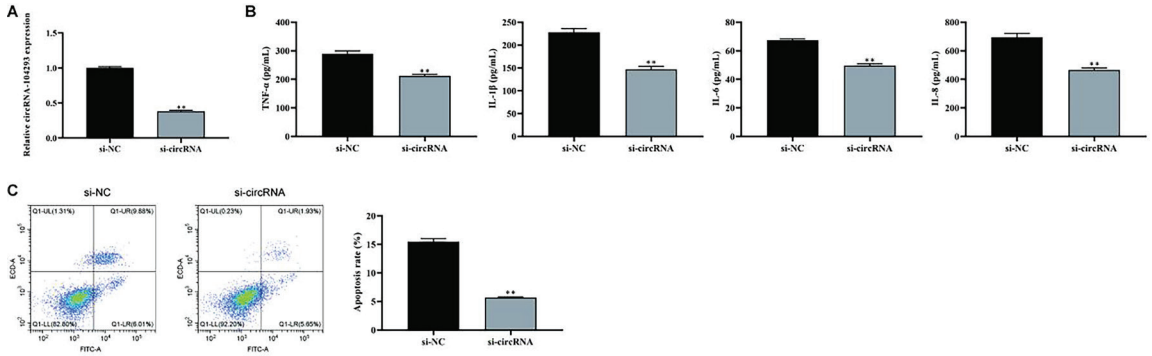

Fig. 2. Si-circRNA_104293 attenuates inflammation in LPS-treated FHC cells. **A.** Transfection efficiency of si-circRNA_104293 was confirmed by quantitative (q)PCR. **B.** ELISA measurements of TNF-α, IL-1β, IL-6, and IL-8 levels across different groups. **C.** Flow cytometry analysis of apoptosis in lipopolysaccharide (LPS)-treated fetal human colon (FHC) cells. (**p < 0.01 vs. si-NC group).

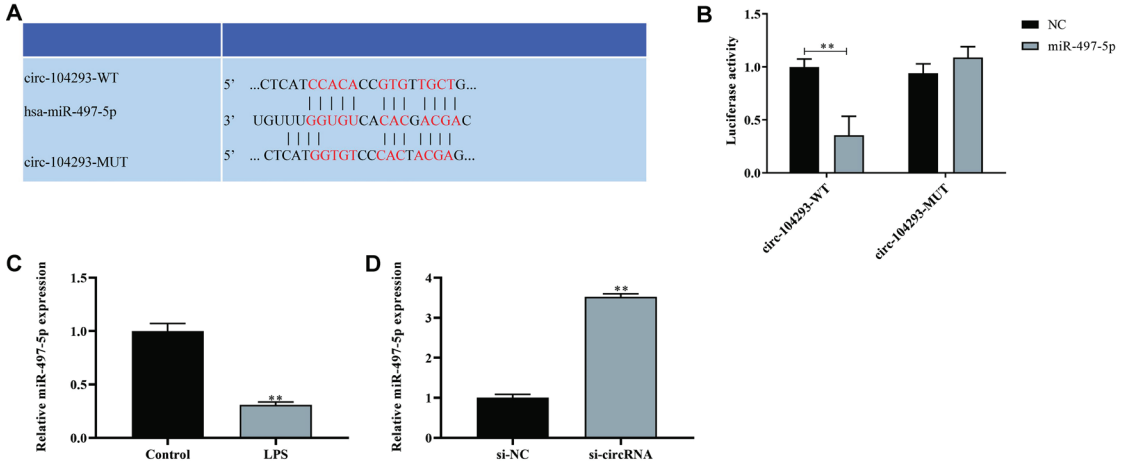

Fig. 3. circRNA_104293 targets miR-497-5p. **A.** Predicted binding site between circRNA_104293 and miR-497-5p. **B.** The dual luciferase assay confirmed the interaction between circRNA_104293 and miR-497-5p. **C.** qPCR analysis of miR-497-5p expression in control and lipopolysaccharide (LPS) groups. **D.** qPCR for miR-497-5p levels in cells treated with si-NC or si-circRNA_104293. (**p<0.01 vs. control or NC group).

miR-497-5p. The efficacy of the miR-497-5p inhibitor was confirmed via qPCR, showing a significant reduction in miR-497-5p levels (Fig. 4A). Immunofluorescence assays revealed that the miR-497-5p inhibitor partially reversed the effects of si-circRNA_104293, markedly decreasing dsDNA and ssDNA levels (Fig. 4B, C). Furthermore, si-circRNA_104293 downregulated inflammatory cytokines, while the miR-497-5p inhibitor partially counteracted this effect (Fig. 4D). Apoptosis assays demonstrated that si-circRNA_104293 reduced apoptosis rates. In contrast, the miR-497-5p inhibitor increased them (Fig. 4E). These findings indicate that circRNA_104293 mitigates inflammation and apoptosis by regulating miR-497-5p.

CircRNA_104293/miR-497-5p alleviated inflammation levels

Western blot analysis revealed that both miR-497-5p mimic and rapamycin downregulated the expression of p-mTOR and p-STAT3 compared to the NC-mimic group, indicating suppression of the mTOR/STAT3 pathway (Fig. 5A). Immunofluorescence as-

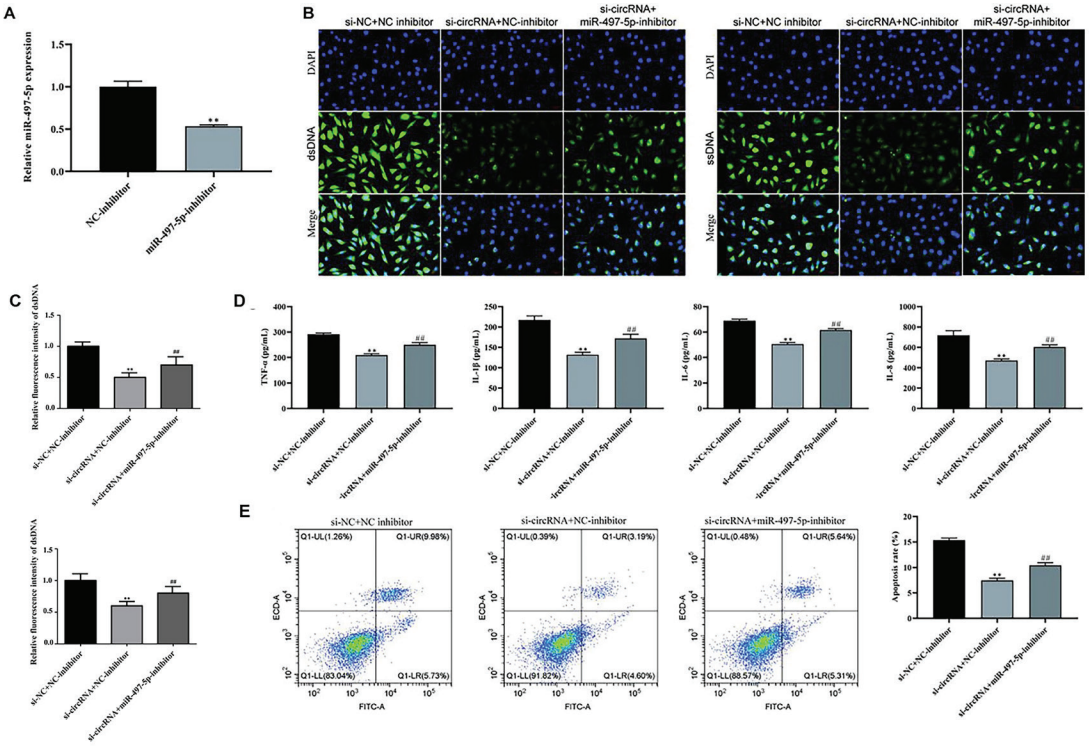

Fig. 4. Si-circRNA_104293 reduces inflammation via miR-497-5p. **A.** qPCR for the miR-497-5p levels in NC-inhibitor and miR-497-5p inhibitor. (**$p < 0.01$) **B-C.** Immunofluorescence analysis for the dsDNA and ssDNA levels in different treatment groups. (**p <0.01, si-circRNA+NC-inhibitor vs si-NC+NC-inhibitor, ## p <0.01, si-circRNA+miR-497-5p-inhibitor vs si-NC+NC-inhibitor). **D**. ELISA for the expression of inflammatory cytokines in different treatment groups. (**p<0.01, si-circRNA + NC-inhibitor vs si-NC + NC-inhibitor, ## p<0.01, si-circRNA + miR-497-5p-inhibitor vs si-circRNA + NC-inhibitor). **E.** Flow cytometry for the cell apoptosis in different groups. (**p<0.01, si-circRNA + NC-inhibitor vs si-NC + NC-inhibitor, ## p<0.01, si-circRNA + miR-497-5p-inhibitor vs si-circRNA + NC-inhibitor).

says showed reduced levels of ssDNA and dsDNA in the miR-497-5p-mimic and rapamycin groups (Fig. 5B, C). Additionally, ELISA results demonstrated decreased levels of inflammatory cytokines in these groups (Fig. 5D). Apoptosis analysis further confirmed that miR-497-5p mimic and rapamycin significantly lowered apoptosis rates compared to the NC-mimic group (Fig. 5E).

DISCUSSION

CircRNA is more stable than linear RNA, making it of great value for clinical diagnosis and prognostic evaluation of CD [17]. Recently, some studies have shown that circRNAs such as circRNA102610, circRNA103516, and circRNA102685 are involved in the inflammatory process of CD. However, the role of most circRNAs in CD pathogenesis remains elusive and therefore requires further exploration[18,20]. circRNA103765 has been identified as a key regulator of CD11 pathogenesis. In this study, significantly increased expression of circRNA104293 was observed in LPS-treated FHC cells and in CD patients. These results suggest a potential role for circRNA104293 in regulating inflammation in CD.

In IBD, TNF-α plays a critical role in the intestinal mucosa through autocrine and paracrine mechanisms [21]. LPS produced by the gut microbiota can directly activate macrophages in the intestinal lamina pro-

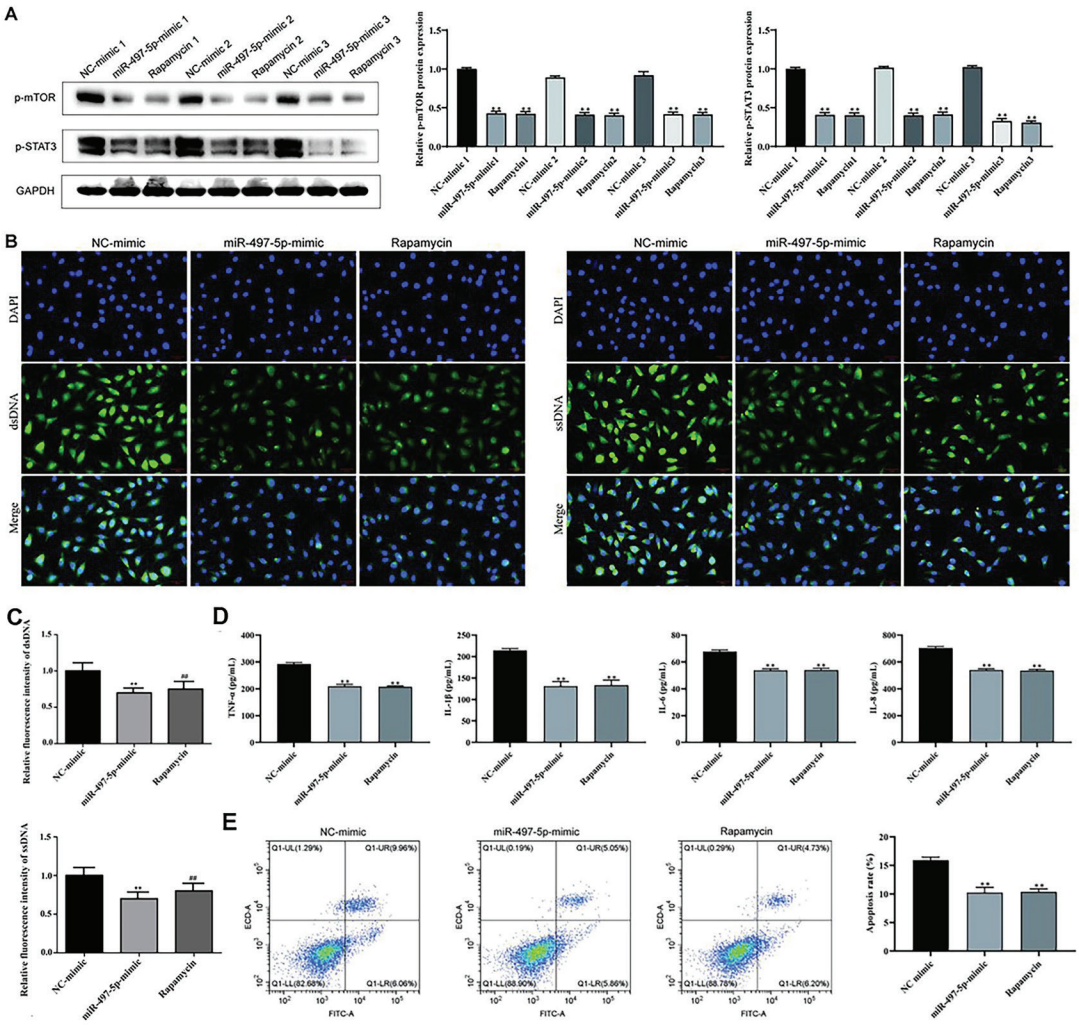

Fig. 5. circRNA_104293/miR-497-5p alleviates inflammation by inhibiting mTOR/STAT3 pathway. **A.** Western blot analysis of p-mTOR and p-STAT3 expression across different groups. **B-C.** Immunofluorescence analysis of dsDNA and ssDNA levels. (**p<0.01, miR-497-5p-mimic vs NC-mimic, ## p<0.01, rapamycin vs NC-mimic). **D.** ELISA measurements of TNF-α, IL-1β, IL-6, and IL-8 levels. **E.** Flow cytometry assessment of cell apoptosis in different groups. (**p<0.01 vs. NC-mimic group).

pria, promote their proliferation, and induce TNF-α release [22]. It has been shown that TNF-α and IL-1β expression are significantly abnormal in mucosal biopsies from pediatric CD patients [23]. In addition, the synergistic effect of TNF-α with interferon γ disrupts barrier function and alters the morphological structure of intestinal epithelial cells, resulting in increased permeability of the intestinal mucosa and vascular wall, ultimately triggering ulcer formation [24, 25]. In the pathogenesis of CD, inhibition of apoptosis leads to excessive accumulation of T cells, which in turn aggravates chronic mucosal inflammation, a process closely related to IL-6 signaling[26,27]. Notably, IL-8 expression is abnormal in the serum and intestinal tissues of immune CD patients, and its level not only reflects disease severity but also serves as an independent indicator of disease activity [28]. In this study, we found that si-circRNA104293 significantly reduced levels of inflammatory factors.

In this study, circRNA104293 was found to play a regulatory role by targeting and inhibiting miR-497-5p expression. It has been shown that miR-497-5p can upregulate IL-6 expression, thereby inhibiting muscle cell atrophy, and affects the inflammatory process by participating in the NF-κB pathway and regulating T cell function [29]. The results of this work, consistently, shows that si-circRNA104293 significantly decreased the rate of apoptosis, whereas the miR-497-5p inhibitor increased it. In addition, si-circRNA104293 effectively reduced the inflammatory response by regulating miR-497-5p, indicating that the circRNA104293/miR-497-5p axis plays a vital role in regulating inflammation in CD. It was also found that si-circRNA104293 significantly reduced dsDNA and ssDNA levels, while miR-497-5p inhibitors partially reversed this effect, further confirming the key role of circRNA104293 in inflammation and cell damage.

In this study, we found that p-mTOR and p-STAT3 expression levels were significantly decreased in miR-497-5p mimic and rapamycin groups compared with NC mimic groups [30]. Previous studies have shown that p-mTOR levels are increased in colonic tissue of CD patients. mTOR, a key molecule regulating cellular energy metabolism, mitochondrial fusion, and glucose and lipid metabolism, has inhibitors that can effectively suppress the expression of inflammatory factors [31]. In addition, STAT3 acts as a multifunctional transcription factor and can activate inflammatory responses in T cells through IL-6-mediated JAK/STAT3 signaling pathway[32]. Blocking IL-6 signaling not only reduces STAT3 activation but also induces monocyte apoptosis, thereby relieving colitis triggered by IL-10 deficiency [33, 34]. In CD patients, total STAT3 and phosphorylated STAT3 levels were significantly increased in inflammatory intestinal mucosa, and phosphorylated STAT3 levels were positively correlated with the degree of inflammatory injury [35]. The results of this study further confirmed that circRNA104293/miR-497-5p significantly reduced CD inflammatory levels by inhibiting the mTOR/STAT3 pathway.

In summary, our findings suggest that the circRNA_104293/miR-497-5p axis regulates LPS-induced inflammatory responses by modulating the mTOR/STAT3 signaling pathway. These results indicate its potential as a therapeutic target in inflammatory processes.

Funding

Chengdu Medical Scientific Research Project (2021333).

Conflict of interest

The authors declare that they have no conflict of interest regarding this study.

Ethics approval and consent to participate

This study was conducted in accordance with the Declaration of Helsinki, and was conducted with approval from the Ethics Committee of The First People's Hospital of Shuangliu District/West China (Airport) Hospital, Sichuan University. Written informed consent was obtained from all participants.

ORCID number of authors

- Xuerui Yin (XY): 0009-0006-6698-8009
- Gaigai Huang (GH): 0009-0008-4424-1179
- Chuan Zheng (CZ): 0009-0005-4178-415X
- Yu Zhou (YZ): 0009-0007-4611-3069
- Rong Chen (RC): 0009-0005-7624-8285

Author contributions

Conceived and designed the study: XY, RC, GH; performed the literature search and data extraction: XY, CZ, YZ; analyzed the data: RC; drafted the manuscript: XY, RC

REFERENCES

1. **Vanhove W, Nys K, Vermeire S**. Therapeutic innovations in inflammatory bowel diseases. Clin Pharmacol Ther. 2016; 99(1): 49-58. *https://doi.org/10.1002/cpt.286*.
2. **Lomer MC, Thompson RP, Powell JJ**. Fine and ultrafine particles of the diet: influence on the mucosal immune response and association with Crohn's disease. Proc Nutr Soc. 2002; 61(1): 123-130. *https://doi.org/10.1079/pns2001134*.
3. **Zhao J, Wang H, Yang H, Zhou Y, Tang L**. Autophagy induction by rapamycin ameliorates experimental colitis and improves intestinal epithelial barrier function in IL-10 knockout mice. Int Immunopharmacol. 2020; 81: 105977. *https://doi.org/10.1016/j.intimp.2019.105977*.
4. **Long SH, He Y, Chen MH, Cao K, Chen YJ, Chen BL, et al.** Activation of PI3K/Akt/mTOR signaling pathway triggered by PTEN downregulation in the pathogenesis of Crohn's disease. J Dig Dis. 2013; 14(12): 662-669. *https://doi.org/10.1111/1751-2980.12095*.
5. **Li L, Wan G, Han B, Zhang Z**. Echinacoside alleviated LPS-induced cell apoptosis and inflammation in rat intestine epithelial cells by inhibiting the mTOR/STAT3 pathway. Biomed Pharmacother. 2018; 104: 622-628. *https://doi.org/10.1016/j.biopha.2018.05.072*.
6. **Li F, Yin YK, Zhang JT, Gong HP, Hao XD**. Role of circular RNAs in retinoblastoma. Funct Integr Genomics. 2022; 23(1): 13. *https://doi.org/10.1007/s10142-022-00942-9*.
7. **Li L, Zhang Q and Lian K**. Circular RNA circ_0000284 plays an oncogenic role in the progression of non-small cell lung cancer through the miR-377-3p-mediated PD-L1 promotion. Cancer Cell Int. 2020; 20: 247. *https://doi.org/10.1186/s12935-020-01310-y*.
8. **Zhang M, Han Y, Zhai Y, Ma X, An X, Zhang S, et al.** Integrative analysis of circRNAs, miRNAs, and mRNAs profiles to reveal ceRNAs networks in chicken intramuscular and abdominal adipogenesis. BMC Genomics. 2020; 21(1): 594. *https://doi.org/10.1186/s12864-020-07000-3*.
9. **Pan H, Li T, Jiang Y, Pan C, Ding Y, Huang Z, et al.** Overexpression of Circular RNA ciRS-7 Abrogates the Tumor Suppressive Effect of miR-7 on Gastric Cancer via PTEN/PI3K/AKT Signaling Pathway. J Cell Biochem. 2018; 119(1): 440-446. *https://doi.org/10.1002/jcb.26201*.
10. **Zhang Y, Li C, Liu X, Wang Y, Zhao R, Yang Y, et al.** circHIPK3 promotes oxaliplatin-resistance in colorectal cancer through autophagy by sponging miR-637. EBioMedicine. 2019; 48: 277-288. *https://doi.org/10.1016/j.ebiom.2019.09.051*.
11. **Ye Y, Zhang L, Hu T, Yin J, Xu L, Pang Z, et al.** CircRNA_103765 acts as a proinflammatory factor via sponging miR-30 family in Crohn's disease. Sci Rep. 2021; 11(1): 565. *https://doi.org/10.1038/s41598-020-80663-w*.
12. **Wu F, Guo NJ, Tian H, Marohn M, Gearhart S, Bayless TM, et al.** Peripheral blood microRNAs distinguish active ulcerative colitis and Crohn's disease. Inflamm Bowel Dis. 2011; 17(1): 241-250. *https://doi.org/10.1002/ibd.21450*.
13. **Syed NH, Mussa A, Elmi AH, Jamal Al-Khreisat M, Ahmad Mohd Zain MR, Nurul AA**. Role of MicroRNAs in Inflammatory Joint Diseases: A Review. Immunol Invest. 2024; 53(2): 185-209. *https://doi.org/10.1080/08820139.2023.2293095*.
14. **Ke J, Chen M, Ma S, Zhang L, Zhang L**. Circular RNA VMA21 ameliorates lung injury in septic rat via targeting microRNA-497-5p/CD2-associated protein axis. Bioengineered. 2022; 13(3): 5453-5466. *https://doi.org/10.1080/21655979.2022.2031406*.
15. **Lou W, Yan J, Wang W**. Downregulation of miR-497-5p Improves Sepsis-Induced Acute Lung Injury by Targeting IL2RB. Biomed Res Int. 2021; 2021: 6624702. *https://doi.org/10.1155/2021/6624702*.
16. **Zhang M, Yang D, Yu H, Li Q**. MicroRNA-497 inhibits inflammation in DSS-induced IBD model mice and lipopolysaccharide-induced RAW264.7 cells via Wnt/β-catenin pathway. Int Immunophar-

macol. 2021; 101(Pt B): 108318. *https://doi.org/10.1016/j.intimp.2021.108318*.

17. **Ma YS, Cao YF, Liu JB, Li W, Deng J, Yang XL, et al.** The power and the promise of circRNAs for cancer precision medicine with functional diagnostics and prognostic prediction. Carcinogenesis. 2021; 42(11): 1305-1313. *https://doi.org/10.1093/carcin/bgab071*.
18. **Yin J, Hu T, Xu L, Li P, Li M, Ye Y, et al.** Circular RNA expression profile in peripheral blood mononuclear cells from Crohn disease patients. Medicine (Baltimore). 2019; 98(26): *e16072. https://doi.org/10.1097/md.0000000000016072*.
19. **Lu JW, Rouzigu A, Teng LH, Liu WL**. The Construction and Comprehensive Analysis of Inflammation-Related ceRNA Networks and Tissue-Infiltrating Immune Cells in Ulcerative Progression. Biomed Res Int. 2021; 2021: 6633442. *https://doi.org/10.1155/2021/6633442*.
20. **Qiao YQ, Cai CW, Shen J, Zheng Q, Ran ZH**. Circular RNA expression alterations in colon tissues of Crohn's disease patients. Mol Med Rep. 2019; 19(5): 4500-4506. *https://doi.org/10.3892/mmr.2019.10070*.
21. **Zhu Y, Mahon BD, Froicu M, Cantorna MT**. Calcium and 1 alpha,25-dihydroxyvitamin D3 target the TNF-alpha pathway to suppress experimental inflammatory bowel disease. Eur J Immunol. 2005; 35(1): 217-224. *https://doi.org/10.1002/eji.200425491*.
22. **Sun L, Rollins D, Qi Y, Fredericks J, Mansell TJ, Jergens A, et al.** TNFα regulates intestinal organoids from mice with both defined and conventional microbiota. Int J Biol Macromol. 2020; 164: 548-556. *https://doi.org/10.1016/j.ijbiomac.2020.07.176*.
23. **Kaminsky LW, Al-Sadi R, Ma TY**. IL-1β and the Intestinal Epithelial Tight Junction Barrier. Front Immunol. 2021; 12: 767456. *https://doi.org/10.3389/fimmu.2021.767456*.
24. **Van Winkle JA, Constant DA, Li L, Nice TJ**. Selective Interferon Responses of Intestinal Epithelial Cells Minimize Tumor Necrosis Factor Alpha Cytotoxicity. J Virol. 2020; 94(21): e00603-20. *https://doi.org/10.1128/jvi.00603-20*.
25. **Coope A, Pascoal LB, da Silva FAR, Botezelli JD, Ayrizono MLS, Milanski M, et al.** Transcriptional and Molecular Pathways Activated in Mesenteric Adipose Tissue and Intestinal Mucosa of Crohn's Disease Patients. Int J Inflam. 2017; 2017: 7646859. *https://doi.org/10.1155/2017/7646859*.
26. **Nakano K, Yamaoka K, Hanami K, Saito K, Sasaguri Y, Yanagihara N, et al.** Dopamine induces IL-6-dependent IL-17 production via D1-like receptor on CD4 naive T cells and D1-like receptor antagonist SCH-23390 inhibits cartilage destruction in a human rheumatoid arthritis/SCID mouse chimera model. J Immunol. 2011; 186(6): 3745-3752. *https://doi.org/10.4049/jimmunol.1002475*.
27. **García de Tena J, Manzano L, Leal JC, San Antonio E, Sualdea V, Alvarez-Mon M**. Distinctive pattern of cytokine production and adhesion molecule expression in peripheral blood memory CD4+ T cells from patients with active Crohn's disease. J Clin Immunol. 2006; 26(3): 233-242. *https://doi.org/10.1007/s10875-006-9016-4*.
28. **Jones SC, Evans SW, Lobo AJ, Ceska M, Axon AT, Whicher JT**. Serum interleukin-8 in inflammatory bowel disease. J Gastroenterol Hepatol. 1993; 8(6): 508-512. *https://doi.org/10.1111/j.1440-1746.1993.tb01643.x*.
29. **Freire PP, Cury SS, Lopes LO, Fernandez GJ, Liu J, de Moraes LN, et al.** Decreased miR-497-5p Suppresses IL-6 Induced Atrophy in Muscle Cells. Cells. 2021; 10(12):3527. *https://doi.org/10.3390/cells10123527*.
30. **Brandt M, Grazioso TP, Fawal MA, Tummala KS, Torres-Ruiz R, Rodriguez-Perales S, et al.** mTORC1 Inactivation Promotes Colitis-Induced Colorectal Cancer but Protects from APC Loss-Dependent Tumorigenesis. Cell Metab. 2018. 27(1): 118-135.e8. *https://doi.org/10.1016/j.cmet.2017.11.006*.
31. **Zhang D, Liu J, Lv L, Chen X, Qian Y, Zhao P, et al.** Total flavone of Abelmoschus

manihot regulates autophagy through the AMPK/mTOR signaling pathway to treat intestinal fibrosis in Crohn's disease. J Gastroenterol Hepatol. 2024; 39(8): 1586-1596. *https://doi.org/10.1111/jgh.16560*.

32. **Wang Y, Liu H, Zhang Z, Bian D, Shao K, Wang S, et al.** G-MDSC-derived exosomes mediate the differentiation of M-MDSC into M2 macrophages promoting colitis-to-cancer transition. J Immunother Cancer. 2023; 11(6): e006166.*https://doi.org/10.1136/jitc-2022-006166*.
33. **Gyamfi J, Lee YH, Eom M, Choi J**. Interleukin-6/STAT3 signalling regulates adipocyte induced epithelial-mesenchymal transition in breast cancer cells. Sci Rep. 2018; 8(1): 8859. *https://doi.org/10.1038/s41598-018-27184-9*.
34. **Akanda MR, Nam HH, Tian W, Islam A, Choo BK, Park BY**. Regulation of JAK2/STAT3 and NF-κB signal transduction pathways; Veronica polita alleviates dextran sulfate sodium-induced murine colitis. Biomed Pharmacother. 2018; 100: 296-303. *https://doi.org/10.1016/j.biopha.2018.01.168*.
35. **Kaur S, Bansal Y, Kumar R, Bansal G**. A panoramic review of IL-6: Structure, pathophysiological roles and inhibitors. Bioorg Med Chem. 2020; 28(5): 115327. *https://doi.org/10.1016/j.bmc.2020.115327*.

Invest Clin 66(4): 378- 389, 2025 https://doi.org/10.54817/IC.v66n4a03

The burden of iron overload in sickle cell disease: insights from South Carolina, USA.

Gilberto Vizcaíno[1,2], Christina M. Abrams[3], Caroline B. Foster[1], Hermes Flórez[1], Natalia Dávila[4] and Sabrina C. Rainey[5]

[1]Department of Public Health Sciences, Medical University of South Carolina, Charleston, SC, USA.
[2]Instituto de Investigaciones Clínicas "Dr. Américo Negrette", Facultad de Medicina, Universidad del Zulia, Maracaibo, Venezuela.
[3]Department of Pediatrics, Division of Hematology/Oncology, Medical University of South Carolina, Charleston, SC, USA.
[4]College of Nursing, Medical University of South Carolina, Charleston, SC, USA.
[5]University of Louisville, Pediatric Hematology Oncology, Louisville, KY, USA.

Keywords: Anemia; Sickle Cell; Iron Overload; Liver Iron Concentration; Ferritin; Liver Function Tests; Chelation Therapy.

Abstract. Red blood cell transfusions can lead to iron overload (IO) in sickle cell disease (SCD). We aimed to determine the relationship between SCD patients with IO and SCD comorbidities. Iron chelation regimen for IO in SCD patients was also studied. A cohort of 245 SCD adult patients receiving care at the Medical University of South Carolina (MUSC) was studied. Information was obtained from medical records. Statistical analysis was performed to examine correlations and odds ratios with 95% confidence intervals. We identified 85 (34.7%) participants who met IO criteria. The results showed a significant association of IO with stroke (OR= 14.67, p= 0.0001), pulmonary hypertension (OR= 4.75, p= 0.0006), acute chest syndrome (OR= 2.46, p= 0.003), and deep vein thrombosis (OR= 1.84, p= 0.04). There was a strong correlation between liver iron concentration (LIC) and ferritin levels (r= 0.5148, p<0.0001). Liver enzymes correlated well with LIC and ferritin levels. Eighty-six percent of participants (74/85) were on chelation therapy, but only 19% of them achieved a good response to the treatment. One-third of SCD individuals developed IO, associated with several comorbidities. Comprehensive measures must include periodic determinations of LIC and ferritin, followed by appropriate chelation therapy to prevent organ damage.

Corresponding author: Gilberto Vizcaíno. Department of Public Health Sciences, Medical University of South Carolina, 135 Cannon Street, Suite 300, Charleston, SC 29425. Email: gilvizcaino@gmail.com

La sobrecarga de hierro en la anemia falciforme: perspectivas desde Carolina del Sur, EEUU.

Invest Clin 2025; 66 (4): 378 – 389

Palabras clave: Anemia de Células Falciformes; Sobrecarga de Hierro; Concentración Hepática de Hierro; Ferritina; Pruebas de Función Hepática; Terapia por Quelación.

Resumen. Las transfusiones de glóbulos rojos pueden provocar sobrecarga de hierro (SH) en la enfermedad de células falciformes (ECF). Nuestro objetivo fue determinar la relación entre pacientes con ECF con SH y comorbilidades asociadas a la ECF. También se estudió el régimen de quelación de hierro para la SH en pacientes con ECF. Se estudió una cohorte de 245 pacientes adultos con ECF atendidos en la Medical University of South Carolina (MUSC). La información se obtuvo de las historias clínicas. Se realizó un análisis estadístico para analizar las correlaciones y las razones de probabilidades (odds ratios) con intervalos de confianza del 95%. Se encontraron 85 (34,7%) participantes con criterios de SH. Los resultados mostraron una asociación significativa de la SH con el ictus (OR = 14,67, p = 0,0001), la hipertensión pulmonar (OR = 4,75, p = 0,0006), el síndrome torácico agudo (OR = 2,46, p = 0,003) y la trombosis venosa profunda (OR = 1,84, p = 0,04). Se observó una fuerte correlación entre la concentración hepática de hierro (CHH) y el nivel de ferritina (r = 0,5148, p<0,0001). Las enzimas hepáticas se correlacionaron adecuadamente con la CHH y los niveles de ferritina. El 86% de los participantes (74/85) recibía terapia de quelación, pero solo el 19% obtuvo una buena respuesta al tratamiento. Un tercio de los pacientes con enfermedad de células falciformes desarrolló sobrecarga de hierro asociada a diversas comorbilidades. Las medidas integrales deben incluir determinaciones periódicas de la CHH y la ferritina, seguidas de un tratamiento de quelación adecuado para prevenir el daño orgánico.

Received: 27-07-2025 Accepted: 07-10-2025

INTRODUCTION

Sickle cell disease is a common hemoglobinopathy, and approximately 4,000 people in South Carolina, USA, live with this disease (SCD) [1]. In the management of SCD, chronic transfusion therapy is used to prevent and treat complications [2]. Each unit of transfused packed red blood cells (pRBCs) provides 200-250 mg of iron, and repeated blood transfusions will lead to iron overload (IO) in SCD patients. Previous studies have shown that the IO resulting from transfusional therapy in other patient populations is associated with significant morbidity and mortality [3]. Iron overload has been considered a major cause of end-organ damage in multitransfused patients with hemoglobinopathies [4], and the source of excessive iron burden in SCD is primarily blood transfusions and intravascular hemolysis.

To assess the degree of IO, liver iron concentration (LIC) can be measured invasively via liver biopsy or noninvasively by

magnetic resonance imaging (MRI). There is a very close correlation between the two methods; thus, MRI has largely eliminated the need for liver biopsies [5]. Ferritin should be used as a measure of IO in SCD patients, but its values should be interpreted with caution for therapeutic decision-making [6]. Iron accumulation depends on the age at which blood transfusions are started, the rate of transfusions, and the nature of the transfusion regimen[7]. Compared with thalassemia, iron deposition in cardiac, renal, or endocrine organs is lower in SCD because intravascular hemolysis promotes biliary and urinary elimination of iron as hemosiderin, heme, and hemoglobin, and the chronic inflammatory state reduces toxic accumulation of iron in macrophages [7–9]. Additionally, there is a difference between multiple simple transfused SCD patients and patients receiving blood with exchange transfusions because there is less liver accumulation of transfused iron in the latter [8,9].

It is complicated to establish if organ damage is caused by iron from transfusion as a treatment for some SCD comorbidities or if damage is a consequence of the complications themselves [5,6]. The non-transferrin-bound iron free in plasma is toxic because it produces radicals with oxidation products that are responsible for a significant part of iron accumulation and cell injury associated with regular multiple transfusions. Additionally, inflammation, as a pathophysiologic mechanism in SCD, leads to increased hepcidin synthesis and decreased iron absorption, with increased iron retention in the reticuloendothelial system [9].

IO is known to increase morbidity and mortality in SCD, although the exact mechanism is unclear [10-12]. This risk of increased mortality could be associated with a high rate of comorbidities [13]. Except for the comorbidities of stroke or the presence of an abnormal transcranial doppler (TCD), whose preventive treatment is based on chronic transfusions [14], it is difficult to determine whether IO induces the presence of comorbidities or whether these comorbidities are independent of IO. It has been shown that in groups of SCD patients with IO, there was a higher mortality rate than those without IO. Those deaths were attributable to sudden death or pneumonia associated with acute chest syndrome [13]. The rate of admission for vasoocclusive crisis related to the prevalence of organ damage and SCD complications only found a meaningful relationship with IO and acute chest syndrome (ACS) [15]. Ferroptosis has also been recognized as a novel mechanism in SCD and an additional avenue for organ damage in SCD patients. In ferroptosis, elevated iron levels trigger cell death by increasing reactive oxygen species (ROS) and lipid peroxides, leading to organ impairment [16].

Iron chelation is the primary treatment for IO in SCD, and it can be initiated if more than 18 transfusions have been received (or >120 cc/kg of PRBC) within a defined period. Additionally, a serum ferritin level >1000 ng/mL on two separate measurements, or hepatic MRI-quantified iron>3 mg/g of dry weight, indicates IO treatment. Because SCD causes a degree of chronic inflammation, ferritin, an acute-phase reactant, is less reliable as a diagnostic tool than in other anemias.

There are three iron chelators currently approved for clinical use: (1) deferoxamine (DFO), (2) deferiprone (DFP), and (3) deferasirox (DFX). DFO is the oldest drug and is administered intravenously or subcutaneously, while DFP and DFX are taken orally [14,15].

The primary aim of this study was to determine the relationship between iron overload and comorbidities in SCD patients. The secondary aims included evaluating the association between liver iron concentration (LIC), serum ferritin levels, liver enzymes, and the characteristics of the iron chelation regimen in chronically transfused SCD patients.

MATERIAL AND METHODS

We conducted a retrospective chart review of the electronic medical records (EMRs) of 245 adults with SCD who receive care at MUSC in Charleston, South Carolina, and are enrolled in the Sickle Cell Disease Implementation Consortium (SCDIC) [17]. The study participants had a diagnosis of SCD, were English-speaking, and aged 15-50. From that population, we identified 85 subjects with both SCD and iron overload (34.7%). EMR data were collected over seven years (2017-2024). The inclusion criteria for this study were a diagnosis of SCD, enrollment in the MUSC-SCDIC-II Registry and REAL Answers projects, and a diagnosis of IO using the previously mentioned parameters. Age, sex, genotype, blood ABO group, comorbidities, ferritin, LIC, liver enzymes, and iron chelation treatment were obtained from the EMR. Patients with iron overload who received a hematopoietic stem cell transplant were excluded from this study.

Institutional review board (IRB) approval was obtained from each of the eight study sites and a central IRB (CIRBI/Advarra) prior to data collection, and a written informed consent was obtained from each participant.

Statistical Analysis

Statistical analysis was performed using GraphPad InStat3 (GraphPad Software, Boston, MA 02110) to analyze frequency distributions for categorical variables and to perform linear regression and Pearson correlation for continuous variables. A 2 x 2 contingency table was used to calculate odds ratios with 95% confidence intervals by Fisher's exact test and to calculate sensitivity and specificity parameters. The reference group for the odds ratio (OR) was adult SCD patients (160/245) without iron overload. A $p<0.05$ was considered statistically significant.

RESULTS

Table 1 describes the demographic characteristics of the 85 (34.7%) subjects with SCD and IO who met inclusion criteria. Seventy-three IO patients (85.9%) were between 18-45 years old with a median age of 32.5 years (range 16-55), 61.2% were female, 95.3% had SS genotype, and 56.5% had blood group O. From 67.0% with IO criteria receiving transfusions (57/85), 51% (29/57) were treated under manual blood exchange regimen, and the rest of them by erythrocytapheresis regimen.

The prevalence of several comorbidities with SCD is described in Table 2. Patients with IO were noted to have a higher rate of four comorbidities: acute chest syndrome (OR= 2.46, p= 0.003), deep vein thrombosis (DVT, OR= 1.84, p= 0.04), stroke (OR= 14.67, p= 0.0001) and pulmonary hypertension (PH, OR= 4.75, p= 0.0006), seen in Table 2 and Fig. 1. Pulmonary hypertension (PH) was defined as a mean pulmonary arterial pressure of at least 25 mm Hg, and a TRV >2.5m/s.

MRI studies, liver biopsy, LIC, and ferritin

Seventy-four percent of subjects with IO initially had MRI/LIC records available (63/85) and 26% had also liver biopsy data available (22/85). Twenty-four percent (20/85) of them did not have a subsequent record of LIC, as measured by liver MRI or liver biopsy, and were followed only with ferritin determination. Cardiac MRI data were available for 25% (21/85) of subjects, and only one patient showed myocardial iron deposition.

The average values at the start and end of the study for LIC were 11.71±8.46 mg/g dry weight (n=59) and 12.88±7.86 mg/g dry weight (n=44), respectively; the average values for ferritin were 3779.5±2852 ng/mL (n=85) and 5055.1±5567.4 ng/mL (n=85), respectively; p=0.06 for both.

There was a strong correlation between LIC (mg/g dry weight) and ferritin level (ng/mL) (r=0.5148, p=0.0001), as seen in Fig. 2. We also observed a strong correlation between serum ferritin and LIC in individuals with serum ferritin levels > 2500 ng/mL (r=0.5220, p=0.0026, n= 31). There was no correlation in patients with serum ferritin levels below 2500 ng/mL (r=0.3133, p= 0.3213; n=12).

Table 1. Demographic characteristics of Iron overload in Sickle Cell Disease.

Characteristics	Iron Overload (N=85)	No Iron Overload (N=160)	Total (N=245)
Age group (years)			
<18	4 (4.7%)	10 (6.3%)	14 (5.7%)
18-24	20 (23.5%)	22 (13.7%)	42 (17.2%)
25-34	24 (28.2%)	65 (40.6%)	89 (36.3%)
35-45	29(34.2%)	43 (26.9%)	72 (29.4%)
>45	8(9.4%)	20 (12.5%)	28 (11.4%)
Median	32.5	31.0	32.0
Gender			
Male	34 (40.0%)	62 (38.8%)	96 (39.2%)
Female	51 (60.0%)	98 (61.2%)	149 (60.8%)
Age (N)			
Male	31.36±10.4 (34)	34.36±11.0 (62)	33.33±10.8(96)
Female	33.43±9.4 (51)	32.51±11.1 (98)	32.75±10.7(149)
Mean±SD	32.61±9.8 (85)	33.26±11.2 (160)	33.05±10.7 (245)
SCD Genotype			
SS	81 (95.3%)	98 (61.3%)	179 (73.1%)
SC	1 (1.2%)	40 (25.0%)	41 (16.7%)
SThal	3 (3.5%)	19 (11.9%)	22 (9.0%)
Other	0 (0%)	3 (1.8%)	3 (1.2%)
Blood Group (ABO)			
Group O	48 (56.5%)		
Group A	20 (23.5%)		
Group B	10 (11.8%)		
Group AB	7 (8.2%)		

Table 2. Sickle Cell Disease Iron overload and comorbidities relationships.

Comorbidity	IO (N=85)	No IO (160)	Total (N=245)	OR (CI95%)	OR *p*-value
ACS	65 (26.5%)	91 (37.1%)	156(63.7%)	2.46 (1.37-4.45)	**0.0032**
DVT	33 (12.2%)	41 (18.0%)	74(30.2%)	1.84 (1.05-3.23)	**0.0406**
Retinopathy	13 (5.3%)	42 (17.1%)	55 (22.4%)	0.50 (0.26-1.01)	0.0548
Stroke*	46(18.8%)	13 (5.3%)	59(24.1%)	13.34 (6.56-27.12)	**0.0001**
CKD	20 (7.8%)	25 (10.2%)	45 (17.9%)	1.66 (0.86-3.21)	0.1650
Anxiety/Depression	39 (16.7%)	61 (23.3%)	100(40.0%)	1.38 (0.80-2.34)	0.2752
AVN	42 (17.1%)	62(25.3%)	104 (42.4%)	1.54 (0.91-2.63)	0.1351
Pulmonary Htn	17 (7.8%)	8(2.9%)	25 (10.7%)	4.75 (1.96-11.54)	**0.0006**

ACS: Acute Chest Syndrome; DVT: Deep Vein Thrombosis; CKD: Chronic Kidney Disease; AVN: Avascular Necrosis; Htn: Hypertension. *Include overt stroke and abnormal transcranial doppler (TCD).

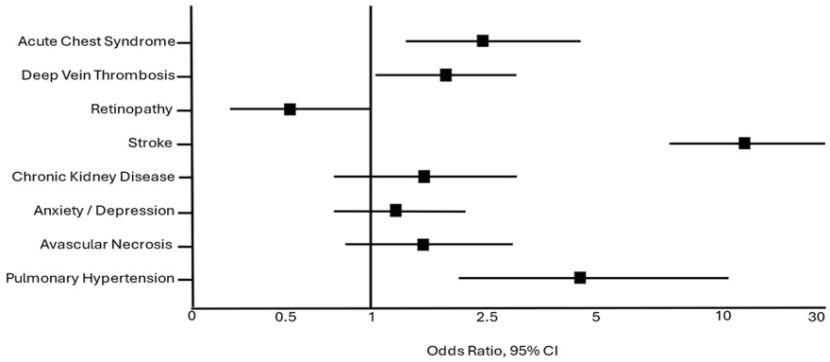

Fig. 1. Odds Ratio for Comorbidities in Sickle Cell patients with IO.

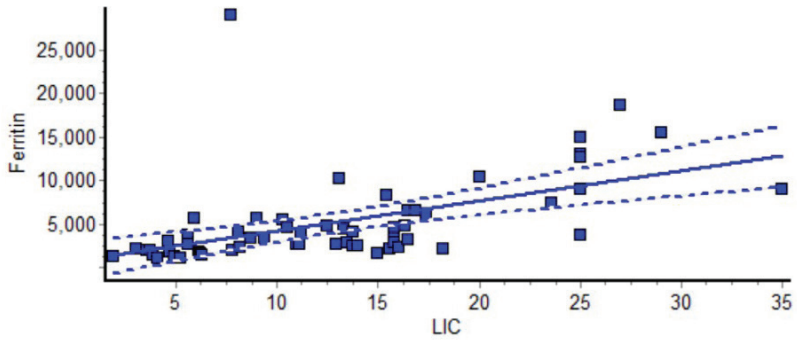

Fig. 2. Linear regression with 95%CI between LIC (mg/g dry weight) and Ferritin (ng/mL) in SCD participants (n=59) diagnosed as Iron overload, r= 0.5148, p<0.0001.

An increasing number of comorbidities was associated with rising LIC and serum ferritin (Table 3). The median number of co-morbidities per patient was 3 (mean 3.12 ± 1.5).

Accuracy estimation of ferritin as a marker of iron overload in SCD participants

Among 69 IO subjects with paired LIC and ferritin levels, 36 had a LIC≥ 10 mg/g dw and 23 had a LIC < 10 mg/g dw. Using a ROC curve and a serum ferritin cut-off of ≥2500 ng/mL, we obtained 78% sensitivity, 74% specificity, 86% positive predictive value, and 61% negative predictive value. In our patient sample, 46 subjects were correctly diagnosed with IO based on their serum ferritin levels (TP), and 13 patients were incorrectly identified as not having IO (FN). The accuracy of the serum ferritin level to diagnose IO was 76% and the area under the curve (AUC) was 76% (Table 4), (Garcia-Casal et al. [18]).

Iron overload and liver enzymes

In SCD individuals with IO, liver enzymes showed a good correlation with LIC and ferritin levels (Supplemental Table 5), except for alkaline phosphatase and LIC. The mean serum values ± SD were AST: 47.8±26.32 U/L, ALT: 33.86±27.36 U/L, and AP: 113.66±55.12 U/L.

Iron chelation treatment

Transfused patients with IO received an average of 22 pRBCs per year with a median of 12 transfusions. Eighty-six percent (74/85) were prescribed chelation therapy with deferasirox (DFX), and two patients were prescribed deferiprone (DFP) chelation therapy. Of those on che-

Table 3. Values of LIC and ferritin associated with the number of comorbidities in subjects with Iron overload.

No comorbidities	LIC (N=43)	Ferritin (N=85)	*p*
1	11.58±5.2 (7)	5538.28±7793.6 (9)	0.0661
2	14.82±7.6 (17)	5748.89±5336.7 (29)	0.0001
3	12.83±9.6 (6)	7026.32±7608.4 (15)	0.0031
4	7.74±4.37 (5)	2588.65±2552.1 (14)	0.0023
>5	11.58±8.17 (8)	3936.66±3800.9 (18)	0.0004

LIC: liver iron concentration (mg/g dry weight), ferritin (ng/mL).

Table 4. Sensitivity and specificity of ferritin as a marker in Sickle Cell Disease to assess iron overload (N=69).

Variable	Value	95% Confidence Interval
Sensitivity	0.7750	0.6159 to 0.8917
Specificity	0.7368	0.4879 to 0.9085
Positive Predictive Value	0.8611	0.7052 to 0.9533
Negative Predictive Value	0.6087	0.3856 to 0.8027
Likelihood Ratio	2.945	
DOR	9.65	

DOR: diagnostic odds ratio, calculated as the effectiveness as an index of iron overload [18]. DOR= (sens x spec) / (1-sens) x (1-spec) = (sens x spec) / (FNs) x (FPs).

Table 5. Correlations between LIC and ferritin versus liver enzymes.

Variable (N)	r	*p*
LIC vs AST (43)	0.5551	**0.0001**
LIC vs ALT (43)	0.5248	**0.0003**
LIC vs AP (43)	0.1393	0.3730
Ferritin vs AST (85)	0.5794	**0.0001**
Ferritin vs ALT (85)	0.6015	**0.0001**
Ferritin vs AP (85)	0.3644	**0.0006**

LIC: liver iron concentration; AST: aspartate transferase; ALT: alanine aminotransferase; AP: alkaline phosphatase. The values of liver enzymes were expressed in U/L, LIC in mg/g dry weight, and ferritin in ng/mL. The reference ranges for liver enzymes were AST (5-34 U/L), ALT (5-45 U/L) and AP (35-150 U/L).

lation therapy with deferasirox, only 19% (14/74) obtained a good response with serum ferritin <1000 ng/mL. Providers followed 54% of these patients with periodic LIC determinations and serum ferritin (40/74), and the remaining patients were followed with serum ferritin alone. Information about the side effects of DFX treatment was scarce and difficult to collect from the data records. Fifty-four percent (40/74) of the subjects were on disease-modifying treatment.

DISCUSSION

These findings show a significant association of IO with several comorbidities in a cohort of SCD patients. Most of the patients were SS genotype young adults receiving frequent blood transfusions. Parameters such as LIC, measured by MRI and/or liver biopsy, were used to diagnose IO in many of these patients, and serum ferritin levels were used as a marker of IO. There was a strong correlation between LIC and serum ferritin when the serum ferritin levels were above 2500 ng/mL. Liver enzymes showed a good correlation with LIC and serum ferritin levels, and chelation therapy with DFX was unsuccessful in most cases.

Previous research has demonstrated that SCD patients with IO have an increased risk of mortality [11,12], and this risk could be associated with a high rate of comorbidities[13]. Moreover, liver injury is associated with mortality in SCD, with increased ferritin and direct bilirubin as predictors of mor-

tality. All patients with advanced liver fibrosis had IO, but not all patients with IO had fibrosis [19]. We have seen an increased number of comorbidities in our study patients with IO, and so this condition may be a predisposing factor for increased morbidity and mortality in SCD patients. In our study, five (2.0%) patients with SCD died, and three of those had IO.

As demonstrated previously [20], our findings showed a stroke or at-risk-of-stroke prevalence of 24% (59/245) in SCD patients. Of the patients with stroke or at risk of stroke, 78% of them had IO (70% stroke, 30% abnormal TCD), making stroke the most common comorbidity that we observed with IO. This high rate of IO could be explained by the use of frequent blood transfusion as primary or secondary prevention in SCD individuals with abnormal TCD or cerebrovascular event[14]. In our study population, none of these patients had recurrent strokes after the initial event.

Sixty-four percent of our study population had ACS, and 41.6% of patients with ACS also had IO. In this population, patients with IO were at a significantly higher risk of ACS. This relationship, at least in part, may be related to the use of simple blood transfusions to improve oxygen-carrying capacity in persons with symptomatic ACS, and to the urgent exchange transfusion performed when there is rapid progression of ACS [21,22].

The prevalence of DVT was 30.2% (74/245) in individuals with SCD, with a predominance in the female sex (66.2%), as has also been described in one other study[23]. A significant relationship between IO and DVT could be explained by the occurrence of a hypercoagulable state in individuals with SCD[24], driven by inflammation, in part due to oxidative stress and iron deposition-induced ferroptosis, leading to thrombogenesis and activation of the coagulation cascade in SCD individuals [25].

Epidemiological studies reveal that PH development is associated with iron overload and other comorbidities [26]. Chronic anemia in sickle cell disease results in cardiac chamber dilation and a compensatory increase in left ventricular mass. Elevated TRV as well as ferritin and the number of red blood cell units transfused, were also found to be associated with a higher risk of death [27]. In the current study, we found that the prevalence of IO associated with PH, as diagnosed by echocardiography, was 7.8%. Additionally, patients with IO were statistically more likely to have PH, with 68% of patients with PH also having IO.

In this study, there was no significant association between IO and other comorbidities such as anxiety and depression. However, we found a 40% prevalence of these mental health issues in the entire cohort of SCD patients. Depression is prevalent in adult patients with SCD and is associated with worse health-related quality of life, so an assessment of anxiety and depression in persons living with SCD is vitally important, given the prevalence of this comorbidity in the general SCD population [12,28].

The relationship between IO and acute kidney injury (AKI) and chronic kidney disease (CKD), although it was not significant in our study, may be a subject of further studies due to the risk of toxicity by iron chelation treatment with an elevated risk of mortality in SCD individuals [29]. Recently, ferroptosis has been implicated in the development of AKI/CKD, as renal cells are particularly vulnerable to IO [30].

Usually, follow-up of patients with SCD and IO is based on periodic MRI measurements of LIC and serum ferritin levels. The current study has demonstrated a strong correlation between LIC and ferritin levels above 2500 ng/mL, with a sensitivity of 78% and a specificity of 74%. This correlation is compatible with other studies [6]. Additionally, this threshold could indicate the need for chelation treatment if LIC cannot be performed [31]. However, when the serum ferritin level is less than 2500 ng/mL, it is less reliable as a marker of LIC. This may be related to serum ferritin levels being af-

fected by chronic inflammation in SCD. Especially during an acute exacerbation of a comorbidity or a vasoocclusive event, serum ferritin may be less reliable for estimating LIC [32]. Additionally, it is important to note that only one-third of the subjects in our study with SCD and elevated serum ferritin levels underwent MRI for LIC measurement, reflecting a lack of appropriate follow-up for screening, diagnosis, and treatment of IO. This observation is in agreement with other studies [31].

Liver enzymes, as a measure of liver function, correlated well with serum ferritin and LIC levels in the SCD cohort with IO. Alkaline phosphatase has been associated with mortality [19], and some studies have reported a correlation between serum ferritin and AST as an estimator of LIC. A serum ferritin/AST ratio >17 μg/U has been highly predictive of IO [33]. Nevertheless, in the population, routine screening of liver enzymes has poor sensitivity and specificity for detecting liver damage [34].

As shown in our study, IO is associated with a greater number of comorbidities. Thus, treating IO intuitively makes sense to reduce the risks associated with this condition. We found that DFX was the most commonly prescribed treatment for IO. Although 86% of IO patients in our study population were prescribed DFX, only 19% achieved ferritin levels <1000 ng/mL during the study period. According to other references [8,15,35], one factor contributing to a limited response to this treatment is poor adherence. While we did not assess compliance with chelation treatment as a cause of poor response in our study, treatment compliance is an important factor and should be evaluated when treating a patient for IO.

This study has several limitations: its observational, retrospective, and cross-sectional design, along with the reliance on medical record abstraction and the patient's self-report of symptoms, could introduce bias and affect the statistical power of the results. In some cases, the evolution of IO is represented solely by serial determinations of serum ferritin, without a matched LIC, and by periodic MRIs. Additionally, it was not distinguished whether the serum ferritin values were reported during vasoocclusive crisis or in the steady state of the patients, thus there is a risk that the vasooclusive event could confound elevated serum ferritin levels. It is well known that ferritin levels increase significantly during a vaso-occlusive crisis [9]. Information on toxicities related to DFX treatment was scarce and difficult to extract from the data records.

In conclusion, iron overload in SCD is a life-threatening condition, often associated with an increased number of comorbidities leading to a declining clinical course with an inadequate quality of life, hepatic complications and premature death. Management suggests that MRI screening for liver iron concentration should be performed every one to two years in patients with SCD receiving chronic transfusion therapy. Serum ferritin levels should be measured after each transfusion; this inexpensive blood test broadly correlates with total body iron burden and, due to its ease of acquisition, is a valuable tool for monitoring trends in iron burden over time [31]. A significant limitation for using ferritin levels as indicator of IO in SCD is that inflammation can raise ferritin levels irrespective of iron burden [2]. Providers should monitor patients and assess adherence with chelation therapy in the treatment of IO. Iron overload in SCD requires preventive care and close monitoring to avoid irreversible organ damage.

Funding

The Sickle Cell Disease Implementation Consortium (SCDIC) has been supported by US Federal Government agreement (167036) from the National Heart, Lung and Blood Institute.

Conflict of interest statement

Authors declare no conflicts of interest.

Ethical approval and informed consent

Institutional review board (IRB) approval was obtained from each of the eight study sites and a central IRB (CIRBI/Advarra) prior to data collection and written informed consent was obtained from each participant.

Consent for publication

Informed consent included agreement to have de-identified data published and disseminated in accordance with publication guidelines for the Sickle Cell Disease Implementation Consortium (SCDIC).

ORCID number of authors

- Gilberto Vizcaíno (GV): 0000-0003-2785-1879
- Christina Abrams (CA): 0000-0002-6296-3844
- Caroline Foster (CF): 0000-0002-3544-3261
- Hermes Flórez (HF): 0009-0003-3812-9926
- Natalia Dávila (ND): 0000-0004-2996-4919
- Sabrina Rainey (SR): 0000-0001-9717-7248

Authors contributions

GV drafted the manuscript and performed the statistical analyses. CA, CF, HF, ND and SR contributed to the concept and design of the study and revised manuscript drafts. All the authors critically reviewed and approved the manuscript.

REFERENCES

1. **Hassell KL.** Population Estimates of Sickle Cell Disease in the U.S. Am J Prev Med. 2010;38(4):S512-S521. *https://doi.org/10.1016/j.amepre.2009.12.022.*
2. **Chou ST, Alsawas M, Fasano RM, Field JJ, Hendrickson JE, Howard J, et al.** American Society of Hematology 2020 guidelines for sickle cell disease: transfusion support. Blood Adv. 2020; 28;4(2):327-355. *https://doi.org/10.1182/bloodadvances.2019001143.*
3. **Harmatz P, Butensky E, Quirolo K, Williams R, Ferrell L, Moyer T, et al.** Severity of iron overload in patients with sickle cell disease receiving chronic red blood cell transfusion therapy. Blood. 2000;96(1):76-79. *https://doi.org/10.1182/blood.V96.1.76.*
4. **Theocharidou E, Suddle AR.** The Liver in Sickle Cell Disease. Clin Liver Dis. 2019;23(2):177-189. *https://doi.org/10.1016/j.cld.2018.12.002.*
5. **Coates TD, Wood JC.** How we manage iron overload in sickle cell patients. Br J Haematol. 2017;177(5):703-716. *https://doi.org/10.1111/bjh.14575.*
6. **Badawy SM, Liem RI, Rigsby CK, Labotka RJ, DeFreitas RA, Thompson AA.** Assessing cardiac and liver iron overload in chronically transfused patients with sickle cell disease. Br J Haematol. 2016;175(4):705-713. *https://doi.org/10.1111/bjh.14277.*
7. **Porter J, Garbowski M.** Consequences and management of iron overload in sickle cell disease. Hematology Am Soc Hematol Educ Program. 2013;2013(1):447-456. *https://doi.org/10.1182/asheducation-2013.1.447.*
8. **Noetzli LJ, Coates TD, Wood JC.** Pancreatic iron loading in chronically transfused sickle cell disease is lower than in thalassaemia major. Br J Haematol. 2011;152(2):229-233. *https://doi.org/10.1111/j.1365-2141.2010.08476.x.*
9. **Marsella M, Borgna-Pignatti C.** Transfusional iron overload and iron chelation therapy in thalassemia major and sickle cell disease. Hematol Oncol Clin North Am 2014;28(4):703-727, vi. *https://doi.org/10.1016/j.hoc.2014.04.004.*
10. **Fung EB, Harmatz P, Milet M, Ballas SK, De Castro L, Hagar W, et al; Multi-Center Study of Iron Overload Research Group.** Morbidity and mortality in chronically transfused subjects with thalassemia and sickle cell disease: A report from the

multi-center study of iron overload. Am J Hematol. 2007;82(4):255-265. *https://doi.org/10.1002/ajh.20809*.

11. **Ballas SK.** Iron overload is a determinant of morbidity and mortality in adult patients with sickle cell disease. Semin Hematol. 2001;38 (1 Suppl 1):30-36. *https://doi.org/10.1016/S0037-1963(01)90058-7*.
12. **Njoku F, Pugh N, Brambilla D, Kroner B, Shah N, Treadwell M, et al.** Mortality in adults with sickle cell disease: Results from the sickle cell disease implementation consortium (SCDIC) registry. Am J Hematol. 2024;99(5):900-909. *https://doi.org/ 10.1002/ajh.27279*.
13. **Piel FB, Jobanputra M, Gallagher M, Weber J, Laird SG, McGahan M.** Co-morbidities and mortality in patients with sickle cell disease in England: A 10-year cohort analysis using hospital episodes statistics (HES) data. Blood Cells Mol Dis. 2021; 89:102567. *https://doi.org/10.1016/j.bcmd.2021.102567*.
14. **Webb J, Kwiatkowski JL.** Stroke in patients with sickle cell disease. Expert Rev Hematol. 2013;6(3):301-316. *https://doi.org/10.1586/ehm.13.25*.
15. **van Tuijn CFJ, Schimmel M, Van Beers EJ, Nur E, Biemond BJ.** Prospective evaluation of chronic organ damage in adult sickle cell patients: A seven-year follow-up study. Am J Hematol. 2017;92(10):E584-E590. *https://doi.org/10.1002/ajh.24855*.
16. **Fortuna V, Lima J, Oliveira GF, Oliveira YS, Getachew B, Nekhai S, et al.** Ferroptosis as an emerging target in sickle cell disease. Curr Res Toxicol. 2024;7:100181. *https://doi.org/10.1016/j.crtox.2024.100181*.
17. **DiMartino LD, Baumann AA, Hsu LL, Kanter J, Gordeuk VR, Glassberg J, et al; Sickle Cell Disease Implementation Consortium.** The sickle cell disease implementation consortium: Translating evidence-based guidelines into practice for sickle cell disease. Am J Hematol. 2018;93(12):E391-E395. *https://doi.org/10.1002/ajh.25282*.
18. **Garcia-Casal MN, Pasricha SR, Martinez RX, Lopez-Perez L, Peña-Rosas JP.** Serum or plasma ferritin concentration as an index of iron deficiency and overload. Cochrane Database Syst Rev. 2021;5(5): Cd011817. *https://doi.org/10.1002/14651858.CD011817*.
19. **Feld JJ, Kato GJ, Koh C, Shields T, Hildesheim M, Kleiner DE, et al.** Liver injury is associated with mortality in sickle cell disease. Aliment Pharmacol Ther. 2015;42(7):912-921. *https://doi.org/10.1111/apt.13347*.
20. **Verduzco LA, Nathan DG.** Sickle cell disease and stroke. Blood. 2009;114(25):5117-5125. *https://doi.org/10.1182/blood-2009-05-220921*.
21. **Yawn BP, Buchanan GR, Afenyi-Annan AN, Ballas SK, Hassell KL, James AH, et al.** Management of sickle cell disease: summary of the 2014 evidence-based report by expert panel members. JAMA. 2014;312(10):1033-1048. *https://doi.org/10.1001/jama.2014.10517*. Erratum in: JAMA. 2015;313(7):729.
22. **Estcourt LJ, Hopewell S, Trivella M, Hambleton IR, Cho G.** Regular long-term red blood cell transfusions for managing chronic chest complications in sickle cell disease. Cochrane Database Syst Rev. 2019;2019(10):CD008360. *https://doi.org/10.1002/14651858.cd008360.pub5*.
23. **Brunson A, Lei A, Rosenberg AS, White RH, Keegan T, Wun T.** Increased incidence of VTE in sickle cell disease patients: risk factors, recurrence and impact on mortality. Br J Haematol. 2017;178(2):319-326. *https://doi.org/10.1111/bjh.14655*.
24. **Naik RP, Streiff MB, Haywood C, Nelson JA, Lanzkron S.** Venous Thromboembolism in Adults with Sickle Cell Disease: A serious and under-recognized complication. Am J Med. 2013;126(5):443-449. *https://doi.org/10.1016/j.amjmed.2012.12.016*.
25. **Ma H, Huang Y, Tian W, Liu J, Yan X, Ma L, Lai J.** Endothelial transferrin receptor 1 contributes to thrombogenesis through cascade ferroptosis. Redox Biol. 2024; 70:103041. *https://doi.org/10.1016/j.redox.2024.103041*.
26. **Gladwin MT, Sachdev V.** Cardiovascular abnormalities in sickle cell disease. J Am Coll

Cardiol. 2012;59 (13):1123-1133. *https://doi.org/10.1016/j.jacc.2011.10.900*.

27. **Gladwin MT, Barst RJ, Gibbs JS, Hildesheim M, Sachdev V, Nouraie M, et al, walk-PHaSST Investigators and Patients.** Risk factors for death in 632 patients with sickle cell disease in the United States and United Kingdom. PLoS One. 2014;9(7):e99489. *https://doi.org/10.1371/journal.pone.0099489*.
28. **Adam SS, Flahiff CM, Kamble S, Telen MJ, Reed SD, De Castro LM.** Depression, quality of life, and medical resource utilization in sickle cell disease. Blood Adv. 2017;1(23):1983-1992. *https://doi.org/10.1182/bloodadvances.2017006940*
29. **Kang H, Han M, Xue J, Baek Y, Chang J, Hu S, et al.** Renal clearable nanochelators for iron overload therapy. Nat Commun 2019;10(1):5134. *https://doi.org/10.1038/s41467-019-13143-z.*
30. **Li S, Han Q, Liu C, Wang Y, Liu F, Pan S, et al.** Role of ferroptosis in chronic kidney disease. Cell Commun Signal. 2024;22(1):113. *https://doi.org/10.1186/s12964-023-01422-8.*
31. **Wilson SR, Sears M, Williams E, Drapekin J, Sivakumar I, Padrino S, et al. GRNDaD investigators.** Gaps in the diagnosis and management of iron overload in sickle cell disease: a 'real-world' report from the GRNDaD registry. Br J Haematol. 2021;195(5):e157-e160. *https://doi.org/10.1111/bjh.17762*.
32. **Puliyel M, Sposto R, Berdoukas VA, Hofstra TC, Nord A, Carson S, et al.** Ferritin trends do not predict changes in total body iron in patients with transfusional iron overload. Am J Hematol. 2014;89(4):391-394. *https://doi.org/ 10.1002/ajh.23650.*
33. **Cippà PE, Boucsein I, Adams H, Krayenbuehl PA.** Estimating Iron Overload in Patients with Suspected Liver Disease and Elevated Serum Ferritin. Am J Med. 2014;127(10):1011.e1-1011.e3. *https://doi.org/ 10.1016/j.amjmed.2014.03.016.*
34. **Ginès P, Castera L, Lammert F, Graupera I, Serra-Burriel M, Allen AM, et al. LiverScreen Consortium Investigators.** Population screening for liver fibrosis: Toward early diagnosis and intervention for chronic liver diseases. Hepatology. 2022;75(1):219-228. *https://doi.org/10.1002/hep.32163.*
35. **Porter J, Bowden DK, Economou M, Troncy J, Ganser A, Habr D, et al.** Health-Related Quality of Life, Treatment Satisfaction, Adherence and Persistence in β-Thalassemia and Myelodysplastic Syndrome Patients with Iron Overload Receiving Deferasirox: Results from the EPIC Clinical Trial. Anemia. 2012;2012:297641. *https://doi.org/*10.1155/2012/297641.

Invest Clin 66(4): 390- 407, 2025 https://doi.org/10.54817/IC.v66n4a04

Comprehensive analysis of autophagy- and glycolysis-related differentially expressed genes involved in chronic inflammation in obese patients.

Simin Yang[1], Rexidanmu Hudabai[1] and Xinwei Su[2]

[1]Department of Anesthesiology, The Fifth Affiliated Hospital of Sun Yat-sen University, Zhuhai, Guangdong, China.
[2]Department of Obstetrics and Gynecology, The Fifth Affiliated Hospital of Sun Yat-sen University, Zhuhai, Guangdong, China.

Keywords: Obesity; Autophagy; Glycolysis; Inflammation.

Abstract. The interaction between glycolysis and autophagy contributes to reprogramming chronic inflammation in obesity, but the knowledge about this interaction remains limited. Publicly available data were used to analyze autophagy- and glycolysis-related differentially expressed genes (A&GRDEGs) in two datasets comparing patients with obesity and normal-weight patients. A total of 5 A&GRDEGs were obtained through screening, namely recombinant eukaryotic translation initiation factor 4E binding protein 1 *(EIF4EBP1)*, transforming growth factor beta 1 *(TGFB1)*, fatty acid synthase *(FASN)*, alpha-synuclein *(SNCA)*, and C-X-C chemokine receptor 4 *(CXCR4)*. Levels of autophagy and glycolysis exhibit substantial predictive value for obesity development and mechanistically contribute to disease pathogenesis through immunometabolic dysregulation.

Corresponding author: Xinwei Su. Department of Obstetrics and Gynecology, The Fifth Affiliated Hospital of Sun Yat-sen University, 52 Meihua East Road, Zhuhai, Guangdong 519000, China. Tel: +86 0756 2528453.
Email: XXinnwei_ss@outlook.com

Análisis exhaustivo de los genes expresados diferencialmente, relacionados con la autofagia y la glucólisis, que intervienen en la inflamación crónica en pacientes obesos.

Invest Clin 2025; 66 (4): 390 – 407

Palabras clave: Obesidad; Autofagia; Glucólisis; Inflamación.

Resumen. La interacción entre la glucólisis y la autofagia contribuye a la reprogramación de la inflamación crónica en la obesidad, pero el conocimiento sobre esta interacción es limitado. Se utilizaron datos públicamente disponibles para analizar los genes expresados diferencialmente relacionados con la autofagia y la glucólisis (A&GRDEG) entre pacientes con obesidad y con peso normal en dos conjuntos de datos. Se obtuvo un total de 5 A&GRDEG mediante cribado, a saber: la proteína recombinante de unión al factor de iniciación de la traducción eucariótica 4E 1 (EIF4EBP1), el factor de crecimiento transformante beta 1 (TGFB1), la sintasa de ácidos grasos (FASN), la alfa-sinucleína (SNCA) y el receptor de quimiocina C-X-C 4 (CXCR4). Los niveles de autofagia y de glucólisis mostraron un valor predictivo elevado para el desarrollo de la obesidad y contribuyen mecánicamente a la patogénesis de la enfermedad mediante la desregulación inmunometabólica.

Received: 03-08-2025 Accepted: 21-09-2025

INTRODUCTION

According to projections, the global population of people living with obesity, a metabolic syndrome, will reach one billion by 2030, affecting one in five women and one in seven men [1] Obesity is characterized by excess weight (body mass index, BMI ≥30 kg/m^2), accompanied by chronic low-grade inflammation, oxidative stress, insulin resistance, hypertension, dyslipidemia, and other abnormalities. It could also increase the susceptibility of individuals to chronic diseases, such as type 2 diabetes mellitus (T2DM), non-alcoholic fatty liver disease (NAFLD), and specific malignancies [2]. Furthermore, adipocytes serve as central metabolic and inflammatory regulators through their endocrine capacity, secreting both pro- and anti-inflammatory mediators, including leptin (pro-inflammatory) and adiponectin (anti-inflammatory), which systemically influence energy homeostasis and immune responses[1]. Leptin and adiponectin exert pro-inflammatory and anti-inflammatory functions, respectively, and mutually regulate carcinogenesis [2].

Adequate lipid storage prevents ectopic lipid accumulation in non-specific organs (e.g. muscle, liver, and heart) and toxic lipid accumulation (e.g., lipotoxicity) and is also associated with stable metabolic function [3]. Lipid droplet accumulation in the liver and other organs has been linked with obesity-associated autophagic dysfunction [4]. The seminal recognition of autophagy through the 2016 Nobel Prize in Physiology or Medicine underscores its pivotal role as a fundamental cellular clearance mechanism for superfluous or deleterious constituents[5]. Chronic inflammation in individuals with obesity may suppress autophagy. Moreover,

obesity-associated autophagic dysfunction may cause protein and organelle degradation, cellular dysfunction, and cell death [6]. Autophagy is presumed to be inactive during obesity owing to the chronic upregulation of mammalian target of rapamycin complex 1 (mTORC1) [7]. Obesity could contribute to an elevated risk of cancer through autophagic impairment; thus, treatment methods involving the enhancement of autophagy may serve as a practical approach against obesity-associated cancers [8].

Metabolism is widely known as a core process underpinning all biological phenomena, supplying energy and building blocks for macromolecules [9]. Restricting glycolysis has been shown to impede cytokine production but not cellular proliferation, suggesting that glycolysis plays a critical role in regulating inflammation [10]. However, information on the exact mechanism by which the interaction between glycolysis and autophagy contributes to reprogramming the progression of chronic inflammation in obesity remains limited.

Individuals with obesity exhibit adipocyte hypoxia, which could lead to the elevated expression of hypoxia-inducible factors, activation of adipocytes, production and release of free fatty acids and pro-inflammatory mediators, induction of circulating monocyte recruitment, and aggregation of adipose tissue macrophages [11]. Studies have revealed that individuals with obesity have a higher macrophage count in white adipose tissues than individuals with normal BMI, showing increases ranging from 10% to >50% of the total cell count [12]. Metabolically activated macrophages show a higher rate of glycolysis and produce more lactic acid in the fatty tissues of individuals with obesity than in the tissues of normal-weight individuals [13]. Alterations in immune cell infiltration dynamics and their secretion of pro-inflammatory cytokines critically contribute to the sustained low-grade inflammation observed in obesity. Consequently, targeting immune cell recruitment and activation has emerged as a key therapeutic strategy for obesity-associated chronic inflammation [14].

In this study, screening was first performed to identify genes frequently involved in autophagy and glycolysis. Next, we leveraged publicly available datasets to compare the expression profiles of autophagy- and glycolysis-related genes between obese and normal-weight individuals. Additionally, we assessed immune cell infiltration patterns and examined their correlations with the differentially expressed genes. These findings could help elucidate the key mechanisms underlying the pathogenesis of chronic inflammation in patients with obesity and provide potential targets for prevention and treatment.

MATERIALS AND METHODS

Dataset download and processing

We obtained two obesity-related gene expression datasets (GSE134913 [15] and GSE59034 [16]) from the Gene Expression Omnibus (GEO) database (https://www.ncbi.nlm.nih.gov/geo/). The GSE134913 dataset included samples. We included 14 pre-surgery samples from obese patients (Obese group) who underwent metabolic surgery and six controls (Control group), forming a subset of 20 samples.

The GSE134913 dataset is a subset of participants from the GSE135066 cohort. It comes from the clinical study "Dynamic Changes in Muscle Insulin Sensitivity after Metabolic Surgery" by Gancheva et al. [15]. The original cohort included six control subjects and 16 obese individuals who had metabolic surgery, with longitudinal gene expression profiling done at three timepoints: before surgery, two weeks after surgery, and 52 weeks after surgery. For this analysis, we included all six control subjects and 14 of the 16 obese participants who had surgery, based on data completeness criteria.

Although aggregate baseline characteristics of the entire cohort are provided in the original publication, detailed demographic and clinical metadata for the specific genet-

ic sequencing subset were unavailable. As a result, participant-level clinical information could not be included in our analyses.

The GSE59034 dataset contained 48 samples. We selected 16 pre-surgery obese samples and 16 controls, yielding a total of 32 samples. This dataset served as the primary cohort for all subsequent analyses. Detailed information about the datasets is provided in Table S1.

Autophagy-related genes (ARGs) and glycolysis-related genes (GRGs) were systematically identified through comprehensive searches of the GeneCards database (https://www.genecards.org), followed by literature validation using PubMed (https://pubmed.ncbi.nlm.nih.gov/) with "Autophagy" [17-19] and "Glycolysis" [20-22] as the primary search terms, respectively. The intersection of ARGs and GRGs defined the autophagy- and glycolysis-related genes (A&GRGs) used in this study (Fig. 1).

Differentially expressed genes analysis

Based on the original study designs, samples were stratified into control and obese groups. Differentially expressed genes (DEGs) were identified using the limma package (v3.58.1) in R (v4.2.2), with significance defined as $|\log FC| > 0.5$ and $p<0.05$. Results were visualized through volcano plots (ggplot2, v3.4.4).

To obtain the autophagy- and glycolysis-related differentially expressed genes (A&GRDEGs), we first intersected all significant DEGs with our curated list of A&GRGs, and a Venn diagram was plotted to provide the A&GRDEGs. Expression patterns of these A&GRDEGs were subsequently displayed as clustered heatmaps (pheatmap package, v1.0.12) in R, using z-score normalized expression values.

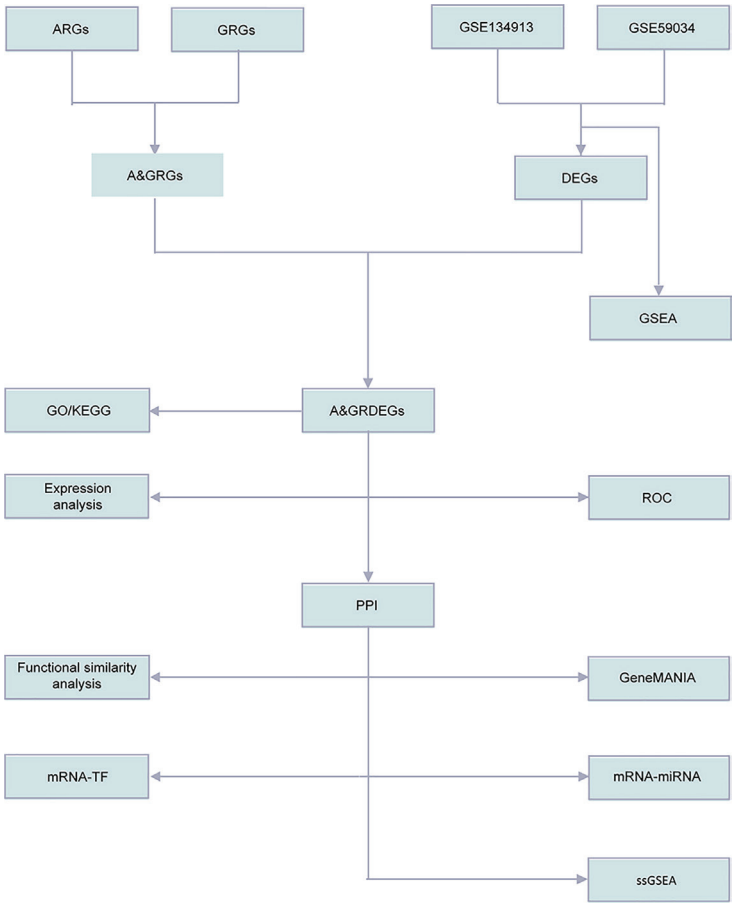

Fig. 1. Technology roadmap.

ARGs, Autophagy Related Genes. GRGs, Glycolysis Related Genes. A&GRGs, Autophagy & Glycolysis Related Genes. A&GRDEGs, Autophagy & Glycolysis Related Differentially Expressed Genes. DEGs, Differentially expressed genes. GSEA, Gene Set Enrichment Analysis. GO, Gene Ontology. KEGG, Kyoto Encyclopedia of Genes and Genomes. ssGSEA, single-sample gene-set enrichment Analysis. ROC, receiver operating characteristic curve. PPI, Protein-protein interaction network. TF, Transcription factors.

Gene ontology and Kyoto Encyclopedia of Genes and Genomes pathway enrichment analyses

Functional enrichment analysis was performed using the clusterProfiler package (v4.10.0) in R. Gene Ontology (GO) and Kyoto Encyclopedia of Genes and Genomes (KEGG) pathway analyses were conducted on the differentially expressed genes. Terms with $p<0.05$ and false discovery rate (FDR; q) <0.25 were considered statistically significant.

Gene Set Enrichment Analysis

Gene Set Enrichment Analysis (GSEA) was conducted on the GSE59034 dataset using the clusterProfiler package. Genes were ranked by $\log_2$ fold-change and analyzed against the 'c2.all.v2022.1.Hs.symbols.gmt' gene set (All Canonical Pathways, n=3,050) from MSigDB, with *Homo sapiens* as the reference species. Significance thresholds were set at $p<0.05$ and q <0.25.

Differential expression and receiver operating characteristic analyses of A&GRDEGs

The expression patterns of A&GRDEGs were compared between the obese and control groups across both datasets. The diagnostic potential was evaluated using receiver operating characteristic (ROC) analysis performed with the pROC package (v1.18.5). Area under the curve (AUC) values were determined to measure the predictive ability.

Analysis of immune infiltration

Immune cell infiltration levels were quantified using single-sample Gene Set Enrichment Analysis (ssGSEA) implemented in the GSVA package (v1.50.0). Correlations among differentially abundant immune cell populations (obese vs. control), and between immune cells and A&GRDEG expression, were analyzed in the GSE59034 dataset. Results were visualized as correlation dot plots (ggplot2).

Statistical analysis

All statistical analyses were conducted using R software (R Foundation for Statistical Computing, Vienna, Austria). Continuous variables were compared with Student's t-test (for normally distributed data) or Wilcoxon rank-sum test (for non-normal data). Multi-group comparisons employed the Kruskal-Wallis test. Categorical variables were analyzed with χ^2 tests or Fisher's exact tests, depending on the situation. Correlations were assessed with Spearman's rank correlation. A two-tailed α level of 0.05 was deemed statistically significant unless otherwise noted.

RESULTS

Identification of A&GRDEGs

Differential expression analysis revealed 628 significant DEGs ($|\log FC| > 0.5$ and $p<0.05$) in the GSE134913 dataset, comprising 316 upregulated and 312 downregulated genes (Fig. 2A). The GSE59034 dataset showed more pronounced differential expression with 904 DEGs under the same thresholds (653 upregulated, 251 downregulated; Fig. 2B). Volcano plots visually represent these expression patterns, highlighting the asymmetric distribution of upregulated versus downregulated genes between datasets.

To identify the A&GRDEGs, we intersected the significant DEGs ($|\log FC| > 0.5$ and $p<0.05$) from both datasets with our curated A&GRG list, revealing five overlapping genes (Fig. 2C): eukaryotic translation initiation factor 4E binding protein 1 *(EIF4EBP1)*, transforming growth factor beta 1 *(TGFB1)*, fatty acid synthase *(FASN)*, alpha-synuclein *(SNCA),* and C-X-C chemokine receptor type 4 *(CXCR4)* (Table 1). We subsequently analyzed and visualized the differential expression patterns of these A&GRDEGs between sample groups in the GSE134913 dataset (Fig. 2D) and in the GSE59034 dataset (Fig. 2E).

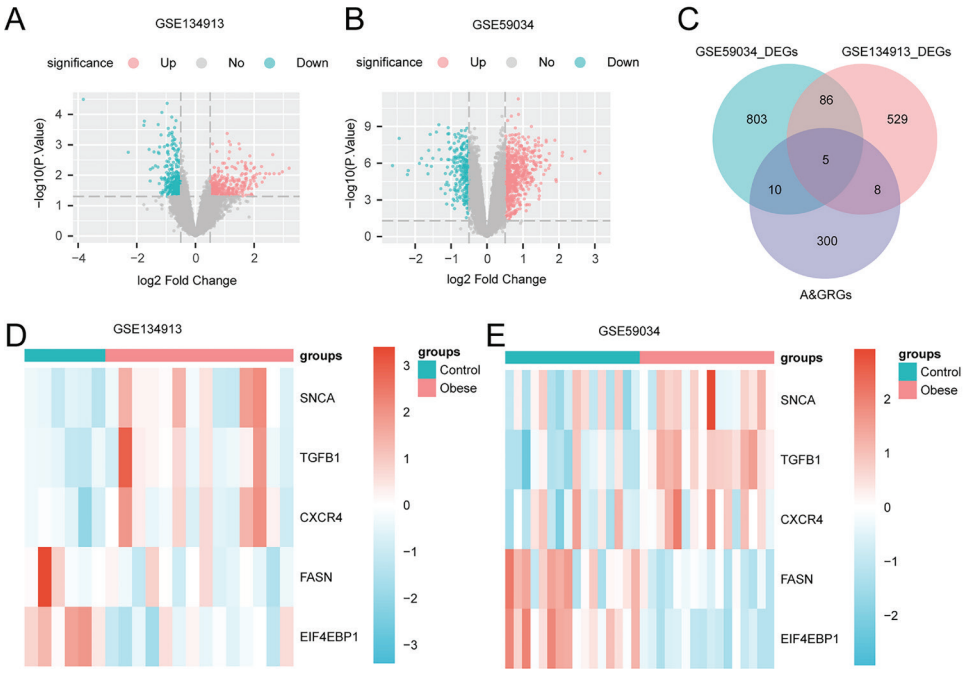

Fig. 2. Differentially expressed genes (DEGs) analysis.
(A) Volcano plot of differential analysis results between the obese and control groups in the GSE134913 dataset. (B) Volcano plot of differential analysis results between the obese and control groups in the GSE59034 dataset. (C) Venn diagram of DEGs in the GSE134913 and GSE59034 datasets and A&GRGs. (D) Differential expression heatmap of DEGs in the GSE134913 dataset. (E) Differential expression heatmap of DEGs in the GSE59034 dataset. Green indicates the control group, and orange indicates the obese group. In the heatmaps, blue represents low expression, and red represents high expression.

Table 1. A&GRDEGs in GSE59034 and GSE134913.

	Gene	logFC	AveExpr	t	p	p adjust	B	group
	EIF4EBP	-0.75697	6.168652	-7.58047	8.52E-09	3.51E-06	10.16121	down
	TGFB1	0.571166	6.797319	5.933876	1.06E-06	4.33E-05	5.525466	up
GSE59034	FASN	-0.64127	10.46345	-4.02795	0.0003	0.002172	0.123576	down
	SNCA	0.596172	7.741707	2.504538	0.017237	0.049432	-3.63114	up
	CXCR4	0.512738	6.194027	2.197896	0.034888	0.085782	-4.25343	up
	EIF4EBP	-0.79216	9.560483	-4.21636	0.00039	0.901994	-3.5489	down
	SNCA	1.325622	9.526431	2.616228	0.016162	0.999958	-4.10701	up
GSE134913	CXCR4	0.785232	7.648631	2.278605	0.033299	0.999958	-4.22823	up
	TGFB1	1.137448	6.567356	2.192964	0.039755	0.999958	-4.25833	up
	FASN	-0.57511	7.727896	-2.11711	0.046404	0.999958	-4.28468	down

Construction and analysis of the prediction model

We systematically investigated the functional associations of the five A&GRDEGs with obesity through comprehensive GO and KEGG enrichment analyses (Table 2). GO analysis identified significant enrichment in biological processes (BP) such as positive regulation of glial cell differentiation, receptor metabolic process, and gliogenesis; cellular

Table 2. Gene Ontology (GO) and Kyoto Encyclopedia of Genes and Genomes (KEGG) enrichment analysis results.

Ontology	ID	Description	Gene Ratio	Bg Ratio	p	p adjust	q	geneID	Count
BP	GO:0032103	positive regulation of response to external stimulus	3/5	442/18800	0.00012461	0.02430796	0.00669754	TGFB1/SNCA/CXCR4	3
BP	GO:0045687	positive regulation of glial cell differentiation	2/5	42/18800	4.8517E-05	0.02430796	0.00669754	TGFB1/CXCR4	2
BP	GO:0043112	receptor metabolic process	2/5	61/18800	0.00010291	0.02430796	0.00669754	TGFB1/SNCA	2
BP	GO:0014015	positive regulation of gliogenesis	2/5	64/18800	0.00011333	0.02430796	0.00669754	TGFB1/CXCR4	2
BP	GO:2000379	positive regulation of reactive oxygen species metabolic process	2/5	71/18800	0.0001396	0.02430796	0.00669754	TGFB1/SNCA	2
CC	GO:0031091	platelet alpha granule	2/5	91/19594	0.0002114	0.00718767	0.00400552	TGFB1/SNCA	2
CC	GO:0031092	platelet alpha granule membrane	1/5	17/19594	0.00433098	0.07362671	0.04103037	SNCA	1
CC	GO:0031093	platelet alpha granule lumen	1/5	67/19594	0.01698227	0.08811426	0.04910392	TGFB1	1
CC	GO:0016234	inclusion body	1/5	74/19594	0.01874314	0.08811426	0.04910392	SNCA	1
CC	GO:0005902	microvillus	1/5	90/19594	0.0227585	0.08811426	0.04910392	TGFB1	1
MF	GO:0003779	actin binding	2/5	439/18410	0.00540893	0.04141684	0.01278836	SNCA/CXCR4	2
MF	GO:0008190	eukaryotic initiation factor 4E binding	1/5	10/18410	0.00271326	0.04141684	0.01278836	EIF4EBP1	1
MF	GO:0034713	Type I transforming growth factor beta receptor binding	1/5	10/18410	0.00271326	0.04141684	0.01278836	TGFB1	1
MF	GO:0004312	fatty acid synthase activity	1/5	13/18410	0.00352609	0.04141684	0.01278836	FASN	1
MF	GO:0043027	cysteine-type endopeptidase inhibitor activity involved in the apoptotic process	1/5	22/18410	0.0059614	0.04141684	0.01278836	SNCA	1
KEGG	hsa04672	Intestinal immune network for IgA production	2/5	49/8164	0.00034888	0.02163052	0.01652586	TGFB1/CXCR4	2
KEGG	hsa04152	AMPK signaling pathway	2/5	121/8164	0.00211594	0.05414617	0.04136804	FASN/EIF4EBP1	2

Table 2. CONTINUATION

Ontology	ID	Description	Gene Ratio	Bg Ratio	p	p adjust	q	geneID	Count
KEGG	hsa04910	Insulin signaling pathway	2/5	137/8164	0.00270445	0.05414617	0.04136804	FASN/EIF4EBP1	2
KEGG	hsa04218	Cellular senescence	2/5	156/8164	0.0034933	0.05414617	0.04136804	TGFB1/EIF4EBP1	2
KEGG	hsa05163	Human cytomegalovirus infection	2/5	225/8164	0.00715783	0.08875712	0.06781104	CXCR4/EIF4EBP1	2

BP: biological process; CC: cellular component; MF: molecular function.

components (CC) such as platelet alpha granule and its subcompartments (membrane, lumen); molecular functions (MF) such as fatty acid synthase activity, TGF-β receptor type I binding, and eukaryotic initiation factor 4E binding. KEGG pathway analysis revealed involvement in the intestinal immune network for IgA production, the insulin signaling pathway, and the AMP-activated protein kinase (AMPK) signaling pathway. Results were visualized as bar charts (Fig. 3A) and bubble plots (Fig. 3B), and functional networks were constructed for BP (Fig. 3C), MF (Fig. 3D), CC (Fig. 3E), and KEGG pathways (Fig. 3F).

Results of Gene Set Enrichment Analysis (GSEA)

GSEA of the GSE59034 dataset revealed significant associations between global gene expression patterns and key biological processes (Fig. 4A), including interleukin-10 signaling (Fig. 4B), neutrophil degranulation (Fig. 4C), Leishmania infection responses (Fig. 4D), and proinflammatory/profibrotic mediator networks (Fig. 4E). These findings, detailed in Table S2, demonstrate broad enrichment in immune-metabolic pathways, highlighting their potential role in obesity-related pathophysiology.

Differential expression and ROC analyses of A&GRDEGs

Wilcoxon rank-sum tests revealed significant differential expression ($p<0.05$) of three A&GRDEGs (*EIF4EBP1*, *TGFB1*, *SNCA*) between obese and control groups in the GSE134913 dataset (Fig. 5A). ROC analysis demonstrated strong diagnostic potential for *EIF4EBP1* (AUC = 0.921, Fig. 5D) and moderate predictive accuracy for *FASN* (AUC = 0.750), *SNCA* (AUC = 0.833), *TGFB1* (AUC = 0.798), and *CXCR4* (AUC = 0.762) (Fig. 5C-E), with AUC values indicating their utility as potential biomarkers for obesity classification.

Consistent analysis of the GSE59034 dataset revealed significant differential expression ($p<0.05$) for all five A&GRDEGs between obese and control groups (Fig. 5B). ROC analysis demonstrated excellent diagnostic performance for *EIF4EBP1* (AUC = 0.980) and *TGFB1* (AUC = 0.910), moderate accuracy for *FASN* (AUC = 0.828), and limited predictive value for *SNCA* (AUC = 0.699) and *CXCR4* (AUC = 0.691) (Fig. 5F-H).

Analysis of immune cell infiltration

Comparative analysis of immune cell infiltration using Wilcoxon rank-sum tests revealed significant abundance differences ($p<0.05$) for 26 of 28 immune cell types between obese and control groups in the GSE59034 dataset (Fig. 6A). Correlation analysis of these differentially abundant immune populations identified a particularly strong positive association (r = 0.98) between activated dendritic cells and myeloid-derived suppressor cells (MDSCs) (Fig. 6B).

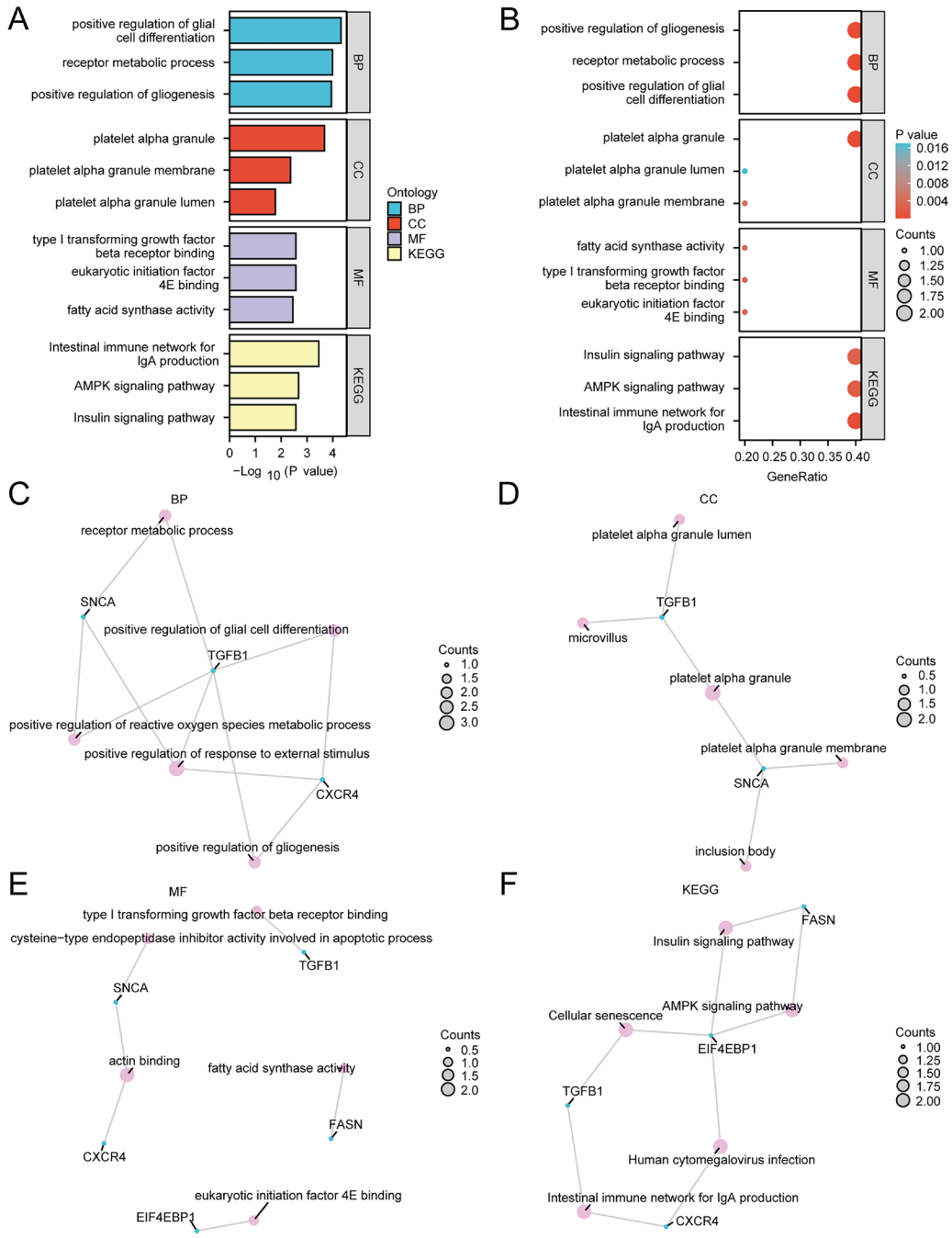

Fig. 3. GO and KEGG analyses.

(A) Bar charts of GO and KEGG analysis results for A&GRDEGs. The vertical axis shows GO and KEGG terms. (B) Bubble charts of GO and KEGG analysis results for A&GRDEGs. The vertical axis shows GO and KEGG terms. (C–E) Network diagrams of GO enrichment analysis for A&GRDEGs (C: BP, D: CC, E: MF). (F) Network diagrams of KEGG enrichment analysis for A&GRDEGs. In the network diagrams (C–F), pink dots represent specific pathways and blue dots represent specific genes. In the bubble charts, the bubble size represents the number of genes, and the bubble color represents the p-value, with redder hues indicating smaller values and bluer hues indicating larger values. The screening criteria for GO and KEGG analyses were $p<0.05$ and $q<0.25$.

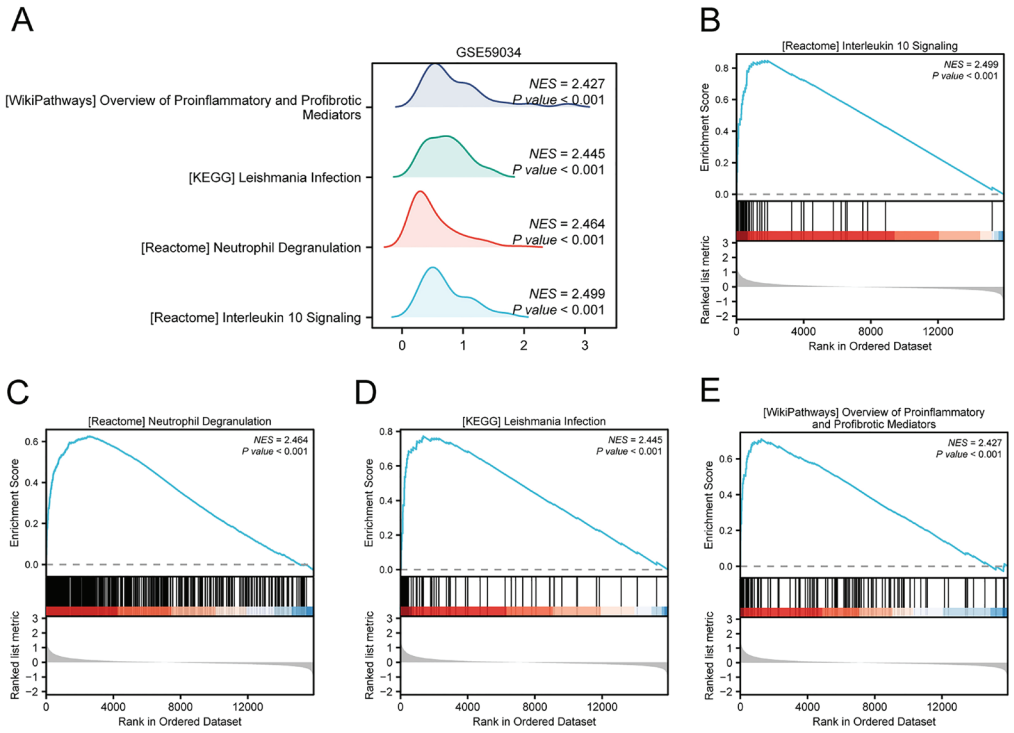

Fig. 4. GSEA of the GSE59034 dataset.

(A) Ridgeline plots of the four main biological functions in GSEA for the GSE59034 dataset. (B–E) Genes in the GSE59034 dataset were significantly enriched in interleukin 10 signaling (B), neutrophil degranulation (C), leishmania infection (D) and overview of proinflammatory and profibrotic mediators (E). The screening criteria for GSEA were $p<0.05$ and $q<0.25$. NES, normalized enrichment score.

Correlation analysis between the 26 differentially abundant immune cell types and A&GRDEG expression levels in GSE59034 revealed a strong positive association between *TGFB1* expression and MDSC infiltration (r = 0.94), and a significant negative correlation between *EIF4EBP1* levels and Th1 cell abundance (r = -0.87) (Fig. 6C).

DISCUSSION

The continuous rise of the obesity rate requires multifaceted and effective prevention and treatment. Inflammatory programs are activated during the early stages of adipose tissue expansion and during chronic obesity, thus perpetuating a proinflammatory phenotype in the immune system. This metabolic dysregulation may elevate the risk of developing severe comorbidities, including insulin resistance, T2DM, cardiovascular disease, NAFLD, certain malignancies, and neurodegenerative disorders [23]. Inhibition of glycolysis has been shown to suppress macroautophagy and chaperone-mediated autophagy, leading to increased lipid accumulation [24]. The mechanisms of both autophagy and glycolysis in obesity-associated diseases are currently hot topics in research. Further research on the regulatory mechanisms of autophagy and the effects of glycolysis levels on obesity and chronic inflammation will help formulate more effective treatment strategies for obesity control.

By phosphorylating the EIF4EBP1, mTOR could dissociate from eIF4E and promote the initiation of translation [25]. Therefore, EIF4EBP1 is believed to be closely related to a wide range of diseases through its regulation of autophagy and glycolysis[26,27].

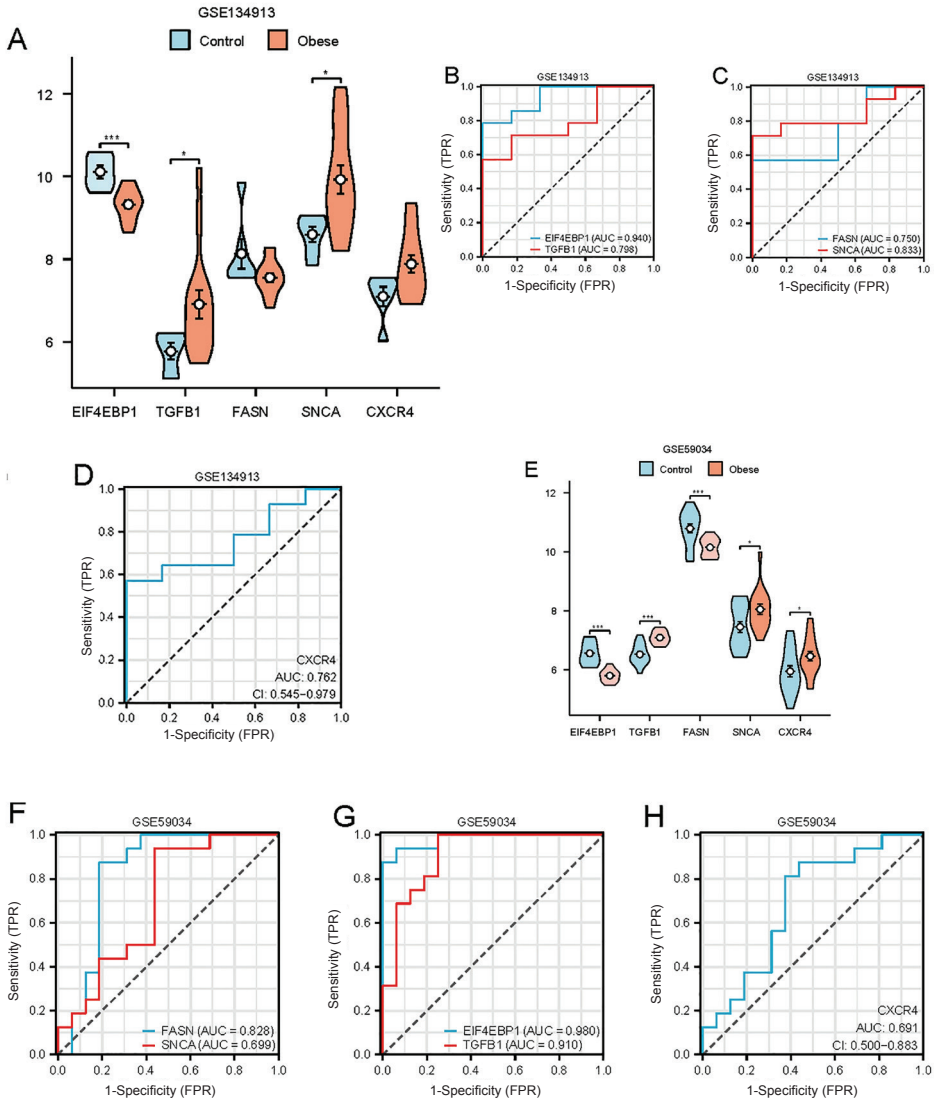

Fig. 5. Differential expression and ROC analyses of A&GRDEGs.

(A) Group comparison plot of A&GRDEGs between the obese and control groups in the GSE134913 dataset. (B) Group comparison plot of A&GRDEGs between the obese and control groups in the GSE59034 dataset. (C–E) ROC curves of A&GRDEGs: *FASN* and *SNCA* (C), *EIF4EBP1* and *TGFB1* (D), and *CXCR4* (E) between different groups (obese or control) in the GSE134913 dataset. (F-H) ROC curves of A&GRDEGs: *FASN* and *SNCA* (F), *EIF4EBP1* and *TGFB1* (G), and *CXCR4* (H) between different groups (obese or control) in the GSE59034 dataset. *$p<0.05$; ***$p<0.001$.

Experimental studies demonstrate that mTOR target proteins EIF4EBP1 and EIF-4EBP2 play critical roles in metabolic regulation. Genetic ablation of both EIF4EBP1 and EIF4EBP2 exacerbates diet-induced obesity in murine models [28]. Conversely, enhanced EIF4EBP1 activity in skeletal muscle confers metabolic protection, mitigating age- and diet-induced insulin resistance while maintaining energy expenditure. This protective effect is associated with reduced white adipose tissue accumulation and preserved brown adipose tissue mass [29]. The above results are consistent with the findings of this

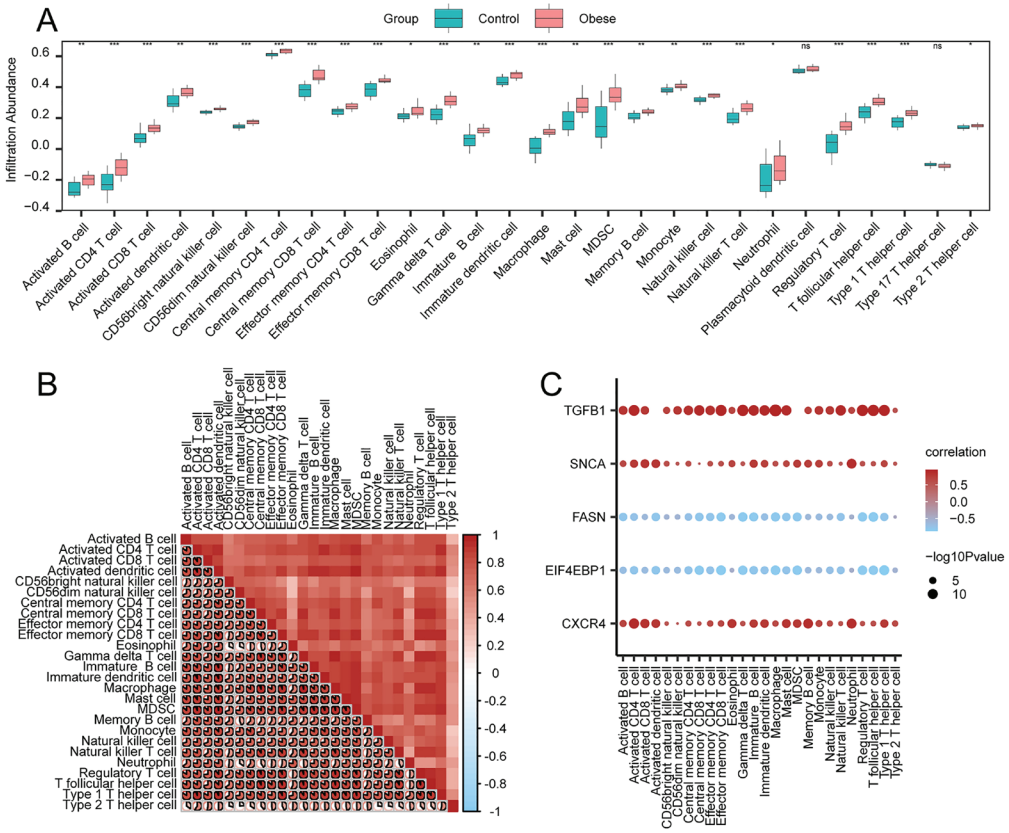

Fig. 6. ssGSEA of the GSE59034 dataset.

(A) Group comparison box plots of immune cells under the obese and control groups in the GSE59034 dataset. (B) Heatmap of correlations among the 26 immune cell types with significant differences in the GSE59034 dataset. (C) Correlation dot plot between the expression levels of A&GRDEGs and the abundance of 26 infiltrating immune cell types. Red indicates positive correlation and blue indicates negative correlation, with the shade of color indicating the strength of correlation. ns $p \geq 0.05$; * $p < 0.05$; ** $p < 0.01$; *** $p < 0.001$.

study, EIF4EBP1 is closely related to the regulatory mechanisms of obesity and chronic inflammation. However, the mechanisms by which EIF4EBP1 regulates obesity and chronic inflammation through autophagy and glycolysis require further study.

Patients with hyperlipidemia exhibit elevated levels of TGF-β1, which could suppress the function of natural killer (NK) cells, whereas restoring NK cell function could improve the prognosis of patients with metabolic syndrome [30]. Studies have shown that TGF-β1 could promote autophagy via the Smad and non-Smad pathways, driving hepatic fibrosis in NAFLD, and the progression of cardiac and renal fibrosis after ionizing radiation [31, 32]. TGF-β1 induces metabolic reprogramming in target cells, shifting energy production from mitochondrial oxidative phosphorylation to glycolytic metabolism – a phenomenon consistent with the Warburg effect observed in many pathological states[33]. Systemic blocking of TGF-β1 signaling regulates glucose tolerance and energy homeostasis, protecting mice from obesity, diabetes, and fatty liver disease [34]. TGF-β1 directly modulates PBX-regulating protein-1expression in both adipose-derived stem cells and mature adipocytes, thereby regulating adipogenic differentiation and insulin

sensitivity [35]. Many studies have shown a relationship between TGF-β1 and obesity and chronic inflammation, consistent with our study. However, there is no research on the mechanism of TGF-β1 inhibiting obesity and chronic inflammation by regulating autophagy and glycolysis levels, which is worthy of further exploration.

FASN is a key enzyme in hepatic de novo lipogenesis, while its upregulation is associated with insulin resistance [36]. Compared with normal-weight patients, FASN expression is significantly downregulated in patients with obesity [37]. Studies have demonstrated that the effect of hepatic FASN deficiency on NAFLD and diabetes is dependent on the etiology of obesity [36]. In mice with diet-induced obesity, adipose-specific *FASN* knockout aggravated high-fat diet-induced metabolic disturbances, exacerbating both hyperglycemia and hepatic dysfunction. These effects may be mediated through impaired hepatic glucose uptake secondary to glycogen accumulation and suppressed glycolytic flux [36]. The elevated *FASN* expression observed in obesity may confer a proliferative advantage to malignant cells through enhanced lipogenesis, potentially promoting tumorigenesis in obese microenvironments [38]. However, research has shown that renal cancer patients with obesity or overweight have a longer median overall survival owing to low *FASN* expression [37]. Therefore, considering the presence of obesity or overweight is important in future interventional treatments targeting the FASN pathway.

The high expression levels of the *SNCA* gene are closely associated with earlier onset, more rapid progression, and more severe manifestation of Parkinson's disease [39]. The *SNCA* gene encodes α-synuclein. Mitochondrial accumulation of α-synuclein aggregates triggers apoptotic pathways through multiple mechanisms, including mitochondrial permeability transition pore opening, calcium efflux, cytochrome C release, and subsequent mitochondrial swelling [40]. Importantly, high-fat diet-induced obesity was shown to accelerate the onset of motor deficits in human α-synuclein-expressing transgenic mice, correlating with premature α-synucleinopathy development and astrogliosis [41]. These findings suggest that diet-induced metabolic dysfunction may represent a significant environmental risk factor for α-synuclein pathology progression. Hence, molecular and cellular mechanisms underlying the interactions between obesity and *SNCA* in cognitive disorders await further elucidation.

CXCR4, the exclusive receptor for chemokine (C-X-C motif) ligand 12, orchestrates neutrophil metabolic reprogramming toward glycolysis and lactate production, while driving neutrophil accumulation in both circulation and psoriatic skin lesions [42]. Beyond its inflammatory functions, metabolic stress induces fat mass and obesity-related protein (FTO)-dependent N6-methyadenosine (m6A) mRNA demethylation, which upregulates CXCR4 expression via autophagic pathways. This mechanism critically contributes to melanoma pathogenesis and confers resistance to PD-1 checkpoint inhibition [43]. Moreover, inhibition of CXCR4 led to the sensitization of osteosarcoma to doxorubicin via the induction of autophagic cell death [44]. In summary, CXCR4 is closely related to inflammation, autophagy, and glycolysis, and hence its regulatory role in patients with obesity warrants further exploration.

Functional enrichment analysis revealed that the five A&GRDEGs were significantly associated with five key biological processes: insulin signaling, AMPK-mediated metabolic regulation, intestinal immune network for IgA production, cellular senescence pathways, and human cytomegalovirus (CMV) infection response. Among these, biological processes such as insulin resistance, AMPK signaling pathway, intestinal IgA immunity, and cellular senescence are thought to be closely related to chronic low-grade inflammation in patients with obesity [45-48]. GSEA of the GSE59034 dataset demonstrated significant enrichment of pro-inflammatory

and pro-fibrotic pathways in obesity. Notably, three metabolic regulators (*EIF4EBP1*, *FASN*, and *TGFB1*) exhibited consistent diagnostic accuracy across both datasets (Fig. 5). These findings implicate autophagy-glycolysis crosstalk in obesity pathogenesis, potentially through the amplification of inflammatory and fibrotic cascades. However, whether these five A&GRDEGs could be applied clinically for the prevention and treatment of obesity needs to be confirmed through further investigations.

Among the five A&GRDEGs, *TGFB1*, *SNCA*, and *CXCR4* expression positively correlated with immune cell recruitment, while *FASN* and *EIF4EBP1* showed significant inverse associations with immune infiltration levels. This dichotomous relationship suggests differential roles in immunometabolic regulation within obese adipose tissue. *TGFB1* showed the strongest positive correlation with MDSCs, while *EIF4EBP1* showed the strongest negative correlation with Th1 cells. Th1 cells, playing a facilitatory role in the pathogenesis of autoimmune diseases and tissue inflammatory responses, is regulated by cytokines IFN-γ [49]. Furthermore, an elevated Th1 cell count was linked with elevated adipose tissue inflammation and insulin resistance, with its cell count increasing alongside increasing obesity [50]. *In vitro* evidence demonstrates that IFN-γ exacerbates adipose tissue inflammation in obesity, while IFN-γ knockout mice show improved metabolic profiles, including enhanced insulin sensitivity and reduced inflammatory markers in high-fat diet models [51]. However, the mechanistic relationship between *EIF4EBP1* expression and Th1 cell infiltration in obese adipose tissue remains unexplored. This knowledge gap highlights the need for focused investigations into *EIF4EBP1*-mediated immunometabolic regulation in chronic inflammation associated with obesity.

This study also has some limitations. First, the results from the two datasets included were not completely consistent, highlighting the need for experimental validation and prospective clinical studies, which represent an important direction for our future research. Second, although screening was performed on obesity-related A&GRDEGs, the specific mechanisms of action involved were not clarified, which warrants further investigation.

In conclusion, levels of autophagy and glycolysis exhibit substantial predictive value for obesity development and mechanistically contribute to disease pathogenesis through immunometabolic dysregulation. These results provide a foundational framework for understanding obesity-associated chronic inflammation, offering new molecular targets for both basic research and potential therapeutic development.

Acknowledgements

The authors gratefully acknowledge the data provided by patients and researchers participating in GEO.

Funding

This research received no specific grant from any funding agency in the public, commercial, or not-for-profit sectors.

Conflict of interests

All authors declare that they have no conflict of interest.

Ethics approval and consent to participate

Not applicable, because GEO belongs to public databases, the patients involved in the database have obtained ethical approval, users can download relevant data for free for research and publish relevant articles, and our study is based on open-source data, and the The Fifth Affiliated Hospital of Sun Yat-sen University does not require research using publicly available data to be submitted for review to their ethics committee, so there are no ethical issues and other conflicts of interest.

Consent for publication

Not applicable.

Availability of data and materials

The original contributions presented in the study are included in the article/Supplementary material; further inquiries can be directed to the corresponding author.

ORCID Numbers

- Simin Yang (SY): 0009-0008-4837-9124
- Rexidanmu Hudabai (RH): 0009-0005-8911-5916
- Xinwei Su (XS): 0009-0001-4289-7018

Authors' contributions

SY designed the research, collected the data, performed the statistical analysis, and drafted the manuscript. RH collected the data and performed the statistical analysis. XS supervised the statistical analysis, reviewed, and edited the manuscript. All authors have approved the final manuscript.

REFERENCES

1. **Ghaben AL, Scherer PE.** Adipogenesis and metabolic health. Nat Rev Mol Cell Biol. 2019;20(4):242-258. *https://doi.org/10.1038/s41580-018-0093-z.*
2. **Kim DS, Scherer PE.** Obesity, Diabetes, and Increased Cancer Progression. Diabetes Metab J. 2021;45(6):799-812. *https://doi.org/10.4093/dmj.2021.0077.*
3. **Calle EE, Kaaks R**. Overweight, obesity and cancer: epidemiological evidence and proposed mechanisms. Nat Rev Cancer. 2004;4(8):579-591. *https://doi.org/10.1038/nrc1408.*
4. **Namkoong S, Cho CS, Semple I, Lee JH**. Autophagy Dysregulation and Obesity-Associated Pathologies. Mol Cells. 2018;41(1):3-10. *https://doi.org/10.14348/molcells.2018.2213.*
5. **Tooze SA, Dikic I.** Autophagy Captures the Nobel Prize. Cell. 2016;167(6):1433-1435. *https://doi.org/10.1016/j.cell.2016.11.023.*
6. **Zhang Y, Sowers JR, Ren J.** Targeting autophagy in obesity: from pathophysiology to management. Nat Rev Endocrinol. 2018;14(6):356-376. *https://doi.org/10.1038/s41574-018-0009-1.*
7. **Dann SG, Selvaraj A, Thomas G.** mTOR Complex1-S6K1 signaling: at the crossroads of obesity, diabetes and cancer. Trends Mol Med. 2007;13(6):252-259. *https://doi.org/10.1016/j.molmed.2007.04.002.*
8. **Behrooz AB, Cordani M, Fiore A, Donadelli M, Gordon JW, Klionsky DJ, et al.** The obesity-autophagy-cancer axis: Mechanistic insights and therapeutic perspectives. Semin Cancer Biol. 2024;99:24-44. *https://doi.org/10.1016/j.semcancer.2024.01.003.*
9. **Soto-Heredero G, Gomez de Las Heras MM, Gabande-Rodriguez E, Oller J, Mittelbrunn M.** Glycolysis - a key player in the inflammatory response. FEBS J. 2020;287(16):3350-3369. *https://doi.org/10.1111/febs.15327.*
10. **Chang CH, Curtis JD, Maggi LB, Jr., Faubert B, Villarino AV, O'Sullivan D, et al.** Posttranscriptional control of T cell effector function by aerobic glycolysis. Cell. 2013;153(6):1239-1251. *https://doi.org/10.1016/j.cell.2013.05.016.*
11. **Jiao P, Chen Q, Shah S, Du J, Tao B, Tzameli I, et al.** Obesity-related upregulation of monocyte chemotactic factors in adipocytes: involvement of nuclear factor-kappaB and c-Jun NH2-terminal kinase pathways. Diabetes. 2009;58(1):104-115. *https://doi.org/10.2337/db07-1344.*
12. **O'Rourke RW, White AE, Metcalf MD, Olivas AS, Mitra P, Larison WG, et al.** Hypoxia-induced inflammatory cytokine secretion in human adipose tissue stromovascular cells. Diabetologia. 2011;54(6):1480-1490. *https://doi.org/10.1007/s00125-011-2103-y.*
13. **Boutens L, Hooiveld GJ, Dhingra S, Cramer RA, Netea MG, Stienstra R.** Unique metabolic activation of adipose

tissue macrophages in obesity promotes inflammatory responses. Diabetologia. 2018;61(4):942-953. *https://doi.org/10.1007/s00125-017-4526-6.*

14. **Jacks RD, Lumeng CN.** Macrophage and T cell networks in adipose tissue. Nat Rev Endocrinol. 2024;20(1):50-61. *https://doi.org/10.1038/s41574-023-00908-2.*
15. **Gancheva S, Ouni M, Jelenik T, Koliaki C, Szendroedi J, Toledo FGS, et al.** Dynamic changes of muscle insulin sensitivity after metabolic surgery. Nat Commun. 2019;10(1):4179. *https://doi.org/10.1038/s41467-019-12081-0.*
16. **Petrus P, Mejhert N, Corrales P, Lecoutre S, Li Q, Maldonado E, et al.** Transforming Growth Factor-β3 Regulates Adipocyte Number in Subcutaneous White Adipose Tissue. Cell Rep. 2018;25(3):551-560.e5. *https://doi.org/10.1016/j.celrep.2018.09.069.*
17. **Sun S, Shen Y, Wang J, Li J, Cao J, Zhang J.** Identification and Validation of Autophagy-Related Genes in Chronic Obstructive Pulmonary Disease. Int J Chron Obstruct Pulmon Dis. 2021;16:67-78. *https://doi.org/10.2147/copd.S288428.*
18. **Fu D, Zhang B, Wu S, Zhang Y, Xie J, Ning W, et al.** Prognosis and Characterization of Immune Microenvironment in Acute Myeloid Leukemia Through Identification of an Autophagy-Related Signature. Front Immunol. 2021;12:695865. *https://doi.org/10.3389/fimmu.2021.695865.*
19. **Wang N, Wei L, Liu D, Zhang Q, Xia X, Ding L, et al.** Identification and Validation of Autophagy-Related Genes in Diabetic Retinopathy. Front Endocrinol (Lausanne). 2022;13:867600. *https://doi.org/10.3389/fendo.2022.867600.*
20. **Zhang D, Zheng Y, Yang S, Li Y, Wang M, Yao J, et al.** Identification of a Novel Glycolysis-Related Gene Signature for Predicting Breast Cancer Survival. Front Oncol. 2020;10:596087. *https://doi.org/10.3389/fonc.2020.596087.*
21. **Zheng J, Guo J, Zhu L, Zhou Y, Tong J.** Comprehensive analyses of glycolysis-related lncRNAs for ovarian cancer patients. J Ovarian Res. 2021;14(1):124. *https://doi.org/10.1186/s13048-021-00881-2.*
22. **Bi J, Bi F, Pan X, Yang Q.** Establishment of a novel glycolysis-related prognostic gene signature for ovarian cancer and its relationships with immune infiltration of the tumor microenvironment. J Transl Med. 2021;19(1):382. *https://doi.org/10.1186/s12967-021-03057-0.*
23. **Saltiel AR, Olefsky JM.** Inflammatory mechanisms linking obesity and metabolic disease. J Clin Invest. 2017;127(1):1-4. *https://doi.org/10.1172/JCI92035.*
24. **Zhang T, Linghu KG, Tan J, Wang M, Chen D, Shen Y, et al.** TIGAR exacerbates obesity by triggering LRRK2-mediated defects in macroautophagy and chaperone-mediated autophagy in adipocytes. Autophagy. 2024;20(8):1741-1761. *https://doi.org/10.1080/15548627.2024.2338576.*
25. **Bjornsti MA, Houghton PJ.** Lost in translation: dysregulation of cap-dependent translation and cancer. Cancer Cell. 2004;5(6):519-523. *https://doi.org/10.1016/j.ccr.2004.05.027.*
26. **Chen C, Chen W, Nong Z, Nie Y, Chen X, Pan X, et al.** Hyperbaric oxygen alleviated cognitive impairments in mice induced by repeated cerebral ischemia-reperfusion injury via inhibition of autophagy. Life Sci. 2020;241:117170. *https://doi.org/10.1016/j.lfs.2019.117170.*
27. **Selvarajah B, Azuelos I, Plate M, Guillotin D, Forty EJ, Contento G, et al.** mTORC1 amplifies the ATF4-dependent de novo serine-glycine pathway to supply glycine during TGF-beta(1)-induced collagen biosynthesis. Sci Signal. 2019;12(582):eaav3048. *https://doi.org/10.1126/scisignal.aav3048.*
28. **Le Bacquer O, Petroulakis E, Paglialunga S, Poulin F, Richard D, Cianflone K, et al.** Elevated sensitivity to diet-induced obesity and insulin resistance in mice lacking 4E-BP1 and 4E-BP2. J Clin Invest. 2007;117(2):387-396. *https://doi.org/10.1172/JCI29528.*
29. **Tsai S, Sitzmann JM, Dastidar SG, Rodriguez AA, Vu SL, McDonald CE, et al.** Muscle-specific 4E-BP1 signaling activation improves metabolic parameters

during aging and obesity. J Clin Invest. 2015;125(8):2952-2964. *https://doi.org/10.1172/JCI77361.*

30. **Hu X, Jia X, Xu C, Wei Y, Wang Z, Liu G, et al.** Downregulation of NK cell activities in Apolipoprotein C-III-induced hyperlipidemia resulting from lipid-induced metabolic reprogramming and crosstalk with lipid-laden dendritic cells. Metabolism. 2021;120:154800. *https://doi.org/10.1016/j.metabol.2021.154800.*
31. **Siapoush S, Rezaei R, Alavifard H, Hatami B, Zali MR, Vosough M, et al.** Therapeutic implications of targeting autophagy and TGF-beta crosstalk for the treatment of liver fibrosis. Life Sci. 2023;329:121894. *https://doi.org/10.1016/j.lfs.2023.121894.*
32. **Ahamed J, Laurence J.** Role of Platelet-Derived Transforming Growth Factor-beta1 and Reactive Oxygen Species in Radiation-Induced Organ Fibrosis. Antioxid Redox Signal. 2017;27(13):977-988. *https://doi.org/10.1089/ars.2017.7064.*
33. **Hewitson TD, Smith ER.** A Metabolic Reprogramming of Glycolysis and Glutamine Metabolism Is a Requisite for Renal Fibrogenesis-Why and How? Front Physiol. 2021;12:645857. *https://doi.org/10.3389/fphys.2021.645857.*
34. **Yadav H, Quijano C, Kamaraju AK, Gavrilova O, Malek R, Chen W, et al.** Protection from obesity and diabetes by blockade of TGF-beta/Smad3 signaling. Cell Metab. 2011;14(1):67-79. *https://doi.org/10.1016/j.cmet.2011.04.013.*
35. **Bruno A, Di Sano C, Simon HU, Chanez P, Patti AM, Di Vincenzo S, et al.** Leptin and TGF-beta1 Downregulate PREP1 Expression in Human Adipose-Derived Mesenchymal Stem Cells and Mature Adipocytes. Front Cell Dev Biol. 2021;9:700481. *https://doi.org/10.3389/fcell.2021.700481.*
36. **Matsukawa T, Yagi T, Uchida T, Sakai M, Mitsushima M, Naganuma T, et al.** Hepatic FASN deficiency differentially affects nonalcoholic fatty liver disease and diabetes in mouse obesity models. JCI Insight. 2023;8(17):e161282. *https://doi.org/10.1172/jci.insight.161282.*
37. **Albiges L, Hakimi AA, Xie W, McKay RR, Simantov R, Lin X, et al.** Body Mass Index and Metastatic Renal Cell Carcinoma: Clinical and Biological Correlations. J Clin Oncol. 2016;34(30):3655-3663. *https://doi.org/10.1200/JCO.2016.66.7311.*
38. **Khandekar MJ, Cohen P, Spiegelman BM.** Molecular mechanisms of cancer development in obesity. Nat Rev Cancer. 2011;11(12):886-895. *https://doi.org/10.1038/nrc3174.*
39. **Ross OA, Braithwaite AT, Skipper LM, Kachergus J, Hulihan MM, Middleton FA, et al.** Genomic investigation of alpha-synuclein multiplication and parkinsonism. Ann Neurol. 2008;63(6):743-750. *https://doi.org/10.1002/ana.21380.*
40. **Malpartida AB, Williamson M, Narendra DP, Wade-Martins R, Ryan BJ.** Mitochondrial Dysfunction and Mitophagy in Parkinson's Disease: From Mechanism to Therapy. Trends Biochem Sci. 2021;46(4):329-343. *https://doi.org/10.1016/j.tibs.2020.11.007.*
41. **Rotermund C, Truckenmuller FM, Schell H, Kahle PJ.** Diet-induced obesity accelerates the onset of terminal phenotypes in alpha-synuclein transgenic mice. J Neurochem. 2014;131(6):848-858. *https://doi.org/10.1111/jnc.12813.*
42. **Chen J, Bai Y, Xue K, Li Z, Zhu Z, Li Q, et al.** CREB1-driven CXCR4(hi) neutrophils promote skin inflammation in mouse models and human patients. Nat Commun. 2023;14(1):5894. *https://doi.org/10.1038/s41467-023-41484-3.*
43. **Yang S, Wei J, Cui YH, Park G, Shah P, Deng Y, et al.** m(6)A mRNA demethylase FTO regulates melanoma tumorigenicity and response to anti-PD-1 blockade. Nat Commun. 2019;10(1):2782. *https://doi.org/10.1038/s41467-019-10669-0.*
44. **Liao YX, Lv JY, Zhou ZF, Xu TY, Yang D, Gao QM, et al.** CXCR4 blockade sensitizes osteosarcoma to doxorubicin by inducing autophagic cell death via PI3K–Akt–mTOR pathway inhibition. Int J Oncol. 2021;59(1):49. *https://doi.org/10.3892/ijo.2021.5229.*
45. **Esser N, Legrand-Poels S, Piette J, Scheen AJ, Paquot N.** Inflammation as a

link between obesity, metabolic syndrome and type 2 diabetes. Diabetes Res Clin Pract. 2014;105(2):141-150. *https://doi.org/10.1016/j.diabres.2014.04.006.*

46. **Foretz M, Guigas B, Viollet B.** Understanding the glucoregulatory mechanisms of metformin in type 2 diabetes mellitus. Nat Rev Endocrinol. 2019;15(10):569-589. *https://doi.org/10.1038/s41574-019-0242-2.*
47. **Huus KE, Petersen C, Finlay BB.** Diversity and dynamism of IgA-microbiota interactions. Nat Rev Immunol. 2021;21(8):514-525. *https://doi.org/10.1038/s41577-021-00506-1.*
48. **Ferrucci L, Fabbri E**. Inflammageing: chronic inflammation in ageing, cardiovascular disease, and frailty. Nat Rev Cardiol. 2018;15(9):505-522. *https://doi.org/10.1038/s41569-018-0064-2.*
49. **Huh JY, Park YJ, Ham M, Kim JB**. Crosstalk between adipocytes and immune cells in adipose tissue inflammation and metabolic dysregulation in obesity. Mol Cells. 2014;37(5):365-371. *https://doi.org/10.14348/molcells.2014.0074.*
50. **Schipper HS, Prakken B, Kalkhoven E, Boes M**. Adipose tissue-resident immune cells: key players in immunometabolism. Trends Endocrinol Metab. 2012;23(8):407-415. *https://doi.org/10.1016/j.tem.2012.05.011.*
51. **Rocha VZ, Folco EJ, Sukhova G, Shimizu K, Gotsman I, Vernon AH,** et al. Interferon-gamma, a Th1 cytokine, regulates fat inflammation: a role for adaptive immunity in obesity. Circ Res. 2008;103(5):467-476. *https://doi.org/10.1161/CIRCRESAHA.108.177105.*

Invest Clin 66(4): 408 - 425, 2025 https://doi.org/10.54817/IC.v66n4a05

Rutin as a potential therapeutic agent for arsenic-induced testicular damage: Antioxidant, anti-inflammatory, and anti-apoptotic effects.

Yunyun Wang[1,#], Zengrong Hua[2,#], Jin Qing Hui[3] and Dandan Qiu[4]

[1]Department of Pharmacy, The First Affiliated Hospital of Zhejiang Chinese Medical University, Zhejiang Hospital of Traditional Chinese Medicine, Hangzhou, Zhejiang, China.
[2]Department of Urology, Huai'an Clinical Medical College of Jiangsu University (Huai'an Hospital of Huai'an City), Huai'an, Jiangsu, China.
[3]Department of Surgical, Shaanxi Kangfu Hospital, Xian, Shaanxi, China.
[4]Department of Urology, The First Affiliated Hospital of Zhejiang Chinese Medical University, Zhejiang Hospital of Traditional Chinese Medicine, Hangzhou Zhejiang, China.
[#]Yunyun Wang and Zengrong Hua are co-first authors; they contributed equally to this work.

Keywords: Apoptosis; Arsenic; Inflammation; Rutin, Spermatogenesis; Testicular Toxicity.

Abstract. Arsenic exposure is associated with male reproductive toxicity, including impaired spermatogenesis, reduced sperm quality, and disrupted hormone levels. Rutin, a natural flavonoid, has demonstrated protective effects in various organs owing to its antioxidant, anti-inflammatory, and antiapoptotic properties. This study aimed to assess the efficacy of rutin in ameliorating testicular toxicity caused by sodium arsenite in laboratory rats. Sprague-Dawley rats were randomly assigned to normal, arsenic control, rutin (25, 50, and 100 mg/kg), and Co-enzyme Q10 (10 mg/kg) treatment groups. Testicular damage was induced by oral administration of sodium arsenite (10 mg/kg, for two days). Rutin and Co-enzyme Q10 were administered orally for 15 and seven days, respectively. The serum hormone levels, sperm parameters, testicular mitochondrial enzymes, oxidative stress markers, inflammatory cytokines, apoptotic proteins, and histopathology were assessed. Arsenic exposure significantly decreased ($p<0.001$) sperm parameters (count, motility, and viability), serum hormone levels (follicle-stimulating hormone, luteinizing hormone, and testosterone), and mitochondrial enzyme activity. Rutin (50 and 100 mg/kg) significantly ($p<0.01$ and $p<0.001$) attenuated arsenic-induced alterations in a dose-dependent manner, improving organ weight, sperm parameters, and hormone levels. Rutin also improved mitochondrial complex activity and testicular architecture. In contrast, elevated oxidative stress (reduced glutathione, superoxide dismutase, nitric oxide, and lipid peroxidation), inflammation (tumor necrosis factor-alpha,

Corresponding author: Dandan Qiu. Department of Urology, The First Affiliated Hospital of Zhejiang Chinese Medical University, Zhejiang Hospital of Traditional Chinese Medicine, Hangzhou Zhejiang, 310006, China. Phone: +8613588454495. Email: qiudandan2000@outlook.com

interleukin-6, and interleukin-1β), and apoptosis (caspase-3 and caspase-9 protein expression) were ameliorated by rutin. In conclusion, rutin demonstrated significant protective effects against sodium arsenite-induced testicular toxicity in rats by reducing oxidative stress, inflammation, and apoptosis. These findings suggest that rutin has therapeutic potential in mitigating arsenic-related reproductive toxicity.

Rutina, un agente terapéutico potencial para el daño testicular inducido por arsénico: Efecto antioxidante, antinflamatorio, y anti-apoptótico.

Invest Clin 2025; 66 (4): 408 – 425

Palabras clave: Apoptosis; Arsénico; Inflamación; Rutina; Espermatogénesis; Toxicidad Testicular.

Resumen. La exposición al arsénico se asocia con toxicidad reproductiva masculina que incluye alteración de la espermatogénesis, reducción de la calidad del esperma y alteración de los niveles hormonales. La rutina, un flavonoide natural, ha demostrado efectos protectores en varios órganos debido a sus propiedades antioxidantes, antiinflamatorias y antiapoptóticas. El propósito del trabajo fue evaluar la eficacia de la rutina para reducir la toxicidad testicular causada por el arsenito de sodio en ratas de laboratorio. Ratas (Sprague-Dawley) fueron asignadas aleatoriamente a grupos de tratamiento normal, control de arsénico, rutina (25, 50 y 100 mg/kg) y coenzima Q10 (10 mg / kg). El daño testicular se indujo mediante la administración oral de arsenito de sodio (10 mg/kg, 2 días). La rutina y la coenzima Q10 se administraron por vía oral durante 15 y 7 días, respectivamente. Se evaluaron los niveles séricos de hormonas, los parámetros de los espermatozoides, las enzimas mitocondriales testiculares, los marcadores de estrés oxidativo, las citocinas inflamatorias, las proteínas apoptóticas y la histopatología. La exposición al arsénico disminuyó significativamente ($p<0,001$) los parámetros espermáticos (recuento, motilidad y viabilidad), y los niveles séricos de hormonas (hormona estimulante del folículo, hormona luteinizante y testosterona) y la actividad de las enzimas mitocondriales. La rutina (50 y 100 mg/kg) atenuó significativamente ($p<0,01$ y $p<0,001$) las alteraciones inducidas por el arsénico de manera dosis-dependiente, mejorando el peso de los órganos, los parámetros espermáticos y los niveles hormonales. La rutina también mejoró la actividad del complejo mitocondrial y la arquitectura testicular, mientras que el estrés oxidativo elevado (glutatión reducido y superóxido dismutasa, óxido nítrico y peroxidación lipídica), la inflamación (factor de necrosis tumoral alfa, interleucina-6 e interleucina-1β) y la apoptosis (expresión de proteínas caspasa-3 y caspasa-9) mejoraron con la rutina. En conclusión, la rutina demostró efectos protectores significativos contra la toxicidad testicular inducida por el arsenito de sodio en ratas al reducir el estrés oxidativo, la inflamación y la apoptosis. Estos hallazgos sugieren que la rutina tiene potencial terapéutico para mitigar la toxicidad reproductiva asociada al arsénico.

Received: 12-08-2025 Accepted: 22-09-2025

INTRODUCTION

Arsenic is a metalloid commonly found in the environment, known for its toxicity and important public health effects [1,2]. It mainly impacts populations through contaminated drinking water, often from natural sources and human activities such as industrial discharge and the use of arsenic-based pesticides [3,4]. According to the World Health Organization (WHO), more than 140 million people worldwide are exposed to arsenic-contaminated water exceeding the safe limit of 10 μg/L [5]. Furthermore, long-term exposure to arsenic has been associated with numerous health problems, including cancer and various non-cancerous conditions like cardiovascular diseases, diabetes, and reproductive issues [6,7]. Sodium arsenite is recognized for causing testicular toxicity through mechanisms such as oxidative stress, apoptosis, and inflammation. Researchers believe that inflammation, oxidative/nitrosative stress, and apoptosis are key factors in arsenic-induced testicular damage [6,8].

The impact of arsenic toxicity on reproductive health has become an increasing concern, particularly regarding the male reproductive system [9]. Arsenic exposure is linked to various reproductive problems, including male infertility, decreased sperm quality, and disruptions in testosterone production. This results in reduced weights of reproductive organs, more sperm abnormalities, and apoptosis in testicular cells [10]. The harmful effects of arsenic on male fertility involve several mechanisms, such as interference with steroidogenesis and mitochondrial dysfunction in reproductive tissues [9]. These disruptions lead to lower testosterone levels, decreased sperm count, and abnormal sperm morphology [11]. Additionally, changes in spermatogenesis and reduced gonadotropin levels have been observed, further emphasizing the reproductive risks of arsenic [3]. Moreover, arsenic exposure causes increased production of reactive oxygen species (ROS), indicating the role of oxidative stress in its genotoxic effects [12]. Researchers have documented that testicular toxicity caused by sodium arsenite is partly due to its ability to induce apoptosis through the p53 pathway, as shown in zebrafish studies where sodium arsenite exposure elevated apoptosis markers and decreased global DNA methylation [13]. Furthermore, experiments with *Caenorhabditis elegans* demonstrated that sodium arsenite can cause cell cycle arrest and germline apoptosis, both of which depend on concentration and exposure time [12].

Several protective agents have been studied to reduce testicular toxicity caused by sodium arsenite. Melatonin has been shown to decrease arsenic-induced testicular cell death, oxidative stress, and tissue damage by boosting antioxidant enzyme activity and lowering lipid peroxidation [14]. Similarly, *Salvia hispanica* (chia seeds) proved effective in decreasing testicular toxicity by improving sperm quality, serum sex hormone levels, and antioxidant enzyme activity, thanks to its flavonoid content and antioxidant properties [15]. Hesperidin and lipoic acid were also tested for their protective effects against liver, kidney, and testicular toxicity when administered with sodium arsenite[16]. Rutin is a natural flavonoid with a wide range of pharmacological benefits, including antioxidant, antimicrobial, antifungal, anti-allergic, anti-cancer, anti-inflammatory, and antiapoptotic effects [4,17-22]. Additionally, rutin has been shown to help manage neurodegenerative diseases and metabolic conditions like diabetes due to its cell-protective effects [19]. Its protective properties have been documented in the liver, kidneys, and heart due to its anti-inflammatory, antioxidant, and antiapoptotic actions, making it a candidate for protecting these organs from toxic agents [4]. However, the impact of rutin on testicular toxicity caused by sodium arsenite has not yet been studied. Given its protective effects on other organs, rutin might provide similar benefits in reducing testicular damage from sodium arsenite. This study examined the effectiveness of rutin in alleviating testicular toxicity caused by sodium arsenite in male rats.

MATERIALS AND METHODS

Experimental design

Rats (male, Sprague-Dawley, weighing 200-220 g, sourced from the animal house of Shaanxi Kangfu Hospital, China) were randomly divided into the following groups (n=6 per group): normal, arsenic control (As), rutin (Sigma Chemical Co., St Louis, Missouri, United States; 25, 50, and 100 mg/kg), and Co-enzyme Q_{10} (Medicines Pvt. Ltd. Mumbai, India; 10 mg/kg). Testicular damage was induced in rats (except the normal group) by oral administration of sodium arsenite (Otto Chemicals, India; 10 mg/kg, for two days) [23,24]. Rats in the arsenic control and normal groups were treated with double-distilled water (10 mL/kg). Three different dosages of rutin (25, 50, and 100 mg/kg) were selected based on previous studies [21,22] and were administered orally for 15 days. Co-enzyme Q_{10} was administered for seven consecutive days before arsenite administration and continued for up to 15 days. On the 16th day, the rats were put under anesthesia using ether, and blood was drawn through retro-orbital puncture. Each blood sample was placed in a separate vial for analysis of serum parameters. Serum follicle-stimulating hormone, luteinizing hormone, and testosterone levels were quantified according to the manufacturer's instructions for the rat-specific ELISA kit (Thermo Scientific, Rockford, IL, USA). The rats were euthanized by carbon dioxide asphyxiation, and the testes were rapidly removed and stored at -80°C for biochemical parameters. Other organs, such as the epididymis and prostate, were isolated and weighed. The epididymal sperm count and motility were determined according to a previously reported method [25].

Biochemical estimation of testis homogenate

Supernatant of the tissue homogenate was employed to estimate lipid peroxidation [malondialdehyde (MDA) content], nitric oxide (NO content), reduced glutathione (GSH), and superoxide dismutase (SOD)] as described previously [26-29]. Testicular mitochondrial enzyme activities, including Complex I (nicotinamide-adenine dinucleotide (NADH) dehydrogenase activity), Complex II (succinate dehydrogenase (SDH) activity), Complex III (mitochondrial redox activity), and Complex IV (cytochrome oxidase assay) were estimated according to previously reported methods [30,31].

Testicular interleukins (interleukins (ILs); IL-6 (ERA31RB) and IL-1β (BMS630)) and tumor necrosis factor-alpha (TNF-α; ERA56RB) were quantified in the testis homogenate using Enzyme-linked immunosorbent assay (ELISA) kits (Thermo Scientific, Rockford, IL, USA). Briefly, 500 mg of testis tissue samples were homogenized with a mechanical homogenizer in 5 ml of phosphate-buffered saline at 3000 rpm. The homogenate was centrifuged for 30 min at 20,000 rpm (4°C) in a cryo centrifuge (Eppendorf), and the supernatant was used to determine ILs and TNF-α. Briefly, the quantification of ILs and TNF-α was performed using the Thermo Scientific Rat ILs and TNF-α immunoassay kit, following the instructions provided. The Rat ILs and TNF-α immunoassay was a 4.5 h solid phase designed to measure rat ILs and TNF-α levels. The assay employed a sandwich enzyme immunoassay principle. A monoclonal antibody specific for rat ILs and TNF-α was pre-coated on the microplates. Standards, control, and samples were pipetted into the wells, and the immobilized antibody thus bound any rat ILs or TNF-α present in the sample. After washing away the unbound substance, an enzyme-linked polyclonal antibody specific for rat ILs or TNF-α was pipetted into the microtitre wells. Any unbound antibody was washed off, and then a substrate solution was added to the wells. The enzymatic reaction produced a blue product that turned yellow upon addition of the stop solution. The intensity of the generated color was measured and was proportional to the amount of rat ILs or TNF-α bound in the initial steps. A standard curve was run

on each assay plate using recombinant ILs or TNF-α in serial dilutions. The sample values were then read and calculations made according to the standard curve. Values were expressed as means ± S.E.M. The levels of ILs or TNF-α were expressed as units per mg of gastric tissue.

The protein expression of caspase-3 and caspase-9 was assessed by western blot in the testis [32-34]. Briefly, the testis was sonicated in Tissue Protein Extraction Reagent (Thermo Fisher Scientific, Inc., Mumbai, Maharashtra, India). The lysates were centrifuged at 10,000 × g for 10 min at 4°C. Protein concentration was determined using a Bicinchoninic Acid (BCA) assay kit (Beyotime Shanghai, China) on ice for 30 min. Equal amounts of extracted protein samples (50 μg) were separated by 10% SDS-PAGE (sodium dodecyl sulfate-polyacrylamide gel electrophoresis) and transferred onto polyvinylidene difluoride membranes. The membranes were blocked with 5% non-fat dry milk at 37°C for 1 hr and incubated overnight at 4°C with the primary antibodies recognizing caspase-3 (ab4051; 1/200 dilution; 31 kDa) and caspase-9 (ab202068; 1/2000 dilution; 46 kDa; Abcam, Cambridge, MA, USA). In addition, an anti-rabbit horseradish-linked secondary antibody (goat anti-rabbit IgG H&L; ab97051) was used, which was incubated at 37°C for 2 hr. Protein bands were visualized using the Chemiluminescent kit (Bio-Rad Laboratories, Inc., Mumbai, Maharashtra, India), and glyceraldehyde 3-phosphate dehydrogenase (GAPDH; EPR6256, ab128915; 1/10000 dilution; 36 kDa) served as the loading control.

Histopathological analysis of testis

Other testis samples were preserved in 10% formalin for 24 hours. These samples underwent dehydration and were immersed in xylene for one hour, repeated three times, followed by treatment with ethyl alcohol at concentrations of 70%, 90%, and 100% for two hours. The infiltration and impregnation process involved treating the samples with paraffin wax twice, with each session lasting 1 hour. The tissue samples were then sliced into sections with a thickness of 3-5μm and stained using hematoxylin and eosin (H&E). The sections were mounted on slides with Distrene Pthalate Xylene (DPX) serving as the mounting medium. A light microscope was used to examine the sections for histopathological characteristics and cell infiltration. The observed changes in histological features were categorized into grades ranging from 0 to 4 according to a previously reported method [35].

Statistical analysis

The data are presented as mean ± standard error of the mean (SEM). GraphPad Prism 5.0 software (GraphPad, San Diego, CA, USA) was utilized for data analysis. Biochemical parameter data were examined using one-way analysis of variance, followed by Tukey's multiple range test for parametric results, while the Kruskal-Wallis test was used for non-parametric outcomes. A p of less than 0.05 was deemed statistically significant. Correlation coefficients were calculated using a two-sided Fisher's test.

RESULTS

Attenuation of arsenic-induced alteration in body weight and organ weights by rutin

Table 1 presents the descriptive results for various body and organ weight parameters across the different treatment groups. The arsenic (As) control group had a significant reduction ($p<0.001$) in organ weights (testes, epididymis, and prostate) and body weight compared with the normal group. CoQ treatment resulted in a significant improvement ($p<0.001$) in body weight and organ weights compared to the arsenic control group. Rutin (50 and 100 mg/kg) administration also effectively ($p<0.01$ and $p<0.001$) and dose-dependently increased the body, testes, epididymis, and prostate weights relative to the arsenic-exposed group.

Table 1. Attenuation of arsenic-induced alteration in body weight, organ weights (testes, epididymis, and prostate), and sperm parameters (count, motility, and viability) by rutin.

Parameters	Normal	As Control	CoQ (10)	R (25)	R (50)	R (100)
Body weight (gm)	281.8 ± 2.86	217.50 ± 3.73###	275.70 ± 2.69***	214.70 ± 2.80	247.00 ± 4.02**	262.20 ± 2.77***
Testes weight (gm)	1.79 ± 0.04	1.03 ± 0.07###	1.59 ± 0.04***	1.07 ± 0.05	1.51 ± 0.06**	1.68 ± 0.02***
Testes weight/Body weight ($\times 10^{-3}$)	6.34 ± 0.15	4.75 ± 0.39###	5.76 ± 0.18***	4.99 ± 0.21	6.13 ± 0.33**	6.41 ± 0.12***
Epididymis weight (gm)	0.51 ± 0.01	0.19 ± 0.02###	0.45 ± 0.02***	0.23 ± 0.01	0.33 ± 0.01**	0.45 ± 0.01***
Epididymis weight/Body weight ($\times 10^{-3}$)	1.80 ± 0.03	0.87 ± 0.07###	1.62 ± 0.07***	1.09 ± 0.07	1.32 ± 0.04**	1.73 ± 0.04***
Prostate weight (mg)	612.30 ± 10.94	308.30 ± 9.78###	560.70 ± 9.02***	298.70 ± 11.44	478.30 ± 11.78**	541.70 ± 11.45***
Prostate weight/Body weight ($\times 10^{-3}$)	2.18 ± 0.04	1.42 ± 0.05###	2.03 ± 0.04***	1.39 ± 0.04	1.94 ± 0.07**	2.07 ± 0.05***
Sperm count (millions/mL)	60.17 ± 1.25	34.00 ± 0.97###	56.83 ± 1.30***	33.83 ± 0.75	45.00 ± 1.21**	51.83 ± 1.25***
Sperm motility (%)	71.33 ± 1.05	40.33 ± 1.02###	62.00 ± 1.00***	44.33 ± 0.95	49.17 ± 1.49**	59.50 ± 0.67***
Dead sperm (%)	28.67 ± 1.05	59.67 ± 1.02###	38.00 ± 1.00***	55.67 ± 0.95	50.83 ± 1.49**	40.50 ± 0.67***
Abnormal sperm (%)	12.17 ± 0.60	36.50 ± 0.43###	17.17 ± 0.54***	34.17 ± 0.48	24.67 ± 0.42**	19.33 ± 0.76***

Data analysis: One-way ANOVA (post-hoc test: Tukey's multiple range test). Data are reported as mean ± SEM (n=6). Statistically significant compared with ###normal rats, ** and ***as control rats. ###$p < 0.001$, **$p < 0.01$ and ***$p < 0.001$. Arsenic (As), Co-enzyme Q_{10} (CoQ (10)) and Rutin (R).

Table 2. Attenuation of arsenic-induced alteration in serum luteinizing hormone, follicle stimulating hormone, testosterone levels and testicular mitochondrial complex activities by rutin.

Parameters	Normal	As Control	CoQ (10)	R (25)	R (50)	R (100)
Serum parameters						
Luteinizing hormone (ng/mL)	1.88 ± 0.04	0.26 ± 0.05###	0.33 ± 0.03	0.36 ± 0.04	0.71 ± 0.05**	1.21 ± 0.04***
Follicle stimulating hormone (ng/mL)	1.37 ± 0.02	0.16 ± 0.02###	0.15 ± 0.02	0.26 ± 0.02	0.64 ± 0.02**	0.92 ± 0.02***
Testosterone (ng/mL)	3.69 ± 0.04	1.41 ± 0.05###	1.32 ± 0.06	1.5 ± 0.06	2.39 ± 0.04**	2.86 ± 0.05***
Testicular parameters						
Complex I (nmole of NADH oxidized/ min/mg protein)	33.36 ± 1.66	7.41 ± 1.80###	30.21 ± 1.79***	10.07 ± 1.35	16.91 ± 1.25**	28.31 ± 2.10***
Complex II (mmole/mg protein)	14.35 ± 0.82	4.38 ± 0.78###	11.86 ± 0.84***	4.74 ± 0.62	9.42 ± 0.67**	11.24 ± 0.58***
MTT assay (OD at 540 nm)	0.45 ± 0.03	0.17 ± 0.03###	0.45 ± 0.03***	0.21 ± 0.02	0.32 ± 0.01**	0.39 ± 0.02***
Complex-IV (nmol cyto-C oxidized/ min/mg protein)	6319.00 ± 280.30	1008.00 ± 212.70###	5293.00 ± 254.70***	1586.00 ± 191.90	3224.00 ± 201.30**	4515.00 ± 342.00***

Data analysis: One-way ANOVA (post-hoc test: Tukey's multiple range test). Data are reported as mean ± SEM (n=6). Statistically significant compared with ###normal rats, ** and ***as control rats. ###$p < 0.001$, **$p < 0.01$ and ***$p < 0.001$. Arsenic (As), Co-enzyme Q_{10} (CoQ (10)), 3-(4,5-dimethylthiazol-2-yl)-2,5-diphenyltetrazolium bromide (MTT) and Rutin (R).

Attenuation of arsenic-induced alteration in sperm parameters by rutin

The arsenic control group showed a significant reduction ($p<0.001$) in cell count and motility compared to the control group. However, the percentage of dead and abnormal sperm was markedly higher ($p<0.001$) in the arsenic control group than that in the normal group. Treatment with CoQ resulted in significant improvements ($p<0.001$) in sperm count and motility compared with the arsenic control group. Furthermore, CoQ administration resulted in a more effective ($p<0.001$) recovery of the percentage of dead and abnormal sperm than arsenic control. Rutin (50 and 100 mg/kg) treatment demonstrated a marked ($p<0.01$ and $p<0.001$) and dose-dependent improvement in sperm parameters relative to the arsenic-exposed group (Table 1).

Attenuation of arsenic-induced alteration in serum follicle-stimulating hormone, luteinizing hormone, and testosterone levels by rutin

Exposure to sodium arsenite significantly decreased ($p<0.001$) the levels of serum follicle-stimulating hormone, luteinizing hormone, and testosterone in the arsenic control group compared with the normal group. Treatment with CoQ and rutin (25 mg/kg) had a minimal impact on serum luteinizing hormone, follicle-stimulating hormone, and testosterone hormone levels. However, rutin (50 and 100 mg/kg) treatments demonstrated effective, dose-dependent increases in all three hormones ($p<0.01$ and $p<0.001$, respectively) compared with the arsenic control group (Table 2).

Attenuation of arsenic-induced alteration in testicular mitochondrial complex activities by rutin

Arsenic exposure led to a significant reduction ($p<0.001$) in mitochondrial complex activity compared to the normal group. The results presented in Table 2 demonstrate that both CoQ and rutin (50 and 100 mg/kg) significantly improved mitochondrial function in arsenic-exposed rats. Specifically, rutin (50 and 100 mg/kg) administration led to notable ($p<0.01$ and $p<0.001$) and dose-dependent increases in mitochondrial complex activities compared with the arsenic control group. However, rutin (25 mg/kg) did not show any significant potential to improve mitochondrial function or mitigate arsenic-induced damage.

Attenuation of arsenic-induced alteration in testicular oxido-nitrosative stress by rutin

The results presented in Table 3 show the effects of rutin treatment on testicular oxido-nitrosative stress. Arsenic exposure caused a substantial ($p<0.001$) decrease in GSH and SOD levels and a marked ($p<0.001$) elevation in nitric oxide and MDA levels in the arsenic control group compared to the normal group. CoQ treatment significantly ($p<0.001$) improved GSH and SOD levels and effectively reduced ($p<0.001$) nitric oxide and MDA levels compared with the arsenic control group. Rutin (25 mg/kg) treatment showed minimal effects in attenuating arsenic-induced elevated testicular oxido-nitrosative stress compared with the arsenic control group. However, rutin (50 and 100 mg/kg) demonstrated marked ($p<0.01$ and $p<0.001$) and dose-dependent protective effects, reflected by restored antioxidant status (GSH and SOD levels) and reduced oxidative stress markers (nitric oxide and MDA) to normal levels (Table 3).

Attenuation of arsenic-induced alteration in testicular inflammatory markers activities by rutin

The results in Table 3 show significant differences in inflammatory cytokine levels between the normal and arsenic control groups. The arsenic control group exhibited markedly elevated ($p<0.001$) levels of ILs (IL-6 and IL-1β) and TNF-α compared with

Table 3. Attenuation of arsenic-induced alteration in testicular oxido-nitrosative stress and inflammatory markers by rutin.

Parameters	Normal	As Control	CoQ (10)	R (25)	R (50)	R (100)
SOD (U/mg of protein)	13.20 ± 1.10	5.19 ± 0.93###	10.66 ± 0.87***	5.45 ± 0.61	8.91 ± 0.93**	10.66 ± 0.96***
GSH (μg/mg of protein)	13.76 ± 0.64	3.90 ± 0.62###	11.04 ± 0.59***	5.36 ± 0.50	8.31 ± 0.76**	10.43 ± 0.56***
MDA (nM/mg of protein)	0.46 ± 0.10	3.14 ± 0.18###	1.97 ± 0.18***	3.00 ± 0.27	2.11 ± 0.04**	1.59 ± 0.19***
NO (μg/mg of protein)	119.00 ± 9.08	284.00 ± 13.96###	143.90 ± 9.97***	261.40 ± 13.64	222.10 ± 12.14**	167.90 ± 9.82***
TNF-α (pg/mL)	157.00 ± 8.15	409.70 ± 12.69###	222.80 ± 14.07***	377.20 ± 14.06	330.30 ± 8.02**	253.70 ± 12.06***
IL-1β (pg/mL)	17.28 ± 3.86	72.12 ± 1.85###	30.57 ± 2.76***	68.46 ± 1.62	48.95 ± 2.70**	42.78 ± 2.41***
IL-6 (pg/mL)	40.50 ± 5.53	152.60 ± 5.18###	59.41 ± 9.32***	155.50 ± 6.21	130.40 ± 7.87**	71.78 ± 7.13***

Data analysis: One-way ANOVA (post-hoc test: Tukey's multiple range test). Data are reported as mean ± SEM (n=6). Statistically significant compared with ###normal rats, ** and ***As control rats. ###$p < 0.001$, **$p < 0.01$ and ***$p < 0.001$. Arsenic (As), Co-enzyme Q_{10} (CoQ (10)), Glutathione (GSH), Interleukin-1 beta (IL-1β), Interleukin-6 (IL-6), Malondialdehyde (MDA), Nitric Oxide (NO), Rutin (R), Superoxide Dismutase (SOD), and Tumor Necrosis Factor-alpha (TNF-α).

the normal group. CoQ treatment substantially ($p<0.001$) lowered ILs (IL-6 and IL-1β) and TNF-α levels compared to the arsenic control group. Rutin (50 and 100 mg/kg) administration resulted in effective ($p<0.01$ and $p<0.001$) and dose-dependent reductions in cytokine levels compared with the arsenic control group. However, a lower dose of rutin (25 mg/kg) did not reduce cytokine levels to levels comparable to those of the arsenic control group, indicating failure to ameliorate arsenic-induced inflammation (Table 3).

Attenuation of arsenic-induced alteration in testicular caspase-3 and caspase-9 protein expressions by rutin

Fig. 1 illustrates the impact of arsenic exposure on markers of apoptosis in the testes, along with their correlation with sperm count. The caspase-3 and caspase-9 protein expression was significantly increased ($p<0.001$) in the arsenic control group compared with that in the normal group. The substantial elevation in caspase-3 and caspase-9 protein expression was markedly downregulated ($p<0.001$) by CoQ treatment compared to the arsenic control group. Treatment with rutin (50 and 100 mg/kg) significantly ($p<0.01$ and $p<0.001$) and dose-dependently reduced both caspase-3 and caspase-9 relative densities compared to the arsenic control (Figs. 1A and 1B). Furthermore, Figs. 1C and 1D reveal a strong inverse correlation between sperm count and the relative densities of caspase-3 ($R^2 = 0.8168$, $p<0.001$) and Caspase-9 ($R^2 = 0.7075$, $p<0.01$), respectively, indicating that lower sperm counts are associated with increased apoptotic activity.

Attenuation of arsenic-induced alteration in testicular histopathology by rutin

Fig. 2 illustrates the histopathological changes in rat testicular tissue after exposure to arsenic and their amelioration across different treatment groups. In the normal group (Fig. 2A), testicular architecture appeared normal, with intact seminiferous tubules containing organized spermatogenic cells and healthy Leydig cells, and no evidence of necrosis. However, it showed mild inflammation (indicated by black arrows). In contrast, the arsenic con-

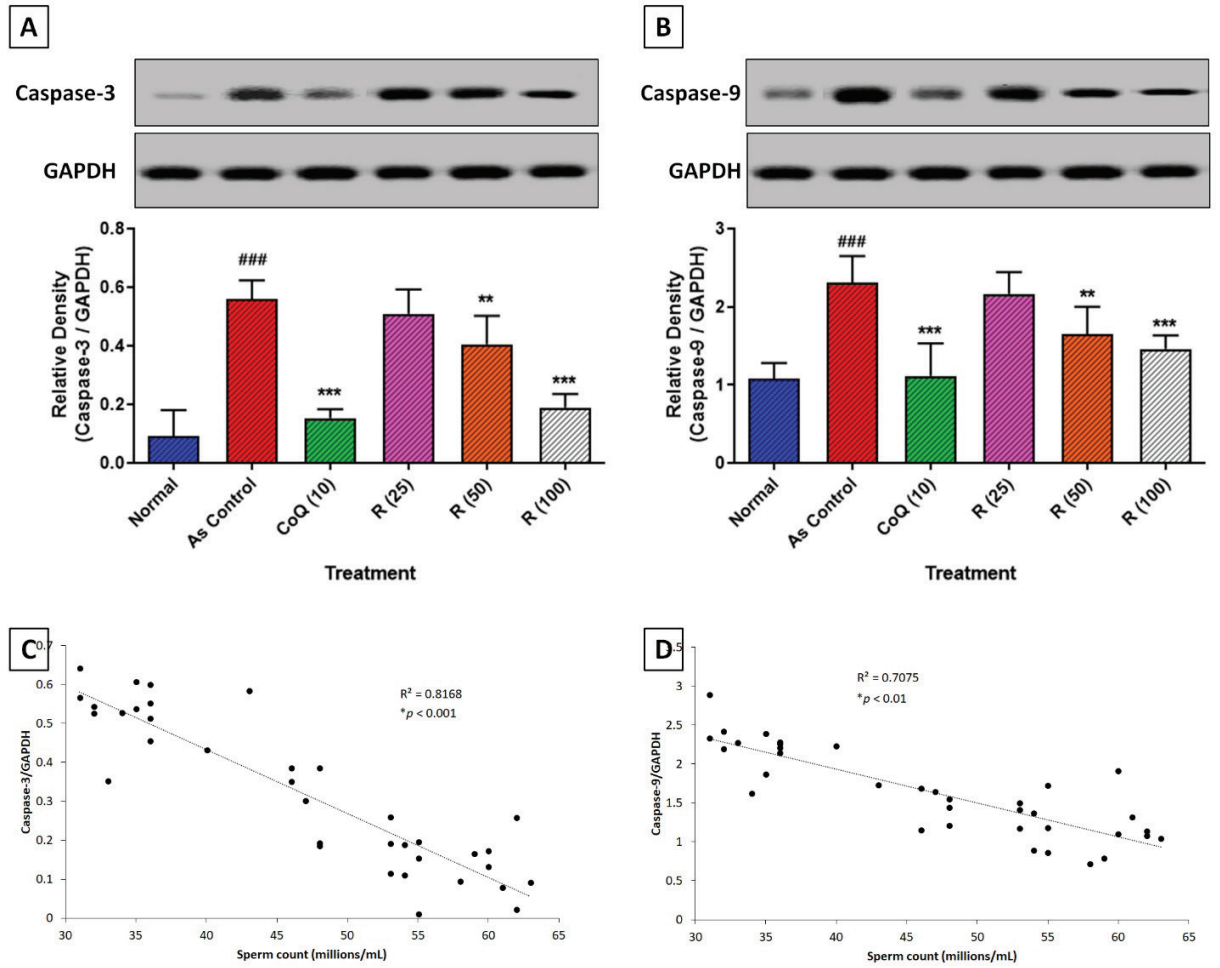

Fig. 1. Attenuation of arsenic-induced alterations in testicular caspase-3 (A) and caspase-9 (B) protein expression by rutin. Correlation of sperm count with caspase-3 (C) and caspase-9 (D) protein expression. Data analysis: One-way ANOVA (post-hoc test: Tukey's multiple range test). Data are reported as mean ± SEM (n=6). Statistically significant compared with ###normal rats, ** and ***As control rats. ###$p < 0.001$, **$p<0.01$ and ***$p<0.001$. Correlation coefficients were determined using a two-sided Fisher's test. Arsenic (As), Co-enzyme Q_{10} (CoQ (10)), Glyceraldehyde-3-Phosphate Dehydrogenase (GAPDH), and Rutin (R). Inflammatory infiltration (black arrow), necrosis (red arrow), and Leydig cells damage (blue arrow).

trol group (Fig. 2B) demonstrated histological aberrations characterized by severe inflammatory infiltration (black arrows), necrosis (red arrows), vacuolated spermatogenic cells (blue arrows), and Leydig cell damage, indicating arsenic-induced toxicity. The quantitative histopathological score in Fig. 2G supports these visual observations, as the arsenic control group exhibited significantly ($p<0.001$) elevated scores for inflammatory infiltration, necrosis, Leydig cell damage, and vacuolated spermatogenic cells than the normal group. Treatment with CoQ significantly reduced ($p<0.001$) these histopathological aberrations compared to the arsenic control group (Fig. 2C), suggesting a protective effect against arsenic-induced testicular injury. The rutin (25 mg/kg) group showed a modest reduction in these scores, but this was not significantly

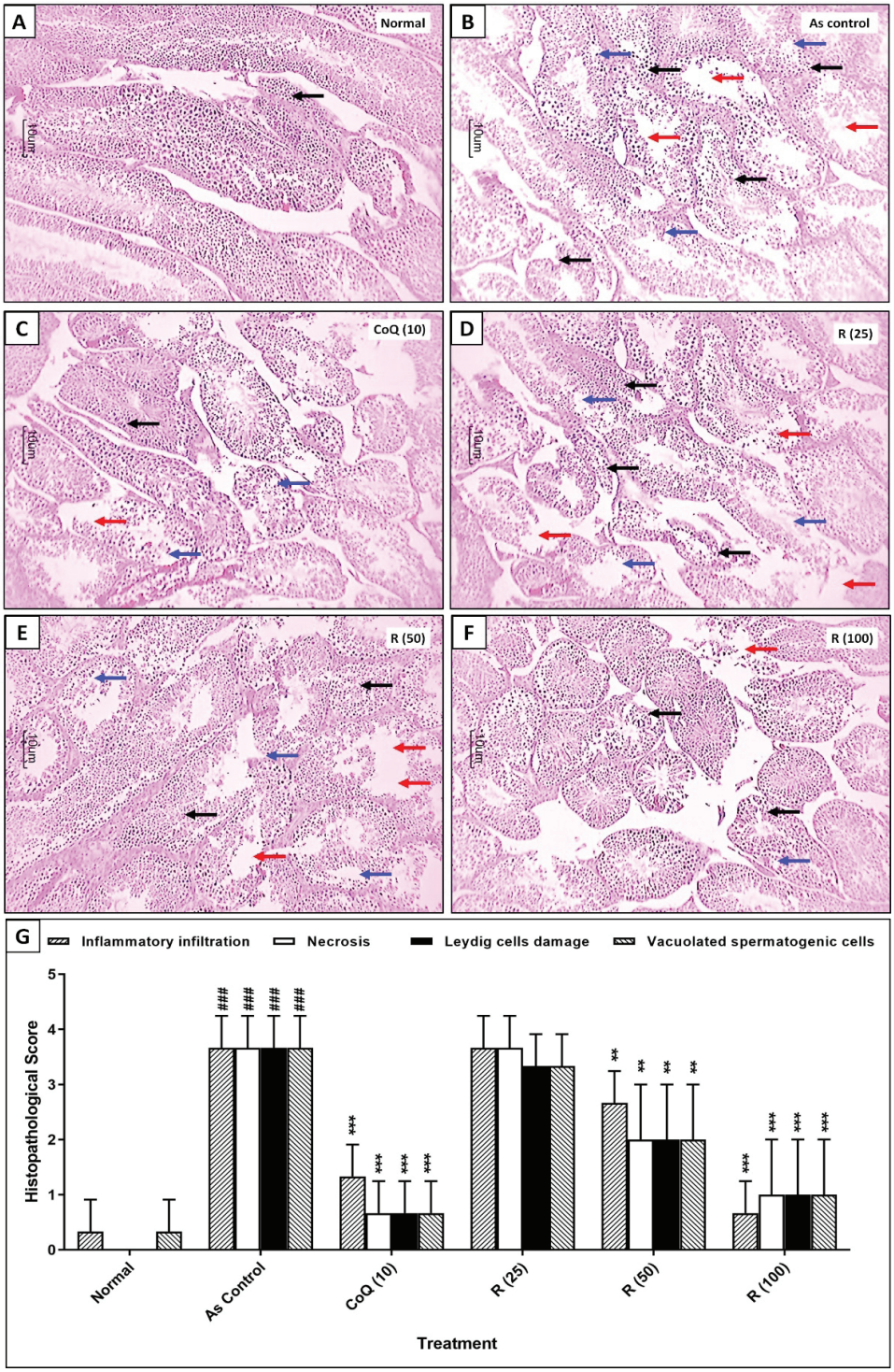

Fig. 2. Attenuation of arsenic-induced alterations in testicular histopathology by rutin treatment. Representative images of testes from each group (A-F). Quantitative analysis of arsenic-induced alterations in testicular histopathology and its attenuation by rutin (G). Data analysis: One-way ANOVA (post-hoc test: Kruskal–Wallis test). Data are reported as mean ± SEM (n=6). Statistically significant compared with $^{###}$normal rats, ** and ***As control rats. $^{###}p < 0.001$, $^{**}p < 0.01$ and $^{***}p < 0.001$. Arsenic (As), Co-enzyme Q_{10} (CoQ (10)), Glyceraldehyde-3-Phosphate Dehydrogenase (GAPDH), and Rutin (R).

different from the higher rutin or CoQ doses (Fig. 2D). Treatment with rutin (50 and 100 mg/kg) showed a significant ($p<0.01$ and $p<0.001$) reduction in arsenic-induced histological aberrations in the testes, reflected in a decrease in inflammatory infiltration, necrosis, Leydig cell damage, and vacuolated spermatogenic cells compared to the arsenic control group (Figs 2E, 2F, and 2G).

DISCUSSION

Arsenic exposure has extensive human health effects, with systemic toxicity affecting multiple organs. It is particularly notorious for its carcinogenic properties, causing skin, lung, and bladder cancers, among others [6]. However, it is crucial to evaluate its adverse effects on male reproductive health as it directly affects male fertility. Arsenic exposure impairs spermatogenesis and reduces sperm quality through oxidative stress and interference with crucial hormonal signaling pathways [11]. Researchers have explored the protective efficacy of phytonutrients, such as lutein and α-lipoic acid, against arsenic-induced oxidative damage in testicular tissues [36]. In the present study, rutin, an herbal intervention, was evaluated for its effects on arsenite-induced testicular damage, and the findings suggested that rutin ameliorated testicular toxicity through its anti-apoptotic, anti-inflammatory, and mitochondrial-protective effects in experimental rats.

Integrative proteomic and metabolomic analyses have shown that arsenic exposure significantly alters the proteome and metabolome in rat testes, affecting spermatogenesis and fertilization through disrupted signaling pathways [37]. Sodium arsenite causes significant testicular damage primarily through oxidative stress, apoptosis, and inflammatory pathways. Studies have demonstrated that chronic exposure to sodium arsenite can lead to a significant decrease in both absolute and relative testicular weight [38]. This reduction in testicular weight is attributed to the toxic effects of arsenic on testicular tissue and its interference with normal spermatogenesis and enzyme activities, including decreased acid phosphatase, sorbitol dehydrogenase, and 17beta-hydroxy-steroid dehydrogenase activities, while increasing lactate dehydrogenase and gamma-glutamyl transpeptidase activities. Additionally, arsenite exposure leads to a notable increase in abnormal sperm forms, along with a decrease in sperm count and motility [38]. Furthermore, arsenic is known to accumulate significantly in reproductive tissues, underscoring its potential to cause prolonged toxic effects [38]. This accumulation in the testes, epididymis, and prostate is linked to oxidative stress and histopathological alterations, indicating that arsenic's effects are more profound at the cellular level [8,14]. In the present study, administration of rutin significantly attenuated arsenite-induced decreases in testes, epididymis, and prostate weights, suggesting its protective efficacy in reproductive organs.

Sodium arsenite led to decreased levels of serum testosterone, luteinizing hormone, and follicle-stimulating hormone, and to significant changes in sperm parameters, including reduced sperm count and motility, and an increase in abnormal sperm[15]. Serum hormone levels, such as testosterone, FSH, and LH, play crucial roles in regulating male reproductive function [39]. Testosterone, which is primarily produced in the testes, is vital for normal male reproductive functions and secondary sexual characteristics. FSH and LH, secreted by the pituitary gland, regulate testicular function, including steroidogenesis and spermatogenesis [40]. Chronic exposure to arsenite is often associated with reduced testosterone levels owing to impaired testicular function. This can be attributed to the direct cytotoxic effects of arsenite on Leydig cells, which are responsible for testosterone production. Additionally, alterations in hormone levels can disrupt the hypothalamic-pituitary-gonadal axis, leading to compensatory changes in LH and FSH levels. In this study, arsenite-induced testicular

damage was reflected in changes in serum testosterone, FSH, and LH levels. However, administration of rutin restored the diminished levels of these hormones in the serum.

Oxidative stress plays a crucial role in arsenic-induced toxicity, impacting various biological systems and leading to significant health issues. Arsenic, a toxic metalloid, can cross cellular barriers and accumulate in tissues, contributing to oxidative stress by generating ROS [41,42]. ROS generation is central to the pathogenesis of arsenic toxicity, as it leads to mitochondrial dysfunction, a critical factor in neurotoxicity, and other health issues [43,44]. Arsenic-induced oxidative stress leads to mitochondrial damage by disrupting the normal balance between antioxidants and pro-oxidants within cells. This disruption impairs mitochondrial membrane potential, promotes cytochrome c release, and triggers apoptosis through caspase activation[42]. On a systemic level, oxidative stress also causes chromosomal instability and DNA damage, leading to further complications, such as carcinogenesis and neurological disorders[44-47]. Moreover, arsenic exposure has been shown to deplete antioxidant capacities and elevate oxidative damage biomarkers, such as malondialdehyde (MDA) and nitric oxide, owing to the heightened oxidative environment[48,49]. These changes underline the oxidative stress mechanism as a cornerstone of arsenic toxicity, which affects various systems, including the reproductive system [50]. Therapeutic strategies to combat arsenic-induced oxidative stress focus on enhancing mitochondrial function and increasing antioxidant defense. Acetyl-L-carnitine (ALC), for instance, has been shown to counteract arsenic-induced oxidative stress by improving antioxidant mechanisms and mitochondrial function, thus offering a potential therapeutic pathway [42]. Other antioxidants, such as curcumin and apigenin, also exhibit protective effects by reducing ROS and supporting cellular antioxidant systems, highlighting their possible roles in mitigating arsenic toxicity[51,52]. In the present investigation, arsenic-induced toxicity, associated with elevated oxidative stress, contributed to various cellular and systemic damage, as reflected by diminished testicular mitochondrial enzyme activity. However, rutin treatment effectively increased testicular glutathione and superoxide levels and reduced malondialdehyde and nitric oxide levels, suggesting its protective effects against arsenic-induced mitochondrial dysfunction, potentially by mitigating oxidative stress and enhancing mitochondrial energy production.

Inflammation is a significant contributor to arsenic-induced testicular toxicity. Pro-inflammatory cytokines, such as TNF-α and interleukins, mediate this process. TNF-α induces apoptosis and promotes inflammatory responses [53]. Inflammation induced by TNF-α can activate various signaling pathways, culminating in oxidative stress and tissue damage [54-56]. It has been observed that arsenic exposure results in the upregulation of inflammatory mediators, such as TNF-α and interleukins, contributing to testicular damage [57]. Furthermore, Caspases 3 and 9 play crucial roles in the apoptotic pathways underlying arsenic-induced testicular toxicity. Caspase-9 is part of the intrinsic or mitochondrial apoptosis pathway, which is often activated by cellular stressors, including toxins such as arsenic. It is responsible for activating downstream effector caspases, including caspase-3 [58,59]. Caspase-3 then executes apoptosis by cleaving cellular substrates, leading to systematic breakdown of cellular components and cell death [60-62]. In arsenic-induced testicular toxicity, activation of these caspases is indicative of enhanced apoptotic activity, contributing to the observed tissue damage and dysfunction [57]. In the current study, arsenic-induced elevated inflammation and apoptosis, mediated by cytokines such as TNF-α and enzymes such as caspases 3 and 9, highlighted the development of arsenic-induced testicular toxicity. However, rutin treatment mitigated the toxic effects induced by chronic exposure to arsenic via

the amelioration of these pathways, suggesting its therapeutic potential against arsenic-induced testicular toxicity.

This study has some limitations. First, the study focused on acute arsenic exposure (two consecutive days), which may not reflect the effects of chronic, long-term exposure often observed in human populations. Second, the study only used sodium arsenite, whereas environmental arsenic exposure often involves multiple arsenic species. Third, this study did not address the bioavailability and metabolism of rutin in rats, which could affect its efficacy in humans. Lastly, the study focused on rutin alone and did not explore its potential synergistic effects with other protective agents.

As a conclusion, rutin demonstrated significant protective effects against sodium arsenite-induced testicular toxicity in rats. Rutin ameliorated arsenic-induced damage by reducing oxidative stress, inflammation, and apoptosis in testicular tissue, while improving sperm parameters and hormone levels. These findings suggest that rutin may have therapeutic potential in mitigating arsenic-related reproductive toxicity, although further research is needed to elucidate its mechanisms of action and clinical applicability fully.

Acknowledgement

Medical writing support for the development of this manuscript, under the direction of the authors, was provided by Yonnova Scientific Consultancy Pvt. Ltd. in accordance with the Good Publication Practice guidelines.

Funding

This study was funded by the Zhejiang Province Medical and Health Science and Technology Plan Project (2021RC096) and the Zhejiang Traditional Chinese Medicine Science and Technology Plan Project (2023ZL370).

Conflicts of interest

The authors declare that they have no conflict of interest regarding this study.

Availability of data

The datasets generated and/or analyzed during the current study are not publicly available due to confidentiality agreements; supporting data can only be made available to bona fide researcher's subject to a non-disclosure agreement.

Ethical approval

All experiments were performed between 09:00 and 17:00. The experimental protocol was approved by the Institutional Animal Ethics Committee of the Shaanxi Kangfu Hospital (approval no. sxkf2025). All procedures involving animals were conducted in accordance with the National Institute of Health Guide for the Care and Use of Laboratory Animals.

ORCID number of authors

- Yunyun Wang (YW): 0009-0007-3462-5323
- Zengrong Hua (ZH): 0009-0008-8248-8148
- Jin Qing Hui (JQH): 0009-0008-5583-9213
- Dandan Qiu (DQ): 0009-0009-1376-7853

Author contributions

Each author has made significant contributions to the development of this manuscript. YW: conceived and designed the evaluation and drafted the manuscript; ZH and DQ: performed data acquisition; YW: participated in developing the assessment, performed parts of the statistical analysis, and helped to draft the manuscript; JQH: revised the manuscript and performed the statistical analysis. All the authors have read and approved the final version of the manuscript.

REFERENCES

1. **Adil M, Kandhare AD, Ghosh P, Bodhankar SL**. Sodium arsenite-induced myocardial bruise in rats: Ameliorative effect of naringin via TGF-β/Smad and Nrf/HO pathways. Chem Biol Interact. 2016;253: 66-77. *https://doi.org/10.1016/j.cbi.2016.05.015.*
2. **Adil M, Kandhare AD, Visnagri A, Bodhankar SL**. Naringin ameliorates sodium arsenite-induced renal and hepatic toxicity in rats: decisive role of KIM-1, Caspase-3, TGF-β, and TNF-α. Ren Fail. 2015;37 (8):1396-1407. *https://doi.org/10.3109/0886022X.2015.1074462*
3. **Kim YJ, Kim JM**. Arsenic Toxicity in Male Reproduction and Development. Dev Reprod. 2015;19 (4):167-180. *https://doi.org/10.12717/DR.2015.19.4.167.*
4. **Rahmani S, Naraki K, Roohbakhsh A, Hayes AW, Karimi G**. The protective effects of rutin on the liver, kidneys, and heart by counteracting organ toxicity caused by synthetic and natural compounds. Food Sci Nutr. 2022;11 (1):39-56. *https://doi.org/10.1002/fsn3.3041.*
5. **World Health Organization**. Obesity and overweight [Internet]. Geneva: World Health Organization; 2020. Available from: *https://www.who.int/news-room/fact-sheets/detail/obesity-and-overweight*
6. **Hong YS, Song KH, Chung JY**. Health effects of chronic arsenic exposure. J Prev Med Public Health. 2014;47(5):245-252. https://doi.org/10.3961/jpmph.14.035.
7. **Mukherjee AA, Kandhare AD, Bodhankar SL**. Elucidation of protective efficacy of Pentahydroxy flavone isolated from Madhuca indica against arsenite-induced cardiomyopathy: Role of Nrf-2, PPAR-gamma, c-fos and c-jun. Environ Toxicol Pharmacol. 2017;56:172-185. *https://doi.org/10.1016/j.etap.2017.08.027*
8. **Souza AC, Marchesi SC, Ferraz RP, Lima GD, de Oliveira JA, Machado-Neves M**. Effects of sodium arsenate and arsenite on male reproductive functions in Wistar rats. J Toxicol Environ Health A. 2016;79(6):274-286. *https://doi.org/10.1080/15287394.2016.1150926.*
9. **Zubair M, Ahmad M, Qureshi ZI**. Review on arsenic-induced toxicity in male reproductive system and its amelioration. Andrologia. 2017; 49(9):e12791. *https://doi.org/10.1111/and.12791.*
10. **Rachamalla M, Chinthada J, Kushwaha S, Putnala SK, Sahu C, Jena G, et al.** Contemporary Comprehensive Review on Arsenic-Induced Male Reproductive Toxicity and Mechanisms of Phytonutrient Intervention. Toxics. 2022; 10(12):744. *https://doi.org/10.3390/toxics10120744.*
11. **Souza ACF, Bastos DSS, Sertorio MN, Santos FC, Ervilha LOG, de Oliveira LL, et al.** Combined effects of arsenic exposure and diabetes on male reproductive functions. Andrology. 2019; 7(5):730-740. *https://doi.org/10.1111/andr.12613.*
12. **Wang S, Zhao Y, Wu L, Tang M, Su C, Hei TK, Yu Z.** Induction of germline cell cycle arrest and apoptosis by sodium arsenite in Caenorhabditis elegans. Chem Res Toxicol. 2007;20(2):181-186. *https://doi.org/10.1021/tx0601962.*
13. **Silva CS, Kudlyk T, Tryndyak VP, Twaddle NC, Robinson B, Gu Q, et al.** Gene expression analyses reveal potential mechanism of inorganic arsenic-induced apoptosis in zebrafish. J Appl Toxicol. 2023;43(12):1872-1882. *https://doi.org/10.1002/jat.4520.*
14. **Uygur R, Aktas C, Caglar V, Uygur E, Erdogan H, Ozen OA**. Protective effects of melatonin against arsenic-induced apoptosis and oxidative stress in rat testes. Toxicol Ind Health. 2016;32(5):848-859. *https://doi.org/10.1177/0748233713512891.*
15. **Omar SM, Zahran NN, Alhotan RA, Hussein EO, Galik B, Saleh AA**. Evaluation of *Salvia hispanica* as a Therapeutic Agent against Sodium Arsenic-Induced Testicular Toxicity in a Male Rats Model. Life (Basel Switzerland). 2024; 14(1):109. *https://doi.org/10.3390/life14010109.*
16. **Pires Das Neves RN, Carvalho F, Carvalho M, Fernandes E, Soares E, de Bastos ML, et al.** Protective activity of hesperidin and lipoic acid against sodium arsenite acute toxicity in mice. Toxicol Pathol. 2004;32(5):527-535. *https://doi.org/10.1080/01926230490502566.*

17. **Negahdari R, Bohlouli S, Sharifi S, Maleki Dizaj S, Rahbar Saadat Y, Khezri K, et al.** Therapeutic benefits of rutin and its nanoformulations. Phytother Res. 2021; 35(4):1719-1738. *https://doi.org/10.1002/ptr.6904.*
18. **Budzynska B, Faggio C, Kruk-Slomka M, Samec D, Nabavi SF, Sureda A, et al.** Rutin as Neuroprotective Agent: From Bench to Bedside. Curr Med Chem. 2019;26 (27):5152-5164. *https://doi.org/10.2174/0929867324666171003114154.*
19. **Hosseinzadeh H, Nassiri-Asl M**. Review of the protective effects of rutin on the metabolic function as an important dietary flavonoid. J Endocrinol Invest. 2014;37 (9):783-788. *https://doi.org/10.1007/s40618-014-0096-3.*
20. **Ganeshpurkar A, Saluja AK**. The Pharmacological Potential of Rutin. Saudi Pharm J. 2017;25 (2):149-164. *https://doi.org/10.1016/j.jsps.2016.04.025*
21. **Niture NT, Ansari AA, Naik SR**. Anti-hyperglycemic activity of rutin in streptozotocin-induced diabetic rats: an effect mediated through cytokines, antioxidants and lipid biomarkers. Indian J Exp Biol. 2014;52 (7):720-727. PMID: 25059040.
22. **Kamalakkannan N, Prince PS**. Antihyperglycaemic and antioxidant effect of rutin, a polyphenolic flavonoid, in streptozotocin-induced diabetic wistar rats. Basic Clin Pharmacol Toxicol. 2006;98:97-103. *https://doi.org/10.1111/j.1742-7843.2006.pto_241.x*
23. **Das J, Ghosh J, Manna P, Sinha M, Sil PC**. Taurine protects rat testes against $NaAsO_2$ induced oxidative stress and apoptosis via mitochondrial dependent and independent pathways. Toxicol Lett. 2009;187(3):201-210. *https://doi.org/10.1016/j.toxlet.2009.03.001.*
24. **Adil M, Visnagri A, Kumar VS, Kandhare AD, Ghosh P, Bodhankar SL**. Protective effect of naringin on sodium arsenite induced testicular toxicity via modulation of biochemical perturbations in experimental rats. Pharmacologia. 2014;5 (6):222-234. *https://doi.org/10.5567/pharmacologia.2014.222.234*
25. **Thangapandiyan S, Miltonprabu S**. Epigallocatechin gallate exacerbates fluoride-induced oxidative stress mediated testicular toxicity in rats through the activation of Nrf2 signaling pathway. Asian Pac J Reprod. 2015;4 (4):272-287. *https://doi.org/https://doi.org/10.1016/j.apjr.2015.07.005*
26. **Kandhare AD, Kumar VS, Adil M, Rajmane AR, Ghosh P, Bodhankar SL**. Investigation of gastro protective activity of Xanthium strumarium L. by modulation of cellular and biochemical marker. Orient Pharm Exp Med. 2012;12: 287-299. *https://doi.org/10.1007/s13596-012-0090-2*
27. **Kandhare AD, Raygude KS, Ghosh P, Ghule AE, Bodhankar SL**. Neuroprotective effect of naringin by modulation of endogenous biomarkers in streptozotocin induced painful diabetic neuropathy. Fitoterapia. 2012;83 (4):650-659. *https://doi.org/10.1016/j.fitote.2012.01.010*
28. **Kandhare AD, Raygude KS, Ghosh P, Ghule AE, Bodhankar SL**. Therapeutic role of curcumin in prevention of biochemical and behavioral aberration induced by alcoholic neuropathy in laboratory animals. Neurosci Lett. 2012;511(1):18-22. *https://doi.org/10.1016/j.neulet.2012.01.019*
29. **Visnagri A, Kandhare AD, Shiva Kumar V, Rajmane AR, Mohammad A, Ghosh P et al.** Elucidation of ameliorative effect of Co-enzyme Q10 in streptozotocin-induced diabetic neuropathic perturbation by modulation of electrophysiological, biochemical and behavioral markers. Biomed Aging Pathol. 2012;2 (4):157-172. *https://doi.org/http://dx.doi.org/10.1016/j.biomag.2012.10.006*
30. **Adil M, Kandhare AD, Dalvi G, Ghosh P, Venkata S, Raygude KS, Bodhankar SL**. Ameliorative effect of berberine against gentamicin-induced nephrotoxicity in rats via attenuation of oxidative stress, inflammation, apoptosis and mitochondrial dysfunction. Ren Fail. 2016;38 (6):996-1006. *https://doi.org/10.3109/0886022X.2016.1165120*

31. **Ketkar S, Rathore A, Kandhare AD, Lohidasan S, Bodhankar SL, Paradkar A, et al.** Alleviating exercise-induced muscular stress using neat and processed bee pollen: oxidative markers, mitochondrial enzymes, and myostatin expression in rats. Integr Med Res. 2015;4 (3):147-160. *https://doi.org/10.1016/j.imr.2015.02.003*
32. **Liu J, Han XC, Wang D, Kandhare AD, Mukherjee-Kandhare AA, Bodhankar SL et al.** Elucidation of Molecular Mechanism Involved in Nephroprotective Potential of Naringin in Ethylene Glycol-Induced Urolithiasis in Experimental Uninephrectomized Hypertensive Rats. Lat Am J Pharm. 2020;39 (5):991-999.
33. **Yao X, Li L, Kandhare AD, Mukherjee–Kandhare AA, Bodhankar SL**. Attenuation of reserpine–induced fibromyalgia via ROS and serotonergic pathway modulation by fisetin, a plant flavonoid polyphenol. Exp Ther Med. 2020;19 (2):1343-1355. *https://doi.org/10.3892/etm.2019.8328*
34. **Zhang K, Kandhare A, Mukherjee-Kandhare A, Bodhankar S**. Apigenin attenuated ethylene glycol induced urolithiasis in uninephrectomized hypertensive rats: A possible role of bikunin, BMP-2/4, and osteopontin. Pharmacogn Mag. 2020;16 (71):455-463. *https://doi.org/10.4103/pm.pm_83_20*
35. **McNamara ER, Madden-Fuentes RJ, Routh JC, Rouse D, Madden JF, Wiener JS, et al.** Evaluation of cold ischemia for preservation of testicular function during partial orchiectomy in the rat model. J Pediatr Urol. 2014;10 (4):593-597. *https://doi.org/10.1016/j.jpurol.2014.06.005*
36. **Prathima P, Pavani R, Sukeerthi S, Sainath SB**. α-Lipoic acid inhibits testicular and epididymal oxidative damage and improves fertility efficacy in arsenic-intoxicated rats. J Biochem Mol Toxicol. 2018;32 (2):e22016. *https://doi.org/10.1002/jbt.22016.*
37. **Huang Q, Luo L, Alamdar A, Zhang J, Liu L, Tian M, et al.** Integrated proteomics and metabolomics analysis of rat testis: Mechanism of arsenic-induced male reproductive toxicity. Sci Rep. 2016;6:32518. *https://doi.org/10.1038/srep32518.*
38. **Pant N, Murthy RC, Srivastava SP**. Male reproductive toxicity of sodium arsenite in mice. Hum Exp Toxicol. 2004; 23(8):399-403. *https://doi.org/10.1191/0960327104ht467oa.*
39. **Oduwole OO, Huhtaniemi IT, Misrahi M**. The Roles of Luteinizing Hormone, Follicle-Stimulating Hormone and Testosterone in Spermatogenesis and Folliculogenesis Revisited. Int J Mol Sci. 2021;22 (23):12735. *https://doi.org/10.3390/ijms222312735*
40. **Oduwole OO, Peltoketo H, Huhtaniemi IT**. Role of Follicle-Stimulating Hormone in Spermatogenesis. Front Endocrinol. (Lausanne). 2018;9:763. *https://doi.org/10.3389/fendo.2018.00763*
41. **Prakash C, Soni M, Kumar V.** Mitochondrial oxidative stress and dysfunction in arsenic neurotoxicity: A review. J Appl Toxicol. 2016; 36 (2):179-188. *https://doi.org/10.1002/jat.3256*
42. **Keshavarz-Bahaghighat H, Sepand MR, Ghahremani MH, Aghsami M, Sanadgol N, Omidi A, et al.** Acetyl-L-Carnitine Attenuates Arsenic-Induced Oxidative Stress and Hippocampal Mitochondrial Dysfunction. Biol Trace Elem Res. 2018;184 (2):422-435. *https://doi.org/10.1007/s12011-017-1210-0*
43. **Thakur M, Rachamalla M, Niyogi S, Datusalia AK, Flora SJS**. Molecular Mechanism of Arsenic-Induced Neurotoxicity including Neuronal Dysfunctions. Int J Mol Sci. 2021;22 (18):10077. *https://doi.org/10.3390/ijms221810077*
44. **Liu L, Trimarchi JR, Navarro P, Blasco MA, Keefe DL**. Oxidative Stress Contributes to Arsenic-induced Telomere Attrition, Chromosome Instability, and Apoptosis. J Biol Chem. 2003;278 (34):31998-32004. *https://doi.org/10.1074/jbc.m303553200*
45. **Cui J, Wang G, Kandhare AD, Mukherjee-Kandhare AA, Bodhankar SL**. Neuroprotective effect of naringin, a flavone glycoside in quinolinic acid-induced neurotoxicity: Possible role of PPAR-gamma, Bax/Bcl-2, and caspase-3. Food Chem

Toxicol. 2018;121:95-108. *https://doi.org/10.1016/j.fct.2018.08.028*

46. **Kandhare AD, Mukherjee AA, Bodhankar SL**. Neuroprotective effect of *Azadirachta indica* standardized extract in partial sciatic nerve injury in rats: Evidence from anti-inflammatory, antioxidant and anti-apoptotic studies. EXCLI J. 2017;16:546-565. *https://doi.org/doi: 10.17179/excli 2017-161.*
47. **Raygude KS, Kandhare AD, Ghosh P, Ghule AE, Bodhankar SL**. Evaluation of ameliorative effect of quercetin in experimental model of alcoholic neuropathy in rats. Inflammopharmacoly. 2012; 20 (6):331-341. *https://doi.org/10.1007/s10 787-012-0122-z*
48. **Xu M, Rui D, Yan Y, Xu S, Niu Q, Feng G, et al.** Oxidative Damage Induced by Arsenic in Mice or Rats: A Systematic Review and Meta-Analysis. Biol Trace Elem Res. 2017; 76 (1):154-175. *https://doi.org/10.1007/s12011-016-0810-4*
49. **Visnagri A, Kandhare AD, Chakravarty S, Ghosh P, Bodhankar SL**. Hesperidin, a flavanoglycone attenuates experimental diabetic neuropathy via modulation of cellular and biochemical marker to improve nerve functions. Pharm Biol. 2014;52 (7):814-828. *https://doi.org/10.3109/138 80209.2013.870584*
50. **Jomova K, Jenisova Z, Feszterova M, Baros S, Liska J, Hudecova D, et al.** Arsenic: toxicity, oxidative stress and human disease. J Appl Toxicol. 2011;31 (2):95-107. *https://doi.org/10.1002/jat.1649*
51. **Biswas J, Sinha D, Mukherjee S, Roy S, Siddiqi M, Roy M**. Curcumin protects DNA damage in a chronically arsenic-exposed population of West Bengal. Hum Exp Toxicol. 2010;29 (6):513-524. *https://doi.org/10.1177/0960327109359020*
52. **Almeer R, Alyami NM**. The protective effect of apigenin against inorganic arsenic salt-induced toxicity in PC12 cells. Environ Sci Poll Res. 2023;30:106625-106635. *https://doi.org/10.1007/s11356-023-29884-w*
53. **El-Khadragy M, Al-Megrin WA, Alsadhan NA, Metwally DM, El-Hennamy RE, Salem FEH, et al.** Impact of Coenzyme Q10 Administration on Lead Acetate-Induced Testicular Damage in Rats. Oxid Med Cell Longev. 2020;2020: 4981386. *https://doi.org/10.1155/2020/4981386*
54. **Devkar ST, Kandhare AD, Zanwar AA, Jagtap SD, Katyare SS, Bodhankar SL, et al.** Hepatoprotective effect of withanolide-rich fraction in acetaminophen-intoxicated rat: decisive role of TNF-α, IL-1β, COX-II and iNOS. Pharm Biol. 2016; 54 (11): 2394-2403. *https://doi.org/10.3109/1388 0209.2016.1157193.*
55. **Honmore VS, Kandhare AD, Kadam PP, Khedkar VM, Natu AD, Rojatkar SR, et al.** Diarylheptanoid, a constituent isolated from methanol extract of Alpinia officinarum attenuates TNF-alpha level in Freund's complete adjuvant-induced arthritis in rats. J Ethnopharmacol. 2019;229:233-245. *https://doi.org/10.1016/j.jep.2018.10.019*
56. **Kandhare AD, Bodhankar SL, Mohan V, Thakurdesai PA**. Effect of glycosides based standardized fenugreek seed extract in bleomycin-induced pulmonary fibrosis in rats: Decisive role of Bax, Nrf2, NF-κB, Muc5ac, TNF-α and IL-1β. Chem Biol Interact. 2015; 237:151-165. *https://doi.org/10.1016/j.cbi.2015.06.019.*
57. **Rao G, Qiao B, Zhong G, Li T, Su Q, Wu S, et al.** Arsenic and polystyrene-nano plastics co-exposure induced testicular toxicity: Triggers oxidative stress and promotes apoptosis and inflammation in mice. Environ Toxicol. 2023;39 (1):264-276. *https://doi.org/10.1002/tox.23970*
58. **Joza N, Susin SA, Daugas E, Stanford WL, Cho SK, Li CY, et al.** Essential role of the mitochondrial apoptosis-inducing factor in programmed cell death. Nature 2001;410(6828):549-554. *https://doi.org/10.1038/35069004*
59. **Zhao P, Wang Y, Yang Q, Yu G, Ma F, Dong J**. Abamectin causes cardiac dysfunction in carp via inhibiting redox equilibrium and resulting in immune inflammatory response and programmed cell death. Environ Sci Pollut Res Int. 2023;30 (11):29494-29509. *https://doi.org/10.1007/s11356-022-24004-6*

60. **Ma T, Kandhare AD, Mukherjee-Kandhare AA, Bodhankar SL**. Fisetin, a plant flavonoid ameliorates doxorubicin-induced cardiotoxicity in experimental rats: the decisive role of caspase-3, COX-II, cTn-I, iNOs and TNF-alpha. Mol Biol Rep 2019;46 (1):105-118. *https://doi.org/10.1007/s11033-018-4450-y*

61. **Visnagri A, Kandhare AD, Bodhankar SL**. Renoprotective effect of berberine via intonation on apoptosis and mitochondrial-dependent pathway in renal ischemia reperfusion-induced mutilation. Ren Fail. 2015;37(3):482-493. *https://doi.org/10.3109/0886022X.2014.996843*

62. **Ghule AE, Kandhare AD, Jadhav SS, Zanwar AA, Bodhankar SL**. Omega-3-fatty acid adds to the protective effect of flax lignan concentrate in pressure overload-induced myocardial hypertrophy in rats via modulation of oxidative stress and apoptosis. Int Immunopharmacol. 2015; 28 (1):751-763. *https://doi.org/10.1016/j.intimp.2015.08.005.*

Invest Clin 66(4): 426- 435, 2025 https://doi.org/10.54817/IC.v66n4a06

Correlations of interleukin-17 and regulatory T cells with the severity of chronic obstructive pulmonary disease and pulmonary function.

Jun Chen, Tingting Zhao, Yingying Gao and Zizhou Zhang

Department of Respiratory and Critical Care Medicine, Changzhou Seventh People's Hospital (Changzhou Geriatric Hospital Affiliated With Soochow University), Changzhou, Jiangsu Province, China.

Keywords: Pulmonary Disease, Chronic Obstructive; Correlation Measures; Interleukins; Respiratory Function Tests; T-Lymphocytes, Regulatory; Disease Severity.

Abstract. We aimed to explore the correlation of interleukin-17 (IL-17) and regulatory T (Treg) cells with the severity of chronic obstructive pulmonary disease (COPD) and pulmonary function. A total of 90 COPD patients, all with a confirmed diagnosis of COPD and without any history of asthma, were included to ensure that the findings are specific to COPD. In addition, a smoking group (healthy smokers, n=90) and a healthy group (healthy non-smokers, n=90) were studied. The COPD group had the highest IL-17 level and the lowest cluster of differentiation 4 (CD4) + Treg cell count, CD25+Treg cell count, and CD4+CD25+Treg cell count in peripheral blood, followed by the smoking and healthy groups ($p<0.05$). The $CD4^+$ Treg cell count, $CD25^+$ Treg cell count, $CD4^+CD25^+$ Treg cell count, forced vital capacity (FVC), forced expiratory volume in one second (FEV_1), and FEV_1/FVC were found to be the highest in the mild group, followed by those of moderate and severe groups ($p<0.05$). The $CD4^+$ Treg cell count, $CD25^+$ Treg cell count, and $CD4^+CD25^+$ Treg cell count displayed positive correlations with FEV_1, FVC, and FEV_1/FVC ($r>0$, $p<0.05$) and negative correlations with the IL-17 level ($r<0$, $p<0.05$). The IL-17 level was negatively correlated with FEV_1, FVC, and FEV_1/FVC ($r<0$, $p<0.05$). Importantly, this study highlights the combined analysis of IL-17 and Treg subsets, which provides additional insights into their joint association with COPD severity beyond IL-17 alone.

Corresponding author: Zizhou Zhang. Department of Respiratory and Critical Care Medicine, Changzhou Seventh People's Hospital (Changzhou Geriatric Hospital Affiliated with Soochow University), Changzhou 213011, Jiangsu Province, China. Email: zhangzzcsph@ph-edu.cn

Correlación de la interleucina-17 y las células T reguladoras con la gravedad de la enfermedad pulmonar obstructiva crónica y la función pulmonar.

Invest Clin 2025; 66 (4): 426 – 435

Palabras clave: Enfermedad Pulmonar Obstructiva Crónica; Medidas de Correlación; Interleucinas; Pruebas de Función Respiratoria; Linfocitos T Reguladores; Gravedad de la Enfermedad.

Resumen. Nuestro objetivo fue explorar las correlaciones entre la interleucina-17 (IL-17) y las células T reguladoras (Treg), así como entre la gravedad de la enfermedad pulmonar obstructiva crónica (EPOC) y la función pulmonar. Se compararon los datos de un grupo con EPOC (pacientes con EPOC tratados entre junio de 2020 y septiembre de 2023, n=90), un grupo de fumadores (fumadores sanos, n=90) y un grupo control (no fumadores sanos, n=90). El grupo de EPOC presentó el nivel más alto de IL-17 y el recuento más bajo de células Treg CD4+, CD25+ y CD4+CD25+ en la sangre periférica, seguido por los grupos de fumadores y de control ($p<0,05$). El recuento de células Treg $CD4^+$, células Treg $CD25^+$, células Treg CD4+CD25+, la capacidad vital forzada (FVC), el volumen espiratorio forzado en el primer segundo (FEV_1) y la relación FEV1/FVC fueron más altos en el grupo leve de EPOC, seguido por los grupos moderado y severo ($p<0,05$). El recuento de células Treg $CD4^+$, células Treg $CD25^+$ y células Treg $CD4^+CD25^+$ mostró correlaciones positivas con FEV1, FVC y FEV_1/FVC ($r>0$, $p<0,05$) y correlaciones negativas con el nivel de IL-17 ($r<0$, $p<0,05$). El nivel de IL-17 se correlacionó negativamente con FEV_1, FVC y FEV_1/FVC ($r<0$, $p<0,05$). La detección combinada de IL-17 y de subconjuntos de Treg es útil para aumentar el valor predictivo de estos en la aparición de EPOC.

Received: 02-03-2025 Accepted: 04-11-2025

INTRODUCTION

Chronic obstructive pulmonary disease (COPD), a chronic inflammatory disease, is pathologically characterized by airflow obstruction of the respiratory tract, and COPD patients usually develop fatigue, shortness of breath, cough, and other typical respiratory symptoms [1,2]. In China, the incidence rate of COPD is 13.6% in people aged over 40 years old and as high as 24.8% in the elderly [3]. The specific pathogenesis of COPD has not been fully elucidated. Still, it is mainly believed to involve mechanisms such as oxidative/antioxidative imbalance, chronic inflammatory responses in the airways and pulmonary parenchyma, and protein/anti-protein imbalance [4]. A study reported that T lymphocytes act as vital players in modulating airway inflammation in COPD, in which helper T (Th) cells are the major players [5]. Cluster of differentiation 4 $(CD4)^+$ T lymphocytes belong to Th lymphocytes, and activated $CD4^+$ T lymphocytes can be classified into Th17 cells and regulatory T (Treg) cells. Th17 and Treg cells repress and antagonize each oth-

er during differentiation, and their balance can confer immune tolerance, whereas an imbalance can induce various autoimmune and infectious diseases [6]. Th17 triggers and progressively amplifies immune responses primarily through the generation of interleukin-17 (IL-17), and a sustained increase in IL-17 content will induce neutrophilic chronic inflammation. As a result, airway inflammation and progressive airway obstruction emerge [7].

Based on this, in the present study, the levels of IL-17 and Treg subsets in the peripheral blood of COPD patients were measured, and their correlations with COPD occurrence and pulmonary function were investigated, aiming to identify targets for the prevention and treatment of COPD.

MATERIALS AND METHODS

Subjects

COPD patients visiting our hospital from June 2020 to September 2023 (a COPD group, n=90), healthy smokers (a smoking group, n=90), and healthy non-smokers (a healthy group, n=90) were enrolled as subjects. The COPD group was composed of 53 males and 37 females aged 49-83 years old, with an average age of (58.52 ± 4.87) years old. The body mass index (BMI) was (22.08 ± 1.87) kg/m^2, the number of cigarettes smoked was (400.36 ± 78.98) cigarettes/year, and the course of disease was (5.64 ± 1.75) years. As to the severity [according to the 2019 Global Initiative for Chronic Obstructive Lung Disease (GOLD) criteria] [8], there were 30 mild cases, 42 moderate cases, and 28 severe cases. The smoking group consisted of 51 males and 39 females aged 45-81 years old, with a mean of (59.48 ± 5.26) years old. BMI was (21.98 ± 1.58) kg/m^2, and the number of cigarettes smoked was (409.54 ± 82.59) cigarettes/year. In the healthy group composed of 55 males and 35 females, the age was 45-80 years old, with an average of (59.11 ± 5.59) years old, and MI was (22.19 ± 1.67) kg/m^2. The age, gender, and BMI were comparable among the three groups ($p>0.05$).

Inclusion and exclusion criteria

The following inclusion criteria were employed: 1) COPD patients meeting the diagnostic criteria for COPD and without a history of acute exacerbation in the past six months [8], 2) smokers with expected results in the pulmonary function test and number of cigarettes smoked ≥200 cigarettes/year, and non-smokers with expected results in the pulmonary function test and no smoking history, and 3) subjects who voluntarily signed the informed consent form.

The exclusion criteria involved: 1) subjects requiring mechanical ventilation due to severe condition, 2) those with rheumatic system diseases, allergic diseases or immune deficiencies, 3) those with acute pulmonary embolism, tuberculosis, bronchiectasis, asthma, cystic fibrosis, and other respiratory diseases, 4) those with coagulation dysfunction, 5) those with severe dysfunction of multiple organs, 6) those with a previous history of pulmonary surgery or lung tumors, 7) those with severe arrhythmia, acute myocardial infarction or myocardial ischemia, or 8) those taking immunosuppressants or glucocorticoids within 4 weeks before enrollment.

Detection of indicators in the peripheral blood

Peripheral venous blood (6 mL, evenly split into two portions) was collected before treatment in the COPD group and on the day of physical examination in the smoking and healthy groups. One portion was subjected to heparin anticoagulation, followed by 10 min of centrifugation (centrifugation radius: 6.5 cm, and centrifugation rate: 3500 rpm). Next, the supernatant was harvested for an enzyme-linked immunosorbent assay (Cat. No. DLR-IL17-Hu, Wuxi Donglin Sci & Tech Development Co., Ltd., China) to measure IL-17 levels. The other portion was subjected to Ficoll density gradient centrifugation using the

relevant kit (Cat. No. 17-1140-02, GE Healthcare Life Sciences, USA) to isolate peripheral blood mononuclear cells (PBMCs). Then, the resulting cell suspension was incubated with monoclonal antibodies against CD4-CD4-fluorescein isothiocyanate (FITC) and CD25-CD25-phycoerythrin (PE) (BD, USA), with immunoglobulin G (IgG)-FITC and IgG-PE as controls. Afterwards, the FAS-Calibur flow cytometer (BD, USA) was employed to detect CD4+ Treg cell count, CD25+ Treg cell count, and $CD4^+CD25^+$ Treg cell count.

Pulmonary function test

The forced expiratory volume in one second (FEV_1) and forced vital capacity (FVC) were determined with the HI-801 pulmonary function tester (CHEST, Japan) on the day of physical examination in the smoking group and the healthy group and before treatment in the COPD group, based on which the FEV_1/FVC value was calculated.

Statistical analysis

Statistical analysis was performed using the SPSS 26.0 software. Measurement data were expressed as mean ± standard deviation ($\bar{x} \pm s$) and subjected to the *t*-test for comparison between two groups and one-way analysis of variance for comparison among multiple groups. Count data were described as [n (%)] and examined by the χ^2 test. Spearman's rank correlation analysis was conducted to explore the correlations between levels of IL-17 and Treg subsets and pulmonary function. Receiver operating characteristic (ROC) curves were plotted, based on which the association between IL-17 levels and Treg subsets and the occurrence of COPD was assessed. $p<0.05$ indicated that the difference was statistically significant.

RESULTS

Levels of IL-17 and Treg subsets in the peripheral blood

The COPD group showed the highest IL-17 levels and the lowest CD4+ Treg cell count, CD25+ Treg cell count, and CD4+CD25+ Treg cell count in peripheral blood, followed by the smoking group and the healthy group ($p<0.05$) (Table 1).

Values of IL-17 and Treg subset levels in the peripheral blood for association with COPD occurrence

The areas under the ROC curves [AUCs, 95% confidence interval (95% CI)) of IL-17 level, $CD4^+$ Treg cell count, $CD25^+$ Treg cell count, and $CD4^+CD25^+$ Treg cell count in the peripheral blood and their combination for associating with the occurrence of COPD were 0.866 (0.813-0.920), 0.885 (0.833-0.936), 0.799 (0.735-0.863), 0.773 (0.705-0.840), 0.949 (0.919-0.979), respectively (Table 2 and Fig. 1).

Table 1. Levels of IL-17 and Treg subsets in the peripheral blood.

Group	n	IL-17 level (ng/L)	$CD4^+$ Treg cell count (%)	$CD25^+$ Treg cell count (%)	$CD4^+CD25^+$ Treg cell count (%)
Healthy	90	13.26±3.84	31.57±4.52	4.53±0.85	3.68±0.75
Smoking	90	28.48±5.65[a]	25.15±5.68[a]	3.21±0.79[a]	3.05±0.64[a]
COPD	90	38.12±6.87[ab]	16.58±4.74[ab]	2.34±0.67[ab]	2.34±0.71[ab]
F		451.893	203.182	182.842	82.202
p		<0.001	<0.001	<0.001	<0.001

[a]$p<0.05$ *vs.* the healthy group, [b]$p<0.05$ *vs.* the smoking group.
Data is expressed as mean ± standard deviation. One-way analysis of variance was used to compare multiple groups. Chronic obstructive pulmonary disease (COPD).

Table 2. Values of IL-17 and Treg subset levels in the peripheral blood for predicting COPD occurrence.

Indicator	Area under the curve	Standard error	Optimal cut-off value	p	95% confidence interval
IL-17	0.866	0.027	32.584ng/L	<0.001	0.813-0.920
$CD4^+$Treg	0.885	0.026	20.025%	<0.001	0.833-0.936
$CD25^+$Treg	0.799	0.033	2.684%	<0.001	0.735-0.863
$CD4^+CD25^+$Treg	0.773	0.034	2.641%	<0.001	0.705-0.840
Combination	0.949	0.015	-	<0.001	0.919-0.979

Chronic obstructive pulmonary disease (COPD).

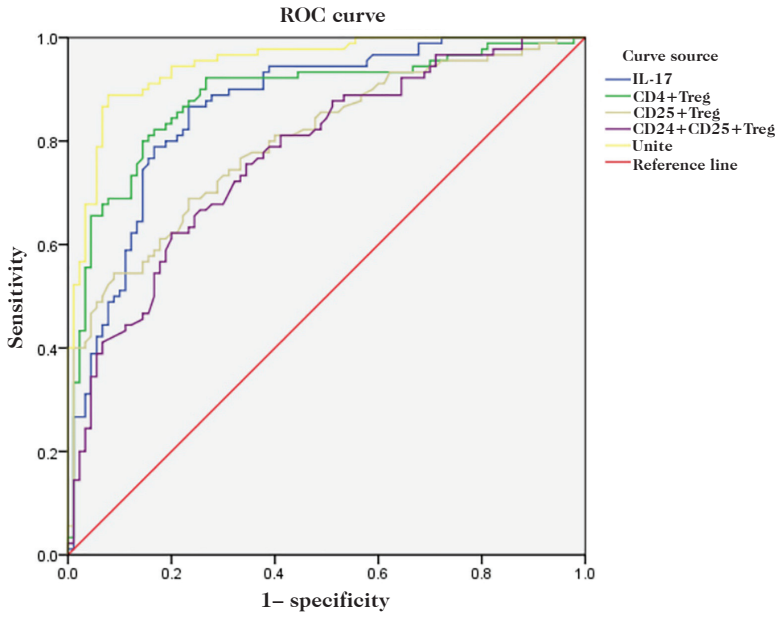

Fig. 1. ROC curves of IL-17 and Treg subset levels in the peripheral blood for predicting Chronic obstructive pulmonary disease (COPD) occurrence.

Levels of IL-17 and Treg subsets in the peripheral blood of COPD patients with different severities

The IL-17 level in the peripheral blood was the highest in the severe group, followed by the moderate group and the mild group, while the $CD4^+$ Treg cell count, $CD25^+$ Treg cell count, and $CD4^+CD25^+$ Treg cell count were the highest in the mild group, followed by the moderate group and the severe group ($p<0.05$) (Table 3).

Pulmonary function in COPD patients with different severities

The FEV_1, FVC, and FEV_1/FVC were the highest in the mild group, moderate in the moderate group, and the lowest in the severe group ($p<0.05$) (Table 4).

Correlations of IL-17 and Treg subset levels in the peripheral blood with pulmonary function

The results of the Spearman's rank correlation analysis showed that the IL-17 level was negatively correlated with FEV_1, FVC, and FEV_1/FVC ($r<0$, $p<0.05$).

Table 3. Levels of IL-17 and Treg subsets in the peripheral blood of COPD patients with different severities.

Group	n	IL-17 level (ng/L)	$CD4^+$ Treg cell count (%)	$CD25^+$ Treg cell count (%)	$CD4^+CD25^+$ Treg cell count (%)
Mild	30	31.25±5.58	20.35±4.65	3.02±0.68	2.89±0.52
Moderate	42	37.85±6.85[a]	14.25±4.58[a]	2.03±0.59[a]	2.11±0.47[a]
Severe	28	45.10±5.87[ab]	10.11±3.68[ab]	1.24±0.49[ab]	1.26±0.57[ab]
F		35.865	40.607	65.732	72.701
p		<0.001	<0.001	<0.001	<0.001

[a]p<0.05 *vs.* the mild group, [b]p<0.05 *vs.* the moderate group. Chronic obstructive pulmonary disease (COPD). Data is expressed as mean ± standard deviation. One-way analysis of variance was used to compare multiple groups.

Table 4. Pulmonary function in COPD patients with different severities.

Group	n	FEV_1 (L)	FVC (L)	FEV_1/FVC (%)
Mild	30	1.89±0.56	3.58±0.71	63.25±6.58
Moderate	42	1.49±0.62[a]	2.95±0.68[a]	57.48±5.59[a]
Severe	28	1.15±0.49[ab]	2.32±0.65[ab]	51.74±6.68[ab]
F		12.343	24.802	24.885
p		<0.001	<0.001	<0.001

[a]p<0.05 *vs.* the mild group, [b]p<0.05 *vs.* the moderate group. Data is expressed as mean ± standard deviation. One-way analysis of variance was used to compare multiple groups. Forced vital capacity (FVC), Forced expiratory volume in one second (FEV_1), Chronic obstructive pulmonary disease (COPD).

In contrast, the $CD4^+$ Treg cell count, $CD25^+$ Treg cell count, and $CD4^+CD25^+$ Treg cell count were positively correlated with FEV_1, FVC, and FEV_1/FVC ($r>0$, $p<0.05$) and negatively correlated with IL-17 level ($r<0$, $p<0.05$) (Table 5).

DISCUSSION

COPD is characterized by airway wall thickening, accumulation of inflammatory mucus, and infiltration of adaptive and innate immune cells. Among them, $CD4^+$ T lymphocytes play a critical role in the pathogenesis of COPD [9,10]. Under normal conditions, the balance of Th subsets helps maintain immune homeostasis, but in COPD, this balance is disturbed, with overactivation of Th17 cells and reduction of Treg cells [11].

Th17 cells secrete IL-17 and IL-22, which recruit neutrophils and other inflammatory cells, thus amplifying airway inflammation. IL-17 also stimulates macrophages, dendritic cells, and fibroblasts to release chemokines, pro-inflammatory cytokines, and proteolytic enzymes, all of which contribute to tissue damage and a decline in pulmonary function [12-14]. Elevated IL-17 further promotes neutrophil and macrophage infiltration, exacerbating airway injury [15]. Smoking additionally aggravates airway obstruction by inducing epithelial damage, mucosal gland hypertrophy, and ciliary dysfunction, and it promotes Th17 proliferation and IL-17 release [16].

In contrast, Treg cells play a protective role by suppressing autoreactive T cells and excessive immune activation [17]. $CD4^+CD25^+$

Table 5. Correlations of IL-17 and Treg subset levels in the peripheral blood with pulmonary function.

Indicator	Coefficient	IL-17	FEV_1	FVC	FEV_1/FVC
IL-17	*r*	-	-0.415	-0.535	-0.552
	p	-	<0.001	<0.001	<0.001
$CD4^+$Treg	*r*	-0.536	0.428	0.585	0.597
	p	<0.001	<0.001	<0.001	<0.001
$CD25^+$Treg	*r*	-0.589	0.448	0.597	0.603
	p	<0.001	<0.001	<0.001	<0.001
$CD4^+CD25^+$Treg	*r*	-0.645	0.487	0.615	0.637
	p	<0.001	<0.001	<0.001	<0.001

Forced vital capacity (FVC), Forced expiratory volume in one second (FEV_1).

Treg cells inhibit effector T-cell proliferation through IL-2 and IFN-γ suppression and TGF-β–mediated pathways [18]. In the present study, comparisons were carried out on the $CD4^+$ Treg cell count, $CD25^+$ Treg cell count, and $CD4^+CD25^+$ Treg cell count among the three groups. The results showed that the CD4+ Treg cell count, CD25+ Treg cell count, and CD4+CD25+ Treg cell count were lowest in the COPD group, moderate in the smoking group, and highest in the healthy group, suggesting immunomodulatory dysfunction in COPD patients and smokers, especially in the former. The $CD4^+$ Treg cell count, $CD25^+$ Treg cell count, and $CD4^+CD25^+$ Treg cell count were the lowest in the severe group, moderate in the moderate group, and the highest in the mild group. According to the Spearman's rank correlation analysis, the $CD4^+$ Treg cell count, $CD25^+$ Treg cell count, and $CD4^+CD25^+$ Treg cell count were positively correlated with FEV_1, FVC and FEV_1/FVC, demonstrating that the level of Treg subsets can reflect the condition of COPD patients to a certain extent, and that patients with a high expression of Treg subsets often have good pulmonary function. This is because CD4+ Treg cells, CD25+ Treg cells, and CD4+CD25+ Treg cells can impede the production of Th1 and Th17 cells via the autocrine transforming growth factor-β (TGF-β) pathway. However, in cases of low Treg expression, they cannot suppress inflammatory cytokines, leading to an imbalance between Th1 and Th2 cell counts. Accordingly, IL-4 expression will be further suppressed, and IL-17 and IFN-γ levels will be increased, resulting in persistently high immune responses, damaging lung and airway tissues, weakening pulmonary function, and thereby inducing COPD [19,20].

Furthermore, the results of the present study also showed that the $CD4^+$ Treg cell count, $CD25^+$ Treg cell count, and $CD4^+CD25^+$ Treg cell count displayed negative correlations with IL-17 level, signifying that the down-regulation of Treg subsets and the high expression of IL-17 (a characteristic inflammatory factor of Th17 cells) will disrupt the balance between Th17 cell count and Treg cell count, increase airway secretions and airway inflammatory responses, affect lung ventilation function, and further damage pulmonary function and lung tissues. The balance between Th17 cell count and Treg cell count should be maintained by taking appropriate measures, thus preventing COPD or its exacerbation [21].

Our study provides novel insights into several aspects. First, our cohort included exclusively COPD patients without asthma, ensuring disease specificity. Second, we simultaneously evaluated IL-17 and Treg subsets, and demonstrated that their combined

imbalance (increased IL-17 and decreased Treg levels) was more strongly associated with COPD severity than IL-17 alone. Third, by stratifying patients by GOLD grade, we revealed dynamic changes in these immune markers across disease progression. Collectively, these findings highlight the importance of the IL-17/Treg axis in COPD immunopathogenesis.

However, several limitations should be recognized. One limitation is that detailed information on inhaled corticosteroid (ICS) use was not systematically collected for all COPD patients. Since ICS therapy may influence cytokine profiles, such as reducing IL-17 levels or affecting Treg responses, its impact on our findings cannot be ruled out. Future studies with more complete treatment records and subgroup analyses are needed to address this. Another limitation is that we did not measure eosinophil and neutrophil counts or their relationship with IL-17 levels. Because these cells are key players in airway inflammation, future research should include them to better understand the connection between IL-17 and innate immune responses in COPD.

In conclusion, IL-17 is upregulated, and Treg subsets are downregulated in COPD, with their imbalance closely linked to impaired lung function and disease severity. The combined detection of IL-17 and Treg subsets may thus offer more informative biomarkers for evaluating COPD progression.

Funding

This study was financially supported by the Applied Basic Research Project of Changzhou Science and Technology Bureau (No. CJ20209030).

Conflict of interest

The authors confirm that the content of this article has no conflict of interest.

ORCID number of authors

- Jun Chen (JC): 0009-0000-7755-4448
- Tingting Zhao (TZ): 0009-0003-7801-2757
- Yingying Gao (YG): 0009-0005-1514-8846
- Zizhou Zhang (ZZ): 0009-0006-9648-3386

Contributions of each author

JC and ZZ designed this study and prepared the manuscript; TZ and YG conducted this study and analyzed the data. All authors have approved the submission and publication of this paper.

REFERENCES

1. **Agustí A, Vogelmeier C, Faner R.** COPD 2020: changes and challenges. Am J Physiol Lung Cell Mol Physiol. 2020; 319(5): L879-L883. *https://doi.org/10.1152/ajplung.00429.2020*
2. **Terry PD, Dhand R.** Inhalation Therapy for Stable COPD: 20 Years of GOLD Reports. Adv Ther. 2020; 37(5): 1812-1828. *https://doi.org/10.1007/s12325-020-01289-y*
3. **Yang IA, Jenkins CR, Salvi SS.** Chronic obstructive pulmonary disease in never-smokers: risk factors, pathogenesis, and implications for prevention and treatment. Lancet Respir Med. 2022; 10(5): 497-511. *https://doi.org/10.1016/S2213-2600(21)00506-3*
4. **Qin K, Xu B, Pang M, Wang H, Yu B.** The functions of CD4 T-helper lymphocytes in chronic obstructive pulmonary disease. Acta Biochim Biophys Sin. 2022; 54(2): 173-178. *https://doi.org/10.3724/abbs.2021009*
5. **Ma R, Su H, Jiao K, Liu J.** Role of Th17 cells, Treg cells, and Th17/Treg imbalance in immune homeostasis disorders in patients with chronic obstructive pulmonary disease. Immun Inflamm Dis. 2023; 11(2): e784. *https://doi.org/10.1002/iid3.784*

6. **Thomas R, Qiao S, Yang X.** Th17/Treg Imbalance: Implications in Lung Inflammatory Diseases. Int J Mol Sci. 2023; 24(5): 4865. *https://doi.org/10.3390/ijms24054865*
7. **Ritzmann F, Lunding LP, Bals R, Wegmann M, Beisswenger C.** IL-17 Cytokines and Chronic Lung Diseases. Cells. 2022; 11(14): 2132. *https://doi.org/10.3390/cells11142132*
8. **Singh D, Agusti A, Anzueto A, Barnes PJ, Bourbeau J, Celli BR, et al.** Global Strategy for the Diagnosis, Management, and Prevention of Chronic Obstructive Lung Disease: the GOLD science committee report 2019. Eur Respir J. 2019;53(5):1900164. *https://doi.org/10.1183/13993003.00164-2019*
9. **Christenson SA, Smith BM, Bafadhel M, Putcha N.** Chronic obstructive pulmonary disease. Lancet. 2022; 399(10342): 2227-2242. *https://doi.org/10.1016/S0140-6736(22)00470-6*
10. **Zhang X, Li X, Ma W, Liu F, Huang P, Wei L, et al.** Astragaloside IV restores Th17/Treg balance via inhibiting CXCR4 to improve chronic obstructive pulmonary disease. Immunopharmacol Immunotoxicol. 2023; 45(6): 682-691. *https://doi.org/10.1080/08923973.2023.2228479*
11. **Cervilha DAB, Ito JT, Lourenço JD, Olivo CR, Saraiva-Romanholo BM, Volpini RA, et al.** The Th17/Treg Cytokine Imbalance in Chronic Obstructive Pulmonary Disease Exacerbation in an Animal Model of Cigarette Smoke Exposure and Lipopolysaccharide Challenge Association. Sci Rep. 2019; 9(1): 1921. *https://doi.org/10.1038/s41598-019-38600-z*
12. **Henen C, Johnson EA, Wiesel S.** Unleashing the Power of IL-17: A Promising Frontier in Chronic Obstructive Pulmonary Disease (COPD) Treatment. Cureus. 2023; 15(7): e41977. *https://doi.org/10.7759/cureus.41977*
13. **Kubysheva N, Boldina M, Eliseeva T, Soodaeva S, Klimanov I, Khaletskaya A, et al.** Relationship of Serum Levels of IL-17, IL-18, TNF-α, and Lung Function Parameters in Patients with COPD, Asthma-COPD Overlap, and Bronchial Asthma. Mediators Inflamm. 2020; 2020: 4652898. *https://doi.org/10.1155/2020/4652898*
14. **Ding F, Han L, Fu Q, Fan X, Tang R, Lv C, et al.** IL-17 Aggravates Pseudomonas aeruginosa Airway Infection in Acute Exacerbations of Chronic Obstructive Pulmonary Disease. Front Immunol. 2022; 12: 811803. *https://doi.org/10.3389/fimmu.2021.811803*
15. **Zhang XF, Xiang SY, Lu J, Li Y, Zhao SJ, Jiang CW, et al.** Electroacupuncture inhibits IL-17/IL-17R and post-receptor MAPK signaling pathways in a rat model of chronic obstructive pulmonary disease. Acupunct Med. 2021; 39(6): 663-672. *https://doi.org/10.1177/0964528421996720*
16. **Upadhyay P, Wu CW, Pham A, Zeki AA, Royer CM, Kodavanti UP, et al.** Animal models and mechanisms of tobacco smoke-induced chronic obstructive pulmonary disease (COPD). J Toxicol Environ Health B Crit Rev. 2023; 26(5): 275-305. *https://doi.org/10.1080/10937404.2023.2208886*
17. **Jia Y, He T, Wu D, Tong J, Zhu J, Li Z, Dong J.** The treatment of Qibai Pingfei Capsule on chronic obstructive pulmonary disease may be mediated by Th17/Treg balance and gut-lung axis microbiota. J Transl Med. 2022; 20(1): 281. *https://doi.org/10.1186/s12967-022-03481-w*
18. **Zhang D, Liu H, Zhao F, Guo P, Li J, Lu T, et al.** Exploring the relationship between Treg-mediated risk in COPD and lung cancer through Mendelian randomization analysis and scRNA-seq data integration. BMC Cancer. 2024; 24(1): 453. *https://doi.org/10.1186/s12885-024-12076-1*
19. **Silva LEF, Lourenço JD, Silva KR, Santana FPR, Kohler JB, Moreira AR, et al.** Th17/Treg imbalance in COPD development: suppressors of cytokine signaling and signal transducers and activators of transcription proteins. Sci Rep. 2020; 10(1): 15287. *https://doi.org/10.1038/s41598-020-72305-y*

20. **Ito JT, Cervilha DAB, Lourenço JD, Gonçalves NG, Volpini RA, Caldini EG, et al.** Th17/Treg imbalance in COPD progression: A temporal analysis using a CS-induced model. PLoS One. 2019; 14(1): e0209351. *https://doi.org/10.1371/journal.pone.0209351*

21. **Liao SX, Chen J, Zhang LY, Zhang J, Sun PP, Ou-Yang Y.** Effects of SOCS1-overexpressing dendritic cells on Th17- and Treg-related cytokines in COPD mice. BMC Pulm Med. 2022; 22(1): 145. *https://doi.org/10.1186/s12890-022-01931-1*

Invest Clin 66(4): 436 - 453, 2025 https://doi.org/10.54817/IC.v66n4a07

Hiperplasia endometrial II: Revisión narrativa sobre diferentes opciones de tratamiento.

José Núñez-Troconis

Departamento de Obstetricia y Ginecología. Universidad del Zulia. Maracaibo-Venezuela.

Palabras clave: Hiperplasia Endometrial; Tratamiento Conservador; Terapia Hormonal; Progestágenos; Tratamiento Quirúrgico.

Resumen. La hiperplasia endometrial comprende un espectro de cambios en el endometrio que van desde un patrón ligeramente desordenado, como la hiperplasia endometrial sin atipias, hasta alteraciones más severas, como la hiperplasia endometrial con atipias, precursora del carcinoma endometrial. Durante los años reproductivos, el riesgo de la hiperplasia está asociado a oligo-anovulación, y durante la menopausia está asociado con factores como la obesidad y la terapia de reemplazo de estrógeno. Esta revisión tiene por objeto, ofrecer un enfoque racional en el tratamiento de la hiperplasia endometrial, incluidos la terapia conservadora como la hormonal y los diferentes métodos quirúrgicos.

Autor de correspondencia: José Núñez-Troconis. Dirección Postal: Calle 73 con Av. 3D y 3E Residencias Atlantis Apto. 2B. Maracaibo. Zulia. Venezuela. 4002. Correo electrónico: jtnunezt@gmail.com

Endometrial hyperplasia II: A narrative review of different treatment options.

Invest Clin 2025; 66 (4): 436 – 453

Keywords: Endometrial Hyperplasia; Conservative Treatment; Hormonal Therapy; Progestogens; Surgical Procedures.

Abstract. Endometrial hyperplasia encompasses a spectrum of endometrial changes, ranging from a mildly disordered pattern, such as endometrial hyperplasia without atypia, to more severe alterations, including endometrial hyperplasia with atypia, a precursor to endometrial carcinoma. During the reproductive years, the risk of hyperplasia is associated with oligo-anovulation, and during menopause, it is associated with factors such as obesity and estrogen replacement therapy. This review aims to offer a rational approach to the treatment of endometrial hyperplasia, including conservative therapy such as hormonal therapy and different surgical methods.

Recibido: 30-07-2025 Aceptado: 21-10-2025

INTRODUCCIÓN

El sangrado por causa de premalignidad o malignidad, representa el 10% del total de los sangramientos uterinos anormales (SUA). La hiperplasia endometrial (HE) es una proliferación precancerosa, no fisiológica y no invasiva del endometrio, que produce un aumento del volumen del tejido endometrial con alteraciones de la arquitectura glandular (forma y tamaño), y de la relación glándula endometrial-estroma superior a 1:1 [1-3]. La mayoría de los casos de HE son el resultado de niveles elevados de estrógenos, combinados con niveles insuficientes de progesterona [4,5]. La estimulación estrogénica sin oposición y en forma crónica en el endometrio, provoca cambios epiteliales glandulares proliferativos, incluida la remodelación glandular, lo que da lugar a glándulas de forma y número variable y de distribución irregular [3,6].

Armstrong y col. [7] reportaron la presencia de HE en el 10% de mujeres premenopáusicas y en el 6% de las mujeres postmenopáusicas con SUA. Se estima que la incidencia de la HE es al menos tres veces mayor que la del cáncer de endometrio (CE). Las estimaciones actuales reportan que la incidencia de HE ronda los 133 a 208 casos por 100.000 mujeres-año, en los países occidentales [8,9]. Las tasas de incidencia de los subtipos de HE son 121 casos por 100.000 años-mujer para la HE no atípica y 16,8 casos por 100.000 años-mujer para la HE atípica [8]. El cáncer de endometrio es la neoplasia maligna ginecológica más común en el mundo occidental[10]. Según Globocan [11], para el año 2020 se reportaron 417.367 nuevos casos de CE en todo el mundo, lo cual representó el 4,5% de todos los canceres femeninos y el segundo más frecuente después del cáncer de cuello uterino (6,5%); provocó la muerte de 97.370 mujeres, o sea, un 23,33% de mujeres a nivel global. En el hemisferio occidental, en el 2020 según Globocan [11], se diagnosticaron 231.723 casos de CE, es decir, el 55,6% y provocó la muerte de 51.470 (52,9%). Históricamente, el CE rara vez aparece en mujeres premenopáusicas, sin embargo, con el

aumento de la obesidad y la creciente prevalencia del síndrome metabólico, los cuadros de HE y de CE han aumentado notablemente en frecuencia [10]. La hiperplasia endometrial con atipias, cuya denominación ha sido cambiada a neoplasia intraepitelial endometrial (NIE), es precursora del CE [2-4]. La prevalencia del CE aumenta con la edad, cerca de una cuarta parte (21,3%) de nuevos diagnósticos ocurren en pacientes menores de 55 años [12,13]. La exposición prolongada a estrógenos, sin oposición es el principal factor de riesgo [14]. La hiperplasia endometrial sin atípia tiene el riesgo de progresar a CE, entre el 1 al 3%, mientras que la HE con atipias o NIE, tiene el riesgo de progresar entre un 14 a 45% [5]; la incidencia de HE con atipias es menor a 1% [7,15].

El objetivo de esta revisión narrativa, consistió en investigar, revisar y analizar los diferentes tratamientos médicos y quirúrgicos que se utilizan en el manejo de la HE.

MATERIAL Y MÉTODO

La presente revisión narrativa fue realizada para revisar, investigar y analizar, los estudios más recientes y relevantes, en relación con los diferentes tratamientos médicos y quirúrgicos en la HE. Se buscaron, revisaron y analizaron publicaciones en los idiomas español e inglés. Siguiendo las guías de PRISMA, se realizó una búsqueda sistemática, por vía electrónica, de publicaciones sobre el tema, en PubMed, MEDLINE, ISI, Springer, Embase, Web of Knowledge, DOAJ, Google Scholar y Cochrane Library, para artículos originales escritos en el idioma inglés y en SciELO, Latindex, Imbiomed-L, Redalyc and Google Scholar para artículos originales escritos en el idioma español e inglés. La búsqueda incluyó palabras clave "sangramiento uterino anormal", "hiperplasia endometrial", "tratamiento médico", "tratamiento quirúrgico", "terapéutica", "manejo" y seguido de términos como: "hiperplasia endometrial y tratamiento médico", o "tratamiento quirúrgico", o "manejo" o "terapéutica", Se incluyeron los artículos publicados en revistas médicas indexadas, y fueron excluidas, aquellas publicaciones que no pudieron ser abiertas electrónicamente; asímismo, fueron excluidos de la revisión: cartas al editor, reportes de casos, estudios sin control y resúmenes de congresos. Se revisaron los artículos publicados desde el año 1970 hasta marzo de 2024. La búsqueda electrónica, la escogencia, el evalúo y el análisis de las publicaciones fueron realizados por el autor.

Tratamiento

Aunque no existe un tratamiento único para la HE, la mayoría de las directrices actuales recomienda las terapias hormonales, o el tratamiento quirúrgico. Los criterios de selección dependerán de la edad de la paciente, la presencia de comorbilidades, de factores de riesgo, fertilidad de la paciente y la presencia o no de atipias en la HE [6,16]. Generalmente las HE sin atípia, responden bien al tratamiento con progestágenos o progestinas (Ps). La terapia hormonal es la recomendada para aquellas pacientes en quienes, por su condición de salud, la cirugía está contraindicada; para mujeres cuya salud general les impide tolerar la cirugía, aunque en los casos donde la HE sin atipias es sintomática (sangrado), otra opción sería la histerectomía. Las mujeres con deseos de fertilidad, se manejan conservadoramente, independientemente si la HE es con o sin atipia [6,17].

Scully y col. [17] recomiendan diferentes opciones de tratamiento, basadas en las probabilidades de progresar a CE (Tabla 1). Bank y col. [18], empleando el sistema de clasificación de NIE, mencionan que su precisión para predecir la progresión de la HE, es mejor que el sistema de la OMS94.

Según la clasificación NIE, la HE benigna presenta el riesgo de malignización en un 0,6% y recomienda 2 opciones: terapia hormonal o ningún tratamiento; la NIE presenta el 19% de riesgo de evolucionar a cáncer y recomienda también 2 opciones de tratamiento: cirugía o terapia hormonal.

Tabla 1. Clasificación según Organización Mundial de la Salud 1994.
Riesgo y Tratamiento

Hiperplasia Endometrial	Riesgo de Progresar a CE*	Opciones de tratamiento
Simple	1%	Hormonal
Compleja	3%	Hormonal o cirugía
Simple con atipias	8%	Cirugía u hormonal
Compleja con atipias	29%	Cirugía u hormonal

*CE: Cáncer de endometrio. Fuente: Scully y col. [17]

Observación:

En 2019, la Sociedad de Obstetricia y Ginecología de Canadá y la Sociedad de Oncología Ginecológica de Canadá [19] recomendaron que las pacientes, con HE sin atipias, pueden ser observadas, y no ser tratadas, igualmente, recomiendan el tratamiento hormonal, en los casos que no se resuelvan con la observación o persistan los sangrados.

Terapia hormonal

Progesterona

El uso de la progesterona por vía oral, en forma micronizada, se ha usado para el tratamiento de la HE sin atipia y con atipia. La administración de la progesterona en dosis de 300 mg por vía oral, durante 10 a 14 días en forma cíclica por 3 meses, se ha empleado para tratar la HE sin atipia y el uso de la misma dosis, pero en forma continua para tratar la HE con atipias [6]. Otra vía de administración de la progesterona, ha sido la vía vaginal, usando el gel o crema al 4% o 8% de progesterona, que corresponde a una dosis de 45 a 90 mg/día [7].

Progestinas o progestágenos

Estos compuestos hormonales, son derivados sintéticos de la progesterona, que presentan una acción similar a ella, sobre el endometrio proliferativo, produciendo la conversión a un endometrio secretor. Las progestinas o progestágenos (Ps) actúan, igual que la progesterona, sobre los receptores de la progesterona (PR) A y B, provocando la transformación del endometrio [7]. Los progestágenos varían en su capacidad de transformar el endometrio secretor o pseudosecretor, o en producir decidualización, determinando su capacidad de disminuir o detener el SUA. La reversión de la HE a un endometrio normal, representa la clave del tratamiento conservador para la prevención del desarrollo del CE [6,7,17,20]. Diferentes autores han reportado que las Ps disminuyen la celularidad glandular al inducir apoptosis e inhibir la angiogénesis en el miometrio subyacente a la HE [21,22].

El uso de las progestinas o progestágenos, es el tratamiento médico de elección para tratar la HE sin atipias y de HE con atipias, en aquellas pacientes que deseen mantener la fertilidad [6,7,20]. Se pueden administrar por vía oral, vía intramuscular, vía vaginal como crema vaginal micronizada, o por vía intrauterina como dispositivos [23,24]. El modo de administración y la duración del tratamiento son esenciales para su éxito. La hiperplasia endometrial sin atipia, suele mostrar una respuesta después de 10 semanas de administración, pero comúnmente se observan respuestas significativas después de 3 meses de tratamiento, siendo el tiempo medio de resolución de 6 meses [6,25].

En mujeres de edad reproductiva con HE sin atipias, las Ps, se pueden administrar durante 12 a 14 días por mes, con el objeto por inducir un sangrado mensual predecible. En mujeres con HE persistente o HE con atipia, ser recomiendan las Ps orales diariamente o Ps parenterales para mantener una exposición continua [7].

Las progestinas son razonablemente bien toleradas por las pacientes, incluso en dosis elevadas, pero uno de los problemas que presentan, son los efectos secundarios, tales como mareos, turgencia mamaria, mastalgia, aumento de peso, dolor de cabeza, náuseas, dolor abdominal, retraso de la menstruación, menstruación abundante, sangramiento uterino irregular, fatiga, dia-

rrea, vómitos y dismenorrea; sin embargo, estos síntomas desaparecen en 48 horas[6,7]. A nivel bioquímico, las Ps por vía oral o parenteral, elevan las lipoproteínas de baja densidad [7]. El empleo de la Ps en el tratamiento no quirúrgico de la HE y CE presenta una resistencia entre 12% al 53% [26]. El fracaso del tratamiento de la HE con Ps puede depender de varios factores, como la edad del paciente, factores de riesgo, presencia de otras comorbilidades y el grado o tipo de HE. Asimismo, Upson y col. [27] reportaron que en pacientes con HE con atipia, la resistencia puede deberse a un nivel bajo o inadecuado de receptores de progesterona RP-A y RP-B particularmente RP-B, o alteración de las funciones de los RP tales como coactivadores o correpresores. También, se han mencionado mecanismos moleculares para la resistencia a la Ps, como son la desregulación del TGF-α. y EGFR en las células glandulares endometriales, la expresión de Fas/FasL y survivina, así como resistencia a la insulina[28,29]. van Hylckama y col. [30] reportaron que el uso del acetato de medroxiprogesterona (AMP) inyectable, aumenta en 3 ó 4 veces, el riesgo de enfermedad venosa tromboembólica (EVT). Visilakis y col. [31] han mencionado, que el uso de Ps solas en altas dosis, en el tratamiento de problemas ginecológicos, aumenta el riesgo de EVT; sin embargo, Heineman y col. [32] reportaron que el uso de Ps no incrementa el riesgo cardiovascular, y que el uso del DIU con Ps tampoco aumenta el riesgo de EVT [30].

Progestinas orales

El uso oral de la Ps para el tratamiento de la HE tiene más de 40 años. Los primeros en usarse fueron el AMP y el acetato de megestrol (AM) [33]. Otras progestinas o progestágenos como la norestisterona, el levonorgestrel (LNG) y el linestrol han sido usados en el tratamiento de la HíE en forma oral continua o cíclica, en diferentes dosis y duración [34-36] (Tabla 2).

Acetato de medroxiprogesterona

El acetato de medroxiprogesterona oral, se puede administrar en dosis de 5 a 10 mg por 10 a 14 días, en forma cíclica por 3 meses o en forma continua por 6 semanas. En pacientes con una respuesta parcial al AMP, se recomienda el uso continuo durante otros 3 meses, por vía oral y a una dosis de 10 mg, cuatro veces al día (Tabla 2). Ushijima y col. [37] reportaron el uso de 600 mg diarios de AMP por 26 semanas, en pacientes con deseos de fertilidad, con diagnóstico de HE con atipias y CE, una respuesta completa en el 82% y una respuesta parcial en el 18% de las pacientes con HE, y en pacientes con CE una respuesta del 55%.

Acetato de megestrol

El acetato de megestrol es una progesterona hidroxilada en el carbono 17, con efectos predominantemente progestacionales y antigonadotrópicos, que se ha demostrado que tiene el potencial de inhibir la proliferación del endometrio. Se recomienda la dosis de 160 a 320 mg/día para el tratamiento de la HE (Tabla 2). Sin embargo, estas dosis producen alteraciones de los perfiles de lípidos séricos y de los niveles de la glucosa [38]. Güven y col. [38] y Gal y col. [39], han reportado remisiones completas de la HE sin y con atipias y del CE en más del 90% de los pacientes. Chandra y col. [6], mencionaron en un estudio realizado en los Estados Unidos de Norteamérica, que usando dosis de 80 mg 2 veces al día durante 12 semanas, lograron una respuesta positiva o remisiones de la HE en 4 semanas.

Acetato de norestisterona o noretindrona

La norestisterona o noretindrona (AN), es una Ps sintética, activa por vía oral, con efectos antiandrógenos y antiestrógenos [40]. Portman y col. [41], demostraron que el AN tiene un papel protector contra el desarrollo de la HE, en mujeres posmenopáusicas tratadas con estrógenos (Tabla 2).

Tabla 2. Progestágenos
Administración, dosis y esquemas de tratamiento.

Progestágeno	Vía administración	Dosis	Esquema	Referencia
Acetato de medroxiprogesterona (AMP)	Oral/ Intramuscular	5-10 mg/ 150 mg	10-14 días x3 meses o continua x 6 semanas a 3 meses/una sola dosis	Chandra y col. [6]
Acetato de megestrol	Oral	160-320 mg	10-14 días x 3 meses o continua x 6 semanas a 3 meses	Güven y col. [38] Gal y col. [39]
Norestisterona o Noretindrona	Oral	O,35-0,5 mg/ ≥1mg	continua x 6 semanas a 3 meses/10-14 días x 3 meses	Portman y col. [41]
Linestrenol	Oral	0,5 mg	10-14 días x 3 meses o continua x 6 semanas a 3 meses	Chandra y col. [6]
Levonorgestrel	Oral	0,75 mg	10-14 días x 3 meses o continua x 6 semanas a 3 meses	Bese y col. [34] Buttini y col. [35] Ozdegirmenci y col. [36]
Desogestrel	Oral	0,75 mg	10-14 días x 3 meses o continua x 6 semanas a 3 meses	Ozdegirmenci y col. [36]
Drosperinona	Oral	4 mg	10-14 días x 3 meses o continua x 6 semanas a 3 meses	Ozdegirmenci y col. [36]
Dienogest	Oral	2 mg	10-14 días x 3 meses o continua x 6 semanas a 3 meses	Ozdegirmenci y col. [36]

Progestinas inyectables

Otra vía de administrar las Ps, en el tratamiento de la HE, es la vía parenteral, específicamente la intramuscular (IM). El progestágeno más comúnmente y frecuentemente usado es el AMP de depósito, en dosis de 150 mg, por vía intramuscular, cada 3 meses (Tabla 2). Esta progestina está bastante bien indicada en paciente menopáusicas o post-menopaúsicas o con resistencia parcial a la terapia oral.

Dispositivo intrauterino liberador de progestina

El levonorgestrel (LNG) es una Ps de segunda generación, común en anticonceptivos orales. Nisker y col. [42] en 1988, encontraron una incidencia de CE de 17,2%, en conejas a las cuales se les había colocado un dispositivo intrauterino, portador de LNG, en uno de los cuernos uterinos, en comparación con las conejas controles que presentaron una incidencia del 42,4% de CE, diferencia que fue significativa ($p<0,05$). El dispositivo intrauterino (DIU) portador y liberador de LNG, es actualmente una opción de tratamiento de la HE [6,7]. Este DIU contiene un depósito de 52 mg de LNG, y se reemplaza cada 5 años. El DIU liberador de Ps libera una dosis alta de Ps al endometrio, con efectos sistémicos mínimos, y es un tratamiento eficaz para tratar la HE [35]. Con el DIU-LNG se consigue una concentración del LNG en el endometrio, 100 veces mayor que

cuando se administra por vía oral [43]. Esta es una opción para pacientes con riesgo de EVT o cuando el cumplimiento del tratamiento es un problema [7]. Con el DIU-LNG más del 50% de las pacientes, desarrollará amenorrea dentro de los 6 meses posteriores a la inserción [44]. Las pacientes con HE tratadas con el DIU-LNG, muestran un endometrio histológicamente normal, después de 6 meses de tratamiento [6]. Pacientes perimenopáusicas con HE sin atipias, tratadas con DIU-LNG, mostraron una tasa de curación o regresión total del 88,1% después de 1 año de uso del DIU [45]. Varma y col. [46], reportaron una regresión histológica del 90%, en pacientes con HE, y Vereide y col. [47] encontraron una remisión del 100% en pacientes con HE, que usaron del DIU-LNG.

Tratamiento y seguimiento

Singh y col. [48], mencionaron 3 principios básicos en el tratamiento de la HE: 1.- descartar la presencia de una neoplasia maligna endometrial coexistente; 2.- prevenir el desarrollo/progresión de malignidad endometrial; 3.- ofrecer el plan de tratamiento que mejor se adapte a las necesidades de la paciente.

En septiembre de 2023, el Colegio Americano de Obstetras y Ginecólogos (ACOG) [49], mencionó, que no hay suficientes evidencias para recomendar ningún agente progestacional de uso oral, sobre otro, y estas pacientes que han sido tratadas con Ps orales deben ser evaluadas histológicamente, después de los 3 a 6 meses de la terapia. La primera opción, es la resolución o regresión completa de la HE, la biopsia mostrará un endometrio atrófico, secretor o proliferativo. La segunda opción, es la resolución o regresión parcial de la HE, es decir, la biopsia endometrial (BE) revelará una HE, pero sin atipia. La tercera opción es la persistencia de la HE sin cambio alguno en la BE, posterior al tratamiento. La cuarta opción es la progresión de la HE al CE; el ACOG menciona que en aquellos casos donde la regresión es parcial o no hay ninguna regresión, se puede considerar 3 a 6 meses más de tratamiento dependiendo del caso, y si no hay respuesta, se debe considerar la opción quirúrgica definitiva [49]. Tampoco hay datos que determinen la duración óptima de la terapia con progesterona o con Ps; esto es particularmente importante en las mujeres en edad reproductiva que desean mantener la fertilidad, ya que, sin tratamiento continuo, es probable que el riesgo de recurrencia aumente con el tiempo, sobre todo en las pacientes que presentan factores de riesgo como anovulación u obesidad. En estas pacientes, el tratamiento con Ps, debe ser oral, continuo o cíclico, durante 3 a 6 meses o más, hasta que la HE revierta, determinado por la BE [25].

Diferentes autores recomiendan el tratamiento con Ps oral o inyectable, durante 3 a 6 meses, con control histológico por BE al terminar la terapia [7,25,49,50]. El tratamiento de la HE con Ps por cualquier vía de administración es eficaz. Gunderson y col. [25], han reportado una resolución completa de la HE del 66% en un plazo de 39 meses, con el uso de Ps. Gallos y col. [50], encontraron al comparar el uso del DIU-LNG con el uso de Ps por vía oral, que el primero es más efectivo en lograr la regresión completa de la HE compleja (92% vs 66%) y de la HE simple con atipia (90% vs 69%), aunque la respuesta completa de la HE sin atipia, ha sido reportada como similar (96% vs 86%).

Según el ACOG [49], hay datos limitados sobre la superioridad del DIU-LNG sobre las Ps orales, en la regresión de la HE con atipias y NIE. Sin embargo, esta sociedad recomienda el DIU-LNG como medicación de primera línea, sobre todo en pacientes con HE sin atipias.

Otras terapias

Danazol

El danazol, es un andrógeno sintético, derivado de la 17α-etiniltestosterona, que suele utilizarse como opción de trata-

miento para la endometriosis [51]. El danazol induce un efecto hipoestrogénico al inhibir la hormona folículo estimulante (FSH) y la hormona luteinizante (LH), produciendo atrofia endometrial [52]. Varios estudios han demostrado los efectos significativos del danazol contra el HE [53-55], siendo sugerido como una alternativa eficaz y segura, para el tratamiento de la HE [54]. Los DIU que contienen danazol (DIU-D), se ha mencionado que podrían ser un método novedoso, alternativo y eficaz para el tratamiento de la HE [56]. Los efectos secundarios del danazol tales como el aumento de peso, calambres musculares, acné, seborrea, disminución del tamaño de los senos, caída del cabello, hirsutismo y engrosamiento de la voz, están relacionados con su acción androgénica; también se ha mencionado que aumenta el riesgo de desarrollar cáncer de ovario en mujeres con endometriosis [57,58].

Genisteína

La genisteína, es un isoflavonoide extraído de los productos de soja, que es un conocido inhibidor de las proteínas tirosinaquinasa y tropoisomerasa II [59,60]. Se ha demostrado que la genisteína suprime los genes inducidos por estrógenos, como c-fos y c-jun, así como la IL-1α y TNF-α, a través de vías mediadas por citoquinas y de los RE[61]. La administración de la aglicona de genisteína a 19 pacientes, a razón de 54 mg diarios, durante 6 meses, provocó una tasa de respuesta positiva del 42% en mujeres premenopáusicas con HE sin atipia, asimismo mostraron una mejoría significativa de los síntomas; igualmente, se encontró una reducción significativa en la tinción de los ER-α y PR, y una tinción mejorada para ER-β1, con regresión completa del sangrado [62]. Los resultados de los diferentes estudios impulsan el uso de aglicona de genisteína para el tratamiento de la HE, particularmente en pacientes sin atipia. Sin embargo, se necesitan más estudios y ensayos clínicos para establecer a la genisteína como un fármaco potente para el tratamiento de la HE.

Metformina

La metformina o N, N-dimetilbiguanida, es una bioguanida que se utiliza en diferentes patologías, entre ellas, la resistencia a la insulina [63]. La metformina se ha asociado a la aparición de la HE [64]. La metformina ha demostrado que tiene efectos antiproliferativos, antiinvasivos y antimetastásicos, en múltiples cánceres [65]. Xie y col. [66], demostraron que la metformina induce la expresión de los RP a nivel de las células endometriales hiperplásicas, por lo que se podría mejorar la eficacia de la terapia con Ps o superar la resistencia a la Ps, causada por el agotamiento de RP, en terapias a largo plazo. Erdemoglu y col. [67], demostraron los efectos antiproliferativos de la metformina en endometrio de ratones tratadas con E_2 o tamoxifeno. Varios estudios han establecido a la metformina, como agente antiestrogénico eficaz, en el control de la HE sin y con atipias [64,68,69].

Agonistas de la hormona liberadora de gonadotrofinas

El endometrio posee receptores de la hormona liberadora de gonadotrofinas (GnRH) y los agonistas de la GnRH pueden competir y regular negativamente estos receptores. Los análogos de la GnRH suprimen el eje hipotálamo pituitario ovárico, inhibiendo la liberación de la FSH y LH por parte de la glándula pituitaria, y, por lo tanto, no hay estímulo de los ovarios para producir Es. Por lo anterior, los análogos de la GnRH tienen un efecto antiproliferativo directo sobre las células endometriales [70], y producen apoptosis de las células endometriales [71]. Se ha empleado una ampolla de estos compuestos (3,75 mg por vía IM cada 28 días, durante 6 meses), en el tratamiento de pacientes con HE sin y con atipias, sin embargo, el 25% de las pacientes mostraron recurrencia de la HE dentro de los 16 meses de la finalización de la terapia [72]. Agorastos y col. [73], trataron pacientes con HE sin y con atipias con 3,75 mg de acetato de leuprolide (análogo de la GnRH) y tibolona, como terapia "add-back", y lograron una completa remisión en todas

las pacientes, pero con un 19% de recurrencia dentro de los 2 años posteriores al cese del tratamiento.

Las desventajas del uso de estos análogos de la GnRH son el alto costo, los síntomas climatéricos y la descalcificación ósea por el uso prolongado de ellos.

Posibles futuras terapias

La HE es una enfermedad compleja que puede ser tratada de diferentes formas simultáneamente, para lograr un tratamiento eficaz. Con el avance en el conocimiento sobre la biología molecular y las vías relacionadas con la progresión de una enfermedad particular, la era de las terapias dirigidas se han convertido en un área o campo de investigación prometedora. Para el desarrollo de agentes terapéuticas de la HE, se requiere una investigación cuidadosa sobre las modulaciones moleculares en la HE y el CE. Dado que la HE es básicamente un problema hormono- dependiente, relacionado con expresiones elevadas de los RE, expresiones bajas y/o respuesta inadecuada de los RP, las investigaciones apuntan hacia el desarrollo de nuevos tratamientos para dicha enfermedad [6]. Sin embargo, para tratar o curar mejor esta patología endometrial, se requiere un conocimiento más profundo de las funciones de REα, REβ o GPRE y sus interacciones.

Antagonistas de la GnRH

Los antagonistas de la hormona liberadora de gonadotropina (anGnRH), son moléculas que actúan en la adenohipófisis, como inhibidores competitivos de los receptores de GnRH (GnRHR), compitiendo contra la GnRH endógena, y una vez que se unen a este receptor, causan la supresión inmediata del eje hipotálamo-hipofisario-gonadal (HPG), con una disminución rápida y sostenida de los niveles de gonadotropina y hormonas sexuales, a través de la regulación negativa, previniendo picos prematuros de hormona luteinizante (LH) [16]. Estos pueden usarse durante cualquier momento de la fase folicular [16]. La supresión del eje HPG está relacionada con la dosis, con dosis más bajas se logra una supresión parcial, y dosis más altas, una supresión completa [16]. Los antagonistas de GnRH inducen un inicio rápido de los efectos clínicos, sin el efecto "flare-up que se observa con los agonistas, y tienen efectos terapéuticos inmediatos, entre 24 a 72 horas, y una vez concluido este tratamiento, la supresión hormonal cesa rápidamente, con normalización de la función gonadal en pocos días, garantizando un aumento de la concentración de GnRH [16]. La ventaja de los anGnRH es su administración por vía oral, además algunos se administran por la vía subcutánea tales, como el acetato de cetrorelix, el acetato de ganirelix y el NalGlu.

El elagolix, el relugolix y el elagolix se administran por vía oral [16]. La dosis y la duración de los anGnRH, dependerán de la patología a tratar. El uso de los antagonistas de la GnRH tiene un futuro en el tratamiento de la HE; su empleo oral presenta una ventaja sobre los agonistas[16].

Las desventajas del uso de los anGnRH, igual que los agonistas, son su alto costo, los síntomas climatéricos y la descalcificación ósea por el uso prolongado de ellos.

Antiestrógenos o moduladores selectivos de receptores estrogénicos

Estos medicamentos compiten con los ligandos de los RE, provocando una regulación negativa de ellos [6]. El fulvestrant (ICI 182,780), es un antagonista no esteroideo del RE que bloquea el RE e inhibe los efectos proliferativos del E en las células tumorales[74]. Igualmente, Long y col. [75] demostraron que este antiestrógeno, también inhibe la aromatasa a nivel celular, ya que se deduce porque afecta la acción de los Es por dos vías diferentes. Se ha usado en el tratamiento del cáncer de mama metastásico con receptores hormonales positivos en mujeres posmenopáusicas y actúa produciendo la degradación de los RE [76]. El acolbifeno (EM-652) y el EM-800, son antiestrógenos no esteroideos que reducen el peso uterino y la expresión de los

RE a nivel uterino/vaginal [77]. El acolbifeno parece ser más eficaz que el fulvestrant para inhibir el CE y la proliferación de las células endometriales inducida por el E_2 [78]. En conjunto, estos hallazgos sugieren que los antiestrógenos o SERM, pueden ser beneficiosos para tratar la HE, al reducir la expresión de RE y actuar como agentes antiproliferativos, pero se requiere más estudios [6]. El 2-[piperidinoetoxifenil]-3-[4-hidroxifenil]-2H-benzo(b)pirano, es un compuesto no esteroideo, triaretileno, triarilpropenona antiestrogénico, que se encontró que inhibía el crecimiento uterino [79,80]. La capacidad de este compuesto para inhibir el crecimiento uterino, se atribuye a su capacidad para antagonizar la acción de los Es e inducir la apoptosis [80]. La actividad de este compuesto, también ha sido validada en cultivo celular de células endometriales humanas con hiperplasia atípica, lo que sugiere su uso potencial como una nueva terapia dirigida para HE, mediante la inhibición de la vía de señalización Wnt, así como la inhibición de la vía de supervivencia celular [81].

Inhibidores de la aromatasa

Los inhibidores de la aromatasa impiden la producción de E, reduciendo los niveles de los Es [82]. Entre los inhibidores de la aromatasa tenemos el letrozole, el anastrozole y el exemestano, los cuales, se usan comúnmente para tratar el cáncer de mama, y se cree que son útiles en el tratamiento de la CE [83,84]. El anastrozole y el letrozole, reducen el grosor del endometrio en pacientes con HE y CE [85]. Tabatabaie y col. [86], y El-shamy y col. [87], recomiendan el uso del letrozole como una buena opción terapéutica para la HE simple sin atipia. Agosastos y col. [88], han reportado que el anastrozole es otra alternativa para el tratamiento de la HE en mujeres posmenopáusicas obesas.

Anticuerpos contra citocinas

Las terapias dirigidas a las citocinas inmunitarias elevadas en HE y CE, también podrían ser una opción prometedora [6]. Guo y col. [89] han demostrado que un anticuerpo neutralizante contra la IL-22 humana, inhibe la proliferación de células estromales del endometrio. Se está estudiando el uso de anticuerpos neutralizantes e inhibidores químicos del IGF-R1, en el CE y podrían tener también aplicabilidad para tratar la HE[90]. Asimismo, se ha demostrado que una quimiocina (motivo C-C), un anticuerpo neutralizante del ligando 2 y un antagonista de CCL 2, inhiben la proliferación de células del estroma endometrial, por lo que podrían, potencialmente, estudiarse para el tratamiento de HE [91].

Diindolilmetano (DIM)

Es un fitoquímico e indol de origen vegetal, presente en verduras crucíferas, como el brócoli, las coles de Bruselas, el repollo, la coliflor y la col rizada. Posee propiedades inmunomoduladoras, antineoplásicas, quimiopreventivas, antioxidantes y antivirales, además tiene propiedades moduladoras sobre los estrógenos. Su derivado estable y activo, el indol-3-carbinol (IC), el diindolilmetano (DIM) promueve el metabolismo de los estrógenos, al aumentar la formación de metabolitos de 2-hidroxiestrógenos, lo que incrementa la actividad antioxidante. Se sabe que el DIM, causa detención del crecimiento y apoptosis de células de cáncer cervical *in vitro,* aunque se desconoce el mecanismo exacto de esta actividad *in vivo* [92-95]. En 2010, Del Priore y col. [92], reportaron el uso de 41 mg de DIM, en 64 pacientes con diagnóstico de neoplasia intraepitelial cervical 2 y 3, sin embargo, sus resultados no fueron superiores a los del placebo. Leong y col. [96], demostraron que el DIM tiene un potente efecto citostático y un fuerte efecto antiproliferativo, en células de cáncer endometrial humano. El uso de este agente en el tratamiento de la HE requiere estudios clínicos en un futuro.

Tratamiento quirúrgico

Cuando se ha completado la maternidad, la opción quirúrgica es quizás la más adecuada.

Hiperplasia endometrial sin atipias

La Sociedad de Obstetras y Ginecólogos de Canadá (SOGC) recomienda la histerectomía total (HT) con ooforosalpingectomía bilateral (OSTB), en pacientes menopaúsicas y posmenopáusicas con HE sin atipias. En pacientes premenopáusicas, la HT está indicada cuando la maternidad se ha completado o cuando falla el tratamiento médico. Cuando hay progresión a HE con atipias o CE y/o recidiva de la HE, la SOGC recomienda la salpingectomía total bilateral con o sin ooforectomía total bilateral. Esto último, debe ser una decisión individualizada, es decir, de la paciente previa discusión con el médico tratante [6,19].

Hiperplasia endometrial con atipias/ Neoplasia intraepitelial endometrial (NIE)

Las recomendaciones del tratamiento quirúrgico de la HE con atipia-NIE son similares a las mencionadas en el manejo de la HE sin atipias [6,19].

Histerectomía total

La histerectomía es el tratamiento más adecuado, en la mayoría de los casos de mujeres con HE con atipia/NIE, que no están interesadas en la maternidad, debido al alto riesgo de complicaciones concurrentes y/o al peligro de progresión al CE. La histerectomía extrafascial por cualquier vía, es apropiada para el tratamiento de HE con o sin atipia/NIE. Sin embargo, se debe considerar el riesgo de encontrar una neoplasia maligna concurrente a la HE con atipia/ NIE, por lo que es recomendable abrir el útero para realizar una observación de la cavidad endometrial y/o una congelación intraoperatoria, para realizar una evaluación del endometrio durante la HT [7,48].

Otras opciones quirúrgicas

En mujeres con HE con o sin atipias, que tienen contraindicaciones médicas para realizar una cirugía mayor, se ha empleado la ablación endometrial (AE), usando diferentes técnicas como ablación con resectoscopio, con electrocauterio, con radiofrecuencia, con balón térmico o con láser. En teoría, la remoción o destrucción del endometrio, podría prevenir la progresión de HE a CE[7]; sin embargo, ninguno de estos métodos, desarrollados originalmente para tratar la menorragia, destruye todo el endometrio, por lo que el uso de estas técnicas es limitado. Hasta que se realicen estudios más amplios con seguimientos más prolongados, la resección o la AE no se pueden recomendar como terapia primaria para la HE [7]. Diferentes autores [6,97] han mencionado que, en la AE, el uso del balón térmico o del resectoscopio es una opción factible, segura y eficaz para tratar la HE simple y compleja con o sin atipias. El ACOG no recomienda el uso de la AE con ninguna técnica [48].

CONCLUSIÓN

Es importante entender y comprender el proceso de origen y evolución de la HE y el CE, asimismo, los factores de riesgo que provocan su desarrollo, para entonces lograr un tratamiento adecuado de esas patologías y evitar la progresión de las lesiones premalignas a malignas; igualmente, colocar tratamientos preventivos en pacientes con factores de riesgo. Para HE sin atipia, la terapia con Ps es el tratamiento más utilizado, sin embargo, a veces se requiere histerectomía, porque no haya respuesta adecuada al tratamiento o porque persiste el sangrado o igual progresión de la enfermedad, por lo que el tratamiento debe ser individualizado, sobre todo en mujeres que han completado su maternidad [6,7,19].

Además de los tratamientos médicos con progesterona, Ps, danazol, ginesteina, metformina y análogos de la GnRH, el tratamiento novedoso con los antiestrógenos, los antagonistas de la GnRH, los inhibidores de la aromatasa y las citoquinas, podrían dar resultados optimistas para la HE; asimismo, la continuación de estudios de mutaciones y SNP en la biología de HE y CE, ayudará a identificar nuevos agentes terapéuticos dirigidos a mejorar el tratamiento de la HE.

Financiamiento

Ninguno.

Conflicto de intereses

El autor no tiene conflictos de intereses.

Número ORCID del autor

- José Núñez-Troconis: 0000-0002-5334-7265

Contribuciones del autor

El autor certifica que diseñó, planificó, revisó las referencias, analizó la información y redactó el manuscrito.

Inteligencia Artificial

El autor certifica que no utilizó inteligencia artificial para la preparación y redacción del manuscrito de esta revisión narrativa.

REFERENCIAS

1. **Montgomery BE, Daum GS, Dunton CJ**. Endometrial hyperplasia: a review. Obstet Gynecol Surv. 2004; 59(5):368-378. *https://doi.org/10.1097/00006254-200405000-00025.*
2. **Höhn AK, Brambs CE, Hiller GGR, May D, Schmoeckel E, Horn LC**. 2020 WHO Classification of Female Genital Tumors. Geburtshilfe Frauenheilkd. 2021; 81(10):1145-1153. *https://doi.org/10.1055/a-1545-4279.*
3. **Ring KL, Mills AM, Modesitt SC**. Endometrial Hyperplasia. Obstet Gynecol. 2022;140(6):1061-1075. *https://doi.org/10.1097/AOG.0000000000004989.*
4. **Sobczuk K, Sobczuk A.** New classification system of endometrial hyperplasia WHO 2014 and its clinical implications. Prz Menopauzalny. 2017; 16(3):107-111. *https://doi.org/10.5114/pm.2017.70589.*
5. **Ricci E, Moroni S, Parazzini F, Surace M, Benzi G, Salerio B, et al.** Risk factors for endometrial hyperplasia: results from a case-control study. Int J Gynecol Cancer. 2002; 12(3):257-260. *https://doi.org/10.1046/j.1525-1438.2002.01105.x.*
6. **Chandra V, Kim JJ, Benbrook DM, Dwivedi A, Rai R.** Therapeutic options for management of endometrial hyperplasia. J Gynecol Oncol. 2016; 27(1):e8. *https://doi.org/10.3802/jgo.2016.27.e8.*
7. **Armstrong AJ, Hurd WW, Elguero S, Barker NM, Zanotti KM**. Diagnosis and management of endometrial hyperplasia. J Minim Invasive Gynecol. 2012; 19(5):562-571. *https://doi.org/10.1016/j.jmig.2012.05.009.*
8. **Reed SD, Newton KM, Clinton WL, Epplein M, Garcia R, Allison K, et al.** Incidence of endometrial hyperplasia. Am J Obstet Gynecol. 2009; 200(6):678. e1-6. *https://doi.org/10.1016/j.ajog.2009.02.032.*
9. **Natarajan P, Vinturache A, Hutson R, Nugent D, Broadhead T.** The value of MRI in management of endometrial hyperplasia with atypia. World J Surg Oncol. 2020; 18(1):34. *https://doi.org/10.1186/s12957-020-1811-5.*
10. **Whitaker L, Critchley HO.** Abnormal uterine bleeding. Best Pract Res Clin Obstet Gynaecol. 2016; 34:54-65. *https://doi.org/10.1016/j.bpobgyn.2015.11.012.*
11. **International Agency for Cancer Research. World Health Organization. The Global Cancer Observatory (GCO).** Corpus uteri. Cancer Today. 2020. Disponible en: *https://gco.iarc.who.int/media/globocan/factsheets/cancers/24-corpus-uteri-fact-sheet.pdf.*
12. **Siegel RL, Miller KD, Wagle NS, Jemal A.** Cancer statistics, 2023. CA Cancer J Clin. 2023; 73(1):17-48. *https://doi.org/10.3322/caac.21763.*
13. **National Cancer Institute.** Surveillance, Epidemiology, and End Results Program. Cancer stat facts: uterine cancer. 2023. Disponible en: *https://seer.cancer.gov/statfacts/html/cervix.html.*
14. **Coulam CB, Annegers JF, Kranz JS.** Chronic anovulation syndrome and associated neoplasia. Obstet Gynecol. 1983; 61(4):403-407. PMID: 6828267.

15. **Göl K, Saraçoğlu F, Ekici A, Sahin I.** Endometrial patterns and endocrinologic characteristics of asymptomatic menopausal women. Gynecol Endocrinol. 2001; 15(1):63-67. PMID: 11293927.
16. **Martínez-Núñez EN, Carvallo-Ruiz DE, Núñez-Troconis JT.** Gynecological uses of GnRH antagonists: review article. Obstet Gynecol Int J. 2022; 13(4):226-238. *https://doi.org/10.15406/ogij.2022.13.00654.*
17. **Scully RE, Bonfiglio TA, Kurman RJ, Silverberg SG, Wilkinson EJ.** International Histological Classification and Typing of Female Genital Tract Tumours. 2nd Ed. New York, NY: Springer-Verlag; 1994: 1–189. *https://doi.org/10.1007/978-3-642-85014-1.*
18. **Baak JP, Mutter GL, Robboy S, van Diest PJ, Uyterlinde AM, Orbo A, et al.** The molecular genetics and morphometry-based endometrial intraepithelial neoplasia classification system predicts disease progression in endometrial hyperplasia more accurately than the 1994 World Health Organization classification system. Cancer. 2005;103(11):2304-2312. *https://doi.org/10.1002/cncr.21058.*
19. **Auclair MH, Yong PJ, Salvador S, Thurston J, Colgan TTJ, Sebastianelli A.** Guideline No. 390-Classification and Management of Endometrial Hyperplasia. J Obstet Gynaecol Can. 2019; 41(12):1789-1800. *https://doi.org/10.1016/j.jogc.2019.03.025.* Erratum in: J Obstet Gynaecol Can. 2020; 42(10):1287.
20. **Jewson M, Purohit P, Lumsden MA.** Progesterone and abnormal uterine bleeding/menstrual disorders. Best Pract Res Clin Obstet Gynaecol. 2020; 69:62-73. *https://doi.org/10.1016/j.bpobgyn.2020.05.004.*
21. **Amezcua CA, Lu JJ, Felix JC, Stanczyk FZ, Zheng W.** Apoptosis may be an early event of progestin therapy for endometrial hyperplasia. Gynecol Oncol. 2000; 79(2):169-176. *https://doi.org/10.1006/gyno.2000.5955.*
22. **Abulafia O, Triest WE, Adcock JT, Sherer DM**. The effect of medroxyprogesterone acetate on angiogenesis in complex endometrial hyperplasia. Gynecol Oncol. 1999;72(2):193-198. *https://doi.org/10.1006/gyno.1998.5106.*
23. **Figueroa-Casas PR, Ettinger B, Delgado E, Javkin A, Vieder C**. Reversal by medical treatment of endometrial hyperplasia caused by estrogen replacement therapy. Menopause. 2001; 8(6):420-423. *https://doi.org/10.1097/00042192-200111000-00006.*
24. **Reed SD, Voigt LF, Newton KM, Garcia RH, Allison HK, Epplein M, et al.** Progestin therapy of complex endometrial hyperplasia with and without atypia. Obstet Gynecol. 2009; 113(3):655-662. *https://doi.org/10.1097/AOG.0b013e318198a10a.*
25. **Gunderson CC, Fader AN, Carson KA, Bristow RE**. Oncologic and reproductive outcomes with progestin therapy in women with endometrial hyperplasia and grade 1 adenocarcinoma: a systematic review. Gynecol Oncol. 2012; 125(2):477-482. *https://doi.org/10.1016/j.ygyno.2012.01.003.*
26. **Brun JL, Belaisch J, Rivel J, Hocké C.** Les hyperplasies endométriales résistant aux progestatifs: alternatives aux traitements traditionnels. [Endometrial hyperplasias resistant to progestins: alternatives to traditional treatments]. Gynecol Obstet Fertil. 2002; 30(3):244-251. *https://doi.org/10.1016/s1297-9589(02)00301-6.*
27. **Upson K, Allison KH, Reed SD, Jordan CD, Newton KM, Swisher EM, et al**. Biomarkers of progestin therapy resistance and endometrial hyperplasia progression. Am J Obstet Gynecol. 2012; 207(1):36.e1-8. *https://doi.org/10.1016/j.ajog.2012.05.012.*
28. **Wang S, Pudney J, Song J, Mor G, Schwartz PE, Zheng W.** Mechanisms involved in the evolution of progestin resistance in human endometrial hyperplasia--precursor of endometrial cancer. Gynecol Oncol. 2003; 88(2):108-117. *https://doi.org/10.1016/s0090-8258(02)00008-2.*
29. **Chen X, Zhang Z, Feng Y, Fadare O, Wang J, Ai Z, et al.** Aberrant survivin expression in endometrial hyperplasia: another mechanism of progestin resistance. Mod

Pathol. 2009; 22(5):699-708. *https://doi.org/10.1038/modpathol.2009.25.*

30. **van Hylckama Vlieg A, Helmerhorst FM, Rosendaal FR**. The risk of deep venous thrombosis associated with injectable depot-medroxyprogesterone acetate contraceptives or a levonorgestrel intrauterine device. Arterioscler Thromb Vasc Biol. 2010; 30(11):2297-2300. *https://doi.org/10.1161/ATVBAHA.110.211482.*
31. **Vasilakis C, Jick H, del Mar Melero-Montes M**. Risk of idiopathic venous thromboembolism in users of progestagens alone. Lancet. 1999; 354(9190):1610-1611. *https://doi.org/10.1016/S0140-6736(99)04394-9.*
32. **Heinemann LA, Assmann A, DoMinh T, Garbe E**. Oral progestogen-only contraceptives and cardiovascular risk: results from the Transnational Study on Oral Contraceptives and the Health of Young Women. Eur J Contracept Reprod Health Care. 1999; 4(2):67-73. *https://doi.org/10.3109/13625189909064007.*
33. **Eichner E, Abellera M.** Endometrial hyperplasia treated by progestins. Obstet Gynecol. 1971; 38 (5):739-42. PMID: 5114224.
34. **Bese T, Vural A, Ozturk M, Dagistanli F, Demirkiran F, Tunedemir M, et al.** The effect of long-term use of progesterone therapy on proliferation and apoptosis in simple endometrial hyperplasia without atypia. Int J Gynecol Cancer. 2006; 16(2):809-813. *https://doi.org/10.1111/j.1525-1438.2006.00533.x.*
35. **Buttini MJ, Jordan SJ, Webb PM**. The effect of the levonorgestrel releasing intrauterine system on endometrial hyperplasia: An Australian study and systematic review. Aust N Z J Obstet Gynaecol. 2009; 49(3):316-322. *https://doi.org/10.1111/j.1479-828X.2009.00981.x.*
36. **Ozdegirmenci O, Kayikcioglu F, Bozkurt U, Akgul MA, Haberal A.** Comparison of the efficacy of three progestins in the treatment of simple endometrial hyperplasia without atypia. Gynecol Obstet Invest. 2011; 72(1):10-14. *https://doi.org/10.1159/000321390.*
37. **Ushijima K, Yahata H, Yoshikawa H, Konishi I, Yasugi T, Saito T, et al.** Multicenter phase II study of fertility-sparing treatment with medroxyprogesterone acetate for endometrial carcinoma and atypical hyperplasia in young women. J Clin Oncol. 2007; 25(19):2798-2803. *https://doi.org/10.1200/JCO.2006.08.8344.*
38. **Güven M, Dikmen Y, Terek MC, Ozsaran AA, Itil IM, Erhan Y**. Metabolic effects associated with high-dose continuous megestrol acetate administration in the treatment of endometrial pathology. Arch Gynecol Obstet. 2001; 265(4):183-186. *https://doi.org/10.1007/s004040000154.*
39. **Gal D, Edman CD, Vellios F, Forney JP.** Long-term effect of megestrol acetate in the treatment of endometrial hyperplasia. Am J Obstet Gynecol. 1983; 146(3):316-322. *https://doi.org/10.1016/0002-9378(83)90754-8.*
40. **Garza-Flores J, Menjívar M, Cardenas M, Reynoso M, García GA, Pérez Palacios G.** Further studies on the antigonadotropic mechanism of action of norethisterone. J Steroid Biochem Mol Biol. 1991; 38(1):89-93. *https://doi.org/10.1016/0960-0760(91)90406-u.*
41. **Portman DJ, Symons JP, Wilborn W, Kempfert NJ**. A randomized, double-blind, placebo-controlled, multicenter study that assessed the endometrial effects of norethindrone acetate plus ethinyl estradiol versus ethinyl estradiol alone. Am J Obstet Gynecol. 2003;188(2):334-342. *https://doi.org/10.1067/mob.2003.91.*
42. **Nisker JA, Kirk ME, Nunez-Troconis JT**. Reduced incidence of rabbit endometrial neoplasia with levonorgestrel implant. Am J Obstet Gynecol. 1988;158(2):300-303. *https://doi.org/10.1016/0002-9378(88)90142-1.*
43. **Nilsson CG, Haukkamaa M, Vierola H, Luukkainen T**. Tissue concentrations of levonorgestrel in women using a levonorgestrel-releasing IUD. Clin Endocrinol (Oxf). 1982; 17(6):529-536. *https://doi.org/10.1111/j.1365-2265.1982.tb01625.x.*
44. **Suhonen SP, Allonen HO, Lähteenmäki P.** Sustained-release estradiol implants and a levonorgestrel-releasing intrauterine device in hormone replacement therapy. Am

J Obstet Gynecol. 1995; 172(2 Pt 1):562-567. *https://doi.org/10.1016/0002-9378(95)90573-1.*

45. **Abu Hashim H, Zayed A, Ghayaty E, El Rakhawy M.** LNG-IUS treatment of non-atypical endometrial hyperplasia in perimenopausal women: a randomized controlled trial. J Gynecol Oncol. 2013; 24(2):128-134. *https://doi.org/10.3802/jgo.2013.24.2.128.*
46. **Varma R, Soneja H, Bhatia K, Ganesan R, Rollason T, Clark TJ, Gupta JK**. The effectiveness of a levonorgestrel-releasing intrauterine system (LNG-IUS) in the treatment of endometrial hyperplasia-a long-term follow-up study. Eur J Obstet Gynecol Reprod Biol. 2008; 139(2):169-175. *https://doi.org/10.1016/j.ejogrb.2008.02.022.*
47. **Vereide AB, Arnes M, Straume B, Maltau JM,** Ørbo **A**. Nuclear morphometric changes and therapy monitoring in patients with endometrial hyperplasia: a study comparing effects of intrauterine levonorgestrel and systemic medroxyprogesterone. Gynecol Oncol. 2003; 91(3):526-533. *https://doi.org/10.1016/j.ygyno.2003.07.002.*
48. **Singh G, Cue L, Puckett Y.** Endometrial Hyperplasia. In: StatPearls [Internet]. Treasure Island (FL): StatPearls Publishing; 2024.
49. **The American College of Obstetricians and Gynecologists (ACOG).** Management of Endometrial Intraepithelial Neoplasia or Atypical Endometrial Hyperplasia: ACOG Clinical Consensus No. 5. Obstet Gynecol. 2023; 142(3):735-744. *https://doi.org/10.1097/AOG.0000000000005297.*
50. **Gallos ID, Shehmar M, Thangaratinam S, Papapostolou TK, Coomarasamy A, Gupta JK.** Oral progestogens vs levonorgestrel-releasing intrauterine system for endometrial hyperplasia: a systematic review and metaanalysis. Am J Obstet Gynecol. 2010; 203(6):547.e1-10. *https://doi.org/10.1016/j.ajog.2010.07.037.*
51. **Greenblatt RB, Dmowski WP, Mahesh VB, Scholer HF.** Clinical studies with an antigonadotropin-Danazol. Fertil Steril. 1971; 22(2):102-112. *https://doi.org/10.1016/s0015-0282(16)38045-1.*
52. **Crosignani P, Olive D, Bergqvist A, Luciano A.** Advances in the management of endometriosis: an update for clinicians. Hum Reprod Update. 2006; 12(2):179-189. *https://doi.org/10.1093/humupd/dmi049.*
53. **Mariani L, Sedati A, Giovinazzi R, Sindico R, Atlante G**. Postmenopausal endometrial hyperplasia: role of danazol therapy. Int J Gynaecol Obstet. 1994; 44(2):155-159. *https://doi.org/10.1016/0020-7292(94)90071-x.*
54. **Soh E, Sato K.** Clinical effects of danazol on endometrial hyperplasia in menopausal and postmenopausal women. Cancer. 1990; 66(5):983-988. *https://doi.org/10.1002/1097-0142(19900901)66:5<983:aid-cncr2820660530>3.0.co;2-6.*
55. **Grio R, Piacentino R, Marchino GL, Bocci A, Navone R**. Danazol in the treatment of endometrial hyperplasia. Panminerva Med. 1993; 35(4):231-233. PMID: 8202337.
56. **Tamaoka Y, Orikasa H, Sumi Y, Sakakura K, Kamei K, Nagatani M, Ezawa S.** Treatment of endometrial hyperplasia with a danazol-releasing intrauterine device: a prospective study. Gynecol Obstet Invest. 2004; 58(1):42-48. *https://doi.org/10.1159/000077882.*
57. **Cottreau CM, Ness RB, Modugno F, Allen GO, Goodman MT.** Endometriosis and its treatment with danazol or lupron in relation to ovarian cancer. Clin Cancer Res. 2003; 9(14):5142-5144. PMID: 14613992.
58. **Vercellini P, Somigliana E, Viganò P, Abbiati A, Barbara G, Crosignani PG**. Endometriosis: current therapies and new pharmacological developments. Drugs. 2009; 69(6):649-675. *https://doi.org/10.2165/00003495-200969060-00002.*
59. **Akiyama T, Ishida J, Nakagawa S, Ogawara H, Watanabe S, Itoh N, et al.** Genistein, a specific inhibitor of tyrosine-specific protein kinases. J Biol Chem. 1987; 262(12):5592-5595. PMID: 3106339.
60. **Yamashita Y, Kawada S, Nakano H.** Induction of mammalian topoisomerase II dependent DNA cleavage by nonintercalative flavonoids, genistein and orobol. Biochem

Pharmacol. 1990; 39(4):737-744. *https://doi.org/10.1016/0006-2952(90)90153-c.*

61. **Lian Z, Niwa K, Tagami K, Hashimoto M, Gao J, Yokoyama Y, Mori H, Tamaya T.** Preventive effects of isoflavones, genistein and daidzein, on estradiol-17beta-related endometrial carcinogenesis in mice. J Cancer Res. 2001; 92(7):726-734. *https://doi.org/10.1111/j.1349-7006.2001.tb01154.x.*
62. **Bitto A, Granese R, Triolo O, Villari D, Maisano D, Giordano D, et al.** Genistein aglycone: a new therapeutic approach to reduce endometrial hyperplasia. Phytomedicine. 2010; 17(11):844-850. *https://doi.org/10.1016/j.phymed.2010.03.024.*
63. **Núñez-Troconis, J.** Uso de la metformina en el síndrome de ovarios poliquísticos. Gac Méd Caracas. 2021;129(1):128-139. *https://doi.org/10.47307/GMC.2021.129.1.14*
64. **Shao R, Li X, Feng Y, Lin JF, Billig H.** Direct effects of metformin in the endometrium: a hypothetical mechanism for the treatment of women with PCOS and endometrial carcinoma. J Exp Clin Cancer Res. 2014;33(1):41. *https://doi.org/10.1186/1756-9966-33-41.*
65. **Núñez-Troconis, J.** Uso de la metformina en cáncer ginecológico. Gac Méd Caracas 2021;129(1):88-106. *https://doi.org/10.47307/GMC.2021.129.1.12.*
66. **Xie Y, Wang YL, Yu L, Hu Q, Ji L, Zhang Y, Liao QP.** Metformin promotes progesterone receptor expression via inhibition of mammalian target of rapamycin (mTOR) in endometrial cancer cells. J Steroid Biochem Mol Biol. 2011; 126(3-5):113-120. *https://doi.org/10.1016/j.jsbmb.2010.12.006.*
67. **Erdemoglu E, Güney M, Giray SG, Take G, Mungan T.** Effects of metformin on mammalian target of rapamycin in a mouse model of endometrial hyperplasia. Eur J Obstet Gynecol Reprod Biol. 2009; 145(2):195-199. *https://doi.org/10.1016/j.ejogrb.2009.04.034.*
68. **Session DR, Kalli KR, Tummon IS, Damario MA, Dumesic DA.** Treatment of atypical endometrial hyperplasia with an insulin-sensitizing agent. Gynecol Endocrinol. 2003; 17(5):405-407. *https://doi.org/10.1080/09513590312331290298.*
69. **Shen ZQ, Zhu HT, Lin JF.** Reverse of progestin-resistant atypical endometrial hyperplasia by metformin and oral contraceptives. Obstet Gynecol. 2008;112(2 Pt 2):465-467. *https://doi.org/10.1097/AOG.0b013e3181719b92.*
70. **Meresman GF, Bilotas MA, Lombardi E, Tesone M, Sueldo C, Barañao RI.** Effect of GnRH analogues on apoptosis and release of interleukin-1beta and vascular endothelial growth factor in endometrial cell cultures from patients with endometriosis. Hum Reprod. 2003; 18(9):1767-1771. *https://doi.org/10.1093/humrep/deg356.*
71. **Fister S, Günthert AR, Emons G, Gründker C.** Gonadotropin-releasing hormone type II antagonists induce apoptotic cell death in human endometrial and ovarian cancer cells in vitro and in vivo. Cancer Res. 2007; 67(4):1750-1756. *https://doi.org/10.1158/0008-5472.CAN-06-3222.*
72. **Agorastos T, Bontis J, Vakiani A, Vavilis D, Constantinidis T.** Treatment of endometrial hyperplasias with gonadotropin-releasing hormone agonists: pathological, clinical, morphometric, and DNA-cytometric data. Gynecol Oncol. 1997; 65(1):102-114. *https://doi.org/10.1006/gyno.1997.4639.*
73. **Agorastos T, Vaitsi V, Paschopoulos M, Vakiani A, Zournatzi-Koiou V, Saravelos H, et al.** Prolonged use of gonadotropin-releasing hormone agonist and tibolone as add-back therapy for the treatment of endometrial hyperplasia. Maturitas. 2004;48(2):125-132. *https://doi.org/10.1016/j.maturitas.2003.08.008.*
74. **Yu K, Huang ZY, Xu XL, Li J, Fu XW, Deng SL.** Estrogen Receptor Function: Impact on the Human Endometrium. Front Endocrinol (Lausanne). 2022; 13:827724. *https://doi.org/10.3389/fendo.2022.827724.*
75. **Long BJ, Tilghman SL, Yue W, Thiantanawat A, Grigoryev DN, Brodie AM.** The steroidal antiestrogen ICI 182,780 is an inhibitor of cellular aromatase activity. J Steroid Biochem Mol Biol. 1998;

67(4):293-304. *https://doi.org/10.1016/s0960-0760(98)00122-8.*

76. **Scott SM, Brown M, Come SE**. Emerging data on the efficacy and safety of Fulvestrant, a unique antiestrogen therapy for advanced breast cancer. Expert Opin Drug Saf. 2011; 10(5):819-826. *https://doi.org/10.1517/14740338.2011.595560.*
77. **Sourla A, Luo S, Labrie C, Bélanger A, Labrie F**. Morphological changes induced by 6-month treatment of intact and ovariectomized mice with tamoxifen and the pure antiestrogen EM-800. Endocrinology. 1997; 138(12):5605-5617. *https://doi.org/10.1210/endo.138.12.5560.*
78. **Tremblay A, Tremblay GB, Labrie C, Labrie F, Giguère V.** EM-800, a novel antiestrogen, acts as a pure antagonist of the transcriptional functions of estrogen receptors alpha and beta. Endocrinology. 1998; 139(1):111-118. *https://doi.org/10.1210/endo.139.1.5702.*
79. **Fatima I, Chandra V, Saxena R, Manohar M, Sanghani Y, Hajela K, et al.** 2,3-Diaryl-2H-1-benzopyran derivatives interfere with classical and non-classical estrogen receptor signaling pathways, inhibit Akt activation and induce apoptosis in human endometrial cancer cells. Mol Cell Endocrinol. 2012; 348(1):198-210. *https://doi.org/10.1016/j.mce.2011.08.018.*
80. **Chandra V, Fatima I, Saxena R, Kitchlu S, Sharma S, Hussain MK, et al**. Apoptosis induction and inhibition of hyperplasia formation by 2-[piperidinoethoxyphenyl]-3-[4-hydroxyphenyl]-2H-benzo(b)pyran in rat uterus. Am J Obstet Gynecol. 2011; 205(4):362.e1-11. *https://doi.org/10.1016/j.ajog.2011.05.024.* Erratum in: Am J Obstet Gynecol. 2020; 222(1):84.
81. **Chandra V, Fatima I, Manohar M, Popli P, Sirohi VK, Hussain MK, et al.** Inhibitory effect of 2-(piperidinoethoxyphenyl)-3-(4-hydroxyphenyl)-2H-benzo(b)pyran (K-1) on human primary endometrial hyperplasial cells mediated via combined suppression of Wnt/β-catenin signaling and PI3K/Akt survival pathway. Cell Death Dis. 2014; 5(8):e1380. *https://doi.org/10.1038/cddis.2014.334.*
82. **Fabian CJ.** The what, why and how of aromatase inhibitors: hormonal agents for treatment and prevention of breast cancer. Int J Clin Pract. 2007; 61(12):2051-2063. *https://doi.org/10.1111/j.1742-1241.2007.01587.x.*
83. **Bershteĭn LM, Maksimov SIa, Danilova MA, Gershfel'd ÉD, Boiarkina MP, Khadzhimba AS, et al.** [Effectiveness of aromatase inhibitors in comparison with metformin for neoadjuvant treatment in patients with endometrial cancer]. Vopr Onkol. 2011; 57(6):737-741. Russian. PMID: 22416390.
84. **Lai CH, Huang HJ.** The role of hormones for the treatment of endometrial hyperplasia and endometrial cancer. Curr Opin Obstet Gynecol. 2006; 18(1):29-34. *https://doi.org/10.1097/01.gco.0000192994.37965.c6.*
85. **Barker LC, Brand IR, Crawford SM.** Sustained effect of the aromatase inhibitors anastrozole and letrozole on endometrial thickness in patients with endometrial hyperplasia and endometrial carcinoma. Curr Med Res Opin. 2009; 25(5):1105-1109. *https://doi.org/10.1185/03007990902860549.*
86. **Tabatabaie A, Karimi Zarchi M, Dehghani-Tafti M, Miratashi-Yazdi A, Teimoori S, Dehghani A**. Comparing letrozole with medroxyprogesterone acetate (MPA) as hormonal therapy for simple endometrial hyperplasia without atypia in adult and middle-aged women. Eur J Gynaecol Oncol. 2013; 34(6):552-555. PMID: 24601050.
87. **El-shamy M, Gibreel A, Refai E, Sadek E, Ragab A.** Aromatase inhibitor "letrozole" versus progestin "norethisterone" in women with simple endometrial hyperplasia without atypia: a prospective cohort trial. Middle East Fertil Soc J. 2012; 17(2):111-115. *https://doi.org/10.1016/j.mefs.2011.11.005.*
88. **Agorastos T, Vaitsi V, Pantazis K, Efstathiadis E, Vavilis D, Bontis JN.** Aromatase inhibitor anastrozole for treating endometrial hyperplasia in obese postmenopausal women. Eur J Obstet Gynecol Re-

prod Biol. 2005; 118(2):239-240. *https://doi.org/10.1016/j.ejogrb.2004.07.002.*

89. **Guo Y, Chen Y, Liu LB, Chang KK, Li H, Li MQ, Shao J.** IL-22 in the endometriotic milieu promotes the proliferation of endometrial stromal cells via stimulating the secretion of CCL2 and IL-8. Int J Clin Exp Pathol. 2013; 6(10):2011-2020. PMID: 2133578.
90. **Bruchim I, Sarfstein R, Werner H.** The IGF Hormonal Network in Endometrial Cancer: Functions, Regulation, and Targeting Approaches. Front Endocrinol (Lausanne). 2014; 5:76. *https://doi.org/10.3389/fendo.2014.00076.*
91. **Li MQ, Li HP, Meng YH, Wang XQ, Zhu XY, Mei J, Li DJ.** Chemokine CCL2 enhances survival and invasiveness of endometrial stromal cells in an autocrine manner by activating Akt and MAPK/Erk1/2 signal pathway. Fertil Steril. 2012; 97(4):919-929. *https://doi.org/10.1016/j.fertnstert.2011.12.049.*
92. **Del Priore G, Gudipudi DK, Montemarano N, Restivo AM, Malanowska-Stega J, Arslan AA.** Oral diindolylmethane (DIM): pilot evaluation of a nonsurgical treatment for cervical dysplasia. Gynecol Oncol. 2010;116(3):464-467. *https://doi.org/10.1016/j.ygyno.2009.10.060.*
93. **Dalessandri KM, Firestone GL, Fitch MD, Bradlow HL, Bjeldanes LF**. Pilot study: effect of 3,3'-diindolylmethane supplements on urinary hormone metabolites in postmenopausal women with a history of early-stage breast cancer. Nutr Cancer. 2004;50(2):161-167. *https://doi.org/10.1207/s15327914nc5002_5.*
94. **Chen DZ, Qi M, Auborn KJ, Carter TH**. Indole-3-carbinol and diindolylmethane induce apoptosis of human cervical cancer cells and in murine HPV16-transgenic preneoplastic cervical epithelium. J Nutr. 2001;131(12):3294-3302. *https://doi.org/10.1093/jn/131.12.3294.*
95. **Savino JA 3rd, Evans JF, Rabinowitz D, Auborn KJ, Carter TH.** Multiple, disparate roles for calcium signaling in apoptosis of human prostate and cervical cancer cells exposed to diindolylmethane. Mol Cancer Ther. 2006;5(3):556-563. *https://doi.org/10.1158/1535-7163.MCT-05-0355.*
96. **Leong H, Firestone GL, Bjeldanes LF**. Cytostatic effects of 3,3′-diindolylmethane in human endometrial cancer cells result from an estrogen receptor-mediated increase in transforming growth factor-α expression. Carcinogenesis. 2001; 22(11):1809-1817. *https://doi.org/10.1093/carcin/22.11.1809.*
97. **Järvelä I, Tekay A, Santala M, Jouppila P**. Thermal balloon endometrial ablation therapy induces a rise in uterine blood flow impedance: a randomized prospective color Doppler study. Ultrasound Obstet Gynecol. 2001;17(1):65-70. *https://doi.org/10.1046/j.1469-0705.2001.00317.*

Invest Clin 66(4): 454 - 466, 2025 https://doi.org/10.54817/IC.v66n4a08

Eficacia comparativa entre el tratamiento quirúrgico y el conservador en el choque fémoroacetabular. Una Revisión sistemática.

Eva M. Lantarón-Caeiro[1,2], Álvaro López-Llorente[3], Gema Santamaría-Gómez[4] y Diego Fernández-Lázaro[5]

[1]Universidade de Vigo. Facultad de Fisioterapia. Campus A Xunqueira. Pontevedra. Galicia. España.

[2]Grupo de Investigación Fisioterapia Clínica (FS1), Instituto de Investigación Sanitaria Galicia Sur (IIS Galicia Sur). SERGAS-UVIGO.

[3]Centro Policlínico Aranda, Aranda de Duero, España.

[4]Departamento de Anatomía y Radiología, Facultad de Ciencias de la Salud, Campus de Soria, Universidad de Valladolid, Soria, España.

[5]Área de Histología y Grupo de Investigación en Neurobiología, Facultad de Ciencias de la Salud, Universidad de Valladolid, Soria, España.

Palabras clave: Síndrome de Pinzamiento Femoroacetabular; Fisioterapia; Artroscopia; Calidad de Vida; Rango de Movimiento Articular.

Resumen. El síndrome o choque de pinzamiento femoroacetabular (PFA), es un síndrome clínico caracterizado por un conflicto de espacio entre el acetábulo y la cabeza femoral, que provoca degeneración precoz y dolor articular, siendo necesario un tratamiento adecuado. Sin embargo, no existe consenso sobre si el tratamiento primario debe de ser quirúrgico o conservador. Por tanto, el objetivo del estudio fue revisar la evidencia científica sobre la efectividad de la fisioterapia respecto a la artroscopia en pacientes con PFA. Siguiendo las directrices "*Preferred Reporting Items for Systematic Review and Meta-Analyses*" (PRISMA), se revisaron sistemáticamente ensayos clínicos aleatorizados publicados en los últimos 15 años, que compararan el tratamiento conservador respecto al artroscópico en el PFA, analizando la función articular y la calidad de vida de los pacientes. La búsqueda se realizó en las bases de datos Medline, "*Physiotherapy Evidence Database*" PEDro y Cochrane. Adicionalmente se evaluó la calidad metodológica mediante las escalas PEDro y CASPe, y el riesgo de sesgo con la herramienta Cochrane. Seis ensayos cumplieron los criterios de selección, incluyendo 744 pacientes entre entre 30 y 50 años de edad. Se observaron mejoras significativas ($p<0,05$), en la calidad de vida de los pacientes con artroscopia de cadera, respecto a los que tuvieron tratamiento conservador. No existe consenso sobre la función articular. En conclusión, el tratamiento del PFA mediante artroscopia, podría mejorar significativamente la calidad de vida de los pacientes con respecto a la fisioterapia. Estos resultados posicionarían al abordaje quirúrgico, como mejor primera opción de tratamiento para el PFA. Sin embargo, se necesitan más estudios, con muestras más grandes, y seguimientos más prolongados para evaluar el abordaje definitivo del PFA.

Autor de correspondencia: Diego Fernández-Lázaro. Departamento de Biología Celular, Genética, Histología y Farmacología, Facultad de Ciencias de la Salud, Universidad de Valladolid, Campus de Soria, Calle Universidad, 1, 42004 Soria, España. Correo electrónico: diego.fernadez.lazaro@uva.es

Comparative efficacy of surgical and conservative treatment for femoro-acetabular impingement. A Systematic Review.

Invest Clin 2025; 66 (4): 454 – 466

Keywords: Femoroacetabular Impingement; Physical Therapy Modalities; Arthroscopy; Quality of Life; Range of Motion, Articular.

Abstract. Femoro-acetabular impingement (FAI) is a clinical syndrome characterized by a space conflict between the acetabulum and the femoral head, which causes premature degeneration and joint pain. For this, an adequate therapeutic approach is necessary. However, there is no consensus on whether the primary treatment should be surgical or conservative. Therefore, the present study aimed to review the available scientific evidence on the effectiveness of physiotherapy compared to arthroscopy in patients with FAI. Following the "Preferred Reporting Items for Systematic Review and Meta-Analyses" (PRISMA) guidelines, we systematically reviewed randomized clinical trials published over the last 15 years comparing conservative treatment with the arthroscopic approach in FAI, analyzing joint function and patient quality of life. The search was performed in the Medline, "Physiotherapy Evidence Database" PEDro and Cochrane databases. In addition, the methodological quality was evaluated using the PEDro and the "Cuestionario Critical Appraisal Skills Programme Español" (CASPe) scales, and the risk of bias was assessed using the Cochrane tool. Six trials met the established selection criteria, including 744 patients aged 30 to 50 years. Significant improvements ($p<0.05$) in quality of life were observed with hip arthroscopy compared with conservative treatment. There is no consensus on joint function. In conclusion, the FAI approach via arthroscopic treatment could significantly improve patients' quality of life compared with physiotherapy. These results would position surgical treatment as the best first-line treatment option for FAI. However, further studies with larger sample sizes and longer follow-ups are needed to evaluate the definitive approach to FAI.

Recibido: 30-06-2025 Accepted: 31-08-2025

INTRODUCCIÓN

El síndrome o choque de pinzamiento femoroacetabular (PFA), es una patología que afecta a la articulación coxofemoral de adultos jóvenes activos, entre 20 y 40 años de edad [1]. Se trata de una alteración biomecánica, derivada de una anomalía morfológica de la cabeza femoral o del acetábulo de la pelvis, que puede conducir a un daño el cartílago articular y la estructura ósea adyacente [2]. El desarrollo del PFA se ha relacionado con numerosos factores de riesgo, tanto genéticos, como derivados de sobrecargas mecánicas repetitivas y acumulativas en la articulación coxofemoral, especialmente en movimientos de flexión y rotación, lo que incrementa su prevalencia en personas físicamente activas [2]. Las manifestaciones clínicas del PFA son diversas, aunque los síntomas

más comunes incluyen dolor, chasquidos o crujidos, bloqueos articulares, rigidez y limitación del rango de movimiento (ROM), que terminan perjudicando la funcionalidad y calidad de vida (QoL) de los pacientes que lo presentan [3]. El dolor, aunque común, presenta una distribución variable entre los pacientes. Su localización puede abarcar desde la zona lateral de la cadera, muslo, nalga y la parte inferior de la espalda, hasta la región de la rodilla [4]. El conjunto de manifestaciones clínicas, ocasiona alteraciones en el patrón de marcha, debilidad muscular y cierta alteración de la sensibilidad en la zona cercana a la cadera [3].

El tratamiento del PFA puede ser conservador o quirúrgico, dependiendo de las características individuales del paciente, como su edad, el estado funcional, la gravedad de los síntomas que refiere, y la integridad ósea y cartilaginosa de la articulación coxofemoral [3]. El tratamiento conservador mediante fisioterapia se orienta a mejorar la funcionalidad del paciente, mediante ejercicios de fortalecimiento, estiramientos miofasciales, terapia manual, y técnicas de estabilización del tronco, control motor y trabajo del core?, dirigidas a mejorar la biomecánica del complejo coxo-lumbo-pélvico [5]. Además, los analgésicos y antiinflamatorios son comúnmente utilizados para el alivio temporal del dolor [5]. Por otro lado, el tratamiento quirúrgico del PFA, se puede realizar mediante técnicas abiertas o mediante la artroscopia de cadera, que es una técnica menos invasiva, que permite una recuperación precoz. Ambas técnicas buscan corregir anomalías óseas y reparar el tejido cartilaginoso dañado [6].

A pesar de la gran prevalencia en la población general y el impacto significativo sobre la calidad de vida de los pacientes que presentan PFA, aún no existe un consenso sobre cuál es el tratamiento más efectivo en el control de los síntomas. Según el conocimiento de los autores, solo se han realizado 2 revisiones sistemáticas en este campo, las cuales incluyeron un número reducido de estudios (3 y 4 respectivamente) [7,8], lo que limita la capacidad de realizar conclusiones firmes, sobre la superioridad de uno u otro enfoque terapéutico. Esta escasez de investigaciones exhaustivas, subraya la necesidad de realizar nuevas revisiones sistemáticas que proporcionen una actualización rigurosa. Por tanto, el objetivo del presente estudio, fue revisar sistemáticamente la evidencia científica disponible, sobre la efectividad del tratamiento conservador de fisioterapia, en comparación con el tratamiento quirúrgico mediante artroscopia en pacientes con PFA, analizando aspectos como la calidad de vida y la funcionalidad de los pacientes.

MATERIAL Y MÉTODOS

Estrategia de búsqueda

La búsqueda bibliográfica se ha realizado en las bases de datos científicas PubMed (Medline), Biblioteca Cochrane y "*Physiotherapy Evidence Database*" (PEDro), entre octubre y diciembre de 2024. La búsqueda se ha llevado a cabo siguiendo las pautas metodológicas específicas "*Preferred Reporting Items for Systematic Review and Meta-Analyses*" (PRISMA) [9] y la correspondiente lista de verificación PRISMA. Se formuló la pregunta de investigación, empleando el modelo de preguntas PICOS [10] de la siguiente manera: P (población): pacientes ≥ 16 años diagnosticados con PFA. I (intervención): tratamiento conservador mediante fisioterapia. C (comparación): tratamiento quirúrgico mediante artroscopia. O (resultados): cuestionarios de funcionalidad y QoL (*Hip Outcome Score-Activity of Daily Life* [HOS-ADL], *International Hip Outcome Score* [iHOT-33], *Global Rating of Change* [GRC], *Short Form Health Survey* [SF-12], *Modified Harris Hip Score* [MHHS] o *Non-Arthritic Hip Score* [NASH]). S (diseño del estudio): ensayos clínicos aleatorizados.

La estrategia de búsqueda utilizó una combinación de "Medical Subject Headings" (MeSH) y palabras libres relevantes que incluían: "*femoroacetabular impingement*" *AND "hip arthroscopy" AND "physiothera-*

py" OR "conservative treatment". Todos los estudios se compararon para delimitar la búsqueda y evitar la repetición de artículos encontrados. Además, se examinó la bibliografía de los estudios incluidos y algunos de los excluidos, con el objetivo de encontrar manuscritos relevantes que pudieran pasar desapercibidos con la estrategia de búsqueda. La búsqueda sistemática fue realizada por dos autores, de manera independiente, y en caso de desacuerdos, un tercer revisor participó en el proceso.

Criterios de selección

Para la selección de estudios se establecieron los siguientes criterios de inclusión: (I) pacientes de 16 o más años de edad, diagnosticados de pinzamiento fémoroacetabular; (II) ensayos clínicos aleatorizados; (III) grupo intervención, tratado mediante fisioterapia, y grupo control, tratado mediante artroscopia; (IV) uso de herramientas de medición validadas y objetivas; (V) explicación detallada del tratamiento de fisioterapia realizado; (VI) explicación de resultados sobre la funcionalidad y calidad de vida del paciente; (VII) publicaciones en inglés o español; (VIII) estudios publicados en los 15 últimos años; (IX) puntuación de 6 o más en el "*Cuestionario Critical Appraisal Skills Programme Español*"? (CASPe) [11] y la escala PEDro [12].

Extracción y síntesis de datos

De cada ensayo incluido en la revisión sistemática, se extrajo la siguiente información: Apellido del primer autor, año de publicación, país de realización del estudio, diseño del estudio, tamaño muestral y características de los participantes (sexo, edad, estatura, peso, pérdida de peso corporal), intervención realizada, parámetros evaluados y resultados obtenidos. Dos investigadores realizaron la extracción de datos mediante una hoja de cálculo. En caso de desacuerdos, un tercer revisor se encargó de la resolución de dudas.

Evaluación de la calidad metodológica

Se evaluó la calidad metodológica de los artículos seleccionados mediante las escalas CASPe [11] y PEDro [12]. Por otro lado, se evaluó el riesgo de sesgo mediante la herramienta de Cochrane [13].

RESULTADOS

Selección de los estudios

La búsqueda bibliográfica resultó en un total de 35 estudios, 20 procedentes de PubMed, 2 de PEDro y 13 de Cochrane. Tras la eliminación de duplicados (n = 5), se analizaron el título y resumen de los 30 artículos restantes, eliminándose 9 estudios más. En una segunda fase, se evaluaron los 21 estudios a texto completo, descartando 15 estudios por no ser ensayos clínicos (n = 5), no realizar fisioterapia (n = 2) y no evaluar variables de interés (n = 8). A continuación, se revisaron las bibliografías de los artículos incluidos y de algunos de los excluidos, para buscar estudios adicionales relevantes, pero no se encontraron nuevos estudios de interés. Finalmente, se seleccionó un total de 6 artículos [14–19] (Fig. 1).

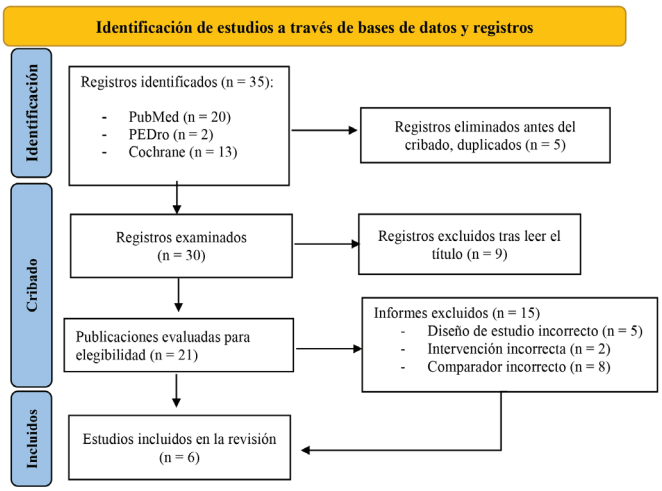

Fig. 1. Diagrama de flujo que ilustra el proceso de identificación y selección de los estudios incluidos en esta revisión, siguiendo las directrices establecidas por PRISMA [9].

Evaluación de la calidad metodológica

En la Tabla 1 se pueden observar las puntuaciones obtenidas en el cuestionario CASPe [11]. Todos los estudios incluidos en la revisión, obtuvieron una puntuación igual o superior a 6 [14–19]. Siendo Hunter y col. [15] el mejor puntuado, con 10 ítems cumplidos y Mansell y col. [17] el peor puntuado con 6 de los 11 ítems. Las principales deficiencias en cuanto a la calidad metodológica se encontraron en los ítems de cegamiento [14–19], aplicabilidad a la población local [16–19] y beneficios que justifican los riesgos y costes[14,16,17,19]. En cambio, la pregunta fue claramente definida, se realizó una asignación aleatoria, no existieron abandonos en el estudio, los grupos fueron similares al comienzo y se valoraron todos los resultados en la totalidad de los estudios seleccionados para la revisión [14–19].

Respecto a la puntuación obtenida a través de la escala PEDro [12] (Tabla 2), todos los artículos seleccionados obtuvieron una puntuación igual o superior a 7 [14–19], pudiendo determinar que la calidad de los artículos era "Buena". Las puntuaciones más altas (9 puntos) fueron obtenidas por Griffin y col. [14] y Mansell y col. [17]. Por el contrario, Martín y col. [18] obtuvieron la menor puntuación, cumpliendo únicamente con 7 de los ítems establecidos. Los ítems de cegamiento de los pacientes y los terapeutas, no fueron cumplidos por ninguno de los estudios, debido a su diseño.

Evaluación del riesgo de sesgo

En la Tabla 3 y Fig. 2, se muestra la evaluación del riesgo de sesgo, realizado mediante la herramienta de evaluación de sesgos de Cochrane [13]. Las puntuaciones obtenidas variaron entre 4 [18,19] y 7 [14,16]. El ítem con mayor riesgo de sesgo fue el número 3, sobre cegamiento del paciente, debido a la imposibilidad de cegar el tratamiento realizado al paciente.

Características de los pacientes y de la intervención

Las características de los participantes y de las intervenciones realizadas han sido detalladas en la Tabla 4. Los 6 estudios sumaron un tamaño muestral de 914 participantes iniciales, de los cuales 744 finalizaron la intervención, lo cual supone un porcentaje de abandono del 18,6%. Todos los participantes habían sido previamente diagnosticados de PFA. El 75% (n = 557) padecían PFA tipo

Tabla 1. Puntuación según el cuestionario CASPe[11] para la evaluación metodológica de los artículos incluidos en la revisión.

Primer autor y año de publicación	Ítems											Total
	1	2	3	4	5	6	7	8	9	10	11	
Griffin y col. [14], (2018)	Sí	Sí	Sí	No	Sí	Sí	Sí	Sí IC >95%	Sí	Sí	No	9
Hunter y col. [15], (2021)	Sí	Sí	Sí	No	Sí	Sí	Sí	Sí IC >95%	Sí	Sí	Sí	10
Klaus y col. [16], (2013)	Sí	Sí	Sí	No	Sí	Sí	Sí	Sí IC >95%	Parcial	Sí	No	8
Mansell y col. [17], (2018)	Sí	Sí	Sí	Parcial	Sí	No	No	Sí IC >95%	Parcial	Sí	No	6
Martin y col. [18], (2021)	Sí	Sí	Sí	No	Sí	Sí	Sí	Sí IC >95%	Parcial	Sí	Sí	9
Palmer y col. [19], (2019)	Sí	Sí	Sí	No	Sí	Sí	Sí	Sí IC >95%	Parcial	Sí	No	8

Abreviaturas = IC: Intervalo de confianza.

Ítems del cuestionario CASPe = 1: Pregunta claramente definida; 2: Asignación aleatoria; 3: Pacientes considerados hasta el final; 4: Cegamiento; 5: Grupos similares al comienzo; 6: Grupos tratados de igual modo; 7: Gran efecto del tratamiento; 8: Precisión del efecto; 9: Aplicabilidad a tu medio o población local; 10: En cuenta todos los resultados; 11: Beneficios justifican riesgos y costes.

Tabla 2. Puntuación según la escala PEDro[12] para la evaluación de la calidad metodológica de los estudios incluidos en la revisión.

Primer autor y año de publicación	ítems													
	1	2	3	4	5	6	7	8	9	10	11	Total	%	Calidad
Griffin y col. [14], (2018)	1	1	1	1	0	0	1	1	1	1	1	**9**	**81,8**	**B**
Hunter y col. [15], (2021)	1	1	0	1	0	0	1	1	1	1	1	**8**	**72,7**	**B**
Klaus y col. [16], (2013)	1	1	0	1	0	0	1	1	1	1	1	**8**	**72,7**	**B**
Mansell y col. [17], (2018)	1	1	1	1	0	0	1	1	1	1	1	**9**	**81,8**	**B**
Martin y col. [18], (2021)	1	1	0	1	0	0	0	1	1	1	1	**7**	**63,6**	**B**
Palmer y col. [19], (2019)	1	1	0	1	0	0	1	1	1	1	1	**8**	**72,7**	**B**

Abreviaturas = 0: criterio no cumplido; 1: criterio cumplido; E: Excelente; B: Bueno.

Ítems de la escala PEDro = 1: criterio de elegibilidad; 2: asignación aleatoria; 3: asignación oculta; 4: comparación inicial; 5: cegamiento de los participantes; 6: cegamiento del terapeuta; 7: cegamiento del evaluador; 8: seguimiento adecuado; 9: análisis por intención de tratar; 10: comparación entre grupos; 11: mediciones puntuales.

Tabla 3. Puntuación del sesgo de los estudios según la herramienta de Cochrane [13].

Primer autor, año de publicación y país	Ítems								T
	1	2	3	4	5	6	7	8	
Griffin y col. [14], (2018)	+	+	−	+	+	+	+	+	**7**
Hunter y col. [15], (2021)	+	−	−	+	+	+	−	+	**5**
Klaus y col. [16], (2013)	+	+	−	+	+	+	?	+	**7**
Mansell y col. [17], (2018)	+	+	−	+	+	+	+	−	**6**
Martin y col. [18], (2021)	+	−	−	−	+	+	+	−	**4**
Palmer y col. [19], (2019)	+	?	−	+	+	+	?	?	**4**

Abreviaturas = +: criterio cumplido; −: criterio no cumplido; ?: indeterminado; T: total.

Ítems de la escala Cochrane= 1: generación de secuencias aleatorias; 2: ocultamiento de la asignación; 3: cegamiento de los participantes; 4: cegamiento del evaluador; 5: seguimiento incompleto; 6: informe de datos; 7: sesgo de publicación; 8: sesgo del observador.

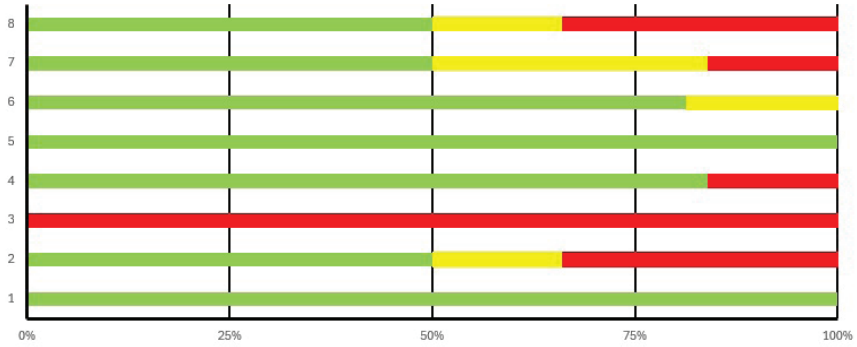

Fig. 2. Puntuación del sesgo de los estudios según la herramienta de Cochrane[13].

Cam, el 12% (n = 89) tipo Pincer y el 13% restante (n = 98), presentaba la morfología mixta. Los participantes comprendían edades entre 30 y 50 años, siendo los pacientes de mayor edad los del estudio de Martin y col. [18]. En cuanto al sexo de los participantes, en todos los ensayos la participación fue mixta [14,15,17–19] a excepción del ensayo de Klaus y col. [16], donde se incluyeron hombres exclusivamente (n = 10). A pesar de todo, la relación mujeres-hombres, fue equitativa, 48% los participantes de sexo femenino (n = 357) y el 52% restante de sexo masculino (n = 387). El índice de masa corporal (IMC) de los participantes fluctuó entre los 25 y 28 kg/m^2 en todos los estudios incluidos, salvo en los ensayos realizados por Griffin y col. [14] y Hunter y col. [15], quienes no detallaron el IMC de la muestra evaluada.

Los participantes de los estudios se dividieron en 2 grupos, el 54% (n = 401) recibió tratamiento conservador de fisioterapia (GF), y el 46% (n = 343) restante, fue tratado quirúrgicamente mediante artroscopia (GQx). El grupo GF recibió sesiones dirigidas al aumento del ROM, disminución del dolor, mejora del control motor y fortalecimiento de la musculatura de la cadera [14]. A su vez, se impartieron charlas de educación sobre el dolor y la patología a los pacientes[14,15]. La duración del tratamiento varió desde las 6 semanas en el ensayo de Klaus y col. [16] hasta las 24 semanas de supervisión del estudio de Martin y col. [18]. Por su parte, el GQx fue intervenido quirúrgicamente mediante artroscopia con resección ósea en todos los estudios seleccionados [14–19].

Evaluación de los resultados

En la Tabla 4 se muestran los resultados obtenidos tras las intervenciones realizadas.

Calidad de vida del paciente

Todos los estudios evaluaron los cambios relacionados con la calidad de vida de los participantes. Las escalas de valoración más repetidas fueron la iHOT-33 [20] y la HOS-ADL [21]. La primera fue utilizada en 4 de los ensayos seleccionados [14,15,17,18]. En los estudios de Griffin y col. [14], Hunter y col. [15] y Martin y col. [18], se observó una tendencia similar en los grupos. Similares hallazgos se obtuvieron mediante la escala HOS-ADL en 4 de los 5 estudios que la utilizaron [15,16,18,19]. Durante los primeros 6 meses de tratamiento se observaron mejoras significativas ($p<0,05$), en ambos grupos respecto al inicio del estudio. En cambio, en las evaluaciones realizadas a los 9 y 12 meses, los cambios respecto a los resultados obtenidos a los 6 meses fueron diferentes en cada grupo. En el grupo GF, las puntuaciones fueron similares a las obtenidas a los 6 meses, sin mostrar diferencias significativas ($p>0,05$). Sin embargo, el grupo GQx, presentó puntuaciones significativamente más altas ($p<0,05$), lo que indica

Tabla 4. Resumen de los estudios incluidos en la revisión sistemática.

Primer autor y año de publicación	Tipo de estudio	Participantes (tamaño y características de la muestra)	Intervención	Parámetros evaluados	Resultados (GF frente a GQx)
Griffin y col.[14], (2018)	Ensayo controlado aleatorizado	**Inicio**: 348 pacientes con PFA **Final**: 298 pacientes - GF (n = 154) - GQx (n = 144) *Edad*: 35,4 ± 9,6 años *Sexo*: 116 ♀, 182 ♂	**GF:** asesoramiento sobre el dolor, ROM y funcionalidad de la articulación, educación y programa de ejercicios individualizado (fortalecimiento, estabilidad y funcionalidad). Seguimiento de programa de ejercicios en casa por teléfono o email 6-10 veces a lo largo de 12-24 semanas. **GQx:** intervención quirúrgica con resección ósea.	Escala iHOT-33 Escala SF-12 Escala EQ-5D-5L	Escala iHOT-33 ↓* Escala SF-12 ↔ Escala EQ-5D-5L ↔
Hunter y col.[15], (2021)	Ensayo controlado aleatorizado	**Inicio**: 99 pacientes con PFA **Final**: 53 pacientes - GF (n = 26) - GQx (n = 27) *Edad*: 32,9 ± 10,5 años *Sexo*: 22 ♀, 31 ♂	**GF**: ejercicio individualizado y progresivo, educación sobre la patología y el alivio del dolor (12 semanas, 6-10 sesiones). **GQx**: intervención quirúrgica con resección ósea.	dGEMRIC Escala HOAMS Escala iHOT-33	dGEMRIC ↑ Escala HOAMS ↔ Escala iHOT-33 ↓*
Klaus y col.[16], (2013)	Ensayo controlado aleatorizado	**Inicio**: 28 pacientes con PFA **Final**: 10 pacientes - GF (n = 6) - GQx (n = 4) *Edad*: 39,6 ± 6,7 años *Sexo*: 10 ♂ *IMC*: 27,6 ± 4,4 kg/m²	**GF**: programa de fisioterapia durante 3 meses (46 sesiones en total) con ejercicio individualizado y progresivo **GQx**: intervención quirúrgica con resección ósea.	Escala HOS-ADL Escala LEFS Escala MHHS Escala NAHS Escala SF-12	Escala HOS-ADL ↓ Escala LEFS ↓ Escala MHHS ↓ Escala NAHS ↓ Escala SF-12 ↔
Mansell y col.[17], (2018)	Ensayo controlado aleatorizado	**Inicio**: 104 pacientes con PFA **Final**: 80 pacientes - GF (n = 66) - GQx (n = 14) *Edad*: 30,1 ± 7,4 años *Sexo*: 33 ♀, 47 ♂ *IMC*: 27,8 ± 4,3 kg/m²	**GF**: tratamiento individualizado (terapia manual, estiramientos, fortalecimiento, estabilidad, control motor y funcionalidad). 2 sesiones semanales durante 6 semanas. **GQx**: intervención quirúrgica con resección ósea. **28 participantes del grupo Fis finalmente fue operado*	Escala HOS-ADL Escala iHOT-33 Escala GRC **Evaluación a los 6, 12 y 24 meses.*	Escala HOS-ADL ↔ Escala iHOT-33 ↔ Escala GRC ↔
Martin y col.[18], (2021)	Ensayo controlado aleatorizado	**Inicio**: 90 pacientes con PFA **Final**: 81 pacientes - GF (n = 39) - GQx (n = 42) *Edad*: 49,4 ± 1,2 años *Sexo*: 39 ♀, 42 ♂ *IMC*: 26,8 ± 1,2 kg/m²	**GF**: disminución del dolor, mejora del ROM y programa de fortalecimiento (24 semanas de supervisión). **GQx**: intervención quirúrgica con resección ósea.	Escala iHOT-33 Escala MHHS	Escala iHOT-33 ↓* Escala MHHS ↓
Palmer y col.[19], (2019)	Ensayo controlado aleatorizado	**Inicio**: 245 pacientes con PFA **Final**: 222 pacientes - GF (n = 110) - GQx (n = 112) *Edad*: 36,2 ± 9,7 años *Sexo*: 147 ♀, 75 ♂ *IMC*: 26,2 ± 4,8 kg/m²	**GF**: programa de fisioterapia individualizado para mejorar el ROM y el control de la articulación (8 sesiones supervisadas durante 5 meses). **GQx**: intervención quirúrgica con resección ósea.	Escala HOS ADL	Escala HOS ADL ↓*

Abreviaturas = n: tamaño muestral; ♀: mujer; ♂: hombre; IMC: Índice de masa corporal; ↓: disminución no significativa (p > 0,05); ↑: aumento no significativo (p > 0,05); ↓*: disminución significativa (p < 0,05); ↔: sin cambios significativos; GF: Grupo fisioterapia: GQx: grupo artroscopia; PFA: impigment femoroacetabular; iHOT-33: International Hip Outcome Tool; SF-12: Short Form 12; EQ-5D-5L: EuroQol EQ-5D-5L; dGEMRIC: resonancia magnética del cartílago con galodinio retardado; HOAMS; Hip Osteoarthritis MRI Scoring System; HOS-ADL: Hip Outcome Score-Activites of Daily Life; LEFS: Lower Extremity Functional Scale; MHHS: Modified Harris Hip Score; NAHS: Nons Arthritic Hip Score; GRC: Global Rating of Charge

que a los 9 y 12 meses las puntuaciones del GQx fueron significativamente superiores a las del GF ($p<0,05$).

En la misma línea, se pudieron observar mejoras no significativas ($p>0,05$) en el GQx en la escala MHHS en los ensayos de Klaus y col. [16] y Martin y col. [18] o en la *Lower Extrimity Functional Scale* (LEFS) evaluada por Klaus y col. [16].

Por el contrario, las escalas SF-12, evaluadas, por Griffin y col. [14] y Klaus y col. [16] o la *EuroQol EQ-5D-5L* (EQ-5D-5L) realizada en el estudio de Griffin y col. [14], no denotaron diferencias significativas ($p<0,05$) entre ambos grupos de estudio.

Funcionalidad de la articulación

Tres de los estudios incluidos evaluaron la funcionalidad de la articulación coxofemoral [14–19]. Sin embargo, solo Klaus y col. [16] observaron diferencias entre los 2 grupos de tratamiento en la NAHS. El grupo GQx, al inicio obtuvo una puntuación de 46,7, a los 3 meses ascendió a los 82,3 y a los 6 meses alcanzó los 86,3 puntos. En cambio, el grupo GF, inició con una puntuación de 67,5 y ascendió a los 75,3 y 77,8 puntos a los 3 y 6 meses respectivamente, observándose una menor mejoría respecto al grupo GQx. Por el contrario, David y col. [15] emplearon el *Hip Osteoartritis MRI Scoring System* (HOAMS), sin encontrar diferencias entre los dos grupos. Mansell y col. [17], tampoco encontraron diferencias entre ambos grupos, medidos por la escala GRC.

Otras pruebas

Como otras pruebas para evaluar el efecto de ambos tratamientos en los pacientes, Hunter y col. [15], optaron por realizar una resonancia magnética del cartílago con galodinio retardado (dGEMRIC). En dicha prueba de imagen, se pudieron observar mejoras no significativas ($p>0,05$) a favor del grupo GF respecto al GQx.

DISCUSIÓN

El objetivo de esta revisión sistemática fue evaluar críticamente, la evidencia científica disponible, sobre la eficacia comparativa del GF frente GQx en la QoL y la funcionalidad de pacientes diagnosticados de PFA. Seis estudios [14–19] cumplieron los criterios de selección establecidos y fueron incluidos en la revisión. En líneas generales, se pudieron observar resultados superiores ($p<0,05$) en el GQx respecto al GF en la QoL valorada mediante escalas y cuestionarios como la iHOT-33 [14,15,18] o la HOS-ADL [16,19] y la funcionalidad por la escala NAHS [17]. Por el contrario, se observaron mejoras no significativas ($p>0,05$) en la prueba de imagen dGEMRIC en el GF respecto al GQx.

Calidad de vida del paciente

Todos los estudios incluidos en la presente revisión evaluaron la calidad de vida de los participantes tras las intervenciones por medio de las diversas escalas ya comentadas[14–19]. Se ha observado una tendencia generalizada a favor del GQx en cuanto a la calidad de vida de los participantes medido por las escalas iHOT-33 y HOS-ADL en comparación con el GF [14,15,18]. Griffin y col. [14] determinaron mejoras significativas ($p<0,05$) 12 meses después de la aleatorización en los pacientes del GQx respecto al GF, teniendo en cuenta el gran tamaño muestral del ensayo ($n = 298$; Fis = 154; Art = 144), son datos que parecen indicar la efectividad de dicho tratamiento. En la misma línea fueron los resultados de Martin y col. [18] o Hunter y col. [15], quienes observaron mejoras significativas ($p<0,05$) a favor del GQx a los 12 meses tras la intervención. En cambio, estos autores encontraron menores diferencias entre ambos grupos a los 6 meses de la intervención [14,15,18]. De esta forma, la artroscopia parece destacar su eficacia en la QoL de los pacientes a largo plazo.

La segunda herramienta que denotó beneficios a favor del GQx fue la HOS-ADL, significativos ($p<0,05$) en el estudio de Palmer y col. [19], y no significativos ($p>0,05$) en el ensayo de Klaus y col. [16], al compararlo con el GF. El tiempo desde la intervención hasta que se realizó la evaluación de la QoL fue de 8 meses para Palmer y col. [19]. En cambio, Klaus y col. [16] compararon ambos grupos de tratamiento a los 3 y 6 meses tras la intervención. Como en la escala iHOT-33, estos resultados indicarían resultados similares entre ambos tratamientos a medio plazo (3-6 meses), y mejoras significativas del GQx al evaluar la calidad de vida de los pacientes al superar el medio año tras la intervención (8-12 meses). Estas mejoras a largo plazo podrían deberse a una mejora en la biomecánica articular generada por la artroscopia que permita prolongar las mejoras [22].

En cuanto a la evaluación de la QoL relacionada con la salud (SF-12 o EQ-5D-5L) evaluadas por Griffin y col. [14] o Klaus y col. [16] no se obtuvieron diferencias entre ambos tratamientos. Esto podría deberse a la falta de sensibilidad de las herramientas seleccionadas o que el tratamiento del PFA no afecte a la QoL de los pacientes en relación con su nivel de salud general.

Funcionalidad de la articulación

En cuanto a la funcionalidad de la articulación coxofemoral, no se observaron diferencias significativas ($p<0,05$) entre los 2 grupos de tratamiento para ninguno de los 3 estudios que la evaluaron [15–17]. Klaus y col. [16] determinaron ligeras mejorías ($p>0,05$) a favor del GQx en la escala NAHS, en consonancia con las investigaciones realizadas por Stähelin y col. [23], quienes observaron mejoras significativas en el GQx evaluado a los 16 meses en cuanto a la reducción del dolor y los síntomas, así como mejora en el ROM de la articulación. En concordancia con nuestros resultados, Philippon y col. [24] obtuvieron similares resultados a los obtenidos en los 6 primeros meses tras el inicio de la intervención en escalas como la NAHS o HOS-ADL.

Pruebas de imagen

Hunter y col. [15] fue el único ensayo que realizó la prueba dGEMRIC, y aunque se observaron ligeras mejoras en el GF respecto al GQx, no fueron significativas ($p>0,05$) a los 12 meses de la intervención. Aunque las diferencias no fueron significativas, se observó una tendencia a favor del GF en cuanto a la estimulación del metabolismo del cartílago acetabular. Esta tendencia podría deberse a un doble motivo. En primer lugar, la intervención quirúrgica provocaría un proceso inflamatorio transitorio que podría afectar a medio plazo, al contenido bioquímico del cartílago [25]. Por otro lado, el tratamiento mediante fisioterapia, derivado del ejercicio físico, podría mejorar el contenido de glucosaminoglicanos en el cartílago acetabular [26].

Seguridad y efectos adversos

En cuanto a los efectos adversos derivados de la intervención, fueron superiores los del GQx. Las principales complicaciones derivadas de la artroscopia fueron infecciones ($n=5$), en los ensayos de Griffin y col. [14], Hunter y col. [15] y Klaus y col. [16]. Otras complicaciones notificadas fueron caídas, fracturas de cadera u osificación heterotópica. Por el contrario, en los GF no se notificaron efectos adversos graves derivados del tratamiento realizado. La tasa de complicaciones fue similar a la de la revisión de Nakano y col. [27], quienes tras evaluar 36.761 casos, reportaron que entorno al 3% de las cirugías, se generaban complicaciones y solo el 0,2% de las mismas, fue de carácter grave. Por último, Mansell y col. [17] reportaron una tasa de artrosis del 10,8% en los pacientes del GQx, respecto al 7,0% del GF. Por lo que, el tratamiento artroscópico, aunque no se encuentre exento de riesgos, parece posicionarse como un tratamiento seguro para los pacientes que lo realicen, tanto a corto, como a largo plazo.

Limitaciones y fortalezas

Entre los estudios incluidos se pueden observar diferencias en cuanto al diseño del estudio, y la variedad de protocolos de intervención

realizados en el GF, tanto por los procedimientos como por la cantidad de sesiones realizadas. Por otro lado, los tamaños muestrales han variado entre los diferentes estudios seleccionados, las características antropométricas y demográficas de las muestras no han sido detalladas en todos los ensayos, y las escalas de valoración han sido heterogéneas.

Tras valorar las limitaciones encontradas durante la revisión, se recomienda interpretar los resultados con precaución y se sugiere la necesidad de una mayor investigación sobre el protocolo fisioterapéutico óptimo para impulsar la rehabilitación de este tipo de pacientes frente al tratamiento artroscópico.

Cabe destacar que las limitaciones encontradas no fueron provocadas por la metodología seguida, ya que se siguieron las reglas PRISMA [9]. A su vez, se realizó la búsqueda en 3 bases de datos diferentes como PubMed (Medline), Biblioteca de Cochrane y PEDro. Se evaluó la calidad metodológica de los artículos seleccionados mediante el cuestionario CASPe [11] y la escala PEDro [12]. Por último, el riesgo de sesgo fue evaluado por la herramienta de Cochrane [13].

CONCLUSIONES

El manejo del PFA mediante tratamiento artroscópico, podría conseguir mayores beneficios a medio-largo plazo, en la QoL de los pacientes, en comparación con el tratamiento conservador basado en fisioterapia. No obstante, las diferencias entre ambos tratamientos son menos evidentes a corto plazo. No existe un consenso claro sobre cuál de los tratamientos es más efectivo en la funcionalidad articular. Estos resultados preliminares sugieren que el tratamiento quirúrgico podría ser una opción más adecuada, aunque es crucial considerar los riesgos asociados al abordaje artroscópico. Es necesario que futuros estudios validen estas conclusiones y proporcionen mayor evidencia sobre la efectividad de ambos tratamientos en la mejora de la función articular.

Agradecimiento

Los autores quieren agradecer al Grupo de Investigación Neurobiología de la Universidad de Valladolid, por su colaboración en la infraestructura informática y por su asesoramiento en el diseño metodológico e interpretación de los resultados.

Financiación

Esta investigación fue financiada por la Consejería de Educación de la Junta de Castilla y León y el Fondo Europeo de Desarrollo Regional (FEDER), mediante el Plan TCUE 2023-2027; (subvención nº 672 067/230003). Investigador Principal Prof. Dr. Diego Fernández-Lázaro.

Conflicto de interés

Los autores declaran no tener ningún conflicto de interés.

Responsabilidades éticas

Los autores declaran que para esta investigación no se han realizado experimentos en seres humanos ni en animales. Además, que en este artículo no aparecen datos de pacientes, y que no han utilizado ningún tipo de inteligencia artificial generativa en la redacción de este manuscrito, ni para la creación de figuras, gráficos, tablas o sus correspondientes leyendas.

Número ORCID de los autores

- Eva María Lantarón-Caeiro (EMLC): 0000-0002-5625-7628
- Álvaro López-Llorente (ALL): 0009-0006-6565-9270
- Gema Santamaría-Gómez (GSG): 0000-0002-6522-8896
- Diego Fernández-Lázaro (DFL): 0000-0002-6522-8896

Contribución de los autores

DFL: concibió y diseñó el estudio, analizó e interpretó los datos, redactó el documento, redactó el borrador original, preparó figuras y/o tablas y aprobó el borrador final versión enviada para publicación; EMLC, ALL y GSG: redactaron el documento, analizaron e interpretaron los datos y revisaron críticamente el artículo.

REFERENCIAS

1. **Ganz R, Parvizi J, Beck M, Leunig M, Nötzli H, Siebenrock KA**. Femoroacetabular impingement: A cause for osteoarthritis of the hip. Clin Orthop Relat Res. 2003; 417: 112–120. *https://doi.org/10.1097/01.blo.0000096804.78689.c2*
2. **Safran MR, Foard SJ, Robell K, Pullen WM**. Incidence of symptomatic femoroacetabular impingement: A 4-year study at a National Collegiate Athletic Association Division I Institution. Orthop J Sport Med. 2022; 10(4): 23259671221084979. *https://doi.org/10.1177/23259671221084979*
3. **Szpak J**. Review of femoroacetabular impingement. J Orthop Physician Assist. 2015; 3(1): 16–23. *https://doi.org/10.2106/JBJS.JOPA.15.00064*
4. **Clohisy JC, Knaus ER, Hunt DM, Lesher JM, Harris-Hayes M, Prather H**. Clinical presentation of patients with symptomatic anterior hip impingement. Clin Orthop Relat Res. 2009; 467(3): 638–644. *https://doi.org/10.1007/s11999-008-0680-y*
5. **Terrell SL, Olson GE, Lynch J**. Therapeutic exercise approaches to nonoperative and postoperative management of femoroacetabular impingement syndrome. J Athl Train. 2021; 56(1): 31–45. *https://doi.org/10.4085/1062-6050-0488.19*
6. **Qiao HY, Zhang YH, Ren YM, Tian MQ**. Arthroscopic versus open treatment for femoroacetabular impingement: A systematic review and meta-analyses. Medicine (Baltimore). 2020; 99(47): e23364. *https://doi.org/10.1097/MD.0000000000023364*
7. **Casartelli NC, Valenzuela PL, Maffiuletti NA, Leunig M**. Effectiveness of hip arthroscopy on treatment of femoroacetabular impingement syndrome: A meta-analysis of randomized controlled trials. Arthritis Care Res (Hoboken). 2021; 73(8): 1140–1145. *https://doi.org/10.1002/acr.24234*
8. **Anzillotti G, Iacomella A, Grancagnolo M, Bertolino EM, Marcacci M, Sconza C, et al**. Conservative vs surgical management for femoro-acetabular impingement: A systematic review of clinical evidence. J Clin Med. 2022; 11(19): 5852. *https://doi.org/ 10.3390/jcm11195852*
9. **Page MJ, McKenzie JE, Bossuyt PM, Boutron I, Hoffmann TC, Mulrow CD, et al**. The PRISMA 2020 statement: An updated guideline for reporting systematic reviews. BMJ. 2021; 372: n71. *https://doi.org/101136/bmj.n71*
10. **da Costa Santos CM, de Mattos Pimenta CA, Nobre MRC.** The PICO strategy for the research question construction and evidence search. Rev Lat Am Enfermagem. 2007; 15(3): 508–511. *https://doi.org/10.1590/S0104-11692007000300023*
11. **Long HA, French DP, Brooks JM**. Optimising the value of the critical appraisal skills programme (CASP) tool for quality appraisal in qualitative evidence synthesis. Res Methods Med Health Sci. 2020; 1(1): 31–42. *https://doi.org/10.1177/2632084320947559*
12. **Moseley AM, Elkins MR, Van der Wees PJ, Pinheiro MB**. Using research to guide practice: The Physiotherapy Evidence Database (PEDro). Brazilian J Phys Ther. 2020; 24(5): 384–391. *https://doi.org/10.1016/j.bjpt.2019.11.002*
13. **Higgins JPT, Altman DG, Gøtzsche PC, Jüni P, Moher D, Oxman AD, et al**. The Cochrane Collaboration's tool for assessing risk of bias in randomised trials. BMJ. 2011; 343: d5928. *https://doi.org/10.1136/bmj.d5928*
14. **Griffin DR, Dickenson EJ, Wall PDH, Achana F, Donovan JL, Griffin J, et al**. Hip arthroscopy versus best conservative care for the treatment of femoroacetabular impingement syndrome (UK FASHIoN): a multicentre randomised controlled trial. Lancet 2018; 391(10136): 2225–2235.

https://doi.org/10.1016/S0140-6736(18)31202-9

15. **Hunter DJ, Eyles J, Murphy NJ, Spiers L, Burns A, Davidson E, et al**. Multi-centre randomised controlled trial comparing arthroscopic hip surgery to physiotherapist-led care for femoroacetabular impingement (FAI) syndrome on hip cartilage metabolism: the Australian FASHIoN trial. BMC Musculoskelet Disord. 2021; 22(1): 697. *https://doi.org/10.1186/s12891-021-04576-z*
16. **Klaus HC**. A randomized controlled trial comparing arthroscopic surgery a randomized controlled trial comparing arthroscopic surgery to conservative management of femoroacetabular impingement. 2013. Western University Open Repository. *https://doi.org/10.71858/123456.*
17. **Mansell NS, Rhon DI, Meyer J, Slevin JM, Marchant BG**. Arthroscopic surgery or physical therapy for patients with femoroacetabular impingement syndrome: A randomized controlled trial with 2-year follow-up. Am J Sports Med. 2018; 46(6): 1306–1314. *https://doi.org/10.1177/0363546517751912*
18. **Martin SD, Abraham PF, Varady NH, Nazal MR, Conaway W, Quinlan NJ, et al.** Hip arthroscopy versus physical therapy for the treatment of symptomatic acetabular labral tears in patients older than 40 years: A randomized controlled trial. Am J Sports Med. 2021; 49(5): 1199–1208. *https://doi.org/10.1177/0363546521990789*
19. **Palmer AJR, Ayyar Gupta V, Fernquest S, Rombach I, Dutton SJ, Mansour R, et al**. Arthroscopic hip surgery compared with physiotherapy and activity modification for the treatment of symptomatic femoroacetabular impingement: Multicentre randomised controlled trial. BMJ. 2019; 364: l185. *https://doi.org/10.1136/bmj.l185.*
20. **Ruiz-Ibán MA, Seijas R, Sallent A, Ares O, Marín-Peña O, Muriel A, et al**. The international Hip Outcome Tool-33 (iHOT-33): Multicenter validation and translation to Spanish. Health Qual Life Outcomes. 2015; 13: 62. *https://doi.org/10.1186/s12955-015-0255-z*
21. **Martin RRL, Philippon MJ**. Evidence of reliability and responsiveness for the hip outcome score. Arthroscopy. 2008; 24(6): 676-682. *https://doi.org/10.1016/j.arthro.2007.12.011*
22. **Samaan MA, Grace T, Zhang AL, Majumdar S, Souza RB**. Short term outcomes of hip arthroscopy on hip joint mechanics and cartilage health in patients with femoroacetabular impingement syndrome. Clin Biomech (Bristol). 2020; 71: 214-220. *https://doi.org/10.1016/j.clinbiomech.2019.11.014.*
23. **Stähelin L, Stähelin T, Jolles BM, Herzog RF**. Arthroscopic offset restoration in femoroacetabular cam impingement: Accuracy and early clinical outcome. Arthroscopy. 2008; 24(1): 51-57.e1. *https://doi.org/10.1016/j.arthro.2007.08.010*
24. **Philippon MJ, Briggs KK, Yen YM, Kuppersmith DA**. Outcomes following hip arthroscopy for femoroacetabular impingement with associated chondrolabral dysfunction: Minimum two-year follow-up. J Bone Joint Surg Br. 2009; 91(1): 16–23. *https://doi.org/10.1302/0301-620X.91B1.21329*
25. **Schmaranzer F, Haefeli PC, Hanke MS, Liechti EF, Werlen SF, Siebenrock KA, et al**. How does the dGEMRIC index change after surgical treatment for FAI? A prospective controlled study: Preliminary results. Clin Orthop Relat Res. 2017; 475(4): 1080–1099. *https://doi.org/10.1007/s11999-016-5098-3*
26. **Roos EM, Dahlberg L**. Positive effects of moderate exercise on glycosaminoglycan content in knee cartilage: A four-month, randomized, controlled trial in patients at risk of osteoarthritis. Arthritis Rheum. 2005; 52(11): 3507–3514. *https://doi.org/10.1002/art.21415*
27. **Nakano N, Lisenda L, Jones TL, Loveday DT, Khanduja V.** Complications following arthroscopic surgery of the hip: A systematic review of 36 761 cases. Bone Joint J. 2017; 99-B (12): 1577–1583. *https://doi.org/10.1302/0301-620X.99B12.BJJ-2017-0043.R2.*

Invest Clin 66(4): 467- 478, 2025 https://doi.org/10.54817/IC.v66n4a09

The ongoing panzootic of avian Influenza A (H5N1) and its potential pandemic threat.

Flor Helene Pujol[1] and José Esparza[2]

[1]Laboratorio de Virología Molecular, CMBC, Instituto Venezolano de Investigaciones Científicas (IVIC), Caracas, Venezuela.
[2]Institute of Human Virology, University of Maryland School of Medicine, Baltimore, MD, USA.

Keywords: Avian Influenza; Pandemics; Panzootic; Influenza A Virus, H5N1 Subtype.

Abstract. The influenza virus is one of the most significant pathogens responsible for respiratory infections and is the human pathogen most frequently associated with epidemics and pandemics. The epidemiological record of influenza suggests that future pandemics caused by this virus are inevitable, even though their timing, origin, and severity remain uncertain. This review focuses on the ongoing panzootic of avian influenza A (H5N1), which is currently spreading across much of the globe. The ongoing panzootic of Influenza A (H5N1) clade 2.3.4.4b has spread rapidly worldwide and is causing concern. The virus has already crossed species barriers, infecting multiple mammalian hosts and causing human cases with varying degrees of severity. While sustained human-to-human transmission has not yet occurred, an increasing frequency of spillover events and the emergence of genotypes with mutations associated with mammalian adaptation are of concern. We assess the potential for this panzootic to evolve into a pandemic and examine the critical measures needed for preparedness and prevention, following a One Health approach.

Corresponding author: Flor H. Pujol. Laboratorio de Virología Molecular, CMBC, IVIC, Caracas, Venezuela. Email: fhpujol@gmail.com

La panzootia actual de influenza aviar A (H5N1) y su potencial amenaza pandémica.

Invest Clin 2025; 66 (4): 467 – 478

Palabras clave: Influenza Aviar; Pandemias; Panzootia; Epizootia; Subtipo H5N1 del Virus de la Influenza A.

Resumen. El virus de la influenza es uno de los patógenos más importantes, causante de infecciones respiratorias, y el agente humano más frecuentemente asociado con epidemias y pandemias. El registro epidemiológico de la influenza sugiere que las futuras pandemias causadas por este virus son inevitables, aunque su momento, origen y gravedad siguen siendo inciertos. Esta revisión se centra en la panzootia actual de la influenza aviar A (H5N1), que actualmente se propaga por gran parte del mundo. La panzootia actual del virus de la influenza A (H5N1), del clado 2.3.4.4b, se ha extendido de manera dramática a nivel mundial y está generando gran preocupación. El virus ya ha cruzado las barreras entre especies, provocando infecciones en múltiples hospedadores mamíferos y causando casos humanos con distintos grados de gravedad. Aunque aún no se ha producido una transmisión sostenida de persona a persona, preocupa la creciente frecuencia de eventos de salto interespecie y la aparición de genotipos con mutaciones asociadas a la adaptación en mamíferos. En esta revisión, evaluamos el potencial de esta panzootia para evolucionar hacia una pandemia y examinamos las medidas críticas necesarias para la preparación y la prevención, siguiendo un enfoque de *Una Sola Salud*.

Received: 07-10-2025 Accepted: 17-11-2025

INTRODUCTION

The influenza virus is one of the most significant pathogens responsible for respiratory infections, distinguished not only by the severity of the illnesses it causes but also by its role in numerous historical epidemics and pandemics [1,2].

While aquatic birds are the natural reservoirs of Influenza A viruses (IAV), these viruses can also infect a broad range of mammalian species, including humans. The epidemiological record of influenza suggests that future pandemics caused by this virus are inevitable, even though their timing, origin, and severity remain uncertain. This review focuses on the ongoing panzootic of avian influenza A (H5N1), which is currently spreading across much of the globe. The virus has already crossed species barriers, leading to infections in multiple mammalian hosts and causing human cases with varying degrees of severity [3]. We assess the potential for this panzootic to evolve into a pandemic and examine the critical measures needed for preparedness and prevention.

Avian Influenza

Influenza viruses belong to the family *Orthomyxoviridae* and are enveloped viruses with a segmented, negative-sense RNA genome. Four genera of influenza viruses have been identified: Influenza A, B, C, and D. Influenza A and B viruses possess eight RNA

segments, whereas Influenza C and D viruses typically contain seven segments, although they frequently package eight [4,5]. Influenza A viruses (IAVs) exhibit a broad host range, infecting birds, humans, and various other mammals. In contrast, Influenza B and C viruses primarily infect humans, while Influenza D virus is predominantly found in bovine hosts [4,6]. In humans, influenza disease is caused mainly by viruses from the A and B genera, with IAVs being of particular concern due to their pandemic potential. These genera are distinguished by the antigenic properties of their internal virion proteins, while IAVs are further differentiated into subtypes by the antigenic properties of their two external proteins [4,6].

The segmented nature of the influenza virus genome facilitates frequent reassortment events. This process occurs when a host is co-infected with two different influenza viruses; during replication, genome segments from both viruses can be packaged together into progeny virions [4,7]. Pigs, which are susceptible to multiple influenza virus subtypes, have traditionally been considered key hosts for reassortment and are often referred to as "mixing vessels" [7]. IAVs display substantial antigenic diversity in their two principal surface glycoproteins: hemagglutinin (H) and neuraminidase (N). This variability allows for a binary classification of IAVs into serotypes, comprising 19 H subtypes and 11 N subtypes, with more than 130 distinct subtype combinations identified to date [8,9]. The primary reservoir of this genetic and antigenic diversity is avian IAVs, which have been the source of multiple influenza pandemics—often through reassortment events between avian and human influenza viruses [7].

Human influenza viruses bind preferentially to α-2,6-linked sialic acid receptors on the surface of epithelial cells, whereas avian influenza viruses have a higher affinity for α-2,3-linked sialic acids. These glycosidic linkages play a critical role in host specificity and cross-species transmission of influenza viruses. Consequently, both the variant and structural configuration of sialic acid receptors influence viral binding affinity to the H glycoprotein of influenza viruses [10].

Avian influenza A viruses (AIAVs) can evolve from low pathogenicity (LPAIV) to highly pathogenic forms (HPAIV), a classification based on their virulence in chickens. A defining molecular feature of HPAIV is the presence of a furin cleavage site in the H protein [3]. Proteolytic cleavage of H into HA1 and HA2 subunits is a crucial step in viral replication, triggering a pH-dependent conformational change that exposes the fusion peptide, enabling fusion with endosomal membranes and subsequent release of the viral genome into the host cytoplasm. HPAIVs contain a polybasic cleavage site that allows processing by furin-like proteases, which are expressed in multiple tissues, thereby facilitating systemic viral dissemination [11].

Notably, HPAIVs have emerged multiple times independently from ancestral LPAIVs, but only among viruses of the H5 and H7 subtypes [12]. Since the first emergence of HPAI H5N1 in 1996, nearly 1,000 human infections have been reported across 24 countries, with a case fatality rate of around 50%[13,14].

The influenza pandemics of the past

Over the past three centuries, ten major influenza pandemics have been documented, averaging approximately three per century (Fig. 1). These events have varied widely in intensity, morbidity, and mortality [1].

In the 18th century, three pandemics were recorded. The first, in 1729–1730, had a global reach, with high morbidity but relatively low mortality—a pattern that was repeated in the subsequent 1732–1733 outbreak. The 1781–1782 pandemic was particularly extensive, reportedly infecting 70–80% of the population, though it also exhibited low mortality [1].

The 19th century witnessed two notable pandemics in 1830–1831 and 1833, which differed in severity, with the latter associ-

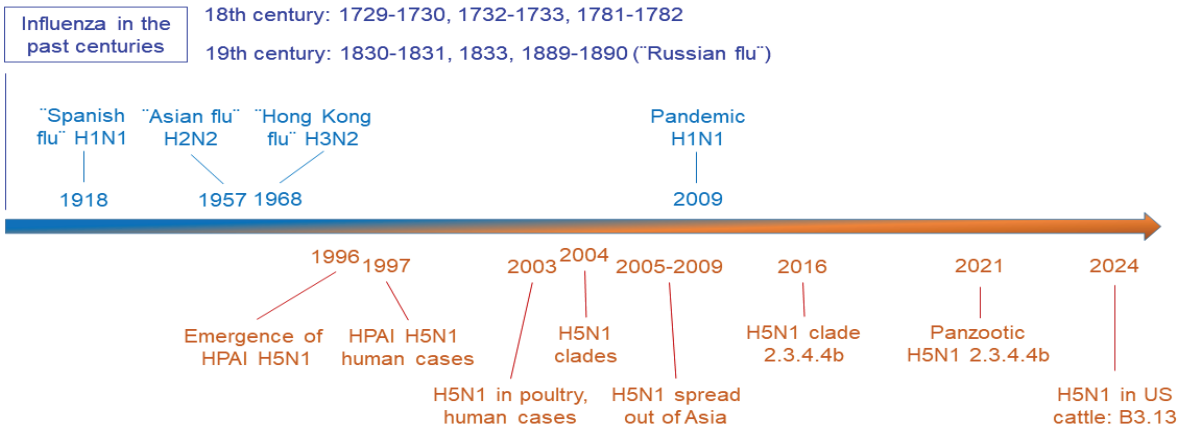

Fig. 1. Major events in human and avian Influenza. The timeline shows the known Influenza pandemics in the past centuries (in blue) and major events in avian influenza over the last two centuries (in orange). The subtype of IAV responsible for the pandemic of the previous two centuries are shown [1,12,18,23,30].

ated with higher mortality. The 1889–1890 pandemic, commonly known as the "Russian flu," was particularly significant because it coincided with the emergence of the germ theory of disease. This conceptual shift—from miasmatic to microbial causation—marked a turning point in public health, paving the way for modern preventive strategies such as improved hygiene and social distancing [1].

The 20th and 21st centuries saw four influenza pandemics, all caused by IAVs. The deadliest of these was the 1918-1919 "Spanish flu," caused by an H1N1 virus. It infected an estimated 500 million people—about 30% of the global population—and resulted in 50 to 100 million deaths over three devastating waves. The impact was magnified by the worldwide disruption and troop movements associated with World War I. Later pandemics included the 1957 "Asian flu" (H2N2) and the 1968 "Hong Kong flu" (H3N2), which were less severe but still responsible for an estimated 1–3 million and 1–4 million deaths, respectively, despite widespread transmission [1].

The only influenza pandemic of the 21st century to date occurred in 2009, caused by a novel H1N1 virus that originated in North America. Although initially feared to rival the severity of the 1918 pandemic, it ultimately proved relatively mild, with an estimated 125,000 to 400,000 deaths worldwide [1].

The panzootic H5N1 clade 2.3.4.4b

In addition to classification by subtype, IAV genome sequences are further categorized based on phylogenetic relationships, including common ancestry and descendant lineages. These classifications include clades (e.g., 1.1, 2.2, 2.3), subclades (e.g., 2.3.2.1c, 2.3.3.4b), lineages (such as Eurasian and American), and genotypes (e.g., A1, B1, B3.13) [3,15,16]. Clades and subclades are defined primarily through phylogenetic analysis of the hemagglutinin (H) gene, reflecting evolutionary divergence. In contrast, genotypes are determined by the constellation of gene segments present in each strain, offering insight into reassortment events and genomic composition [16].

The subclade 2.3.4.4b emerged in 2016 (Fig. 1) in an H5N8 virus in China and subsequently spread across Asia and into Europe. This virus caused an unexpected epidemic peak in 2020/2021 [17]. The 2.3.4.4b H5N8 rearranged with a LPAI H5N1 around 2020, leading to the 2.3.4.4b H5N1. This vi-

rus caused the wave of 2021/2022, the current panzootic, with several human cases, and was the most devastating avian influenza epidemic [17,18]. After this subclade was introduced into North America, several reassortment events with circulating LPAIVs led to the emergence of new genotypes. At least three genotypes have circulated among infected marine birds in South America since 2022, and these genotypes have also shown infectivity and virulence toward marine mammals [19,20].

Both avian- and human-type receptors are present in swine respiratory epithelia. Swine are generally the intermediate hosts involved in the reassortment and adaptation of AIAVs to mammals before spillover to humans. However, new evolutionary pathways may be considered for the emergence of a pandemic, given the frequent infection of many mammalian species (both marine and terrestrial), particularly cattle in the USA[20,21].

Cattle are typically infected with the Influenza D virus but not with IAVs. However, during the current panzootic, the first documented spillover of Influenza A into cows involved an H5N1 virus of genotype B3.13—originally circulating in wild animals (Fig. 1). This genotype is a reassortant between B3.6 and an LPAIV endemic in the United States. Phylogenetic evidence suggests that a single spillover event was responsible for the emergence of this panzootic clade in cattle [22]. In cattle, the primary site of AIAV replication appears to be the udder, as mammary tissue expresses avian-type α-2,3-linked sialic acid receptors. This raises the possibility of virus transmission through unpasteurized milk. The initial spillover event is believed to have occurred in Texas, USA, with subsequent spread to cattle in other states likely facilitated by contaminated milking equipment [18]. Since February 2024, at least two additional spillover events involving a different genotype, D1.1, have been reported in U.S. cattle [23,24]. Alarmingly, the first fatal human case associated with this panzootic in the United States was linked to infection with this genotype [23].

Most human cases of H5N1 infection during the current panzootic have been mild so far. However, this apparent low pathogenicity may be partly attributed to host-related factors, including the young age of many patients and the presence of pre-existing immunity to N1 and other conserved cellular immunity epitopes [25,26]. In contrast, experimental infection of ferrets with the H5N1 genotype B3.13—currently circulating in U.S. cattle—resulted in high lethality [27]. Another study reported reduced mortality in mice infected with a clade 2.3.4.4b H5N1 virus, despite the strain exhibiting high pathogenicity in chickens [28]. Notably, differences in pathogenicity among genotypes within the panzootic clade have also been observed in both teals and poultry [29].

These findings underscore the potential for this lineage's pathogenicity to evolve further through reassortment and mutation. Comprehensive studies are urgently needed to assess the virulence and transmissibility of these viruses in humans. Regardless of the current severity, it is imperative to implement preparedness and response plans now to mitigate the risk of a future influenza pandemic.

Pandemic risk?

The current panzootic caused by Influenza A-H5N1 has been marked by frequent spillover events into a wide range of terrestrial and marine mammalian species, with around 50 species affected to date [3,30,31]. The United States currently reports the highest number of human cases associated with this outbreak, with 70 confirmed infections between 2024 and the end of April 2025 [13]. However, this number remains below the highest annual record of human H5N1 cases, which occurred in 2015, when 145 cases were reported globally, 136 of them in Egypt alone [13].

A prerequisite for the development of a pandemic is that the panzootic influenza

virus acquires the ability not only to infect humans, but also to sustain efficient human-to-human transmission—something that has not occurred to date. Efficient human-to-human transmission of avian influenza viruses likely requires the cumulative acquisition of several key mutations (Fig. 2) [30-33].

H mutations enhancing affinity for human receptors: Adaptation to the human α-2,6-linked sialic acid receptor is critical. Notably, only four mutations were sufficient to render an Influenza A-H5N1 virus transmissible, via respiratory droplets, in ferrets[34]. More recently, a single mutation, Q226L, in the H of bovine H5N1 (genotype B3.13) was shown to switch viral specificity toward mammalian receptors [35]. Three additional mutations have been identified as key contributors to increased human receptor affinity [32].

PB2 mutations enabling polymerase adaptation to mammalian ANP32 proteins: ANP32A and ANP32B, which serve as host cofactors for the viral polymerase, differ between avian and mammalian species. Several mutations have been characterized that allow avian influenza polymerases to utilize mammalian ANP32 proteins [36] efficiently. Some of these mutations have already been detected at low frequency in viruses infecting cattle [22].

Increased viral stability at low pH: Avian influenza viruses generally exhibit reduced stability in acidic environments such as the human upper respiratory tract, posing a barrier to transmission [33].

Host immune history: Pre-existing immunity to seasonal human influenza viruses, whether from prior infection or vaccination, may influence susceptibility and clinical outcomes following exposure to H5N1 viruses [37].

The eventual emergence of a pandemic influenza virus can result not only from the gradual accumulation of key mutations but also, frequently, from reassortment events[20,21]. Traditional "mixing vessels" for such reassortment have been pigs; however, emerging evidence highlights other hosts with high reassortment potential, including humans, minks, ferrets, seals, dogs, cats, and various bird species—particularly turkeys, chickens, quails, and ducks [20,21]. Interestingly, current data suggest that pigs may be less susceptible to the current panzootic IAV than some other mammals [38,39].

Although several key mutations associated with mammalian adaptation have been detected in viruses isolated from infected mammals during this panzootic [21], none of the sequenced viral isolates to date possess the whole constellation of mutations required for efficient human-to-human trans-

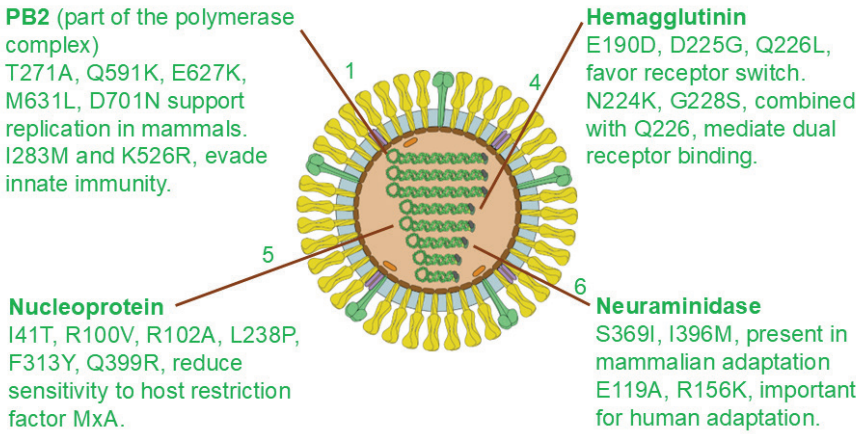

Fig. 2. Major mutations in four of the AIAV associated with efficient mammalian transmission and replication. Mutations in four viral proteins, potentially related to human adaptation, are shown [22,30,32-36].

mission. Nevertheless, the extensive geographic spread of the panzootic clade and its ability to infect a broad range of mammalian hosts raise significant concerns about the potential emergence of a pandemic strain [40].

Preparedness

According to the World Health Organization [41], influenza virus activity is classified into six distinct phases, progressing from circulation limited to animals to widespread human transmission at the global level (Table 1). This framework is divided into two overarching stages: Phases 1–3, which focus on preparedness, and Phases 4–6, which emphasize response and mitigation.

In Phase 1, no influenza viruses circulating among animals have been reported to cause infections in humans. Phase 2 is characterized by an animal influenza virus - circulating among domesticated or wild animals - that has caused human illness and is therefore considered a potential pandemic threat. Phase 3 occurs when an animal or human-animal reassortant influenza virus causes sporadic cases or small clusters of disease in people but does not lead to sustained human-to-human transmission or community-level outbreaks. In Phase 4, human-to-human transmission results in localized community outbreaks, indicating a significant increase in pandemic risk. Phase 5 is marked by community-level outbreaks in at least two countries within one WHO region. In contrast, Phase 6 -defined by community outbreaks in multiple WHO regions - signifies the onset of a global pandemic [41].

Although the global spread of the A (H5N1) panzootic remains a serious concern, no sustained human-to-human transmission has been reported as of May 2025. Consequently, the human influenza epidemic remains classified as Phase 3, highlighting the urgent need to bolster preparedness efforts and prevent escalation to a pandemic. To mitigate this risk, countries must develop and implement coordinated response strategies at both national and international levels, emphasizing proactive preventive measures. Since 2021, the World Health Organization (WHO) has been working with Member States to draft a global treaty on pandemic prevention, preparedness, and response. This treaty was formally adopted by consensus at the 78th World Health Assembly in May 2025. It establishes guidelines for the timely sharing of epidemiological data, genomic analysis of emerging pathogens, and critical information related to potential vaccines and treatments [42].

Table 1. World Health Organization pandemic phases descriptions.

Phase	Description	Estimated probability of pandemia
1	No animal influenza virus reported as causing human cases	Uncertain
2	An animal influenza virus has caused infection in humans	Uncertain
3	An animal or human-animal reassortant virus has caused a small number of human cases but has not resulted in significant human-to-human transmission	Uncertain
4	Human-to-human transmission able to sustain community-level outbreaks	Medium to high
5	Community-level outbreaks in at least two countries in one WHO region	High to certain
6	Community-level outbreaks in an additional WHO region	Pandemic in progress

Adapted from World Health Organization [41].

National preparedness plans should incorporate robust communication strategies to promote public adherence to non-pharmaceutical interventions (NPIs). For influenza, these include individual-level protective behaviors such as staying home when symptomatic, covering coughs and sneezes, and practicing frequent hand hygiene. At the community level, recommended measures may include temporary school closures, suspending childcare services, and canceling mass gatherings during periods of heightened transmission. When a novel pandemic influenza virus emerges, the combined implementation of NPIs and antiviral therapies can significantly reduce transmission rates, particularly in the early stages before a vaccine becomes widely available [41-44].

Pandemic preparedness for influenza depends heavily on early detection of novel strains, particularly those that originate in animal reservoirs through spillover events. Over the past two decades, repeated zoonotic influenza outbreaks have underscored the vital importance of sustained surveillance in both human and animal populations, especially among birds and swine. As noted earlier in this paper, the most pressing current threat is the ongoing panzootic of avian influenza A (H5N1). However, other avian influenza subtypes continue to circulate in more localized contexts. Genetic reassortment during coinfections plays a critical role in the emergence of pandemic-capable strains. While the surface glycoproteins H and N are traditionally viewed as central to influenza infectivity and host specificity, increasing evidence indicates that internal viral genes -particularly those encoding the polymerase complex- also significantly contribute to virulence and disease severity [44]. Since 1952, the World Health Organization has led a global initiative to monitor circulating influenza viruses, enabling a coordinated international response to emerging influenza threats [45].

Given that a future pandemic influenza virus is likely to emerge from an avian influenza strain affecting poultry, control strategies must integrate biosecurity measures, epidemiological surveillance, targeted culling, and vaccination with strain-specific immunogens [46-48]. Culling should be prioritized in outbreaks involving HPAI strains, mainly when rapid transmission occurs within poultry populations. Protective measures for farm workers are also essential to minimize the risk of zoonotic transmission. A similar level of urgency applies to controlling H5N1 infections in other livestock species, such as cattle [49].

During the preparedness phase, early interventions should focus on securing vaccine and antiviral stockpiles [48-51] and on expanding the healthcare system capacity to ensure effective clinical management during a pandemic. Notably, at least three experimental vaccines targeting early H5N1 influenza virus strains have demonstrated the ability to elicit cross-reactive binding and cross-neutralizing antibodies against the HPAI clade 2.3.4.4b in humans, suggesting they could serve as interim protective tools while updated vaccines are developed[52]. Furthermore, a novel H5-based mRNA vaccine has recently been shown to generate a robust adaptive immune response in cattle[53]. Nevert heless, the final formulation of a pandemic influenza vaccine must be tailored to the specific viral strain in circulation at the time of emergence to ensure optimal efficacy.

CONCLUSIONS

The unprecedented epidemiology of the panzootic AIAV (H5N1) clade 2.3.4.4b has already resulted in devastating impacts on poultry and wild mammal populations. It now poses an emerging threat to livestock, further complicating the pre-pandemic landscape. Although several human infections have been reported, the mortality rate to date has been lower than in previous outbreaks. While it remains impossible to predict with certainty when or how a new influ-

enza pandemic might emerge, the current spread of AIAV (H5N1) is deeply concerning and demands urgent preparedness efforts. A coordinated One Health approach—integrating human, animal, environmental health, and, evidently, vaccines—is essential to address this evolving threat effectively. This requires strong collaboration among animal, environmental, and public health sectors to assess risks, strengthen early prevention, coordinate outbreak responses, and develop effective countermeasures. To reduce future pandemic risks, urgent action is needed, not only to protect people at the highest risk of zoonotic infection (such as farm workers) but also to prevent transmission among wild and domestic animals and humans. Efforts should target the underlying factors that enable such outbreaks and ensure rapid risk assessment and response to every zoonotic event [54].

ORCID number of authors

- Flor H. Pujol (FHP): 0000-0001-6086-6883
- José Esparza (JE): 0000-0002-2305-6264

Conflict of interest

The authors declare no conflict of interest.

REFERENCES

1. **Esparza J**. Lessons from history: What can we learn from 300 years of pandemic flu that could inform the response to COVID-19? Am J Public Health. 2020; 110: 1160-1. *https://doi.org/10.2105/AJPH.2020.305761.*
2. **Taubenberger JK, Kash JC**. Influenza virus evolution, host adaptation, and pandemic formation. Cell Host Microbe. 2010; 7: 440-51. *https://doi.org/10.1016/j.chom.2010.05.009.*
3. **Butt SL, Nooruzzaman M, Covaleda LM, Diel DG**. Hot topic: Influenza A H5N1 virus exhibits a broad host range, including dairy cows. JDS Commun 2024; 5: S13-S19. *https://doi.org/10.3168/jdsc.2024-0638.*
4. **Krammer F, Smith GJD, Fouchier RAM, Peiris M, Kedzierska K, Doherty PC, et al**. Influenza. Nat Rev Dis Primers 2018; 4: 3. *https://doi.org/10.1038/s41572-018-0002-y.*
5. **Nakatsu S, Murakami S, Shindo K, Horimoto T, Sagara H, Noda T, Kawaoka Y**. Influenza C and D Viruses Package Eight Organized Ribonucleoprotein Complexes. J Virol 2018; 92: e02084-17. https://doi.org/10.1128/JVI.02084-17.
6. **Sreenivasan CC, Sheng Z, Wang D, Li F**. Host Range, Biology, and Species Specificity of Seven-Segmented Influenza Viruses-A Comparative Review on Influenza C and D. Pathogens 2021; 10: 1583. *https://doi.org/10.3390/pathogens10121583.*
7. **Steel J, Lowen AC**. Influenza A virus reassortment. Curr Top Microbiol Immunol, 2014; 385: 377-401. *https://doi.org/10.1007/82_2014_395.*
8. **Raza MA, Ashraf MA, Amjad MN, Din GU, Shen B, Hu Y**. The peculiar characteristics and advancement in diagnostic methodologies of influenza A virus. Front Microbiol, 2025; 15: 1435384. *https://doi.org/10.3389/fmicb.2024.1435384.*
9. **Karakus U, Mena I, Kottur J, El Zahed SS, Seoane R, Yildiz S, et al**. H19 influenza A virus exhibits species-specific MHC class II receptor usage. Cell Host Microbe. 2024; 32: 1089-1102. e10. *https://doi.org/10.1016/j.chom.2024.05.018*
10. **Zhao C, Pu J**. Influence of Host Sialic Acid Receptors Structure on the Host Specificity of Influenza Viruses. Viruses. 2022; 14: 2141. *https://doi.org/10.3390/v14102141.*
11. **de Bruin ACM, Spronken MI, Bestebroer TM, Fouchier RAM, Richard M**. Conserved Expression and Functionality of Furin between Chickens and Ducks as an Activating Protease of Highly Pathogenic Avian Influenza Virus Hemagglutinins. Microbiol Spectr, 2023; 11: e0460222. *https://doi.org/10.1128/spectrum.04602-22.*

12. **Lycett SJ, Duchatel F, Digard P**. A brief history of bird flu. Philos Trans R Soc Lond B Biol Sci. 2019; 374(1775): 20180257. *https://doi.org/10.1098/rstb.2018.0257.*
13. **Centers for Disease Control and Prevention**. Past Reported Global Human Cases with Highly Pathogenic Avian Influenza A (H5N1) (HPAI H5N1) by Country, 1997-2025. 2025.Accessed on September 25, 2025. *https://www.cdc.gov/bird-flu/php/avian-flu-summary/chart-epi-curve-ah5n1.html.*
14. **Charostad J, Rezaei Zadeh Rukerd M, Mahmoudvand S, Bashash D, Hashemi SMA, Nakhaie M, Zandi K.** A comprehensive review of highly pathogenic avian influenza (HPAI) H5N1: An imminent threat at doorstep. Travel Med Infect Dis, 2023; 55: 102638. *https://doi.org/10.1016/j.tmaid.2023.102638.*
15. **Elsmo EJ, Wünschmann A, Beckmen KB, Broughton-Neiswanger LE, Buckles EL, Ellis J, et al**. Highly Pathogenic Avian Influenza A(H5N1) Virus Clade 2.3.4.4b Infections in Wild Terrestrial Mammals, United States, 2022. Emerg Infect Dis. 2023; 29: 2451-2460. *https://doi.org/10.3201/eid2912.230464.*
16. **Youk S, Torchetti MK, Lantz K, Lenoch JB, Killian ML, Leyson C, et al.** H5N1 highly pathogenic avian influenza clade 2.3.4.4b in wild and domestic birds: Introductions into the United States and reassortments, December 2021-April 2022. Virology. 2023; 587: 109860. *https://doi.org/10.1016/j.virol.2023.109860.*
17. **Zeng J, Du F, Xiao L, Sun H, Lu L, Lei W, et al**. Spatiotemporal genotype replacement of H5N8 avian influenza viruses contributed to H5N1 emergence in 2021/2022 panzootic. J Virol, 2024; 98: e0140123. *https://doi.org/10.1128/jvi.01401-23.*
18. **Peacock TP, Moncla L, Dudas G, VanInsberghe D, Sukhova K, Lloyd-Smith JO, et al**. The global H5N1 influenza panzootic in mammals. Nature. 2025; 637(8045): 304-313. *https://doi.org/10.1038/s41586-024-08054-z.*
19. **Bruno A, de Mora D, Olmedo M, Garces J, Marzal A, García-Bereguiain MA**. Highly pathogenic avian influenza A (H5N1) virus outbreaks in South America in 2022–2024: a comprehensive review of an ongoing panzootic. Virology. 2025; 610: 110602. *https://doi.org/10.1016/j.virol.2025.110602.*
20. **Ruiz-Saenz J, Martinez-Gutierrez M, Pujol FH.** Multiple introductions of highly pathogenic avian influenza H5N1 clade 2.3.4.4b into South America. Travel Med Infect Dis. 2023; 53: 102591. *https://doi.org/10.1016/j.tmaid.2023.102591.*
21. **Abdelwhab EM, Mettenleiter TC**. Zoonotic Animal Influenza Virus and Potential Mixing Vessel Hosts. Viruses. 2023; 15: 980. *https://doi.org/10.3390/v15040980.*
22. **Nguyen TQ, Hutter CR, Markin A, Thomas M, Lantz K, Killian ML, et al**. Emergence and interstate spread of highly pathogenic avian influenza A(H5N1) in dairy cattle in the United States. Science. 2025; 388(6745): eadq0900. *https://doi.org/10.1126/science.adq0900.*
23. European Food Safety Authority; European Centre for Disease Prevention and Control; European Union Reference Laboratory for Avian Influenza; Alexakis L, Buczkowski H, Ducatez M, Fusaro A, Gonzales JL, Kuiken T, et al. Avian influenza overview December 2024-March 2025. EFSA J. 2025; 23: e9352. *https://doi.org/10.2903/j.efsa.2025.9352.*
24. **Zhang G, Shi Y, Ge H, Wang Y, Lu L, Jiang S, Wang Q**. Genomic signatures and host adaptation of H5N1 clade 2.3.4.4b: A call for global surveillance and multi-target antiviral strategies. Curr Res Microb Sci. 2025; 8: 100377. *https://doi.org/10.1016/j.crmicr.2025.100377.*
25. **Krammer F, Hermann E, Rasmussen AL**. Highly pathogenic avian influenza H5N1: history, current situation, and outlook. J Virol, 2025; 99: e0220924. *https://doi.org/10.1128/jvi.02209-24.*
26. **Sidney J, Kim A-R, de Vries RD, Peters B, Meade PS, Krammer F, et al**. Targets of influenza human T-cell response are mostly conserved in H5N1. mBio. 2025; 16: e0347924. *https://doi.org/10.1128/mbio.03479-24.*

27. **Gu C, Maemura T, Guan L, Eisfeld AJ, Biswas A, Kiso M, et al.** A human isolate of bovine H5N1 is transmissible and lethal in animal models. Nature. 2024; 636(8043): 711-8. *https://doi.org/10.1038/s41586-024-08254-7.*
28. **Mahmoud SH, Khattab MS, Yehia N, Zanaty A, Arafa AES, Khalil AA**. Pathogenicity of Highly Pathogenic Avian Influenza A/H5Nx Viruses in Avian and Murine Models. Pathogens. 2025; 14: 149. *https://doi.org/10.3390/pathogens14020149.*
29. **Alkie TN, Embury-Hyatt C, Signore AV, Baldwin F, Hisanaga T, Xu W, et al**. Comparative pathogenicity of three A(H5N1) clade 2.3.4.4b HPAI viruses in blue-winged teal and transmission to domestic poultry. mSphere. 2025; 10: e0002125. *https://doi.org/10.1128/msphere.00021-25.*
30. **Capelastegui F, Goldhill DH**. H5N1 2.3.4.4b: a review of mammalian adaptations and risk of pandemic emergence. J Gen Virol. 2025; 106: 002109. *https://doi.org/10.1099/jgv.0.002109.*
31. **Xie Z, Yang J, Jiao W, Li X, Iqbal M, Liao M, Dai M.** Clade 2.3.4.4b highly pathogenic avian influenza H5N1 viruses: knowns, unknowns, and challenges. J Virol. 2025; 99: e0042425. *https://doi.org/10.1128/jvi.00424-25.*
32. **Good MR, Suja D, Guthmiller JJ.** The sweet side of H5N1 influenza virus infection. PLoS Pathog. 2025; 21: e1012847. *https://doi.org/10.1371/journal.ppat.1012847.*
33. **Long JS, Mistry B, Haslam SM, Barclay WS**. Host and viral determinants of influenza A virus species specificity. Nat Rev Microbiol. 2019; 17: 67–81. *https://doi.org/10.1038/s41579-018- -0115-z.*
34. **Imai M, Watanabe T, Hatta M, Das SC, Ozawa M, Shinya K, et al.** Experimental adaptation of an influenza H5 HA confers respiratory droplet transmission to a reassortant H5 HA/H1N1 virus in ferrets. Nature; 2012; 486(7403): 420-428. *https://doi.org/10.1038/nature10831.*
35. **Lin TH, Zhu X, Wang S, Zhang D, McBride R, Yu W, et al**. A single mutation in bovine influenza H5N1 hemagglutinin switches specificity to human receptors. Science. 2024; 386(6726): 1128-34. *https://doi.org/10.1126/science.adt0180.*
36. **Peacock TP, Sheppard CM, Lister MG, Staller E, Frise R, Swann OC, et al.** Mammalian ANP32A and ANP32B Proteins Drive Differential Polymerase Adaptations in Avian Influenza Virus. J Virol. 2023; 97: e0021323. *https://doi.org/10.1128/jvi.00213-23.*
37. **Garretson TA, Liu J, Li SH, Scher G, Santos JJS, Hogan G, et al**. Immune history shapes human antibody responses to H5N1 influenza viruses. Nat Med. 2025; 31: 1454-8. *https://doi.org/10.1038/s41591-025-03599-6.*
38. **Kaplan BS, Torchetti MK, Lager KM, Webby RJ, Vincent AL.** Absence of clinical disease and contact transmission of HPAI H5NX clade 2.3.4.4 from North America in experimentally infected pigs. Influenza Other Respir Viruses. 2017; 11: 464-470. *https://doi.org/10.1111/irv.12463.*
39. **Kwon T, Trujillo JD, Carossino M, Machkovech HM, Cool K, Lyoo EL, et al.** Pathogenicity and transmissibility of bovine-derived HPAI H5N1 B3.13 virus in pigs. Emerg Microbes Infect. 2025; 14: 2509742. *https://doi.org/10.1080/22221751.2025.2509742.*
40. **Krammer F, Schultz-Cherry S**. We need to keep an eye on avian influenza. Nat Rev Immunol. 2023; 23: 267-8. *https://doi.org/10.1038/s41577-023-00868-8.*
41. **WHO Global Influenza Programme & World Health Organization**. Pandemic influenza preparedness and response: a WHO guidance document. 2009. World Health Organization. Accessed on May 25, 2025. *https://iris.who.int/handle/10665/44123.*
42. **World Health Organization**. Intergovernmental Negotiating Body to draft and negotiate a WHO convention, agreement or other international instrument on pandemic prevention, preparedness and response. 2025. Accessed on May 5, 2025. *https://apps.who.int/gb/ebwha/pdf_files/WHA78/A78_10-en.pdf.*

43. **Qualls N, Levitt A, Kanade N, Wright-Jegede N, Dopson S, Biggerstaff M, et al**. Community Mitigation Guidelines to Prevent Pandemic Influenza – United States, 2017. MMWR. 2017; 66: 1-34. *https://www.cdc.gov/mmwr/volumes/66/rr/rr6601a1.htm.*
44. **Harrington WN, Kackos CM, Webby RJ.** The evolution and future of influenza pandemic preparedness. Exp Mol Med. 2021; 53: 737-749. *https://doi.org/10.1038/s12276-021-00603-0.*
45. **Ziegler T, Mamahit A, Cox NJ**. 65 tears of influenza surveillance by a World Health Organization-coordinated global network. Influenza Other Respir Viruses. 2018; 12: 558-565. *https://doi.org/10.1111/irv.12570.*
46. **Cargnin Faccin F, Perez DR**. Pandemic preparedness through vaccine development for avian influenza viruses. Hum Vaccin Immunother. 2024; 20: 2347019. *https://doi.org/10.1080/21645515.2024.2347019.*
47. **Centers for Disease Control and Prevention**. Highly Pathogenic Avian Influenza A(H5N1) Virus: Interim Recommendations for Prevention, Monitoring, and Public Health Investigations. 2024. Accessed on May 4, 2025. *https://www.cdc.gov/bird-flu/prevention/hpai-interim-recommendations.html.*
48. **Cohen J.** Bird Shots. Science. 2023; 380(6640): 24-7. *https://doi.org/10.1126/science.adi1004.*
49. **Lewis N, Beer M**. Stop H5N1 influenza in US cattle now. Science. 2024; 385(6705): 123.2024. *https://doi.org/10.1126/science.adr5866.*
50. **Medina-Armenteros Y, Cajado-Carvalho D, das Neves Oliveira R, Apetito Akamatsu M, Lee Ho P.** Recent Occurrence, Diversity, and Candidate Vaccine Virus Selection for Pandemic H5N1: Alert Is in the Air. Vaccines. 2024; 12: 1044. *https://doi.org/10.3390/vaccines12091044.*
51. **Jones JC, Yen HL, Adams P, Armstrong K, Govorkova EA.** Influenza antivirals and their role in pandemic preparedness. Antiviral Res. 2023; 210: 105499. *https://doi.org/10.1016/j.antiviral.2022.105499.*
52. **Khurana S, King LR, Manischewitz J, Posadas O, Mishra AK, Liu D, et al.** Licensed H5N1 vaccines generate cross-neutralizing antibodies against highly pathogenic H5N1 clade 2.3.4.4b influenza virus. Nat Med. 2024; 30: 2771-2776. *https://doi.org/10.1038/s41591-024-03189-y.*
53. **Souza CK, Santos JJS, Boggiatto P, Sterle H, Arruda B, Palmer MV, et al.** H5 influenza virus mRNA-lipid nanoparticle (LNP) vaccination elicits adaptive immune responses in Holstein calves. 2025. bioRxiv preprint. */https://doi.org/10.1101/2025.05.01.651548.*
54. **Koopmans MPG, Barton Behravesh C, Cunningham AA, Adisasmito WB, Almuhairi S, Bilivogui P, et al.** The panzootic spread of highly pathogenic avian influenza H5N1 sublineage 2.3.4.4b: a critical appraisal of One Health preparedness and prevention. Lancet Infect Dis. 2024; 24: e774-e781. *https://doi.org/10.1016/S1473-3099(24)00438-9.*

FE DE ERRATA

En el trabajo **"Estudio experimental sobre el efecto regulador de Qinggan Dongyin en la homeostasis de los linfocitos T en ratones MRL/lpr"**, publicado en el Vol. 66 número 3, septiembre de 2025, es necesario hacer unas correcciones a saber: en las páginas 274 y 275 deben sustituirse las Tablas 1 y 2 por esta nueva versión.

ERRATUM

In the article **"Experimental study on the regulatory effect of Qinggan Dongyin on T lymphocyte homeostasis in MRL/lpr mice"**, published in Vol. 66, Issue 3, September 2025, the following corrections are necessary: on pages 274 and 275, Tables 1 and 2 should be replaced with this updated version.

Table 1. Distribution of CD4 + T, CD8 + T, Th1, Th2, Th17 and Treg cells in the spleen of mice in each group.

	Control group (n=6)	Model group (n=6)	QGDY group (n=6)
CD4+ T (%)	19.67 ± 0.63	15.37 ± 0.21***	17.52 ± 0.32###
CD8+ T (%)	12.65 ± 0.55	6.38 ± 0.29***	9.49 ± 0.17###
Th1 (%)	0.82 ± 0.16	3.61 ± 0.39**	1.60 ± 0.06##
Th2 (%)	0.75 ± 0.07	3.38 ± 0.35***	1.58 ± 0.03###
Th17 (%)	1.36 ± 0.20	2.83 ± 0.10***	1.97 ± 0.13###
Treg (%)	2.59 ± 0.08	0.69 ± 0.30**	1.61 ± 0.04##

Note: Cells of CD4-positive T cells (CD4+ T), CD8-positive T cells (CD8+ T), T-helper 1 cells (Th1), T-helper 2 cells (Th2), T-helper 17 cells (Th17), Regulatory T cells (Treg) in model and treatment group compared with the control group using one-way ANOVA method, and the mean ± standard deviation (SD) is used for the result representation. **p<0.01, ***p<0.001; compared with the model group, ###p<0.001, ##p<0.01.

Table 2. Concentrations of IFN-γ, IL-6, TNF-α, IL-17A, TGF-β and PFP in the plasma of mice in each group.

	Control group (n=6)	Model group (n=6)	QGDY group (n=6)
IFN-γ (ng/L)	113.07 ± 31.21	457.42 ± 218.77*	166.81 ± 22.34#
IL-6 (pg/mL)	28.07 ± 8.76	80.29 ± 39.76*	40.66 ± 47.38
TNF-α (ng/L)	80.11 ± 44.98	373.12 ± 146.68**	186.70 ± 111.87#
IL-17A (pg/mL)	17.69 ± 7.18	108.23 ± 38.61**	50.77 ± 32.63#
TGF-β (ng/L)	27.20 ± 18.38	177.47 ± 78.95**	69.97 ± 26.65#
PFP (ng/L)	47.41 ± 14.01	14.64 ± 8.78**	34.95 ± 20.50

Note: The cytokines of Interferon-gamma (IFN-γ), Interleukin-6 (IL-6), Tumor Necrosis Factor-α (TNF-α), Interleukin-17A (IL-17A), Transforming Growth Factor-beta (TGF-β), Perforin (PFP) in model and treatment groups compared with the control group using One-way ANOVA method, and the mean ± standard deviation (SD) is used for the result representation. *p<0.05, **p<0.01; compared with the model group, #p<0.05.

Índice de Autores Vol. 66, Nos. 1-4, 2025

Investigación Clínica
Vol. 66 Nº 4 / December 2025
Bilingual - Abstracts in Spanish and English

Contents

Investigación Clínica
Vol. 66 Nº 4 /Diciembre 2025
Bilingüe - Resúmenes en Español e Inglés

Contenido